University of Southampton

Faculty of Engineering, Science and Mathematics

School of Geography

Changes in Hydrological Extremes and Climate Variability in the Severn Uplands

Eloise M. Biggs

Thesis for the degree of Doctor of Philosophy

September 2009

UNIVERSITY OF SOUTHAMPTON

ABSTRACT

FACULTY OF ENGINEERING, SCIENCE AND MATHEMATICS

SCHOOL OF GEOGRAPHY

Doctor of Philosophy

CHANGES IN HYDROLOGICAL EXTREMES AND CLIMATE VARIABILITY IN THE SEVERN UPLANDS

By Eloise Marie Biggs

Hydrological extremes within the UK have increased in intensity, frequency and persistence over recent years and are predicted to increase in variability throughout the 21st century. Past and future changes in hydrological extremes relative to climate change were investigated within Severn Uplands, a climate sensitive catchment. Using the Mann-Kendall trend detection test, time-series analysis over a 30-year period revealed a significant increase in winter and autumn precipitation and a decrease in summer precipitation. The analysis of flow time-series indicated an increase in winter and July flows and a decrease in spring flows. Changes in climate variability over the same period showed increases in air temperature and SST, and a reduction in snow cover. Climate variables were found to largely correlate with hydrological extremes which were characteristic of certain weather types and largely influenced by the NAO.

To model future flows within the Severn Uplands a hydrological model (HEC-HMS) was used to simulate hydrological processes. The extreme hydrological event of November-December 2006 was used to calibrate the model. The difference between using radar and gauge precipitation data to drive the model was quantified. Radar data resulted in the smallest prediction accuracy followed by gauge-corrected radar data (corrected using the mean-field bias where gauge rainfall was interpolated using cokriging) and then gauge precipitation which had the largest prediction accuracy. Model accuracy was sufficient using the gauge corrected radar and gauge precipitation data as inputs, so both were altered for future predictions to investigate the propagation of uncertainty. Predicted changes in temperature and precipitation by the UKCIP02 scenarios were used to alter the baseline extreme event to predict changes in peak flow and outflow volume. Both radar- and gauge-driven hydrological modelling predicted large flow increases for the 21st century with increases up to 8% by the 2020s, 18% by the 2050s and 30% by the 2080s. Discrepancies between predictions were observed when using the different data inputs.

Contents

List of Figures

List of Tables

Declaration of authorship

I, Eloise Biggs, declare that the thesis entitled 'Changes in hydrological extremes and climate variability in the Severn Uplands'

and the work presented in the thesis are both my own, and have been generated by me as the result of my own original research. I confirm that:

- this work was done wholly or mainly while in candidature for a research degree at this University;
- where any part of this thesis has previously been submitted for a degree or any other qualification at this University or any other institution, this has been clearly stated;
- where I have consulted the published work of others, this is always clearly attributed;
- where I have quoted from the work of others, the source is always given. With the exception of such quotations, this thesis is entirely my own work;
- I have acknowledged all main sources of help;
- where the thesis is based on work done by myself jointly with others, I have made clear exactly what was done by others and what I have contributed myself;
- none of this work has been published before submission

Signed:

Date: 30th September 2009

Acknowledgements

"A PhD is just like surfing. The waves keep coming. Some you want to ride, some you don't. And periodically, there is always one wave larger than the others."

Professor Peter M. Atkinson (2005)

Above all I would like to express my sincerest gratitude to my principal supervisor Professor Peter Atkinson for his invariable and invaluable efforts which have continuously strengthened my research. The above quote was one of the first things Pete said to me upon my arrival. Quite an outlandish declaration, but on reflection, his statement does indeed have some metaphorical similarity to the PhD research process. Thanks also to the other members of my supervisory team, Professor David De Roure and Dr. Craig Hutton, for all their contributions and many good ideas. Special recognition is essential for Dr. Danius Michaelides; without his technical support in assisting with processing large datasets and converting them into manageable files, large portions of this research would not have been possible. Much appreciation also goes to Dr. Steve Darby for taking on the roll of internal examiner and providing comments during my upgrade.

A number of organisations and certain individuals within them have provided data and information fundamental to my research. Many thanks go to Richard Cross, Claire French, Richard Severn, Bhavika Tailor, Mathew Wells (all at the Environment Agency), Thomas Evans (US Army Corps), the Met Office and CEH Wallingford.

Thanks to all staff and postgraduates (both past and present) within the School of Geography who have provided ideas and helped resolve both trying and trivial issues: Professor Nigel Arnell, Professor Mike Clark, Professor Mary Edwards, Professor Dave Martin, Dr. Arnis Asmat Dr. Matthew Charlton, Dr. Edith Cheng, Dr. Jeganathan Chockalingam, Dr. Peter Gething, Dr. Charlie Kerr, Dr. Pete Langdon, Dr. Julian Leyland,

Dr. Jeff Neal, Dr. Nick Odoni, Dr. Sally Priest, Dr. Elly Pryce, Dr. Kathryn Rose, Dr. Matt Wilson, Dr. Jim Wright, Aizam Adnan, Nicola Batchelor, Sam Bateman, Sam Cockings, Kate Cudworth, Emily Forster, Maggie Harriss, Duncan Hornby, John Hurst, Duncan Kitts, James Macmillen, Marc Naura, Rich Treves, Tri Van, Gary Watmough and Justyn Willsmore.

Finally, thanks to all my family and friends for providing endless encouragement and support.

Abbreviations

AM	Annual maxima
CEH	Centre for Ecology and Hydrology
CN	Curve number
CO_2	Carbon dioxide
CSI	Critical success index
DEFRA	Department of Environment, Food and Rural Affairs
DEM	Digital elevation model
DSS	Data storage system
ECS	School of Electronics and Computer Science
ENSO	El Niño Southern Oscillation
GCM	Global climate model
GS	Gilbert skill score
GIS	Geographical information system
HadAM	Hadley Centre atmospheric model
HadCM	Hadley Centre coupled model
HadGEM	Hadley Centre global environmental model
HadRM	Hadley Centre regional model
HEC	Hydrologic Engineering Centre
HMS	Hydrologic modelling system
IDW	Inverse-distance weighting
IPCC	Intergovernmental Panel on Climate Change
ISAT	Impervious surface analysis tool
MBF	Mean field bias
MAE	Mean average error
MAP	Mean areal precipitation

MCRM	Midlands catchment runoff model
MK	Mann-Kendall
NOA	North Atlantic oscillation
NAOI	North Atlantic oscillation index
NOAA	National Oceanic and Atmospheric Administration
ONI	Oceanic Niño Index
QMED	Discharge median
RAS	River analysis system
RCM	Regional climate model
RHS	River habitat survey
RMS	Root mean square
RMSE	Root mean square error
RMSF	Root mean square factor
SAR	Synthetic aperture radar
SCS	Soil conservation service
SMD	Soil moisture deficit
SRES	Special report on emissions scenario
SST	Sea surface temperatures
UKCIP	United Kingdom climate impacts programme
UKCP	United Kingdom climate projections
USAGE	United States Army Corps of Engineers
USGS	United States Geological Survey

CHAPTER 1

Introduction

Flooding is a persistent problem in present-day society, with millions of people affected by its potentially devastating impacts. It is estimated that more than one third of the world's land area is exposed to flooding which affects 82% of the world's population who reside in these areas (Pelling, 2004). Out of all natural catastrophes throughout the world, flood disasters account for about a third (by number and economic losses) and are responsible for more than half of the fatalities. Trend analysis reveals that major flood incidents and the losses generated by them have increased dramatically in recent years (White, 2001). Essentially, flooding becomes a problem only where there is conflict with human use, and as populations continue to expand rapidly, and development pressures increase accordingly, society is indisputably becoming more vulnerable to natural hazards. Nonetheless, the natural aspects of flooding may also be playing a role in increased risk. Our climate is changing, be it natural- or human-induced, and it is these changes that need to be accounted for now to prepare for the future. This chapter provides an introduction to fluvial flood issues in the UK and introduces how a changing climate has, and will continue to influence flood characteristics.

1.1 FLUVIAL FLOODING

Fluvial flood inundation generally arises as a result of heavy or continuous rainfall causing soil to become waterlogged and the flow capacity of the river to be exceeded, resulting in water overflowing the river banks onto adjacent land (HR Wallingford 2005). The surrounding land is known as the floodplain and being a flood-prone area it is hazardous to

people, animals and all material assets. Various mitigating circumstances can abet flood inundation, yet precipitation is one of the main drivers of out-of-bank flow. Precipitation events that give rise to serious flooding are often outcomes of four main contributory factors: (i) intensity of precipitation; (ii) duration of precipitation; (iii) the wetness of the ground; and (iv) the response of the rainfall catchment (Collier *et al*., 2002). Over the last decade especially, the UK has suffered from multiple fluvial flood events, all of which were driven primarily by periods of severe precipitation.

1.2 UK FLOODING

Flooding is the most damaging and costly natural hazard in the UK (Brown and Damery 2002), costing the nation billions of pounds every year. Currently, 8% of England's land area is at risk from fluvial or tidal river flooding and approximately 10% of the population of England and Wales live within areas potentially at risk from flooding or coastal erosion (Culshaw *et al.* 2006). Property worth over £220 billion and agricultural land worth £7 billion is also located within these risk areas. Flooding in the UK is so severe that total annual average damages, just by maintaining present levels of protection for fluvial, sea and tidal inundation, amount to £784 million (DEFRA 2001a). Nationwide, urban land area is estimated to have increased by 50% between 1930 and 1990 (Environment Agency, 2001a). Urbanisation stems from development pressures and as demand continues to increase, risks associated with flood inundation increase accordingly. Nonetheless, strategic policy and planning can reduce exposure to flooding through planning control and defence schemes which help to alleviate impacts (Moore *et al.* 2005).

Recent severe flood events in the UK have prompted the government to inject vast quantities of funding into improving flood policy and defences, and to finance immediate further research into how flood mitigation measures can be enhanced. Major flood incidents over the last decade have received extensive media and academic coverage, highlighting where current problems and concerns rest. In particular, the floods of autumn 2000 and summer 2007 had severe impacts nationwide. Circumstances leading up to these two major events are described as follows.

Autumn 2000 floods

Autumn 2000 was the wettest year on record across England and Wales with the heaviest autumn rainfall since records began in 1766 (Alexander and Jones, 2001; Howe and White, 2002). Following a wet spring and a dry summer season, a period of storminess began in September with a series of powerful wave depressions sweeping across the UK (Lawrimore et al., 2001). Recurrent heavy rainfall in October and November caused prolonged, extensive and, in places, repeated flooding as ground saturation remained high. With catchments waterlogged, rivers responded rapidly to even minimal rainfall amounts. Flood levels in many places were the highest on record. A breakdown of nationwide flood incidents shows that 40% occurred where no flood defences existed, 28% from overtopping, outflanking or failure of defences, and 32% from ordinary watercourses, inadequate surface drainage and third party defences (Environment Agency, 2001a). Total damages amounted to costs of £1 billion across England and Wales (White and Howe, 2002).

Summer 2007 floods

The Pitt Review (Pitt, 2008) appraised the summer floods of 2007 and stated that *"the floods that devastated England last year ranked as the most costly flood in the world in 2007"* even despite an overwhelming loss of life elsewhere. 48,000 households and nearly 7,300 businesses were flooded and inundation caused the most significant loss of essential services since the Second World War. Heavy rainfall was the result of a series of statistically unusual patterns of weather which have been attributed to two major causes; the position of the Polar Front Jet Stream and high North Atlantic sea surface temperatures (Lane, 2008; Marsh and Hannaford, 2007). The period from May to July was the wettest period since national records began in 1766. In June, heavy thunderstorms led to wide extents of ground saturation and slow moving depressions in July resulted in the greatest flood inundation peaks.

In light of the autumn 2000 floods the Environment Agency (2001a) disclosed that any further increases in the more modest of floods or the severity of extreme events would stretch the resources of the Agency and its partners beyond their current operating capabilities. It was following the autumn 2000 floods that the flood issue was finally given

national prominence. Referring to the title of an Environment Agency (2001a) report published in the spring following the autumn 2000 floods, many *lessons* were indeed *learned*. And it was following these extreme floods that the British government finally began to question the role of climate change (Moore *et al.* 2005).

Multiple extreme flood events since the turn of the century have emphasized the need to strengthen the ability to identify and interpret changes in the magnitude, frequency and seasonality of flooding across the UK (DEFRA, 2001b). During the summer of 2007 resources were stretched yet again, with extensive, unexpected flooding inundating much of the nation with little that could be done to prevent property from being damaged due to fast-rising river levels. The summer 2007 floods led to the resurfacing of issues brought on by the Easter 1998 floods when inundation events were mainly concentrated in the Midlands region (DEFRA, 2001b) and flood defence, investment, policy and operations were all profoundly affected (Moore *et al.* 2005). Prior to 1998, UK flooding was perceived by the majority of the UK population as being something that happened relatively rarely (White and Howe, 2002). Issues raised from severe flooding in 1998 and 2000 were reiterated by the 2007 floods, emphasizing the imminent need to tackle resource requirements and mitigate the impacts of climate change if these extreme events are to be successfully "lived with".

1.3 FUTURE FLOOD IMPLICATIONS

Adaptation to change requires the determination of how climate has altered over recent years and how forecasts of future scenarios are likely to influence present conditions. Current climate change is exacerbating the flooding problem, with more frequent and intense floods resulting from enhanced winter precipitation amounts, which is discussed in detail in Chapter 2. Prolonged and widespread flooding over Northern Europe in recent years has raised the question of the likely effects of precipitation changes on hydrological regimes and, in particular, the effect on flood frequency and severity (Bell *et al.*, 2007). Many UK flood defences will reach the end of their design life over the next decade (POST 2001) and the Government's funding for defence construction and repair has been declared insufficient (Brown and Damery 2002). Without allowance for accommodating the predicted impacts of climate change flooding costs could increase significantly, with annual average damages rising by 50% in fluvial areas (DEFRA 2001a).

Future river flows are set to intensify and will be dependent on the extent of change in climatic variables influencing the catchment, as well as basin morphology and the configuration of the drainage network and stream channels (Arnell, 2003a; Collier and Fox, 2003). A change in seasonality might be expected to cause changes in flood behaviour, particularly an increase in winter flooding given the links between flooding and rainfall (Robson, 2002). The Environment Agency (2009a) states that over the 21st century there is a higher likelihood of flooding from more frequent and severe extreme weather. An increase in flood severity is expected under a changing climate which will result in adverse environmental and socioeconomic impacts. The Foresight Project (Evans *et al.*, 2004) estimates that flood risk could be up to three times greater from increased rainwater in flood-prone areas over the coming century.

1.4 SUMMARY

With flood events seemingly a common occurrence across the UK and likely to increase in frequency and severity in the future, Chapter 2 explores where extremes in precipitation and flows can be identified in the literature and how the concept of "climate change" is influencing the hydrological system. Both climate and hydrological modelling are reviewed in detail, assessing what has previously been achieved in relation to specific climate and hydrological models, and where current problems are to be found in order to model fluvial and climate systems more accurately. Particular attention is given to precipitation, the primary agent of out-of-bank flow and the main hydrological model driver.

1.5 RESEARCH AIM

The overall aim of this research is to determine how hydrological extremes within a climate sensitive catchment have changed over recent years and how they are likely to be affected under future conditions given current climate change predictions. Hydrological modelling is used as an intermediary process in order to predict future extremes using past hydrological extreme events. Uncertainty is inherent with scientific research and is duly reported at each stage, with an overall emphasis on uncertainty propagation throughout the research. Research is outlined in Figure 1.1 and detailed objectives are stated following a review of the literature in Chapter 2.

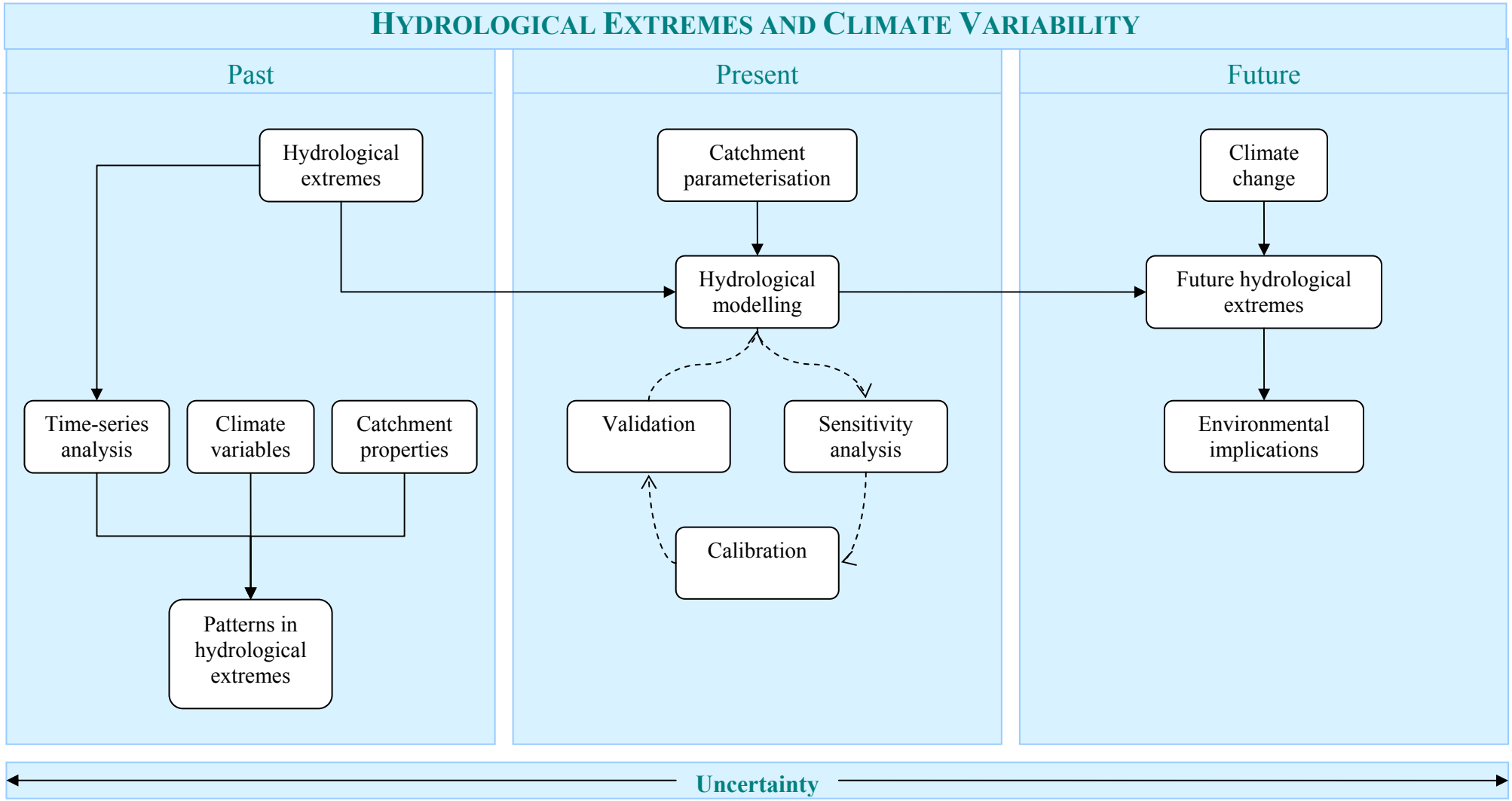

Figure 1.1 Broad overview of research outline

CHAPTER 2

Literature Review

"If we are to understand how flooding may be affected by future alterations in our climate, it will probably be necessary to work towards characterising the links between climatic conditions, rainfall patterns and flooding."

(Robson, 2002, p1341)

Flooding is a prominent global issue and its relationship to climate change is as uncertain as ever. The previous chapter highlighted recent nationwide changes in flood inundation. In this chapter, literature is explored, presenting evidence for a recent increase in precipitation at sites across the UK in relation to a changing climate. Rainfall is one of the main drivers influencing river flows and is likely to be highly responsive to changes in climate. With the general public perception that both the occurrence and magnitude of extreme flood events in the UK are increasing (DEFRA, 2001b; Randall *et al.*, 2007) research into both flow and precipitation extremes is reviewed to support this claim. Climate modelling is discussed with particular reference to the UK Hadley Centre modelling suite. The latter part of this chapter looks into the accuracy of hydrological modelling with respect to rainfall inputs and issues linked with climate change altering the hydrological system over the coming century. Finally, a series of aims and objectives, derived from the reviewed research, are formulated as the basis for investigation within this study.

2.1 CLIMATE CHANGE

Climatic change can arise from several natural forcing mechanisms such as solar activity, orbital variations, volcanic eruptions, changes in ocean and atmospheric circulation

patterns, and modifications in greenhouse gas composition. Recent concerns regarding abrupt climate change are currently at the forefront of political, scientific and public debate with the link to increases in greenhouse gas concentrations, principally carbon dioxide (CO_2), being thoroughly scrutinised. Anthropogenic forcing leading to an enhancement of the natural greenhouse effect is thought to be having a drastic impact on our climate. It is only by accounting for human activities that temperature rise during the 20th century can be adequately explained (Crowley, 2000; Hegerl *et al.*, 2007). Although global warming reduction efforts may have an effect at slowing warming, these will not become apparent until later in the 21st century. Warming for the next 30 to 40 years has already been pre-determined by past and current emissions and it is for this reason that there is a pressing need to adapt to climate change (Hulme *et al.*, 2002).

2.1.1 Global warming

Currently, Earth's climate system is undergoing a period of rapid warming with associated effects having global-scale implications. There is a substantial array of evidence to back this assertion and it is therefore impossible to ignore such a major global occurrence. CO_2 gas, water vapour and cloud droplets absorb terrestrial radiation which directly warms the troposphere. These particles reflect longwave radiation and radiate heat partly back to the ground which temporarily retains heat in the troposphere (Knapp, 1986). This phenomenon is referred to as the *greenhouse effect* and an increase in particulates has resulted in increased warming of the troposphere, hence an enhanced greenhouse effect. Over the last 100 years, global temperatures have risen by about 0.6 ºC, with 0.4 ºC of this warming occurring since the 1970s (Hulme *et al.*, 2002). During this timeframe human activities, particularly the burning of fossil fuels, have caused a rapid increase in atmospheric CO_2 and other greenhouse gases, gases which prior to the industrial age had remained at near stable concentrations for thousands of years (Hegerl *et al.*, 2007). The recent IPCC assessment on climate change, released in 2007, states that during the last half-century human influence on climate has dominated over all other causes of global average surface temperature changes. Rapid warming since the 1970s has occurred in a period when greenhouse gas increase has prevailed over all other factors. Time-series analyses of global temperature records conclude that the 1990s was the warmest decade on record (Brohan *et al*., 2006), and studies of over 400 proxy climate records analysed by Jones (2006) concur

with time-series findings declaring that the 20th century was the warmest century, and the 1990s the warmest decade, of the entire millennium.

2.1.2 UK warming

Throughout the UK, climate has changed consistently with worldwide warming. Central England temperature records show temperature rises of almost 1 ºC over the 20th century, with all UK regions experiencing rapid warming since the late 1970s (Perry, 2006) and unprecedented warming during the 1990s (Jones and Hulme, 1997). Environmental and socioeconomic response indicators affected by climate shifts also echo warming patterns with a changing climate identified in proxy records, ranging from trends in the tourism industry to bird populations (DEFRA, 2004). The repercussions of global warming are set to continue and by the 2080s atmospheric carbon dioxide concentrations may be two to three times higher than that of pre-industrial concentrations. Climate models project global temperature increases of between 2.2ºC and 5.3ºC (Christensen *et al.*, 2007) by the end of the 21st century and average annual temperatures across the UK may increase between 2ºC and 3.5ºC (Hulme *et al.*, 2002) with summer temperature increases up to 4°C (Jenkins *et al.*, 2009). Douville *et al.* (2002) state that nearly all land areas will warm more rapidly than the global average and that the greatest warming will occur at northern high latitudes in winter. All IPCC (2001) models predict that water vapour concentration will increase in a warmer atmosphere which will enhance equatorial convection and intensify the global hydrological cycle.

2.1.3 Precipitation change

Increases in greenhouse gases in the atmosphere produce global warming through an increase in downwelling infrared radiation and, thus, not only increase surface temperatures but also enhance the hydrological cycle, as much of the heating at the surface goes into evaporating surface moisture (Trenberth, 1999). A rise in global water vapour concentration has resulted in an increase in mean global precipitation (Osborn and Hulme, 2002). This process is often referred to in the literature as an intensification or acceleration of the hydrological cycle. Atmospheric moisture content increases with a warmer climate due to a rise in surface evaporation and the water holding capacity of the atmosphere, at a

rate of about 7% per °C (Trenberth *et al.*, 2007). This leads to more precipitable water in the atmosphere accompanied by consequential changes in worldwide precipitation regimes.

Over many Northern Hemisphere mid-to-high latitude land areas, including the UK, more intense precipitation events have been observed. The trend in changing winter rainfall, and associated trends in runoff, is strongly linked to large-scale atmospheric circulation changes related to the North Atlantic Oscillation (NAO) and weather type descriptors (Wilby and Wigley, 1997; Shorthouse and Arnell, 1999; Fowler and Kilsby, 2002). Resultant enhanced westerly airflows and a more northerly storm track has led to increases in winter precipitation over Northern Europe (Hannaford and Marsh, 2007). Furthermore, the variability of the winter NAO over the last 50 years has been linked to North Atlantic sea surface temperatures (SSTs). The NAO Index is the difference between pressure systems centred over the Azores and Iceland. The NAO regulates precipitation variability and when in its positive phase airflow across the UK is more westerly, originating from the Atlantic, resulting in windier, wetter and milder winters. There has been an upward trend in positive NAO values since the 1960s (Osborn, 2000) which correlates with recent global warming and UK precipitation changes (Fowler and Hennessy, 1995).

Precipitation records for the UK show little evidence of longer-term trends but the long-term rainfall series averaged across the UK indicates that rainfall is probably increasing rather than decreasing (DEFRA, 2001b). Wetter winters have been observed since 1960 (Jones *et al*., 1997; Perry 2006) and the frequency of wet days (days when rainfall ≥ 10 mm) has increased (Hulme *et al.*, 2002). Giorgi *et al.* (2001) found an increase in the frequency of precipitation events exceeding 30 mm per day. Across the country, the contribution of most intense rainstorms to winter precipitation has increased, as has the proportion of winter precipitation that falls in five day or longer sequences of "heavy" rain (Osborn *et al.*, 2000; Hulme *et al.*, 2002). The proportion of precipitation received in winter relative to summer has changed over time, so that winters have never been as wet relative to summer in about 240 years of measurements as they have been over the last 30 years; winters have been getting wetter and summers have been getting drier (Hulme *et al.*, 2002). Osborn and Hulme's (2002) analysis of heavy rainfall events shows that total winter precipitation has increased almost everywhere in the UK, particularly in the west. The implications of warming on summer rainfall are less clear-cut, but a continued reduction in average rainfall totals combined with a greater concentration of intense rainfall into shorter periods is generally indicated (Hanna *et al.*, 2008).

2.2 EXTREMES

Global repercussions of a changing climate are likely to result in an increase in the frequency and magnitude of hydrological extremes within the UK (DEFRA, 2001a). River flows represent the integrated response to all hydrometeorological processes operating within a catchment and provide a more direct assessment of hydrological variability than characterisations based on precipitation (Svensson *et al.*, 2006). However, evidence for trends in rainfall is globally greater than that for changes in flooding and it is sometimes difficult to identify significant trends in the UK flood series to demonstrate an increase in flood events (Robson *et al.*, 1998; Robson, 2002). Some research has been conducted into changes in flow extremes, but as flood events are often hard to isolate a viable proxy to support evidence of flood increases is provided by data analysis of rainfall extremes (Lamb, 2001).

2.2.1 Flow

Precipitation and evaporation are the most important drivers of the hydrological system and changes in these primary processes significantly influence the timing and volume of runoff and streamflow, changes in soil water storage, groundwater-surface water interactions and the variability of hydrological processes (Murphy and Charlton, 2006; Wang *et al.*, 2006). Since the beginning of the 20th century positive trends in flood frequency have been identified by Robson and Reed (1996) at several UK sites. Hannaford and Marsh (2007) found significant positive trends in all high-flow indicators analysed, primarily in maritime-influenced, upland catchments in the north and west of the UK. There is high confidence that the timing and amount of runoff in fluvial systems is changing, and there is a very high confidence that catchments with substantial snow packs will experience major changes as temperature continues to rise (Miller, 2003). As stated in Chapter 1, precipitation is the main driver of fluvial flooding in the UK. Recent severe flooding in the UK has been attributed to multi-day rain events. Given projected changes in atmospheric circulation patterns, flood events are likely to become more common, particularly if the Polar Front Jet Stream shifts location and strength in upcoming years; storms which normally bring high rainfall to Scotland could possibly strengthen and shift southwards.

2.2.2 Precipitation

There is evidence for increasing rainfall extremes in Britain over the last 30 to 40 years, especially for longer durations, for example 30- or 60-day running totals (DEFRA, 2001a). Osborn *et al*. (2000) suggest that since the 1960s there has been an upward trend in extreme rainfall, in particular, an increase in short-duration winter rainfall intensities. Fowler and Kilsby (2003) found that over the last 40 years there have been significant but regionally varying changes in extreme rainfall, with more multi-day, prolonged heavy rainfall events in northern and western regions of the UK. This reflects on Lamb's (2001) research that recent extreme events have characteristically been multi-day, with unremarkable one-day totals.

2.2.3 Future changes

Changes in the frequency of hydrologic extremes may be one of the most significant consequences of climate change. Under a changing climate even the smallest of alterations to the mean, standard deviation or variance of a distribution can result in a large change to the frequency or intensity of the extremes (Meehl *et al.*, 2000). Many critical impacts of climate are controlled by extreme events rather than mean values (Salinger and Griffiths, 2001) yet Wang *et al.* (2006) state that most flood impact studies relating to climate change have looked at changes in mean climate values rather than the extremes, with research at a fine temporal resolution of daily precipitation and river discharge very limited. Arnell (2003a) suggests that in addition to changes in mean climate determining the potential frequency with which extremes are exceeded, changes in climate variability from day-to-day and year-to-year will influence changes in the frequency of extremes.

Several scenario-based climate modelling studies predict that the frequency of extreme rainfall events is likely to increase, signifying a significant reduction in return periods for extreme rainfall events (Huntingford *et al.*, 2003) and an increase in the proportion of precipitation occurring as extreme events (Karl *et al.*, 1995). The sensitivity of a shift in heavy precipitation events is thought to increase with the return period of the event, such that a comparatively small increase in the frequency of weak or moderate precipitation events may result in pronounced increases in the frequency of heavy events (Frei *et al.*, 2000). Two factors which may be influencing changes in extremes were identified by Frei

et al. (2000); the first being a change in the general circulation of the atmosphere affecting the preferred track of Atlantic storms and the second that global warming is inducing a global moistening of the atmosphere.

The continuing amplification of hydrological processes through global warming may have severe consequences in the UK, especially in terms of an increase in significant flood events (Fowler and Kilsby, 2003) with several global climate model (GCM) scenario simulations inferring an increase in frequency of extreme river discharges in the future. Natural variability alone is unlikely to be responsible for all the observed increase in high river flows (Svensson *et al.*, 2006). The possibility of climate change in decades to come further emphasises the need for early warning and flood forecasting particularly in floodplain areas at immediate and high risk. Samuels (2004) recognises the need for further research into forecasting floods caused by extreme precipitation event conditions. In recent years many studies have considered the potential effects of climate change on runoff in the UK, yet many of these consider only a limited number of catchments (Pilling and Jones, 1999). The primary method of understanding how variables in the hydrological system have, and are likely to change, is through the use of climate and hydrological models.

2.3 CLIMATE MODELLING

Predicting future climate precisely is not possible. Therefore, any assessment of impacts of climate change on river flows and water resources must use scenarios of feasible future changes (Arnell, 2004). Globally, climate models can simulate future climate systems at coarse spatial resolutions for a range of scenarios based on how the planet is predicted to change over coming years. Climate change at various locations depends upon the emissions scenario and the models which are used to apply the emissions scenario to the local climate (Arnell, 2004). Climate models are available at a global or regional scale.

2.3.1 Global Climate Models

General circulation models (GCMs; also termed global climate models) represent numerically the physical processes of the atmosphere, ocean, cryosphere and land surface. GCMs provide global estimates of many climate variables and are able to simulate the

response of the global climate system to future conditions based on a series of assumptions including population growth, energy demand, greenhouse gas emissions, land use change and the general behaviour of the climate system over long time scales. GCM modelling uses two main parameters, firstly the 'emission scenario' which reflects CO_2 concentrations in the atmosphere, and secondly 'climate sensitivity' which is the assumed response of the climate system to a doubling of the 1961-1990 CO_2 content in the atmosphere (Prudhomme *et al.,* 2003).

The most recent GCM in the UK is the HadGEM1 produced by the Hadley Centre in 2006. The new 2007 IPCC climate change assessments are based on model outputs from this GCM. Prior to this model climate evaluations were conducted using HadCM3 outputs, also produced by the Hadley Centre. Current UK climate scenarios (at the time of conducting this research) are based on this model (new scenarios were released in June 2009). The HadCM3 model has an atmospheric horizontal spatial resolution of 2.5 º latitude x 3.75 º longitude with 19 vertical layers. The ocean model has 20 layers and the spatial resolution is 1.25 º latitude x 1.25 º longitude (Gordon *et al.*, 2000).

GCM outputs are not generally considered to be adequate for hydrological modelling as they are generated at very coarse spatial and temporal resolutions in comparison to river basin scales. In particular, extremes are poorly modelled, as intensities, frequencies and distributions are less well simulated (Randall *et al.*, 2007). Downscaling processes are utilised to simulate climate impact studies at the hydrological scale (Prudhomme *et al.,* 2003). The HadCM3 GCM was used to drive a regional climate model which was used to produce the most recent UK climate change scenarios, as described below.

2.3.2 Regional Climate Models

Dynamic downscaling is a technique that uses complex algorithms at a fine grid resolution, describing the atmospheric processes nested within the GCM outputs (Prudhomme *et al.,* 2003). These are termed regional climate models (RCMs) and their resolution is significantly greater for hydrological modelling in comparison to GCMs. Advances in downscaling techniques have allowed hydroclimatological modelling to be carried out at increasingly fine spatial resolutions. Statistical rainfall downscaling methods have been developed which, when calibrated against weather-station measurements, relate the large-

scale circulation, temperature and moisture to likely rainfall extent and duration over smaller areas (Huntingford *et al.*, 2003). Statistical downscaling is often less costly than implementing dynamic downscaling techniques and is therefore often used for climate scenario generation in hydrological impact studies. As an example, Sharma *et al.* (2007) looked into downscaling issues for using GCM outputs as hydrological model inputs in the Ping River Basin, Thailand. Bias-correction and spatial disaggregation methods were used to increase the accuracy of GCM precipitation scenarios. These corrected forecasts were found to increase accuracy in basin level runoff observations.

Although RCMs show substantial increases in accuracy in modelling spatial weather patterns compared with GCMs, accurate reproduction of some weather statistics still remains problematic (Semenov, 2007). However, RCM spatial resolution has increased dramatically over the years with current rainfall extremes represented well by RCMs. This notable skill provides confidence in RCM ability to estimate extreme rainfall under future climate conditions and accurately examine how future precipitation characteristics are set to affect basin hydrology. Fowler *et al.* (2005) state that RCMs currently provide the most accurate available information for estimating changes in extreme rainfall.

HadRM3H is an ensemble-based RCM developed by the Hadley Centre for northern Europe. The spatial resolution is 50 km and the model uses future scenarios of 30-year time periods on a daily timescale (Fowler and Kilsby, 2007). Results from Ekström *et al.* (2005) using the HadRM3H model indicate that the return period magnitude for a 1-day rainfall event will increase by 10% nationwide by 2100. A study by Fowler *et al*. (2005) found that HadRM3H shows acceptable proficiency in estimating statistical properties of mean and extreme rainfall for the baseline period 1961-1990 for most UK regions. They also found that almost all problems relating to the representation of extreme rainfall events by the HadRM3H model were related to orographic enhancement of mean rainfall. Nevertheless, RCMs can resolve important atmospheric processes such as orographic precipitation more accurately than the driving GCM (Jones *et al.,* 1995). Building on the work by Fowler *et al.* (2005), Fowler and Kilsby (2007) pioneered the use of daily HadRM3H data directly in a UK hydrological impact study, following the proposal by Lamb (2001). HadRM3H integrations are at the forefront of modelling European climates and they were used to produce the UKCIP02 climate change scenarios for the UK (Hulme *et al.*, 2002).

2.3.3 UKCIP02 Scenarios

Climate change scenarios that provide conceivable descriptions of how things may change in the future have continually evolved in recent years. The most recent scenarios depicting future climate conditions in the UK are those developed by the Climate Impacts Programme. Outputs from the coupled HadCM3 and HadAM3H model provide the boundary conditions to drive a high spatial resolution atmospheric regional model (HadRM3) for Europe which is nested within the GCM. Results for the UK are in the form of the UKCIP02 scenarios, released in 2002 (UKCP09 scenarios were released towards the end of this research in June 2009 and so were not used in this study, but are further discussed in Chapter 9). The UKCIP02 scenarios supersede the UKCIP98 scenarios by modelling with a higher effective sensitivity, considering the effects of changing sulphate aerosol concentrations and improving the way thermal expansion of ocean waters and the dynamics of land glaciers are modelled (Hulme *et al.*, 2002). They also addressed user requirements to provide greater regional detail, estimates of changes to extremes of weather and sea level, advice on the possibility of rapid climate change and guidance on how to handle uncertainty. There is a relatively high confidence attached to UKCIP02 scenario outputs (Hulme *et al.*, 2002).

The UKCIP02 scenarios reflect upon the four different emissions scenarios that essentially span the IPCC SRES emissions range (see Table 2.1 for details). These consist of 40 future scenarios which follow four different storylines (each is considered equally probable) as described in the IPCC Special Report on Emissions Scenarios (Nakicenovic, *et al.*, 2000). The conventional 30-year period from 1961-1990 was used as the baseline period for the UKCIP02 scenarios and all changes in climate were calculated relative to this period. The "double-nesting" method used meant that only four regional climate model experiments, three for the A2 emissions scenario and one for the B2 scenario (relating to UKCIP02 named scenarios: low emissions, medium-low emissions, medium-high emissions and high emissions), could be conducted just for the 2080s (2071 to 2100) due to high computational costs. Regional climates for the higher (A1F1) and lower (B2 and B1) scenarios for the 2020s (2011 to 2040) and 2050s (2041 to 2070) were subsequently derived using the pattern-scaling procedure which entails taking results from existing GCM simulations and scaling RCM patterns up or down according to global temperature changes estimated by simple climate models for different emissions scenarios or assumptions about climate sensitivity (IPCC, 2001).

Outputs are divided according to the standard climatological seasons, defining winter as December-January-February, spring as March-April-May, summer as June-July-August and autumn as September-October-November. UKCIP02 scenarios are at a fine enough spatial resolution to be appropriate for hydrological impact studies by incorporation into a suitable hydrological model. The UKCIP02 scenarios are now widely used in the UK for climate change impact studies. However, studies up until 2006 used proportional changes in climate variables, with little direct use of RCM data in hydrological studies. Kay *et al.* (2006a) advanced research by using data derived directly from the Hadley Centre RCM as input to a distributed rainfall-runoff model.

Table 2.1 UKCIP02 emissions scenarios and their derivation from the SRES emissions scenarios (adapted from Hulme *et al.*, 2002)

UKCIP02	SRES	Derivation	Description
Low emissions	B1	HadRM3 ensemble simulation for A2 emissions scaled to the HadCM3 global temperature for B1 emissions	Clean and efficient technologies; reduction in material use; global solutions to economic, social and environmental sustainability; improved equity; population peaks mid-century
Medium-Low emissions	B2	HadRM3 ensemble simulation for A2 emissions scaled to the HadCM3 global temperature for B2 emissions	Local solutions to sustainability; continuously increasing population at a lower rate than in A2; less rapid technological change than in B1 and A1F1
Medium-High emissions	A2	HadRM3 ensemble simulation for A2 emissions	Self-reliance; preservation of local identities; continuously increasing population; economic growth on regional scales
High emissions	A1F1	HadRM3 ensemble simulation for A2 emissions scaled to the HadCM3 global temperature for A1FI emissions	Very rapid economic growth; population peaks mid-century; social, cultural and economic convergence among regions; market mechanisms dominate; reliance on fossil fuels

2.4 HYDROLOGICAL MODELLING

"Nowhere is flooding a simple linear response to precipitation. We understand how precipitation is translated into river flows through modelling the hydrological runoff of rainfall. Modelling also helps us to understand how changes in all aspects of precipitation – amount, intensity, duration, location and clustering – will affect the flooding system."

Evans *et al*., 2004, p231

There is a need for a great deal of research into how precipitation forecasts can be effectively presented to hydrologists and how they can be used in combination with hydrological models to provide indications of future flows and river levels (Collier *et al*.,

2002). Additionally, Tilford *et al*. (2003) identified a lack of knowledge in the coupling of meteorological and hydrological models, and suggest that the reliability of rainfall-runoff modelling needs improvement, particularly under extreme conditions. Collier *et al.* (2002) stated that "the most extreme hydrometeorological events that are likely to be experienced in the UK have received only limited study from the point of view of underlying consistency and predictability." Model structure for extreme fluvial events also needs to be addressed as does the uncertainty of climate change. A report prepared by DEFRA (2001a) into the October/November 2000 floods concludes that there is a need for the enhancement and development of rainfall and flood flow data resources, advancement in methods for flood risk analysis and linking hydrological and climate models to estimate catchment flood risk in a changed climate.

2.4.1 Rainfall-runoff

The quality of forecasts will, in general, depend on the quality of the simulation model, the accuracy of the precipitation and boundary forecasts, and the efficiency of the data assimilation procedure (Madsen *et al.*, 2000). An ideal model fully replicates processes and their spatial and temporal variability. However, complete replication of reality is impossible and so accuracy is limited accordingly (Ball and Luk, 1998). For the majority of flood risk studies one-dimensional modelling is usually considered appropriate (Environment Agency, 2006). Rainfall-runoff models are one-dimensional models which represent the conversion process of rainfall to river flows using observational data as the model driver. An array of model parameters represents catchment characteristics, with time-series data used as inputs. Hydrological research using rainfall-runoff models is extensive and many investigations into the processes of linking climate change and hydrology have been achieved. Sefton and Boorman (1997) investigated regional climate change impacts on UK streamflows using climate change scenarios to perturb historical climate data, a rainfall-runoff model and a GIS to extrapolate results to other catchments. Reynard *et al.* (2001) used a continuous flow simulation model to look at the impact of climate change scenarios on flood regimes in large UK catchments and Cameron *et al.* (2000) reviewed rainfall-runoff modelling under a changed climate in an upland catchment in Wales.

2.4.1.1 HEC-HMS

The HEC Hydrologic Modelling System (HEC-HMS; USACE, 2006) is a simple one-dimensional numerical hydrological model developed by the United States Army Corps of Engineers (see Chapter 3 for further details). Studies using HEC-HMS are exhaustive, particularly within the US. Elsewhere in the world, research using this modelling system, and in particular to investigate climate change, has received limited attention, but research that has been undertaken has been successfully applied. Some examples include Garcia *et al.* (2008) who looked at water resource modelling in northern Spain, Foody *et al.* (2004) who investigated flash flooding in the Eastern Desert, Egypt and Yener *et al.* (2007) who used HEC-HMS to model runoff scenarios in the Yuvacik basin, Turkey. In terms of climate change, McColl and Aggett (2007) used HEC-HMS to forecast future flows with different land use scenarios and Amengual *et al.* (2007) investigated future climate change and its hydrological implications in Catalonia, Spain, using HEC-HMS forced with MM5 mesoscale rainfall forecasts. This combination was also adopted by Anderson *et al.* (2002), but for Northern California. These latter two studies also made use of the HEC-HMS gridded precipitation modelling component and research in Spain is one of the very few places outside the US to utilise gridded precipitation data obtained from radar imagery with the HEC-HMS model.

2.4.2 Radar rainfall

Recent efforts in river forecasting have focused on quantifying rainfall amounts from radar images (Anderson *et al*., 2002). As the spatial and temporal resolution of distributed gridded data has increased it has become more desirable to incorporate gauge-corrected radar imagery into hydrological modelling to increase accuracy. By using rainfall data from both radar and gauge sources the accuracy of a modelling system can be determined. Peters and Easton (1996) speculated there to be substantial differences between simulations based on grid-distributed and spatially-averaged rainfall. Research by Charley (1988) showed that large amounts of rainfall were recorded by radar but missed by rain gauges due to the positioning of rainfall relative to the gauges. Cutis and Clyde (1999) found that even the larger scale trends in the rainfall surface can sometimes be mischaracterised by standard rainfall spatial interpolation techniques.

Weather radar exploits the interaction between electromagnetic waves propagating through the atmosphere and hydrometeors (raindrops, snowflakes and hail) to infer rainfall intensities from the power of back-scattered energy. Radar signals are also pulsed so that object distance can be inferred. Radar can observe moderate and high precipitation rates fairly accurately, yet shows serious weakness in identifying light rain and drizzle (Golding, 2000). During heavy rainfall (events in excess of 6 hours) radar generally provides a more accurate estimation compared to estimations from rain gauges, especially during widespread frontal events. Also, for short duration, intense rainfall events such as thunderstorms it is unlikely that even the most sophisticated techniques can provide great accuracy, and weather radar may provide more useful estimates (Tilford *et al.*, 2003). This is particularly true should there be an increase in convective-induced flood events.

Lewis and Harrison (2007) stated that "relatively little attention has been specifically given to radar data quality over upland areas, despite the uncertainties involved in radar measurement in such regions" and limited work has been completed with regard to calibration of distributed models (Muleta and Nicklow, 2005). Mountainous regions are one of the primary geographical areas where the challenge of extreme rainfall estimation is particularly acute, and rapid hydrological regimes benefit greatly from the use of weather radars (Andrieu et al., 1997; Krajewski and Smith, 2002; Hossain *et al.,* 2004). Recently, more studies have been undertaken to assess the advantages of radar data in such locations across the UK. Cranston and Black (2006) presented an assessment of radar data quality in central Scotland, with results indicating no consistent error bias and concluding that radar were of sufficient quality for hydrological modelling in steep Scottish upland catchments. In upland catchments across England and Wales Lewis and Harrison (2007) assessed radar data quality and found that radar measurements at closer ranges, generally within a 50 km radius, were found to have smaller errors in their estimates and this was found to be the most important factor affecting radar data quality. Some catchments showed a systematic underestimation of surface rainfall which is commonly observed in areas of higher topography (Kitchen and Blackall, 1992). Orographic corrections and subsequent scaling of adjustment factors shifted rainfall estimates closer to those recorded by the gauge network and making such corrections locally is likely to increase the predictive power of the rainfall-runoff modelling.

Recently, the use of gridded precipitation has started to have a role in predicting hydrological regimes under future climates. HEC-HMS developments have advanced to incorporate radar imagery into the modelling process. Nevertheless, research using radar data outside the conterminous United States is somewhat limited. From the few examples that exist, Amengual *et al.* (2007) modelled flash-flooding in Catalonia, Spain using radar forecasts and Hall and Catchley (2006) studied the coupling of a hydrological model with the MM5 mesoscale meteorological model to predict rainfall on a 1 km grid at 1 hour time resolution in Wales. Contrastingly, research using gridded precipitation data within the United States is plentiful. Anderson *et al*. (2002) used 48-hour rainfall forecasts through the use of a mesoscale model (MM5) and HEC-HMS to translate predicted precipitation into runoff forecasts. Ahrens and Maidment (1999) used HEC-HMS with NEXRAD (next generation radar data from the US National Weather Service) data to look at flood forecasting in the Buffalo Bayou basin, Texas. Hoblit and Curtis (2001) did the same for a basin near Heppner, Oregon. Research by Giannoni *et al.* (2003) used fine temporal and spatial resolution radar rainfall observations on a 5-minute temporal and 1 km² spatial scale for modelling hydrological processes in the Mississippi River basin. The combination of high-resolution radar rainfall estimates and distributed hydrologic modelling is of great potential benefit for flood forecasting (Giannoni *et al.*, 2003).

Progress in the use of weather radar as input to flood forecasting models has been slow to be established operationally within the UK (Moore *et al.,* 2004). In general, throughout the UK there is caution in the automated use of weather radar data as input to hydrological models for real-time flood forecasting. This is due to reasons concerning the lack of consistent data quality in time and space of the weather radar estimates of rainfall (Vehvilainen *et al.*, 2004). Moore *et al.* (2004) declare that it is uncertain how changes in radar data quality of recent years feed through to flood forecasting performance. Radar estimates generally increase forecasting accuracy in small catchments of less than 500 km². However, during extreme precipitation or critical flooding situations radar precipitation data is advantageous even in large catchments for shortening the response times (Vehvilainen *et al.*, 2004). Bell and Moore (1998a; 1998b) found a substantial increase in accuracy when using good quality radar data over rain gauges in small catchments. Extreme hydrological events are usually the most damaging and often unexpected. It is these periods which need to be forecast accurately, especially if future changes in extremes are to be adequately mitigated.

2.4.3 Future simulations

Caution should always be exercised when applying a model to conditions beyond the range for which it was calibrated (Sefron and Boorman, 1997). To simulate runoff realistically outside of the calibration period, a model must have an adequate description of hydrological rainfall-runoff processes. The suitability of a model when operated under extreme flows is a key factor to consider in model selection. For example, there can be a high risk of inaccurate results in using purely data-based methods such as correlations outside their range of calibration (Tilford *et al*., 2003). To investigate the possible future effects that climate change may have on river flows a hydrological model can be forced with the output from a climate model. Detailed precipitation inputs are required by hydrological models and therefore the fine spatial resolution of a RCM is suitable to capture the variability of rainfall (Gutowski *et al.*, 2003).

RCM outputs have been used to force hydrological models for numerous sites around the world. Arnell *et al.* (2003a) estimated changes in runoff in southern Africa using the HadRM3H regional climate model outputs and Hay *et al.* (2002) used RCM data as direct input to a hydrological model for a daily time-step in four US catchments. Using RCM data directly from UK climate change scenarios is a relatively recent phenomenon. Fowler and Kilsby (2007) claimed that their study in northwest England was the first to incorporate RCM data from HadRM3H directly in a hydrological impact study. Also, Leander and Buishand (2007) resampled RCM output to simulate extreme river flows for the Meuse basin in Western Europe. In the same year, Bell *et al.* (2007) developed a simple modelling framework which translated RCM estimates of rainfall into estimates of river flow. Precipitation inputs for their model were daily rainfall interpolated onto a 5 km grid from a network of rain gauges and a 25 km grid of hourly precipitation from a RCM. There is a desire to further Bell *et al.*'s research by determining how climate change scenarios will influence rainfall radar data at even finer spatial and temporal scales and how such events can be adequately hydrologically simulated.

2.5 HYDROCLIMATOLOGY IN THE 21ST CENTURY

By the 2020s the effects of climate change on average annual runoff are typically predicted to be greater than the effects of natural multi-decadal variability in approximately two-thirds of the world, and by the 2080s this will increase to between 70 and 90% (Arnell, 2003b). Global mean runoff is predicted to increase by 7.3% by 2050 (Wetherald and Manabe, 2002). Across Ireland, the impacts of climate change on fluvial sites was researched by Steele-Dunne *et al.* (2008) and findings show that expected changes in climate amplify the seasonal cycle in streamflow of all catchments studied. Increases in winter and reductions in summer streamflow and precipitation are expected for 2021-2060 simulations. Murphy and Charlton (2006) investigated changes across Ireland of catchment storage, streamflow and extreme events by using statistically downscaled GCM outputs to force a lumped, conceptual rainfall-runoff model for the 2020s, 2050s and 2080s. Their study found that the magnitude and frequency of flood events increases in the future, with the greatest increases associated with higher return period floods. Predicted hydrological changes in Ireland act as a relevant baseline for changes across the UK, given similar dominant weather systems which is thought to be the main factor driving changes in precipitation extremes.

Due to increases of CO_2 concentration in the atmosphere, the UK is likely to experience changes in its rainfall regime, as indicated by most climate simulations, over the coming century (Prudhomme *et al.,* 2003; Giorgi *et al.*, 2001). Heavy rainfall events are predicted to increase in frequency and intensity (McGuiffe *et al.*, 1999; Hulme and Jenkins, 1998) and the UK climate scenarios (Figures 2.1 to 2.5) suggest that by the 2080s winter precipitation will become more frequent and winter daily precipitation intensities that are experienced, on average, once every two years may become up to 20% heavier. Precipitation increases range from 5 to 15% for the Low Emissions scenario, to in excess of 30% for some areas under the Medium-High and High emissions scenarios (Hulme *et al*., 2002). Changes in winter precipitation predict increases of up to 33% along the western side of the UK (Jenkins *et al.*, 2009). Research by Fowler *et al.* (2005) and Ekstrom *et al.* (2005) also estimate magnitude increases of 10 to 30% in rainfall events up to a 50 year return period by the end of the century. Climate models predict that human influences will be the main cause for an increase in many types of extreme events, including extreme rainfall (Hegerl *et al.*, 2007).

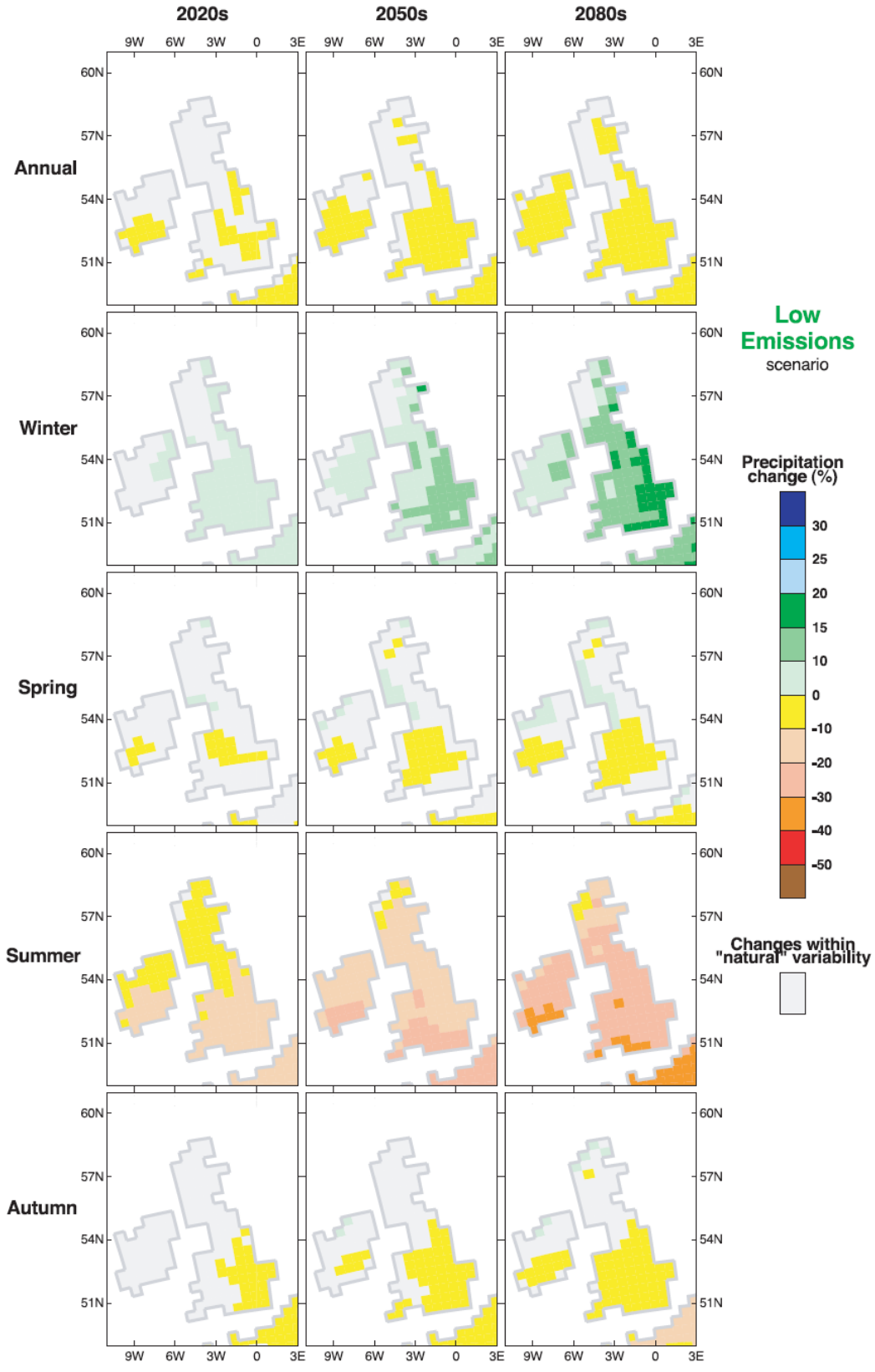

Figure 2.1 Change in average annual and seasonal precipitation (with respect to model-simulated 1961-1990 climate) for thirty-year periods centred on the 2020s, 2050s and 2080s for the **Low Emissions** scenario. Grey areas show changes within an estimate of "natural" variability, one standard deviation of model-simulated 30-year average climates. Note the asymmetric scale (Source: Hulme *et al*., 2002; p33)

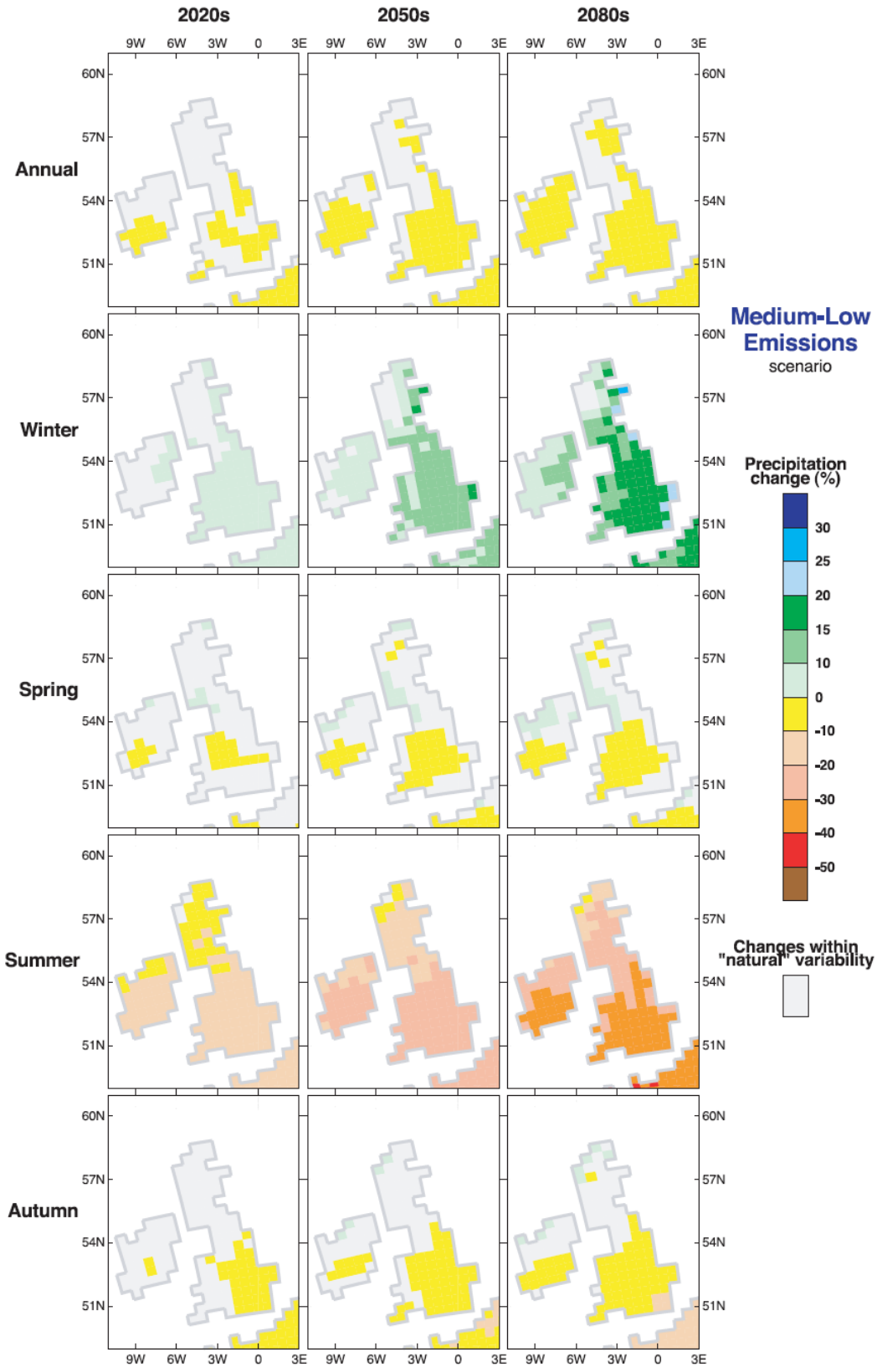

Figure 2.2 Change in average annual and seasonal precipitation (with respect to model-simulated 1961-1990 climate) for thirty-year periods centred on the 2020s, 2050s and 2080s for the **Medium-Low Emissions** scenario. Grey areas show changes within an estimate of "natural" variability, one standard deviation of model-simulated 30-year average climates. Note the asymmetric scale (Source: Hulme *et al.*, 200; p34)

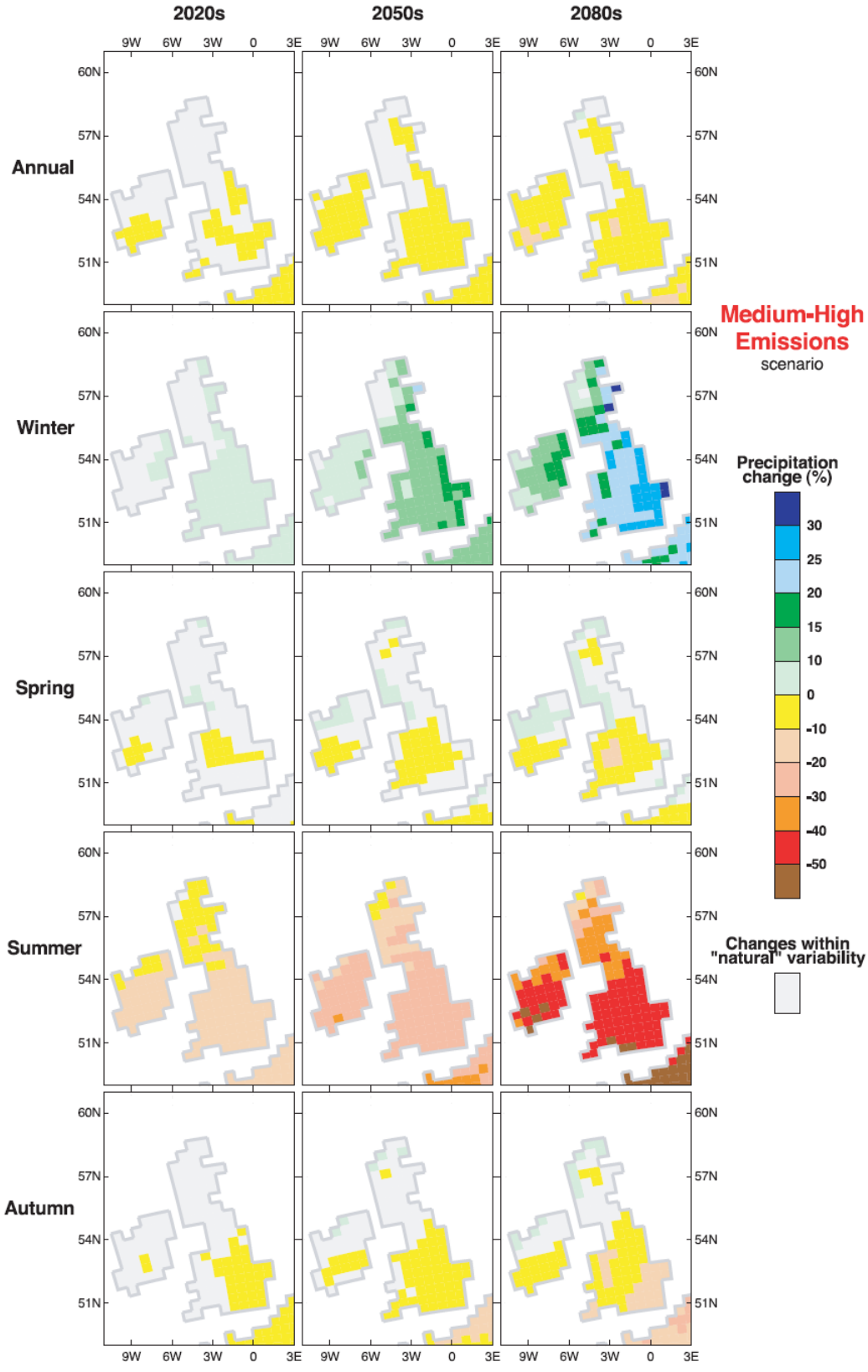

Figure 2.3 Change in average annual and seasonal precipitation (with respect to model-simulated 1961-1990 climate) for thirty-year periods centred on the 2020s, 2050s and 2080s for the **Medium-High Emissions** scenario. Grey areas show changes within an estimate of "natural" variability, one standard deviation of model-simulated 30-year average climates. Note the asymmetric scale (Source: Hulme *et al*., 2002; p35)

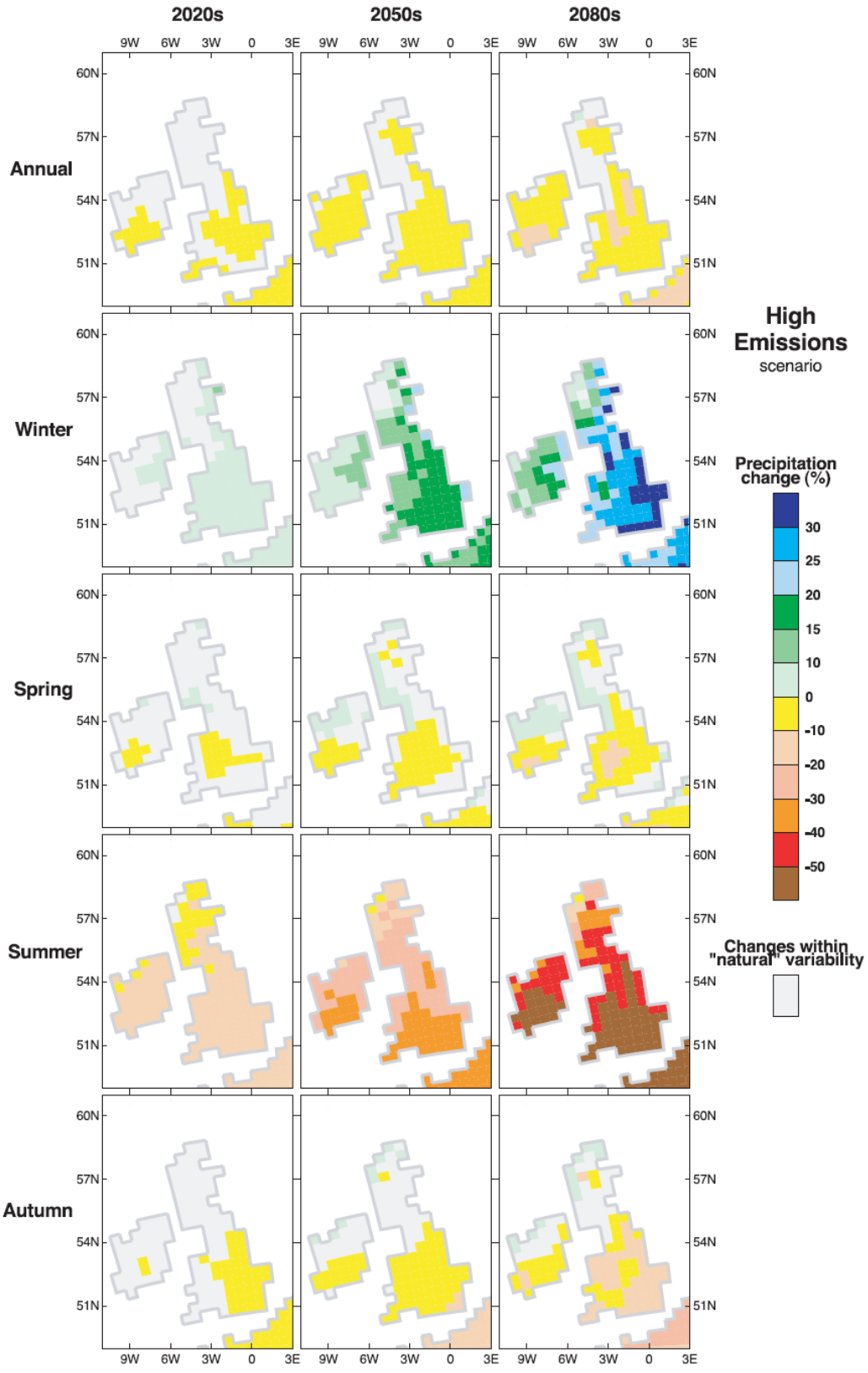

Figure 2.4 Change in average annual and seasonal precipitation (with respect to model-simulated 1961-1990 climate) for thirty-year periods centred on the 2020s, 2050s and 2080s for the **High Emissions** scenario. Grey areas show changes within an estimate of "natural" variability, one standard deviation of model-simulated 30-year average climates. Note the asymmetric scale (Source: Hulme *et al.*, 2002; p36)

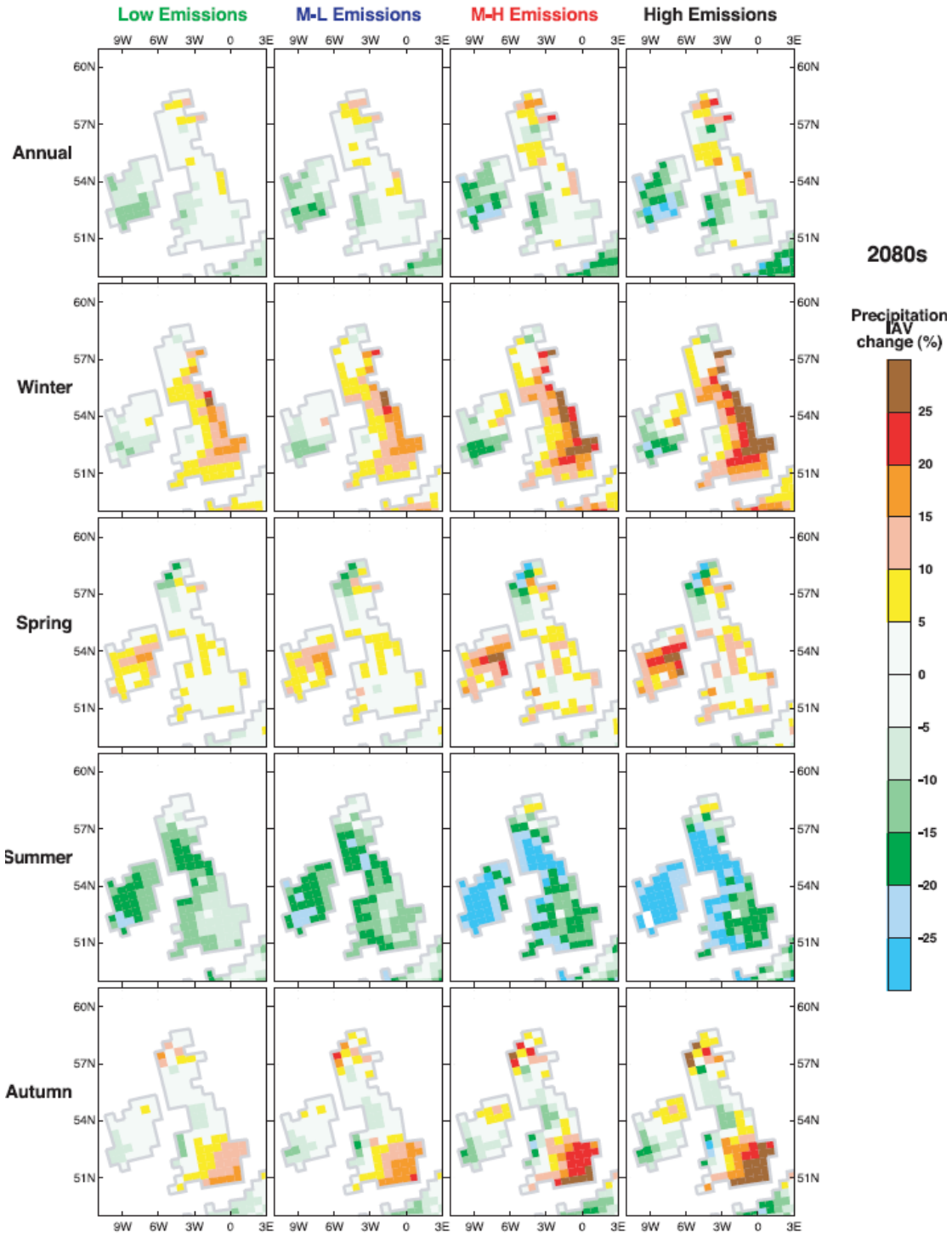

Figure 2.5 Relative changes in the inter-annual variability of annual and seasonal precipitation for the 2080s and for the four scenarios. Changes are the percentage change in standard deviation, with respect to 1961-1990. Data were de-trended before analysis (Source: Hulme *et al.,* 2002; p41)

Across Northern Europe extremes of precipitation are likely to increase in winter due to warming being greatest within the winter season (Christensen *et al.*, 2007; Douville *et al.*, 2002). Jones and Reid (2001), and later Huntingford *et al.* (2003), analysed changes in UK

extreme rainfall, both concluding that drastic increases in the heaviest rainfall would be apparent by the end of the 21st century. Large projected increases in the magnitude of longer duration extreme rainfall events in parts of England are relevant to note, as it was this type of rainfall which resulted in the widespread UK flooding in autumn 2000 (Ekström *et al.*, 2005). Average spring and autumn rainfall is predicted to change less drastically than winter, but also less consistently across the UK (Kay *et al.*, 2006b).

Not all researchers envisage an increase in precipitation for the UK. Kay *et al.* (2006b) indicated that rainfall across the UK will generally decrease and, therefore, concluded that a change in the temporal distribution of rainfall must be resulting in the increased flooding. Kay *et al.* (2006b) also predicted a reduction in flood frequency at certain UK sites due to changes earlier in the year. Decreased rainfall and higher temperatures in the summer and autumn will lead to higher soil moisture deficits (SMD) which are likely to delay the onset of the flood season until the increased winter rainfall has reduced SMDs to zero. The Environment Agency (2003) speculate that if rainfall increases by a rise in the number of rain days then flood frequency may still reduce due to an increase in potential evaporation. Fowler and Kilsby (2007) postulate that by 2070-2100 potential evaporation may increase by +10 to +20% in all months, with July to September showing slightly larger increases than other months.

2.6 SUMMARY

To summarise, global temperatures are rising and as a result the hydrological cycle is undergoing intensification. The UK is following global temperature trends with records indicating an increase in mean annual temperatures. Over northern hemisphere land masses, including the UK, precipitation regimes have changed, signifying a general increase in the intensity, frequency and persistence of rainfall. Repercussions of a changing climate have resulted in an increase in the number of extreme events. Evidence provided supports an increase in rainfall and flow extremes across the UK with increases forecast to continue into the future. Climate modelling provides a key tool for predicting future changes to the UK climate and hydrological modelling provides an essential method for accurately monitoring climate-induced changes of catchment hydrology.

2.7 RESEARCH OBJECTIVES

Given the vast array of literature explored looking at past, present and future changes in hydrological extremes and modelling, a series of objectives providing the basis for analytical investigations within four analysis chapters are now outlined. These build on the main research aim stated in Chapter 1, by firmly grounding research ideas in the literature.

1. Trends in extremes and climate variability

Extreme events will always lead to the possibility of severe flooding and an improved understanding is continually sought after. Haylock and Nicholls (2000) affirm that more detailed studies of climate extreme trends on high quality and consistent data are needed if we are to be able to determine whether climate extremes are varying. Many previous climate change studies have focused on changes in mean values of climate variables rather than extremes (Hundecha and Bárdossy, 2005). It is changes in the frequency and intensity of extremes rather than changes in the climate average that will impact most upon society (Huntingford *et al.*, 2003). Hegerl *el al.* (2004) and Groisman *et al.* (2005) state that changes in extreme rainfall may be more robustly detectable than changes in means and totals. Evidence reviewed suggests a noticeable change in the frequency and intensity of extreme events. Therefore, rather than focusing research into changes in climatic means, focus is directed to investigating changes in the extremes of hydrological distributions. Understanding more about the distribution of extreme rainfall is necessary if rainfall duration as well as intensity is to be predicted under future projected climates (Sefton and Boorman, 1997).

Limited research has been undertaken into both precipitation and flow extremes within small-scale river basins. Precipitation change is very location-dependent and at present there is low confidence in changes in frequency, intensity, and persistence (Miller, 2003). The main objectives defined are:

- Has the intensity, frequency and persistence of extreme precipitation and flow events increased over the last 30 years within a small-scale river basin?
- Do these changes correspond to the reviewed national time-series analyses?

- Can such changes be explained by climate variability and/or changes in catchment characteristics?

2. Hydrological modelling

This analysis chapter deals with the development of the hydrological model for a small-scale UK catchment. Data were collated and the necessary processing steps were performed. This step was an essential prerequisite for the subsequent analyses chapters. One main objective is defined:

- Can HEC-HMS model accurately an extreme hydrological event within a selected UK catchment using gauge precipitation data as the model driver?

3. Comparison, correction and performance of precipitation data

HEC-HMS is engineered specifically for hydrological modelling in the US and the model is tailored to use US formatted data, predominantly NEXRAD radar data. The UK equivalent to NEXRAD is the Met Office's Nimrod radar imagery. Modelling a UK river system with an American model using UK input data poses problems relating to data projections and file formats. Although previous hydrological studies in the UK have adopted the HEC modelling suite, no previous research has investigated the use of Nimrod images with HEC-HMS. However, the model is well tested and extending research to river systems outside the US is a plausible option given the ease of access to both the model and the input data. Giannoni *et al.* (2003) state the need to increase the accuracy of radar rainfall estimates for extremes and also increase the quantitative characterisation of the error structure. The main objectives defined are:

- What are the discrepancies between gauge and radar rainfall data for an observed extreme hydrological event?
- Can this error be attributed to particular sources?
- How well does the radar data perform in predicting flow extremes using HEC-HMS and is there any increase in accuracy over using the gauge network?

- Can bias correction of radar data on a local scale using a gauge-adjustment technique increase hydrological prediction accuracy?
- What is the overall performance capability of HEC-HMS?

4. Climate projections and future hydrological extremes

An important task is to identify the most likely causes of rapid climate change and the regions in which they are most likely to impact. Where there is a potential for severe impacts, a lack of predictability should not delay adaptation assessments. For instance, rapid regional climate change can alter rainfall patterns, making historical records obsolete for design purposes (Jones, 2000). An indication of changing extremes is provided in this chapter and coupled with the analysis undertaken in Chapter 5, a clear basis for future hydrological extremes within a small-scale UK catchment is defined. Using the UKCIP02 climate scenarios for the UK, local changes are investigated to determine the scale of future extremities. The main objectives defined are:

- How is the local climate predicted to change under the UKCIP02 scenarios?
- What is the predicted change to hydrological extreme events given projected changes in precipitation and temperature?
- What are the wider implications should extremes become *more* extreme?
- What other environmental factors need to be considered?

Chapter 9 provides an overall discussion regarding the interlinking findings of all the analyses conducted. The main focal point of the discussion raises issues surrounding error propagation and the uncertainty associated with all stages of the analysis.

CHAPTER 3

Methods

This chapter describes all the methods used in the four subsequent analysis chapters which investigate (i) time-series trend analyses, (ii) hydrological model creation and simulation of extreme flows, (iii) model input data (precipitation) comparison, correction and performance evaluation, and (iv) climate change scenarios and future extreme flows. Theses methods are shown in Figure 3.1, which illustrate how the processes for analysing extremes in a small hydrological basin fit together.

3.1 TREND ANALYSIS

Trends in time-series data can be identified using either parametric or non-parametric tests. Parametric tests depend on fitting a model to the empirical distribution of a given variable, so that when the distribution is unknown, or is likely to be fitted best by a non-Gaussian model, non-parametric statistical methods can be useful and in many cases advisable (Sneyers, 1992; Rodrigo *et al.*, 1999). Hydrological extremes are not usually fitted well by a Gaussian model (DEFRA, 2001b) and often contain a number of outliers; therefore, it is sensible to use robust non-parametric methods that do not assume normality. As the median and distribution tail-ends play a vital role in analysing time-series data, the use of non-parametric methods is largely justified for trend analysis (Sneyers, 1990). Before a trend detection test can be performed the data in question need to be tested to assess population characteristics to ensure the correct methods are instigated.

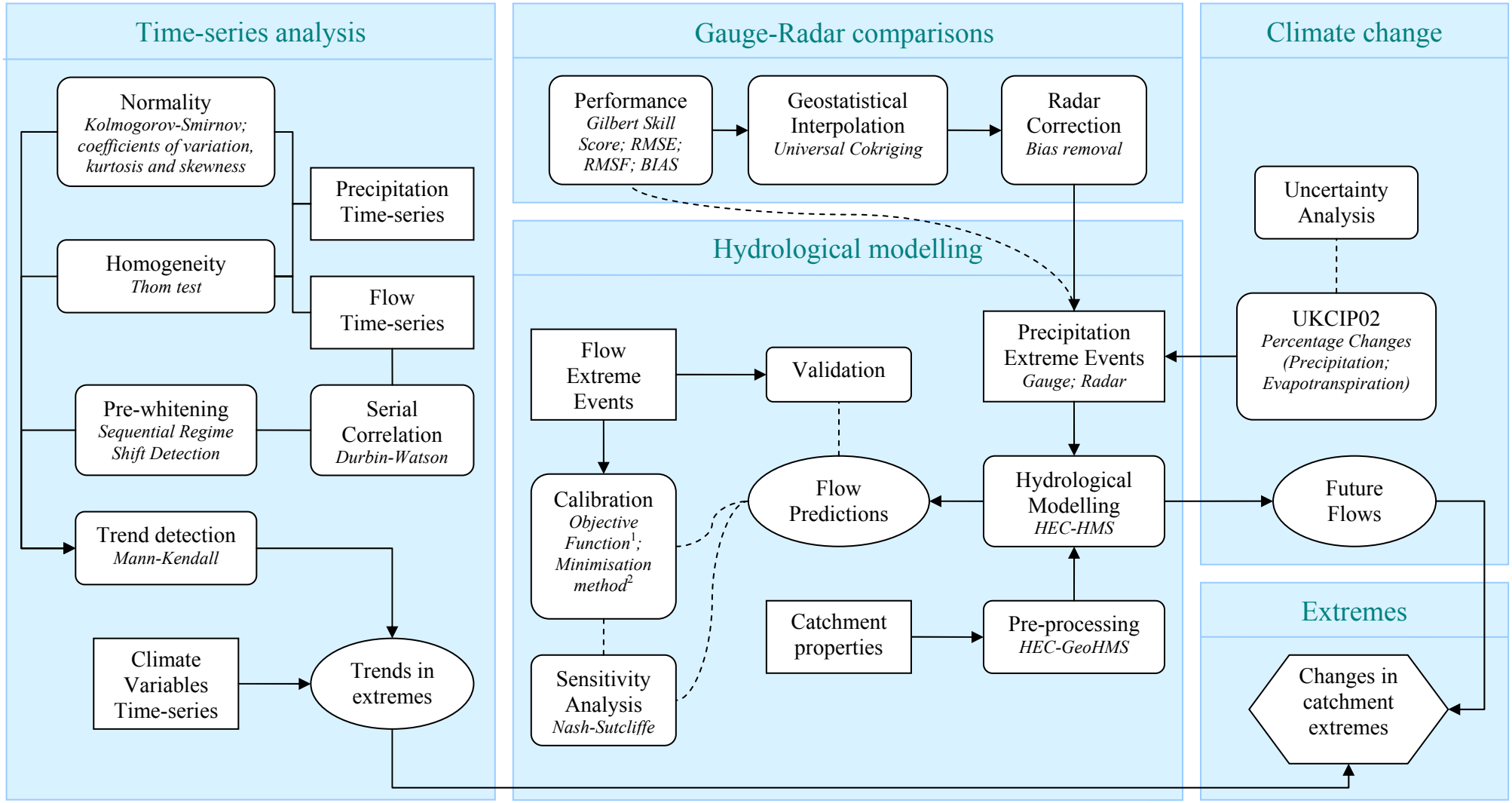

Figure 3.1 Overview of research methods indicating data inputs (square), methods for analysis (rounded-square) and outputs (oval). Overall output is an overview of catchment changes in extremes (hexagonal).

[1]Sum of the squared residuals; peak-weighted RMS
[2]Univariate-gradient; Nelder and Mead

3.1.1 Testing for homogeneity

A numerical climatic series is said to be homogeneous when the observed variation is purely resultant from fluctuations in weather and climate (Lázaro *et al.*, 2001). Testing for homogeneity in a given variable can identify possible error sources affecting data accuracy, for example, that which would result from changes to the gauging station and its environment. The non-parametric Thom test was implemented to check the homogeneity of time-series records (Thom, 1966). This test explores the variation of a series with respect to a central value, usually the median. The number of uninterrupted runs, R, of values larger and smaller than the median is counted. Under the null hypothesis this statistic has an approximately normal distribution with mean $E(R) = (N+2)/2$ and variance $Var(R) = [N(N-2)]/[4(N-1)]$ where N is the number of observations in the time-series. The statistic is defined as

$$Z = \frac{R - E(R)}{\sqrt{Var(R)}} \tag{3.1}$$

and if $|Z| \leq 2.58$ then the null hypothesis of homogeneity is accepted at the $\alpha < 0.01$ confidence level.

3.1.2 Testing for normality

Testing to see if a Gaussian model provides a good fit to the distribution of a time-series can be achieved using various methods. The Kolmogorov-Smirnov normality test compares the observed cumulative distribution function of the sample data with an expected normal distribution. Should the difference be sufficiently large, the null hypothesis of normality is rejected at an appropriate confidence level and the alternative hypothesis of a non-Gaussian distribution is accepted. Other test statistics which are useful in describing data distributions are the coefficients of variation, kurtosis and skewness. The coefficient of variation determines the ratio of the standard deviation of the data to the mean. The kurtosis coefficient measures how peaked a distribution is and the skewness coefficient measures the asymmetry of a distribution. A Gaussian distribution has kurtosis and skewness coefficient values of zero.

3.1.3 Testing for serial correlation

Hydrological time-series data are often lacking serial independence. Streamflow is regulated by storage in the river basin, with carry-over of flow from one time interval to the next, resulting in correlation between values. Positive serial correlation inflates the variance of the estimated time-series mean and, therefore, the time-series contains less information about the mean than a random series (Matalas and Langbein, 1962). Given positive autocorrelation amongst observations the chance of a trend statistic being significant is overestimated, even when no trend is present. Normally precipitation data do not need to be checked for persistence (Dahmen and Hall, 1990).

The serial correlation coefficient aids the validation of time-series independence. Detecting signs of serial correlation can be achieved by determining the presence of autocorrelation in the residuals and whether or not the correlation between two adjacent error terms is zero. Based on the assumption that errors are generated by a first-order autoregressive process, the Durbin-Watson test statistic is calculated as

$$d = \frac{\sum_{t=2}^{n} (e_t - e_{t-1})^2}{\sum_{t=q}^{n} e_t^{\,2}} \tag{3.2}$$

where e_i is the i^{th} residual, $e_{i\text{-}1}$ is the residual of the previous observation and n is the number of observations. The critical values for the lower d_L and upper d_U bounds of the Durbin-Watson test statistic are extracted from a table (e.g. Savin and White, 1977) at the chosen confidence level of α. If $d > d_U$ no correlation exists, if $d < d_L$ positive correlation exists and if d is between the two bounds the test is inconclusive. Any missing observations are omitted from the calculations.

If serial correlation is found to be present in a time-series then the process of prewhitening data may be performed. Most climate series contain red noise and are serially correlated due to the nature of variability (Zhang *et al.*, 2000). Prewhitening a time-series removes a serial correlation component such as an autoregressive (AR) process (red noise) prior to applying the trend detection test. In this research, prewhitening was conducted using the ordinary least squares estimate of AR1 (see Rodionov, 2006a) and was performed using the "sequential regime shift detection" software (Rodionov, 2006b).

3.1.4 Testing for trends

The Mann-Kendall test (Mann, 1945; Kendall, 1975) is a rank-based non-parametric test, particularly suitable for censored, missing and non-Gaussian distributed variables, which searches for a trend in a time-series without stipulating whether the trend is linear or non-linear (Maidment, 1993). Data are assumed to consist of a uniformly sampled time-series and the test indicates the direction and significance of any trend. Much research has been undertaken using the Mann-Kendall test to detect trends in climatological and hydrological time-series (e.g. Rao, 1993; Kothyari and Singh, 1996; Brunetti et al., 2000; Yue and Hashino, 2003, Abdul and Burn, 2006; Jiang et al., 2007; Modarres and Silva, 2007), and this particular non-parametric test has been shown to be more powerful than some parametric tests when dealing with skewed data (Önöz and Bayazit, 2002).

The time-series is defined as $x_1, x_2, \ldots, x_n$ where the values of x are treated as a random sample of n independent, identically distributed variables and F_i is the continuous cumulative distribution function of x_i, i=1, 2, ..., n. The Mann-Kendall test statistic, S, is defined as

$$S = \sum_{k=1}^{n-1} \sum_{j=k+1}^{n} Sgn(x_j - x_k) \tag{3.3}$$

where x_j and x_k are sequential data values for the dataset record length n. The test statistic represents the number of positive differences minus the number of negative differences for all the differences between adjacent points in the time-series considered, and equates to the sum of the *Sgn* series, which is defined as

$$Sgn(x_j - x_k) = \begin{cases} 1 & if \quad x_j > x_k \\ 0 & if \quad x_j = x_k \\ -1 & if \quad x_j < x_k \end{cases} \tag{3.4}$$

Kendall (1975) gives the mean and variance of S, $E(S)$ and $V(S)$ respectively, under the null hypothesis, H_0, of randomness, given the possibility that there may be ties in the x values, as

$$E(S) = 0 \tag{3.5}$$

$$V(S) = \frac{1}{18}\left\{ n(n-1)(2n+5) - \sum_{i=1}^{n} t_i\left[(t_i - 1)(2t_i + 5)\right]\right\} \tag{3.6}$$

where t is the extent of any given tie. Σt_i denotes the summation over all ties and is only used if the data series contain tied values. The standard normal variate Z is calculated by

$$Z = \begin{cases} \dfrac{S-1}{\sqrt{V(S)}} & if \quad S > 0 \\ 0 & if \quad S = 0 \\ \dfrac{S+1}{\sqrt{V(S)}} & if \quad S < 0 \end{cases} \tag{3.7}$$

The null hypothesis of randomness H_0 states that the data ($x_1, x_2, \ldots, x_n$) are a sample of n independent and identically distributed random variables. Mann (1945) showed that under H_0, the distribution of S is symmetrical and is normal in the limit as n approaches infinity. The alternative hypothesis H_1 of a two-sided test is that the distributions of x_j and x_k, are not identical for all $k, j < n$ with $k \neq j$. Thus, in a two-sided test for the trend, H_1 should be accepted if $|Z| > Z_{\alpha/2}$, where $F_n(Z_{\alpha/2}) = \alpha/2$, F_n being the standard normal cumulative distribution function and α being the significance level for the test. Positive values of Z indicate an upward trend and negative values indicate a downward trend.

3.2 HYDROLOGICAL MODELLING

The HEC-HMS hydrological model was used for simulating catchment hydrological processes, and was described briefly in Chapter 2. HEC-HMS represents a catchment by linking up individual subbasins and separating the hydrological cycle into manageable sections. Mass and energy fluxes entering the system are represented by a series of deterministic mathematical models. The HEC-HMS technical reference manual (Scharffenberg and Fleming, 2006) details mathematically how the various models within HEC-HMS work and is the basis for the following descriptions and equations of each of the three main components that constitute the system. Each of the individual modelling methods was selected according to dataset availability and methods which graphically fitted the observed flow data the most accurately.

Table 3.1 Description of mathematical models used in this research (Ford and Hamilton, 1996)

Model	Description
Event	Simulates single events (a few hours to a few days)
Continuous	Longer simulation; both during and between events
Lumped	Spatial variations unaccounted
Empirical	Based on observations; no process of conversion
Conceptual	Based on pertinent natural processes
Measured parameter	Determined from system properties based on measurements
Fitted parameter	Immeasurable parameters; found by fitting model with observed values
Deterministic	Inputs, parameters and processes are certain; free of random variation

3.2.1 Basin model

The basin model provides a physical representation of the catchment. A dendritic network connects hydrologic elements for simulating surface runoff, infiltration losses, baseflow contributions, open-channel flow and water storage areas. Table 2.1 provides a summary and categorisation of the models used in this research. HEC-HMS primarily hosts event and lumped models, with all models being deterministic. Ford and Hamilton (1996) provide a description of the categorisation of these mathematical models, which is summarised in table 3.1. The basin model groups parameters into four main categories of loss, baseflow, transform and routing, as detailed below.

3.2.1.1 Loss

Losses were calculated following the deficit and constant method; a quasi-continuous variation on the initial and constant loss method, yet initial loss recovers after a prolonged period of no rainfall. Parameters include the initial deficit, D_i, which indicates the amount of water required to saturate the maximum storage; the maximum storage, S_{Max}, specifying the amount of water the soil layer can hold (as a depth); the constant (infiltration) rate, Q_R, when the soil layer is saturated; and the percentage of the subbasin which is directly connected impervious area, I. The moisture deficit is tracked continuously and calculated as the initial abstraction volume less the precipitation volume, plus the recovery volume during precipitation-free periods.

Throughout an event, the maximum potential rate of precipitation loss, f_c, is constant. Therefore, if p_t is the mean-areal precipitation (MAP) depth during a time interval t to $t+\Delta t$, the excess, pe_t, during the interval is defined by:

$$pe_t = \begin{cases} p_t - f_c & if \;\; p_t > f_c \\ 0 & otherwise \end{cases} \qquad (3.8)$$

The initial loss, I_a, represents interception and depression storage (depressions in catchment topography) which occur prior to the onset of runoff. Runoff only occurs once the accumulated precipitation on the previous area exceeds the initial loss volume. Excess is given by:

$$pe_t = \begin{cases} 0 & if \;\; \sum p_i < I_a \\ p_t - f_c & if \;\; \sum p_i > I_a \;\; and \;\; p_t > f_c \\ 0 & if \;\; \sum p_i > I_a \;\; and \;\; p_t < f \end{cases} \qquad (3.9)$$

D_i, S_{Max} and Q_R parameters were extracted from an existing parameter dataset (MCRM, 2005). I was calculated using the impervious surface analysis tool (ISAT) extension for ArcGIS (NOAA, 2007) by using land cover and population density coefficients.

3.2.1.2 Baseflow

Baseflow from groundwater and soil contributions, which is normally present even in the absence of rainfall, was modelled using the recession process, determined from the recession constant (rate at which baseflow recedes) and threshold ratio (resetting the baseflow). The relationship is defined by Q_t, the baseflow at any time t, to an initial value as

$$Q_t = Q_0 \, k^t \qquad (3.10)$$

where Q_0 is the initial baseflow at time zero and k is an exponential decay constant. The starting baseflow value, Q_0 (flow rate in m^3s^{-1}), is an initial condition of the model and k is defined as the ratio of the baseflow at time t to the baseflow one day earlier. The recession baseflow model is applied at the start of simulation of a storm event and later in the event as delayed subsurface flows reach the catchment channels. After direct runoff has peaked, the user-specified ratio-to-peak threshold defined the time at which the recession model of equation 3.10 describes the total flow. Subsequent total flows are computed using equation 3.10 with Q_0 as the specified threshold value. At the threshold flow, baseflow is defined by the initial baseflow recession. Thereafter, baseflow was computed indirectly, defined as the recession flow less the direct surface-runoff. When direct surface runoff reached zero (all

rainfall has run off the catchment), the total flow and baseflow were identical. Unless the direct runoff plus initial baseflow recession contribution exceeded the threshold, the streamflow hydrograph ordinates were defined by the recession model alone after the threshold flow occurred (Figure 3.2).

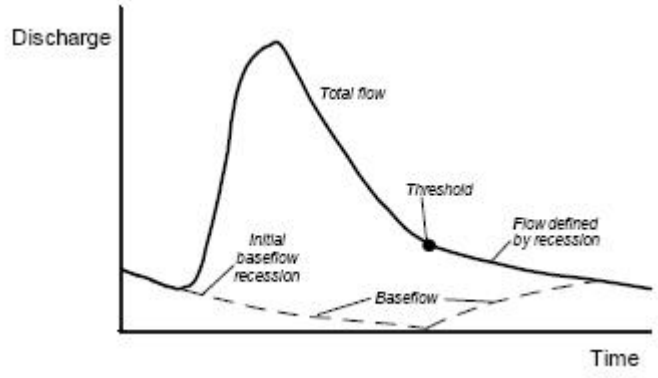

Figure 3.2 Hydrograph showing baseflow component of runoff (after Scharffenberg and Fleming, 2006)

Baseflow parameters included the initial flow, the recession ratio and the threshold flow. The initial flow was an initial condition which was extracted from time-series data. The recession constant k depends on the baseflow source. If $k = 1$, baseflow contributions are constant, with $Q_t = Q_0$. Otherwise, to model the exponential decay typical of natural catchments k must be less than 1.

3.2.1.3 Transform

The Clark unit hydrograph and Modclark transform methods depict hydrograph characteristics. The Clark unit hydrograph is an instantaneous synthetic unit hydrograph which has no duration and is used in conjunction with point precipitation. Runoff is the result of one inch of uniformly generated excess precipitation which is then translated and routed through a reservoir to account for the storage effects of the basin. This excess precipitation is applied uniformly over a catchment which is broken into time-area increments. The two critical processes of translation (movement of excess water) and attenuation (reduction of discharge magnitude as excess water is stored) are represented in the catchment unit hydrograph, transforming excess precipitation to runoff. Two parameters represent these hydrograph processes: firstly, time of concentration T_c which defines the time it takes a wave of water to propagate from the most distant point of the

catchment to the outlet, and secondly, the storage coefficient R, an index of the temporary storage of precipitation excess in the catchment as it drains to the outlet point.

Short-term storage (soil, surface and channel) effects in the catchment are represented using the linear reservoir model, which represents the transformation of precipitation excess to runoff. The model begins with the continuity equation

$$\frac{dS}{dt} = I_t - O_t \tag{3.11}$$

where dS/dt is the rate of change of water in storage at time t, I_t is the average inflow to storage at time t, and O_t is the outflow from storage at time t. Using this linear reservoir model storage S_t at time t is related to outflow as

$$S_t = RO_t \tag{3.12}$$

where R is a constant linear reservoir parameter. Combining and solving the equations using a simple finite difference approximation gives

$$O_t = C_A I_t + C_B O_{t-1} \tag{3.13}$$

where C_A, C_B are routing coefficients calculated from

$$C_A = \frac{\Delta t}{R + 0.5\Delta t} \tag{3.14}$$

$$C_B = 1 - C_A \tag{3.15}$$

The average outflow during period t is

$$\overline{O_t} = \frac{O_{t-1} + O_t}{2} \tag{3.16}$$

The aggregated impacts of all catchment storage are represented using Clark's model and conceptually the reservoir may be considered to be located at the catchment outlet. Clark's model also uses a linear channel model to route water from remote parts to the linear reservoir at the outlet with delay (translation), but with no attenuation. This delay is represented using the linear routing model properties, defined implicitly by a time-area histogram, computed as:

$$\frac{At}{A} = \begin{cases} 1.414\left(\frac{t}{T_c}\right)^{1.5} & for\ t \le \frac{T_c}{2} \\ 1 - 1.414\left(1 - \left(\frac{t}{T_c}\right)\right)^{1.5} & for\ t \ge \frac{T_c}{2} \end{cases} \tag{3.17}$$

where A_t is the cumulative catchment area contributing at time t, A is the total catchment area, and T_c is the time of concentration of catchment. This specifies the catchment area contributing to flow at the outlet as a function of time. To get inflow, I_t, to the inflow linear reservoir, the area is multiplied by unit depth and divided by Δt. Application of this implementation requires only the time of concentration T_c parameter which was approximated using the Soil Conservation Service (SCS) method (Kent, 1973) as

$$T_c = \frac{Lag}{0.6} \tag{3.18}$$

where *Lag* is the time between the centre of mass of the excess rainfall and the peak of its incremental outflow hydrograph. For catchments where runoff is nearly uniform it is sufficient to relate lag to time of concentration in this way and the lag is calculated from physical properties of the catchment.

$$Lag = \frac{L^{0.8}(S+1)^{0.7}}{1900Y^{0.5}} \tag{3.19}$$

where L is the length of the main channel to the farthest divide in feet, Y is the slope of the catchment in percent and S is a retardance factor approximated from the curve number CN representing the hydrologic soil-land cover interactions within the catchment. S equates to

$$S = \frac{1000}{CN} - 10 \tag{3.20}$$

where CN is the hydrologic curve number for the subbasin. SCS curve numbers were computed within a GIS framework, assigning hydrologic soil groups that depict infiltration rates to different land use types, creating a matrix of CN numbers. Area-weighting techniques were used to determine average CN values.

The basin storage coefficient R is the second parameter required to translate precipitation into runoff and is computed as the flow at the inflection point on the falling limb of the

hydrograph divided by the time derivative of flow (Clark, 1945). The relationship between R and T_c is generally constant over a given region such that the constant k is estimated as

$$k = \frac{S_c}{S_c + T_c} \tag{3.21}$$

Both the Clark time of concentration and storage coefficient parameters were calculated as initial approximations.

The modified Clark unit hydrograph, ModClark**,** is a quasi-distributed transform method based on the Clark conceptual unit hydrograph. The catchment is represented as a collection of grid cells each with a time-travel index (eliminating the time-area curve), each of which is scaled by the overall time of concentration. Translation time from the grid cell to the outlet (T_{cell}) is computed as

$$T_{cell} = T_c \frac{d_{cell}}{d_{\max}} \tag{3.22}$$

where d_{cell} is the travel distance from the cell to the outlet and d_{max} is the travel distance for the cell that is most distant from the outlet. Cell area is specified and the volume of inflow to the linear reservoir for each time interval is computed as the area multiplied by the precipitation excess. Storage is accounted for using the same linear reservoir model incorporated in the Clark model.

3.2.1.4 Routing

Channel routing was defined from the Muskingum-Cunge routing method, which is a finite-difference scheme based on the continuity equation and storage-discharge relation of the Muskingum method. The Muskingum method includes non-physically based parameters which are difficult to estimate and is based on a series of assumptions that are often violated in natural channels; the Muskingum-Cunge method overcomes these limitations. A combination of the continuity and diffusion equations using a linear approximation yields the convection diffusion equation (Miller and Cunge, 1975)

$$\frac{\partial Q}{\partial t} + c\frac{\partial Q}{\partial x} = \mu\frac{\partial^2 Q}{\partial x^2} + cq_L \tag{3.23}$$

where c is the wave celerity (speed)

$$c = \frac{dQ}{dA} \tag{3.24}$$

and μ is the hydraulic diffusivity

$$\mu = \frac{Q}{2BS_o} \tag{3.25}$$

where B is the top width of the water surface. A finite difference approximation of partial derivatives is combined with the Muskingum storage and continuity equations to give

$$O_t = C_1 I_{t-1} + C_2 I_t + C_3 O_{t-1} + C_4 (q_L \Delta x) \tag{3.26}$$

where the coefficients are

$$C_1 = \frac{\frac{\Delta t}{K} + 2X}{\frac{\Delta t}{K} + 2(1 - X)} \tag{3.27}$$

$$C_2 = \frac{\frac{\Delta t}{k} - 2X}{\frac{\Delta t}{K} + 2(1 - X)} \tag{3.28}$$

$$C_3 = \frac{2(1 - X) - \frac{\Delta t}{K}}{\frac{\Delta t}{K} + 2(1 - X)} \tag{3.29}$$

$$C_4 = \frac{2\left(\frac{\Delta t}{K}\right)}{\frac{\Delta t}{K} + 2(1 - X)} \tag{3.30}$$

and the parameters K and X are (Cunge, 1969; Ponce, 1978)

$$K = \frac{\Delta x}{c} \tag{3.31}$$

$$X = \frac{1}{2}\left(1 - \frac{Q}{BS_o c\Delta x}\right) \tag{3.32}$$

A representative cross-section is used to describe the routing reach, using 8 pairs of *x, y* (distance, elevation) values (points 1,2 left overbank, 3 left bank, 4,5 channel, 6 right bank, 7,8 right overbank) extracted from cross-section data. Reach length and slope were estimated using topographic data in a GIS. Both channel and floodplain Manning's *n* friction coefficients were calculated following Cowan's (1956) method for estimating roughness using the equation

$$n = \left(n_b + n_1 + n_2 + n_3 + n_4\right)m \tag{3.33}$$

where n_b is the basic roughness coefficient depicting the characteristics of a straight, uniform, smooth channel in natural materials. This basic *n* value is subject to modification factors allowing adjustment for surface irregularities n_1, channel cross-section changes n_2, obstructions n_3, vegetation n_4 and channel meandering *m*. For floodplain frictional coefficients n_2 is assumed to equal zero and *m* to equal one. Look-up tables (Cowan, 1956) were used to estimate these coefficients.

At confluences HEC-HMS makes the basic assumption that no water is stored; the downstream flow at time *t* is equal to the sum of the upstream flows:

$$O_t = \sum_r I_t^r \tag{3.34}$$

where I_t^r is the flow in channel *r* at time *t*; O_t is the outflow from the confluence period *t*.

3.2.2 Meteorological model

Precipitation, evapotranspiration and snowmelt comprise the meteorological model. Precipitation inputs were entered as point sources (rainfall gauges), which use a weighting method to estimate spatial distributions, or as gridded data (radar imagery) which uses a distributed grid approach. For the point observations each rain gauge was assigned a time and depth weight for areal weighting. The mean areal precipitation (MAP) depth was inferred from the depths at gauges using an averaging scheme, calculated as

$$P_{MAP} = \frac{\sum_i \left(w_i \sum_t p_i(t) \right)}{\sum_i w_i} \tag{3.35}$$

where P_{MAP} is the total storm MAP depth over the subbasin, $p_i(t)$ is the precipitation depth measured at time t at gauge i, and w_i is a weighting factor assigned to gauge i. If gauge i is not a recording device, only the quantity $\Sigma p_i(t)$, the total storm precipitation at gauge i, will be available and used in the computation. Thiessen polygons provided the areal-based weighting scheme used to create the depth weights for each subbasin. Precipitation depth at any point within a catchment is the same as the precipitation depth at the nearest gauge in or near the catchment. Thus, a weight was assigned to each gauge in proportion to the area of the catchment that was closest to that gauge.

Time weights were calculated following the inverse-distance-squared method which computes $P(t)$, the watershed precipitation at time t, by dynamically applying a weighting scheme to precipitation measured at catchment precipitation gauges at time t. The scheme relies on the concept of nodes that are positioned within a catchment such that they provide adequate spatial resolution of precipitation in the basin. HEC-HMS computes the precipitation hyetograph for each node using gauges near to that node. To select these gauges, hypothetical north-south and east-west axes were constructed through each node and the nearest gauge was found in each quadrant defined by the axes, as follows

$$w_C = \frac{\frac{1}{d^2_C}}{\frac{1}{d^2_C} + \frac{1}{d^2_D} + \frac{1}{d^2_B} + \frac{1}{d^2_A}} \tag{3.36}$$

where w_C is the weight assigned to gauge C, d_C is the distance from the node to gauge C in the north-eastern quadrant, d_D is distance from the node to gauge D in the south-eastern quadrant, d_B is distance from the node to gauge B in the south-western quadrant, and d_A is distance from the node to gauge A in the north-western quadrant of grid. Weights for gauges D, B and A are computed similarly. With the weights computed, the node hyetograph ordinate at time t was computed for all times t as:

$$P_{node}(t) = w_A p_A(t) + w_B p_B(t) + w_C p_C(t) + w_D p_D(t) \tag{3.37}$$

Subbasin rainfall totals were indexed using annual precipitation totals sourced from the National Water Archive (Centre for Ecology and Hydrology) according to rain gauge location within the catchment.

The grid-based precipitation method requires a grid cell parameter file which contains four necessary attributes for cells in each subbasin (i) cell *x*-coordinate from grid origin (ii) cell *y*-coordinate from grid origin (iii) proportion of the cell in the specified subbasin and (iv) the flow length from the cell to the outlet. This was achieved within a GIS environment.

Evapotranspiration is modelled as vaporisation of water directly from soil and vegetative surfaces and transpiration through plant leaves (Cunderlik and Simonovic, 2004). The potential evapotranspiration rate for all time periods within the month was computed as the product of the monthly value and the pan coefficient. The pan coefficients were extracted from an existing parameter dataset (MCRM, 2005) and the monthly potential evapotranspiration (*PE*) values were calculated using the Blaney-Criddle equation which determines *PE* by the Penman-Monteith formulation, as

$$PE_t = P_t(\alpha T + \beta) \tag{3.38}$$

where T is temperature in °C, P_t is the mean daily percentage for the month of total annual daytime hours and α and β are coefficients with values extracted from previous research.

3.2.3 Control specifications

The control specifications determine the temporal aspects (range and interval) of the data in question. The start date/time, finish data/time and time interval were stated under the specifications. Time-series data (flow and precipitation) and paired data (channel cross-sections and reservoir functions) were also stored within HEC-HMS. Precipitation and discharge data (sourced from Environment Agency archives) were entered as time-series data from the data storage system program HEC-DSSVue (USACE, 2005).

3.3 MODEL OPTIMISATION

Hydrological processes can never be exactly replicated in a virtual environment. Therefore, all rainfall-runoff model calibrations and subsequent predictions are subject to uncertainty, predominantly arising from error in initial and boundary conditions and in the observational data used for calibration. Optimisation of hydrological models is necessary for increasing accuracy of predictive simulations. There are four stages involved in assessing the accuracy of model outputs. These are

(i) *Sensitivity analysis* – assessing the impact of changes in uncertain parameter values on model outputs to isolate sensitive parameters for model calibration
(ii) *Calibration* – the selection of model parameter values that fit predicted data to observed data as accurately as possible within acceptable limits
(iii) *Validation* – using an independent data set(s) to test a calibrated model
(iv) *Uncertainty analysis* – assessing the range of likely model outcomes given parameter uncertainty, model error and exogenous factors

3.3.1 Sensitivity Analysis

Hydrological rainfall-runoff models are often governed by exhaustive parameter sets. It is computationally demanding, and often unnecessary, to optimise all parameters within a model. Sensitivity analysis identifies parameters which are particularly sensitive within the modelling system enabling greater understanding between the physical processes and their representation in the model (McCuen, 1973). All loss, transform and baseflow parameters within the model were tested for sensitivity using selected subbasins (routing coefficients were not tested as they were deemed sufficiently accurate). Sensitivity was assessed with respect to four predicted variables and two performance measures.

Sensitivity of predicted variables was measured using the local gradient of the response surface in the direction of the chosen parameter axis. The change in total discharge, total baseflow, peak discharge and total loss across the parameter space was used to define a normalised sensitivity index S_i, calculated as:

$$S_i = \frac{dZ / dx_i}{x_i} \tag{3.39}$$

where i is the parameter with value x_i and Z is the value of the predicted variable at that point in the parameter space. These values were plotted as a sensitivity plot, where the greater the change in gradient of the cumulative distribution across the parameter space the higher the model sensitivity to the parameter.

The performance measure used compares simulations from strategic sampling of the parameter space to that of the uncalibrated model using the Nash-Sutcliffe efficiency index E_f (Nash and Sutcliffe, 1971), calculated as

$$E_f = 1 - \frac{\sum_{i=1}^{n}\left(\hat{Y}_i - Y_i\right)^2}{\sum_{i=1}\left(Y_i - \overline{Y}\right)^2} \tag{3.40}$$

where $\hat{Y}_i$ are the predicted values and Y_i the measured values of the dependent variable Y, $\overline{Y}$ is the mean of the measured values and n is the sample size. E_f will return a value of 1 for a perfect fit, a value close to 0 is equivalent to saying that the hydrological model is no better than a one-parameter "no-knowledge" model and negative values indicate that the model is performing worse than a "no-knowledge" model (Beven, 2001).

Wilby (2005) used the E_f method, but stated that the criterion is biased towards high flows and suggested using a secondary index. Consequently, the absolute mean error, *MAE*, was used in addition to E_f values, where

$$MAE = \frac{1}{n}\sum_{i=1}^{n}\frac{\left|Y_i - \hat{Y}_i\right|}{Y_i} \tag{3.41}$$

and terms are defined as in Equation 3.40.

3.3.2 Calibration

Model calibration was achieved using the HEC-HMS optimisation procedure using a combination of methods to ensure optimal model accuracy was achieved. Two objective functions were used to measure the goodness-of-fit between the computed outflow and observed flow data. Firstly, the sum of the squared residuals function (Diskin and Simon, 1977) where increased weight is given to large errors and less to small errors. The objective function Z is calculated as

$$Z = \sum_{i=1}^{NQ} \left(q_o(i) - q_s(i) \right)^2 \tag{3.42}$$

where NQ is the number of computed hydrograph ordinates, q_o is the observed flow and q_s is the simulated flow. Secondly, the peak-weighted RMS error function (USACE, 2000) is a modification of the standard root mean square error that gives greatly increased weight to flows above average and less weight to flows below average, and is determined from

$$Z = \left\{ \frac{1}{NQ} \left[\sum_{i=1}^{NQ} \left(q_o(i) - q_s(i) \right)^2 \left(\frac{q_s(i) + q_o(mean)}{2 q_o(mean)} \right) \right] \right\}^{1/2} \tag{3.43}$$

where $q_o(mean)$ is the mean of the observed flows and all other terms are defined as in Equation 3.42. Both objective function methods are implicitly a measure of comparing peak magnitude, timing and volume of the two hydrographs.

Two methods were used to minimise the objective functions and find optimal parameter values. The univariate-gradient search algorithm adjusts and evaluates one parameter at a time whilst holding the other values constant. That is, if x^k represents the parameter estimate with objective function $f(x^k)$ at iteration k, the search defines a new estimate x^{k+1} at iteration $k+1$ as

$$x^{k+1} = x^k + \Delta x^k \tag{3.44}$$

in which Δx^k is the correction to the parameter. The aim of the search is to select a correction value so that the estimates move toward the parameter that yields the minimum value of the objective function. Reaching the minimum value normally requires a recursive

application of the equation. The method is detailed in full in the USACE technical reference manual (2000). The second minimisation method is the Nelder and Mead algorithm which uses a downhill simplex (a set of alternative parameter values) that evaluates all parameters simultaneously and determines which parameter to adjust. Parameter estimates are formulated based on prior iteration knowledge. The Nelder and Mead algorithm evolves the simplex to find a vertex at which the objective function is a minimum. Again, more details on this process are described in USACE (2000). During either minimising method HEC-HMS checks at each iteration to ascertain that the trail values of the parameters are within the feasible range and adjusts itself accordingly if they are not.

The objective functions and minimising algorithms were used to optimise the sensitive parameters determined during the sensitivity analysis process. Once optimisation for all method combinations (univariate-gradient and sum of squared residuals; univariate-gradient and peak-weighted RMS; Nelder and Mead and sum of squared residuals; Nelder and Mead-peak and weighted RMS) was complete the optimal parameter sets were used to substitute the initial parameter values and the model re-run. The resulting outflow hydrographs were compared to the observed hydrographs for specific locations and the accuracy was determined using five comparison measures: (i) the Nash-Sutcliffe efficiency index, as described in Equation 3.40; (ii) the absolute mean error as defined in Equation 3.41; (ii) the Pearson product-moment correlation coefficient ρ which measures the cofluctuation between two variables, calculated as

$$\rho = \frac{1}{n-1}\sum_{i=1}^{n}\left(\frac{x_i - \bar{x}}{\sigma_x}\right)\left(\frac{y_i - \bar{y}}{\sigma_y}\right) \tag{3.45}$$

where n is the number of observations, x_i is the simulated value, y_i is the observed value, $\bar{x}$ and $\bar{y}$ are the sample means and σ_x and σ_y are the sample standard deviations. A correlation of 1 indicates a perfect positive linear relationship between variables and a correlation of -1 indicates a perfect negative linear relationship; (iv) the coefficient of determination R^2 which calculates the proportion of variability in a dataset that is accounted for by a statistical model, such that

$$R^2 = 1 - \frac{\sum_{i=1}^{n}(y_i - x_i)^2}{\sum_{i=1}^{n}(y_i - \bar{y})^2} \tag{3.46}$$

where the numerator is the sum of the squared errors and the denominator is the total sum of squares, with terms defined as in Equation 3.45; and (v) the root mean squared error (RMSE) which gives particular emphasis to differences of high absolute values and is formulated as

$$\mathrm{RMSE} = \sqrt{\frac{1}{n}\sum_{i=1}^{n}\left(\frac{x_i - y_i}{y_i}\right)^2} \tag{3.47}$$

Again, terms are defined as in Equation 3.45.

3.3.3 Validation

Testing a calibrated model outside the range of data to which the model was calibrated against is essential for assessing parameter accuracy. Running the model for alternative time periods, where observed data are of a similar nature, was completed to ensure consistency in optimal parameter sets. As only extreme heavy precipitation and high flows were investigated, both calibration and validation of the hydrological model were performed on time periods characteristic of these extremes. The resulting hydrographs were compared to the observed flows using the same five measures detailed previously (Equations 3.40, 3.41, 3.45, 3.46 and 3.47).

3.3.4 Uncertainty Analysis

Uncertainty is inherent with rainfall-runoff modelling and the optimisation of parameter sets reveals little about associated uncertainty. The uncertainty associated with modelling results even at the post-calibration stage requires an uncertainty analysis to be performed. Uncertainty estimation aims at assessing the probability of a certain quantity (i.e. peak discharge) being within a certain interval (Beven, 2001). Error and uncertainty were

discussed for each modelling stage, and where appropriate uncertainty bands were either qualitatively stated or quantitatively measured.

3.4 RADAR AND GAUGE COMPARISONS

3.4.1 Raw data

An initial determination of how well the radar data predicted the occurrence of rainfall, in comparison to corresponding gauge values, is conducted using skill-indicating validation scores. These scores are used by national weather providers to decipher radar data prediction accuracy for various rainfall threshold values. The Critical Success Index (CSI) for different thresholds is defined as the number of stations for which both the observed and predicted rainfall amounts are above the threshold, divided by the total number of occasions on which that event was predicted and/or observed (De Bruijn and Brandsma, 2000). However, the CSI does not account for events which occur purely by chance. Therefore, a skill dependent CSI, the Gilbert Skill Score (GS) was used. This score is the number of correct forecasts in excess to those that would be validated by chance, divided by the number of cases when there was a threat that would have not been foreseen by chance (Schaefer, 1990). It is expressed mathematically as follows

$$GS = \frac{(X - C)}{X - C + Y + Z} \tag{3.48}$$

where C equates to

$$C = \frac{(X + Y)(X + Z)}{(X + Y + Z + W)} \tag{3.49}$$

Schaefer (1990) denotes these terms as the number of positive forecasts which correspond to an occurrence of the event (X), the number of events which occurred in conjunction with a negative forecast (Y), the number of positive forecasts which were not accompanied by an event (Z) and the number of negative forecasts which did not have any associated events. C is the number of random forecasts that will validate by change.

A number of methods were employed to quantify the amount of error associated with radar forecasts. Error and uncertainty in derived surface precipitation from radar estimates arise in both reflectivity measurements and attempts at relating measurements to that at ground-level. The RMSE (Equation 3.47) was used as a measure of the quantitative agreement between the gauge and radar time-series. Lewis and Harrison (2007) state that RMSE is highly correlated with the magnitude of surface rain-rate such that poorly performing radars in light rain could appear more accurate in predicting reference data than relatively accurately performing radar in heavy rainfall. RMSE overemphasises the large difference which may result from erroneous data (Gjertsen *et al.*, 2004) and for rainfall amounts the root-mean square factor (RMSF) has been found to provide more information than the RMSE (De Bruijin and Brandsma, 2000). Therefore, in addition to RMSE, the RMSF was used as it overcomes this problem. RMSE is interpreted as giving scale to the additive error whereas RMSF is interpreted as giving scale to the multiplicative error (Golding, 1998) and is calculated as

$$RMSF = \exp\left\{\frac{1}{n}\sum_{i=1}^{n}\left[\ln\left(\frac{R_i}{G_i}\right)\right]^2\right\}^{1/2} \tag{3.50}$$

where R_i is radar precipitation and G_i is rain gauge precipitation at observation i and n is number of observations. Radar time-series were calculated by extracting cell values located at each of the gauging station locations and amalgamated to coincide with the temporal resolution of the gauge time-series. The closer the RMSF value is to 1, the more accurate the forecast (De Bruijn and Brandsma, 2000). In addition to RMSE and RMSF, the Pearson product-moment correlation coefficient (Equation 3.45) was used and systematic bias was estimated for time-series totals as

$$BIAS = \frac{1}{n}\sum_{i=1}^{n}(G_i - R_i) \tag{3.51}$$

where terms are defined as in Equation 3.48.

3.4.2 Geostatistical interpolation

Geostatistics uses the understanding of statistical variation as an important source of information for increasing the accuracy of predictions of an attribute at unsampled points, given a limited set of measurements (Burrough, 2001). Geostatistical interpolation methods assume that the spatial variation of a continuous climatic variable is too irregular to be modelled by a mathematical function and its spatial variation could be more accurately predicted by a probabilistic surface. This continuous variable is called a regionalised variable, which consists of a drift component and a random spatial correlation component (Vincente-Serrano *et al.*, 2003). The statistical properties of the measured points are utilised, quantifying the spatial autocorrelation among measured points and accounting for the spatial configuration of the sample points around the prediction location (Apaydin *et al.*, 2004). A geostatistical methodology was used to interpolate the gauge rainfall field and the resultant interpolated surfaces were subsequently used to correct the radar imagery.

3.4.2.1 Cokriging

Sophisticated geostatistical techniques, such as kriging, provide a more accurate surface estimation than any of the more commonly used interpolation techniques (Prudhomme and Reed, 1999). These techniques are variants of the basic linear estimators. Kriging is more accurate over simple interpolation methods because prediction estimates are accompanied by prediction standard errors (quantification of the uncertainty in the predicted value) and tend to be less biased (Goodall and Maidment, 2002). Predictions obtained using kriging methods are based on a weighting average of data available at neighbouring weather stations. The weighting is chosen so that the calculation is not biased and variance is minimal (Vincente-Serrano *et al*., 2003). Kriging is based on the assumption that the property being interpolated can be treated as a regionalised variable (Ricart, 2004). If the assumptions required to krige a surface are fully met, then kriging by definition will be the best linear unbiased predictor (Agnew and Palutikof, 2000).

Cokriging is a multivariate extension of kriging. Cokriging has the potential, at least in theory, to outperform both univariate kriging and regression because it simultaneously incorporates information on the spatial dependence both in the primary (gauge rainfall) and secondary (elevation/radar rainfall) variables, as well as the cross-correlation between the

two variables (Kelly and Atkinson, 1993). All cokriging estimators are required to be unbiased and to minimise the error variance under the constraint that the expected error is zero. One important advantage of the cokriging estimator is that its error variance is always smaller than or equal to that corresponding to the Kriging estimator, which ignores secondary information.

When the multivariate spatial linear model is given with a trend it is called universal cokriging, also known as cokriging with a trend, and was the method selected to interpolate the gauge precipitation surface. Universal cokriging provides both an estimator of the trend parameters and the best linear unbiased predictor of the variables at unknown locations, and requires knowledge of trend shapes as well as spatial correlation structures (Militino *et al.*, 2001). This technique was adopted by Apaydin *et al.* (2004) to interpolate climate data in Turkey and by Stein *et al.* (1991) to interpolate soil moisture deficits in the Netherlands. Universal cokriging assumes that there is an overriding trend in the data which can be modelled by a deterministic function (i.e. by a polynomial). This trend is subtracted from the original measured points and the autocorrelation is modelled from the random errors. Once the model is fitted to the random errors, before making a prediction, the polynomial is added back to the predictions to give meaningful results (Apaydin *et al.*, 2004). The trend component is not constant within the search neighbourhoods; it depends on the coordinates of the location being estimated and of the data locations (Goovaerts, 1997). For extrapolation beyond the extent of the sample points universal kriging is considered to be the most accurate method to use (Goovaerts, 1997) therefore universal cokriging was adopted.

Cokriging uses information on several variables. The main variable of interest is Z_1, and both autocorrelation for Z_1 and cross-correlations between Z_1 and all other variables are used to make more accurate predictions. Universal cokriging assumes the model

$$Z_1(s) = \mu_1(s) + \varepsilon_1(s)$$
$$Z_2(s) = \mu_2(s) + \varepsilon_2(s) \qquad (3.52)$$

where μ_1 and μ_2 are the n-order trends at location s and ε_1 and ε_2 are types of random error where there is autocorrelation for each of them and cross-correlation between them. These components are estimated using semivariogram and covariance models.

3.4.2.3 The semivariogram

The semivariogram is a function which represents the spatial dependence in a given variable. It must be computed and modelled for kriging and cokriging. The semivariogram captures the spatial dependence between samples by plotting semivariance against separation distance, on the premise that close samples tend to be more similar than more distanct samples (spatial autocorrelation). This gives a measure of dissimilarity between observations. The semivariogram model is used to obtain estimates for the weighting parameters and the selection of the model depends on the behaviour of the experimental semivariogram at the origin. For a parabolic behaviour the Gaussian model is best suited and for linear the spherical or exponential model can be used.

The semivariogram formula involves calculating half the squared difference between the values of the paired locations. The semivariogram is defined as

$$Y(s_i, s_j) = 0.5 \operatorname{var}\left(Z(s_i) - Z(s_j)\right) \tag{3.53}$$

where *var* is the variance and s_i and s_j are two locations. Covariance is a scaled version of correlation and is a similarity function as the covariance function decreases with distance. Both the semivariogram and the covariance provide information on the spatial autocorrelation of the datasets. Semivariance and covariance modelling determines the best-fit model that will pass through the points in the semivariogram. Modelling the semivariance is an iterative process and requires the following parameters to be estimated.

(i) Lag number and size

The lag size is the size of a distance class into which pairs of locations are grouped (binning). Lag size should equate to the approximate minimum distance among samples. When samples are located on a sampling grid, the grid spacing is usually a standard indicator for lag size. The lag size multiplied by the number of lags equate to approximately half the largest distance among all points.

(ii) Range, sill and nugget

Once the semivariance reaches equilibrium this is the end of the range, and the equilibrium value is known as the sill; the plateau that the semivariogram model reaches. The sill constitutes the partial sill plus the nugget. The nugget is caused by discontinuities which, over a short distance, are a consequence of geographic discontinuity. The variogram nugget indicates the variation among repeated measurements at the same point. The nugget effect consists of measurement error and micro-scale variation and the presence of a nugget in the semivariogram suggests that variable is not spatially continuous given zero measurement error. A non-zero nugget occurs when there is substantial error in the measuring instrument (Longley *et al.*, 2005).

(iii) Anisotropy

Anisotropy occurs if the pattern of semivariance changes with direction. If direction is considered then the variogram is described as anisotropic, and if not, then isotropic. If the variation of the range as a function of direction can be approximated by an ellipse (linear transformation) then geometric anisotropy must be considered and if fitted by a second-degree curve, then zonal anisotropy should be used. Creutin and Obled (1982) noted that strong anisotropy corresponds closely with geomorphological features. If points were close to the fitted variogram model in one direction and spread out in another, then directional autocorrelation was likely present in the data. If this was the case, anisotropy was modelled and the changing scatter of empirical semivariogram values when the angle of search direction was altered was well fitted by the model.

3.4.2.4 Cross-validation

Because all variants of kriging are exact interpolators no estimation error occurs at rain gauge locations. Therefore, cross-validation was used to determine accuracy of predictions for known locations. A single precipitation value from the sample dataset was excluded and its value re-estimated from the remaining samples using all other available information. Positive cross-validation errors indicated overestimation of the actual precipitation by the cross-validation estimate, whereas a negative cross-validation error indicated the reverse. Cross-validation statistics examined were the mean error, RMSE,

average standard error and the RMS standardised error. The objective of cross-validation is to assist a decision about which model provides the most accurate predictions. For optimal accuracy the mean error should be close to 0, the root-mean-square error and average standard error should be as small as possible and the root-mean-square standardised error should be close to 1.

3.5 RADAR CORRECTION

Following gauge-radar comparisons, the radar imagery was corrected according to the reference of the gauge records by using the interpolated gauge rainfall surface. Removing systematic error (bias) from radar data was achieved by applying a correction factor. Bias correction of radar estimates used the multiplicative factor F by defining the mean gauge and radar accumulations as

$$F = \frac{\frac{1}{n}\sum_{i=1}^{n} Gi}{\frac{1}{n}\sum_{i=1}^{n} Ri} \tag{3.54}$$

where G_i and R_i are the ith gauge-radar paired variates and n is the number of pairs. Mean field bias adjustment is the simplest method and, therefore, its use is widespread and has commonly been applied to correct radar rainfall data (Gjertsen et al., 2003; Dinku and Anagnostou, 2002; Wilson and Brandes, 1979). The multiplicative correction factor was applied to each of the radar composite images to eliminate bias. An advantage of adjusting bias at the final radar product level is that is handles all sources of systematic radar errors combined (Dinku and Anagnostou, 2002). Once bias removal was completed, the average difference D was calculated as an indicator of the random error measured by comparison to the gauges, defined as

$$D = \frac{100}{n}\sum_{i=1}^{n} \frac{G_i - \overline{R_i}}{G_i} \tag{3.55}$$

where $\overline{R_i}$ is the mean of the adjusted radar accumulations.

3.6 CLIMATE SCENARIOS

Precipitation data sourced from both gauge and radar archives were altered according to future climate change scenarios. The simplest technique of altering historical data with climate change factors is simple proportional change. This method has been widely used by hydrologists (e.g. Arnell and Reynard, 1996; Reynard et al., 1999; Prudhomme et al. 2002) and future climatic series are created by applying monthly climate change factors to all values within the month (Environment Agency, 2003). A couple of examples from the UK include Lane *et al.* (2007) who used the proportional method to study interactions between climate change and flood risk in a temperate upland environment in the north-east of England; and Weatherhead *et al.* (2005) who altered weather data using scaling factors derived from the 50 km by 50 km UKCIP02 baseline and scenarios climatology. Scaling proportions were calculated for use in this research using a method which forced baseline data using the UKCIP02 climate change scenarios for the 2020s, 2050s and 2080s. Both precipitation and evaporation, the two main climate processes which are envisaged to change and alter hydrological regimes in the future, were altered. Once change proportions were calculated for both the precipitation and evapotranspiration data the perturbed time-series data were inputted into HEC-HMS to calculate changes in runoff regimes under likely future conditions for each of the four emissions scenarios under the three time periods.

3.6.1 Precipitation

Radar precipitation data were perturbed directly using the UKCIP02 scenarios. A set of 5 km² spatial resolution model outputs were obtained from the UKCIP archives. This finer spatial resolution was achieved in the UKCIP02 scenarios by interpolating the 50 km² climate changes using a basic form of statistical downscaling and using an observed baseline dataset (Hulme *et al.*, 2002). The percentage changes C applied to the time-series values were calculated as

$$C = 100\left(\frac{P_{t+1} - P_t}{P_t}\right) \tag{3.56}$$

where P is the precipitation value at the baseline time period t or the future time period t+1. Changes were applied to the radar data for every 1 km² cell within the 5 km² cells. The gauge precipitation data were altered using the monthly values extracted from the UKCIP02 tile in which the gauge was located.

3.6.2 Evaporation

Potential evaporation values were calculated following the method by Walsh and Kilsby (2006) which used Equation 3.38. Future monthly temperature values were extracted from the UKCIP02 scenario data and input into the calculations.

3.7 SUMMARY

All methods have been fully described and where appropriate mathematical formulae provided. The application of methods is detailed in the analyses chapters with respect to the selected datasets and chosen study site.

CHAPTER 4

The Severn Uplands

The River Severn flows in a general southward direction from its source in Plynlimon, traversing for approximately 354 km in and out of Wales and England, to its outlet into the Bristol Channel. On a European scale the Severn basin is relatively small, yet on a national scale the Severn is the largest single river basin in England and Wales, with the longest river in Britain and spanning a total catchment area of 11,420 km² (Environment Agency, 2006). The river is divided into three main reaches; the Severn Uplands, the Middle Severn and the Severn Vale. In practice, the Severn has been very carefully managed to preserve its 'natural' appearance (Wood, 1987).

In strategic terms, relatively remote, near-natural catchments can be the most valuable for understanding hydrological processes (Marsh, 2002), particularly in terms of evaluating climatic influences on hydrology. The River Habitat Survey database indicates that the Severn Uplands has experienced only slight and localised channel modification and from a total of 108 sites surveyed within the catchment 89% have been classified as 'pristine/semi-natural' or 'predominantly unmodified' in terms of habitat modification (RHS, 2008). Additionally, for simulating river flows with respect to changes in precipitation, a basin with a high rainfall-runoff component is preferential, where alternative sources of flooding such as groundwater have minimal influence. For these reasons, the Severn Uplands was selected as an ideal near-natural catchment suitable for modelling rainfall-runoff processes and analysing changes in precipitation regimes. This chapter describes basin characteristics and justifies rainfall-runoff modelling suitability for assessing the impacts of climate change in this particular region.

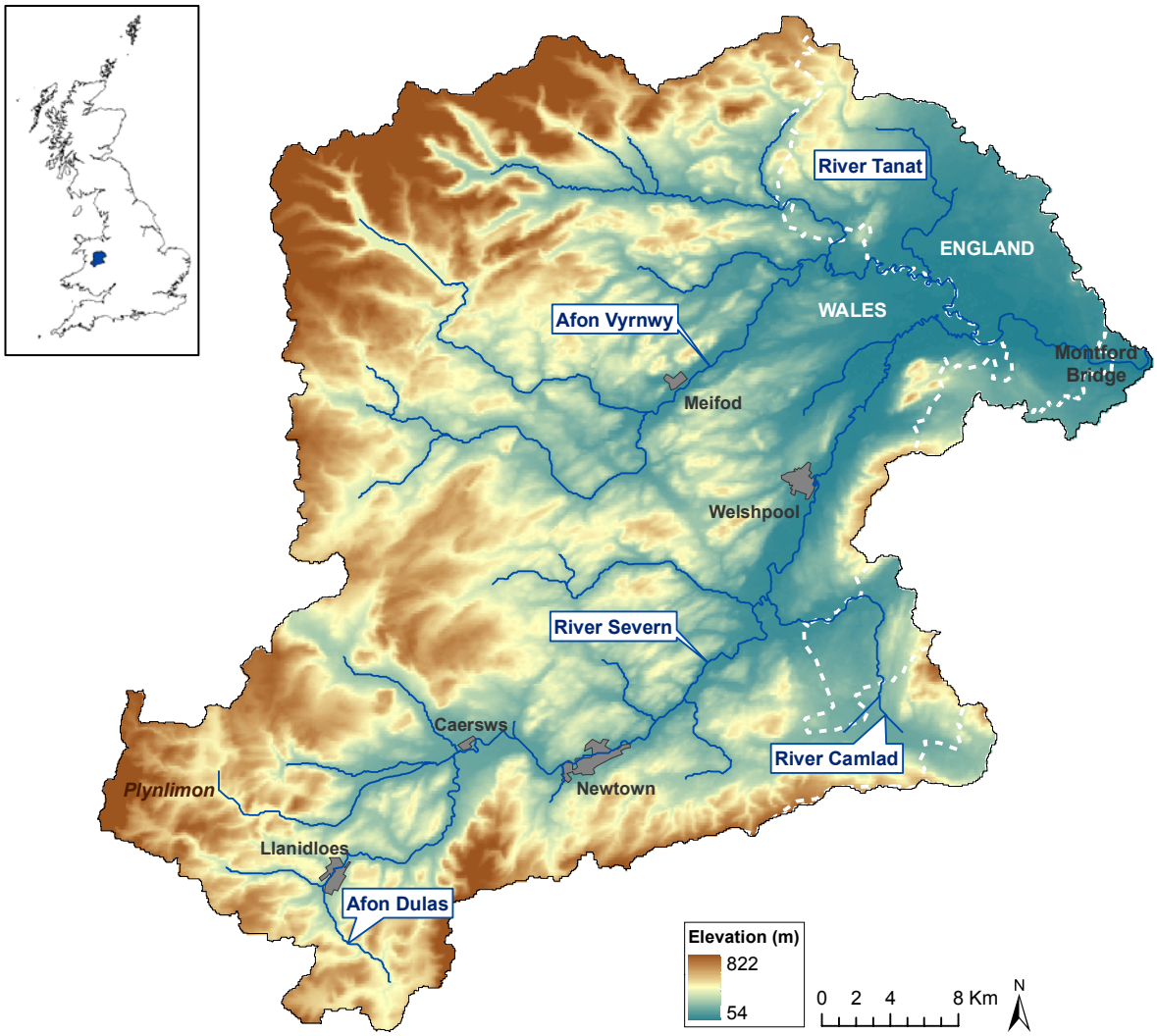

Figure 4.1 The Severn Uplands (Inset: location within the UK)

4.1 LOCATION

From rising on the Plynlimon peak of Bryn-Cras, Powys, to the confluence with the River Perry just upstream of Shrewsbury in Shropshire, the upper reaches of the River Severn flow a distance of 115km and drain an area of 2,065 km². The area upstream of Montford Bridge is known as the Severn Uplands and 86% of this catchment is located within Central Wales (Environment Agency, 2006). The source of the river lies 613 m above sea level with elevation drastically falling to 156 m at Llanidloes and lowering to 55 m on the eastern catchment edge at Montford Bridge, just west of Shrewsbury (Figure 4.1).

4.2 TOPOGRAPHY

North Wales has a complex topography, with mountain ranges either cross-cutting or sub-parallel to the tracks of prevailing westerly weather systems, leading to a complex relationship between rainfall patterns and altitude (Hall and Cratchley, 2005). The western edge of the Severn Uplands catchment is bordered by the Cambrian mountain range and to the north-west the Snowdonia National Park encroaches on the upper reaches of the catchment. Towards the east of the basin the hills give way to the Shropshire Plain, a wide expanse of flat floodplains, and a stark contrast in elevation is observed to that of the steep-sided, incised river valleys in the mountainous west. Rapid elevation reductions, coupled with steep-sided slopes, bode well for rapid runoff, particularly given the nature of the basin geology.

4.3 GEOLOGY

Strata spanning the Palaeozoic and early Mesozoic dominate the geology of the area. Bedrock comprises of Permian Bridgnorth and Triassic Sherwood Sandstone Formations to the north-east (poorly cemented sandstones with layers of thin marls and conglomerates), Silurian mudstones to the south-west and a small area of Carboniferous strata between the two (limestones, Millstone Grit and coal). Overlying much of the north-east catchment are deposits of glacial and post-glacial sands, gravels and clays. To the south-west are surface deposits of alluvium and river terrace gravels. The wide floodplain of the Severn-Vyrnwy confluence lies on sandstone bedrock which provides the primary aquifer in the Severn Uplands (Environment Ageny, 2006). Hydrogeology indicates that the majority of the catchment consists of areas underlain by impermeable rocks, generally without groundwater except at shallow depths (Figure 4.2). Loosely packed soils such as peat dominate the Severn Uplands and act as a sponge for rainfall. These absorb and retain water acting as a temporary store for slow release into the channel. However, once peat is saturated all additional water falling on the peat will flow as surface runoff. Clays retain less water and result in rapid runoff. In the very north-east of the catchment there are highly productive aquifers with intergranular flow which result in high permeability. Also in the north-east are smaller regions of locally important fissured and intergranular aquifers (moderate permeability) and concealed aquifers (mixed permeability). Superficial deposits comprise of boulder clay and morainic drift, glacial sand and gravel, alluvium, river terrace

and peat (Figure 4.2). The geology to the far north-east of the catchment, in contrast to the remainder of the basin, generates higher throughflow and baseflow components feeding into channel flows. However, as the catchment mainly constitutes geology of an impermeable nature, surface runoff processes dominate across much of the Severn Uplands.

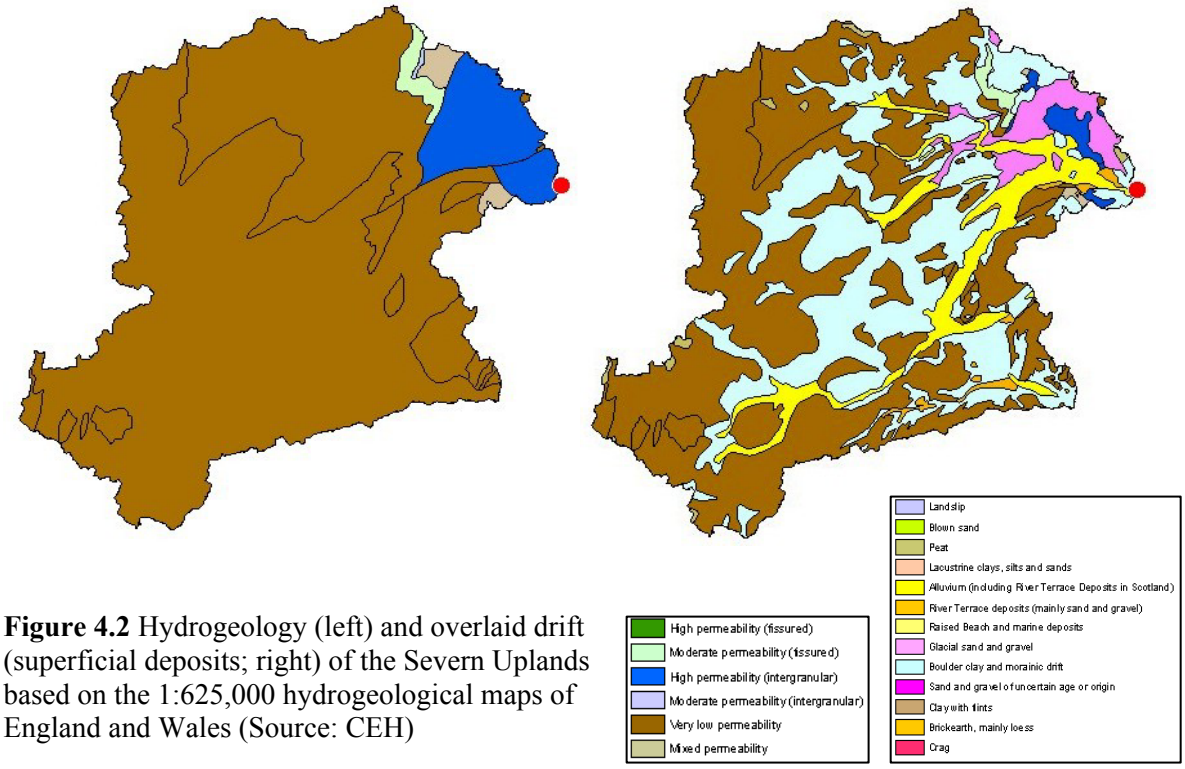

Figure 4.2 Hydrogeology (left) and overlaid drift (superficial deposits; right) of the Severn Uplands based on the 1:625,000 hydrogeological maps of England and Wales (Source: CEH)

4.4 GEOMORPHOLOGY

Climatic changes which took place over Britain between 12,000 and 8,000 BP have strongly influenced the Severn drainage. Since this initial evolution of the Severn basin the Upper Severn has retained an active fluvial system. Between Dolwen and Penstrowed the River Severn represents one of the most unstable sections of natural channel remaining in England and Wales (Gregory, 1997). Although a challenge to model hydraulically, this fluvial instability emphasises the vital importance of understanding changes in hydrological extremes for such high-energy environments. Downstream the river flows as a single-thread gravel-bed river through the flat valleys and wide alluvial floodplains. The reduced gradient facilitates rapid bar accumulation and associated channel planform changes and bank erosion. Due to rapid migration over the floodplain the river has changed

location considerably over the past 100 years and has created a series of meander cutoffs and oxbow lakes. Bed material transport events are relatively frequent along this length of channel.

Within this precipitation-fed system changes in climate variability can often lead to positive feedback mechanisms where flow regimes are modified as a consequence of changes in rainfall, which in turn adjust sediment budgets and together result in geomorphological alterations of the catchment. In a relatively pristine setting these changes have little direct effect, however, the transportation of flows and sediment to downstream reaches, where the geology is less constraining and land use becomes a significant factor, flood inundation becomes critically important.

Downstream of Welshpool to the confluence with the Vyrnwy, the Severn is laterally stable and is prone to flooding due to a lower bankfull channel capacity. The floodplain is over 2 km wide in some places and the channel has entrenched as much as 6 m into the floodplain at places. Due to this high channel and floodplain storage the flood wave is effectively delayed and so peak discharge observations are higher at Abermule compared to the downstream site of Montford, especially for more extreme discharges (Gregory, 1997). Limitations arise for one-dimensional flood modelling when floodplains are frequently inundated due to inaccurate modelling of river flows. These inaccuracies also translate during hydrological model calibration, so, although flow extremes are important in the downstream reaches, it is flows upstream of the Severn-Vyrnwy confluence which will provide more accurate locations for modelling the impacts of future climate change.

4.5 HYDROLOGY

Tributaries of the River Severn form an integral part of the whole Severn Uplands river system. Three main tributaries feed into the Upper Severn; the Camlad, Tanat and Vyrnwy. Surface water streams from the mountains are steep and flashy and during periods of intense rainfall high-flows can be quickly transferred downstream. Average flow rates range from 0.5 $m^3 s^{-1}$ in the catchment headwaters (Plynlimon) to around 43 $m^3 s^{-1}$ at Montford. Within the Severn Uplands river sinuosity is high, with the exception of the upper reaches where channels are constrained by the surrounding topography and underlying geology (Environment Agency, 2005). Channel width near the source is

approximately 1 m and by the time water reaches Montford Bridge the river has widened to 42 m. Sandstone in the north-east catchment acts as a natural aquifer providing groundwater for abstraction and baseflow to support river flows during dry periods.

Lake Vyrnwy and Llyn Clywedog are two artificial dams built on the tributaries of the River Severn in the headwaters of the catchment. Both dams are owned by Severn Trent Water Ltd. and water release is managed by the Environment Agency. Table 4.1 provides a structural comparison of the dams. Lake Vyrnwy, a large artificial reservoir located at the headwaters of the River Vyrnwy was created from dam construction in 1889. The main purpose of the reservoir is to supply water to North-West England, predominantly Liverpool, with only a small proportion of the stored water entering the River Vyrnwy. Although not designed for flood storage control the reservoir does have a limited effect in managing flood risk. Maximum release is 450 Ml day^{-1} with normal compensation releases of 25-35 Ml day^{-1}.

Dam construction in 1986 across the River Clywedog, near Bryntail, created Llyn Clywedog. Controlled water release from this reservoir helps maintain flows in the River Severn with maximum release set at 200 Ml day^{-1}. Storage of water in this reservoir has a negligible effect on flood alleviation downstream as numerous tributaries join the Severn in this upstream area. Reservoir volume is notionally allocated as 65% for abstraction for water supply, 5% for flood attenuation and 30% for ecological and environmental river requirements (Environment Agency, 2006). Llyn Clywedog supports the provision of water supplies to 6 million people and electricity is generated as water is released for regulation purposes (Environment Agency, 2002a). Both reservoirs have negligible effects on highflows within the channel network, particularly at greater distances downstream of the dams (Gilman, 2002).

Table 4.1 Statistics on Lake Vyrnwy and Llyn Clywedog reservoirs (Environment Agency, 2002a)

	Units	**Vyrnwy**	**Clywedog**
Area	km^2	4.54	2.5
Length	km^2	7.6	9.5
Capacity	Ml	59,666	50,000
Dam Height	m	43.9	72
Maximum Depth	m	25.6	66

4.6 CLIMATE

The strong maritime influence in the Severn Uplands leads to high rainfall quantities and frequencies (Starkel *et al.*, 1991). Dominant weather systems bring precipitation from the south-west with air streams being forced to uplift by the Cambrian mountain range. Rainfall totals more than 2500 mm annum^{-1} in the Plynlimon area. Rainfall to the east, around Shrewsbury, is considerably less at only 660 mm annum^{-1} (Environment Agency, 2000). Figure 4.3 illustrates average annual rainfall in the Severn Uplands where the west-east rainfall gradient can be clearly observed. Precipitation during autumn and winter generally originates from weather fronts and low pressure systems (depressions) and tends to be of higher volume than rainfall associated with summer convective storms. This combined with the topographic affect can result in heavy rainfall falling on a near-saturated upper catchment during autumn and winter (Environment Agency, 2008). A waterlogged basin enhances the direct translation of rainfall into surface runoff.

Average temperatures (1971-2000) over north-west England and north Wales are 6.1 °C maximum, 0.9 °C minimum for January and 18.9 °C maximum, 10.9°C minimum for July, with an annual average of 12 °C (Met Office, 2007). Temperatures are cool enough in the mountains to warrant snowfall part of the year, and following any thawing of the snow-pack, the fluvial system is supplied with the melt-water released.

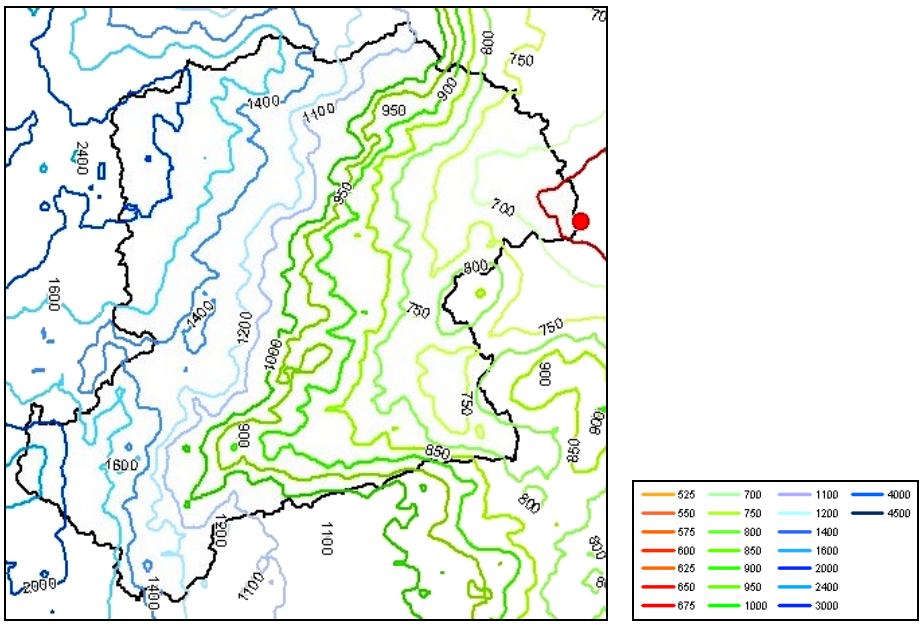

Figure 4.3 Average annual rainfall (mm) of the Severn Uplands (Source: CEH)

4.7 LAND USE

The Severn Uplands has a population of approximately 75,000 people (Environment Agency, 2005), with main urban developments being the riverside towns of Llandiloes, Oswestry, Newtown, and Welshpool. Industry consists of quarrying, high-tech business parks and light industrial estates. Tourism and agriculture are of great regional economic importance. Pasture and sheep farming covers the hillsides, dairy farming dominates the valleys and arable farming is concentrated in the lowland areas. Agriculture in the Severn catchment has intensified over the last 60 years, with increased stocking levels, changes in animal husbandry and alterations in farming practices (Environment Agency, 2008). Grassland, including managed grassland (pasture and sheep farming) is widespread and represents approximately 70% of land cover. Rain-fed blanket bogs and mires are prevalent in the Welsh Mountains and Shropshire Hills. Woodland covers around 17% of the catchment with coniferous and deciduous forests predominantly found in the Shropshire Hills and around the Vyrnwy and Clywedog lakes. Afforestation has taken place since the First World War and the area covered by woodland has risen significantly over the last 25 years. The upper River Severn and Vyrnwy provide a particularly good aquatic habitat and many protected species, such as the Otter and Atlantic salmon exist here. Around the confluence area wet washlands and grasslands are the principle land cover, with a wide range of wetland habitats including reed beds, fens and wet woodlands. Figure 4.4 illustrates the spatial distribution of land use within the Severn Uplands.

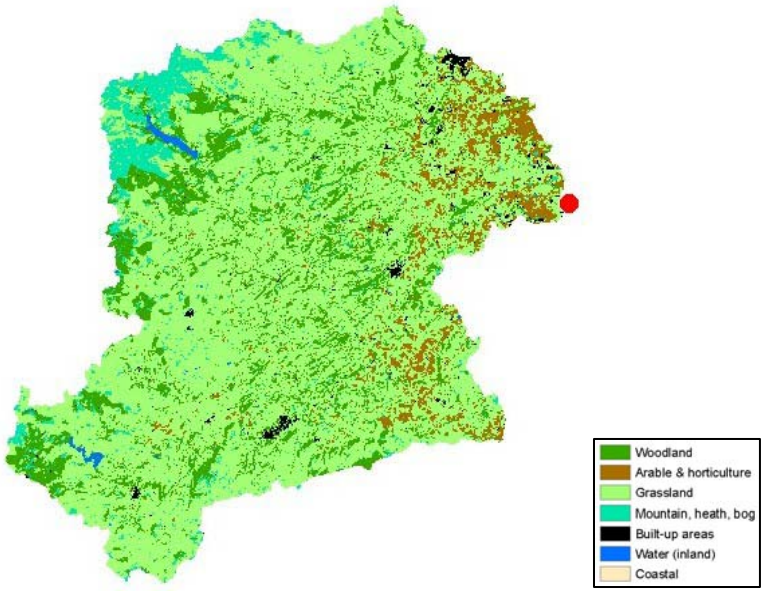

Figure 4.4 Land use within the Severn Uplands at 50 m spatial resolution. The seven broad classes are aggregates of 27 land cover categories based on the Land Cover Map 2000 (Source: CEH)

4.8 FLOODING

Flooding in the Severn is generally caused by rainfall in the Welsh mountains causing a 'plug' of water to pass down the river (Environment Agency, 2005). Extensive areas of agricultural land are at risk of flooding throughout the catchment, especially around the Severn-Vyrnwy confluence area. Around the confluence area (approximately 50 km^2) major flooding occurs above the 5 to 15 year return period. Floodwaters are held back by an argae system and after the flood peak has passed water returns to the Severn and Vyrnwy rivers through sluice gates or by pumping (Environment Agency, 2006). The argae banks prevent flooding at low return periods which is of vital importance as this area reduces flows downstream by up to 17% (Environment Agency, 2008), protecting communities such as Shrewsbury by storing substantial volumes of water. Very few communities are protected by defences within the Severn Uplands catchment. Properties at risk from flooding are located within Penybontfawr, Llanyblodwel, Pontrobert, Meifod, Llanymynech, Llanfechain, Llanfyllin, Maesbury, Morda, Pant, Church Stoke, Llanidloes and Llandinam. Towns with flood protections are Caersws, Welshpool and Newtown.

Recently, there have been many high profile flood events within the Severn catchment, such as those which occurred in Easter 1998, Autumn 2000 and Summer 2007. Rainfall in the autumn of 2000 in Wales was exceptional in terms of intensity, cumulative quantity and severity (Environment Agency, 2001b). During the Autumn 2000 floods the continuous heavy rainfall caused the Vyrnwy reservoir to spill as there was insufficient time for the reservoir level to fall. Hundreds of properties along the Severn's upper catchment were inundated as there was no flood protection. Frequent incidents of flooding occurred from 30th October to 10th November as the Severn river basin experienced prolonged high flow episodes with sustained periods of over-bank flows (DEFRA, 2001b). An estimated 30,000 ha of agricultural land was affected across Wales, resulting in crop damage, stock losses and severe disruption to farming activity (Environment Agency, 2001b). As these flood locations were undefended there was little that could be achieved by the Environment Agency to prevent major flooding (Environment Agency, 2001a).

Natural catchments in the UK mainly flood due to prolonged rainfall in the winter, when soils are wet and storm runoff is readily generated (Wheater, 2006). During autumn and winter the Severn Uplands generally floods due to heavy precipitation from weather fronts and low pressure systems, combined with orographic enhancement (Environment Agency,

2008). During these seasons, precipitation falls on a near-saturated catchment due to the impermeable nature of catchment geology and a build up of water storage. The headwater regions of the Severn catchment are frequently saturated following heavy orographic rainfall and this seasonal waterlogging of soils during the winter period results in the primary runoff process being saturation excess over land flow (Marshall *et al*. 2006). (Howe *et al*., 1967). The hydrological implications of a saturated catchment include low soil moisture deficits and infiltration capacity, maximum surface detention and storage of water, and rivers at or near bankfull stage (Howe *et al*., 1967). Snowmelt has traditionally influenced runoff regimes in upland areas particularly during winter and spring. Recently however, due to a significant decline in snow cover, snowmelt is contributing less to runoff, especially during the winter months (this is further discussed in Chapter 5).

Changes in runoff regimes in the Severn have been noted for decades now. Wood (1987) provided evidence supporting an increase in runoff regime flashiness in the upper Severn reaches in recent years, with hydrograph lag time shortening by as much as 40% and recording higher percentage runoff. Rainfall-runoff modelling of the Severn has been extensive along its reach with research pioneered by the likes of Bailey (1981). However, although much modelling work has been carried out on the Severn it has generally been constrained to sites further downstream and within the Plynlimon study area. Even the majority of nationwide surveys, as discussed in Chapter 2, have not included sites analysed within this region.

In terms of climate change, some research has focused on the Severn basin. Reynard *et al*. (2001) stipulate that the flood event on the Severn, with a 50-year return period, will be 20% larger by the 2050s. More frequent flooding is seen to be less affected by climate change, with the 5-year event increasing by 15%. In terms of flow, Reynard *et al*. (2001) found that a daily mean flow of 300 $m^3 s^{-1}$ is currently exceeded 22 days per annum on average, whereas by the 2050s the frequency rises to 30 days per year. For a more extreme flow of 600 $m^3 s^{-1}$ they find that this is exceeded on average approximately once per year with the future 2050s climate scenario compared to once every 10 years. In 2003 the Environment Agency undertook climate change impact modelling at a downstream location of the River Severn and also found an overall percentage increase in flows by the 2080s. A separate study by the Environment Agency (2005) included coverage of the Severn Uplands and investigated the possible impacts of an increase in peak flow with predicted effects evident from combined future change scenarios (UKCIP98 climate,

urbanisation and rural land management). Results showed an increase of over a metre in water level for the Vyrnwy and Camlad tributaries, and just under a metre for the Upper Severn. These findings are important given the extensive amount of flooding presently occurring in the Severn Uplands.

4.9 SUMMARY

Possible future changes in the Severn catchment are likely to fall under urban development, land use and land management, or climate change (Environment Agency, 2008). This chapter has indicated the suitability of the Severn Uplands to investigate the effects of a changing climate. Murphy and Charlton (2006) state that the lower the catchment water storage capacity, the greater the sensitivity to climate change. This places the Severn Uplands in a sensitive zone for climate induced change as most of the catchment is impermeable, particularly in the west where rainfall is high and combined with steep relief resultant runoff processes are rapid. With a strong rainfall-runoff relationship established within a predominantly rural environment, the Severn Uplands was justifiably selected for investigating the interactions between changes in flow extremes and climate variability, in particular the link to precipitation extremes.

CHAPTER 5

Trends in Extremes and Climate Variability

This chapter investigates precipitation and flow hydrological extremes in the Severn Uplands over a 30-year period from 1977 to 2006. A non-parametric trend detection method was used to analyse monthly, seasonal and annual time-series records across the catchment. The latter part of the chapter explores spatial and temporal patterns in various climate and land cover characteristics in an attempt to identify explanatory variables for trends in precipitation and flow extremes over the time period in question.

5.1 DATA SELECTION

Six rain gauges (Cefn Coch, Dolydd, Llangynog, Llanyfyllin, Pen-y-Coed and Welshpool) and five flow gauges (Abermule, Llanyblodwel, Llanymynech, Montford and Rhos-y-Pentref) were analysed for time-series trends. Gauges were selected based on an adequate record length and less than 11% missing data (Table 5.1). Less that 15% missing data was selected following Haylock and Goodess (2004) who investigated extreme rainfall across Europe and rejected stations with more than 17% missing values and ideally accepted those with less than 10% missing. Climate-driven trend analysis requires rivers where artificial disturbances are minimal, but also there has to be an adequately long time-series record of sufficient quality. Bower *et al.* (2004) state that "long-term" records equate to a minimum length of 25 years. All flow gauge records in the Severn Uplands catchment met this minimum requirement, having lengths of 30 years. However, the number of long-term rain gauge records was limited. Therefore, records ranging from 23 to 30 years were selected to ensure a more complete spatial analysis. All gauge records started on 1st October for the specified water year and finished on 30th September 2006. Data were

obtained from Environment Agency archives at a daily temporal resolution. Gauge locations are mapped in Figure 5.1 with attributes detailed in Table 5.1.

5.2 HOMOGENEITY, NORMALITY AND SERIAL CORRELATION

Large extremes in a time-series of daily maxima are often rare events induced by a distinctive set of weather conditions. Homogeneity adjustments, as discussed in chapter 3, of daily time-series data are very difficult to implement and Anguilar *et al.* (2003) make no recommendations to apply them at this *daily* scale. Therefore, the *annual* maxima time-series records were tested for homogeneity. Thom test *Z*-values indicate that all variables were homogeneous at $\alpha < 0.01$ for the annual data series (Table 5.2). Descriptive statistics of the flow and rainfall daily time-series indicate that the variance was large for all variables, as indicated by the coefficient of variation, C_v, given as a percentage. The distributions also indicate large positive skewness, C_s, and large kurtosis, C_k, indicative of excessive leptokurtic distributions. The Kolmogorov-Smirnov test statistic, *KS*, rejected normality for all variables at a confidence level of $\alpha < 0.01$. Given the non-Gaussian distribution of variables, the Mann-Kendall (MK) non-parametric test was selected as a suitable trend analysis method.

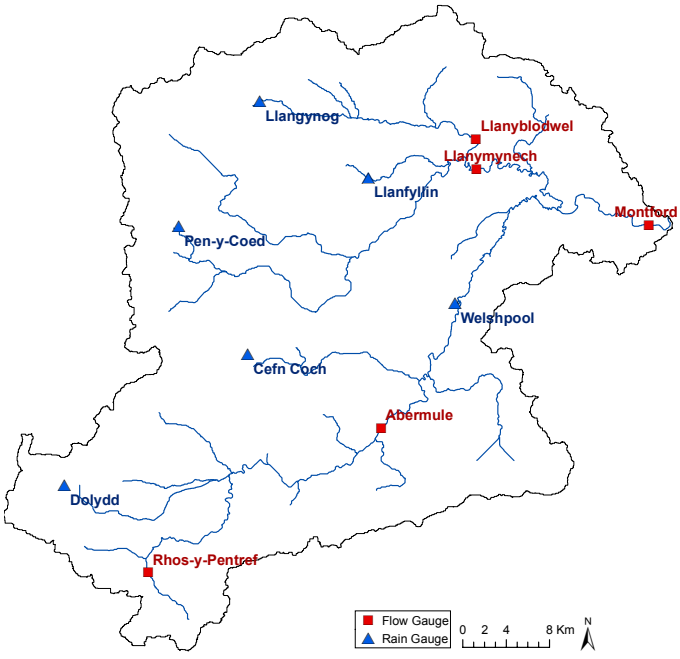

Figure 5.1 Location of precipitation and flow gauges used in trend analysis

Table 5.1 Precipitation and flow gauging station details including when time-series records commenced (water year) and the percentage of data missing from each daily dataset.

No.	Station Name	Type	River	Elevation *m*	Latitude	Longitude	Type	Starts	% Missing
2014	Abermule	Flow	Severn	90	52° 32' 45"	3° 14' 22"	Velocity-Area	1977	0
1338	Cefn Coch	Rain	n/a	310	52° 37' 52"	3° 24' 58"	Tipping Bucket	1983	0
1152	Dolydd	Rain	n/a	294	52° 30' 03"	3° 39' 42"	Tipping Bucket	1980	1.0
1334	Llanfyllin	Rain	n/a	156	52° 45' 38"	3° 15' 23"	Tipping Bucket	1981	8.4
1700	Llangynog	Rain	n/a	166	52° 49' 20"	3° 24' 24"	Tipping Bucket	1982	10.7
2038	Llanyblodwel	Flow	Tanat	85	52° 47' 54"	3° 07' 34"	Flat-V Weir	1977	0
2028	Llanymynech	Flow	Vyrnwy	68	52° 46' 37"	3° 05' 13"	Velocity-Area	1977	0
2005	Montford	Flow	Severn	64	52° 43' 56"	2° 50' 35"	Velocity-Area	1977	0
1009	Pen-y-coed	Rain	n/a	304	52° 43' 03"	3° 30' 52"	Tipping Bucket	1982	6.6
2025	Rhos-y-Pentref	Flow	n/a	184	52° 25' 48"	3° 32' 45"	Trapezoidal Flume	1977	0
1221	Welshpool	Rain	Severn	74	52° 39' 29"	3° 08' 07"	Tipping Bucket	1981	3.2

Table 5.2 Descriptive statistics are identified using the minimum X_{min}, maximum X_{max}, median X_{med}, mean $\overline{X}$ and standard deviation σ of the dataset, where X is the sample population. Normality of the time-series is defined by the coefficients of variation C_v, skewness C_s, kurtosis C_k and the Kolmogorov-Smirnov (KS) test statistic. Z is the Thom test statistic for determining the homogeneity.

Station	X_{min}	X_{max}	X_{med}	$\overline{X}$	σ	C_v	C_s	C_k	KS	Z
Abermule	0.49	328.50	22.84	20.12	28.18	140.05	3.46	17.03	0.25	0.37
Cefn Coch	1.20	61.00	5.50	7.67	7.02	91.59	2.26	7.23	0.18	-0.20
Dolyyd	1.20	110.00	7.50	10.91	11.15	102.19	2.54	9.63	0.19	0.59
Llangynog	1.20	73.00	6.00	8.65	7.99	92.42	2.11	6.60	0.18	0.00
Llanyblodwel	0.15	152.09	4.34	8.54	11.68	136.72	3.35	17.31	0.24	0.00
Llanyfyllin	1.20	82.00	5.00	7.04	6.47	91.97	2.61	12.49	0.19	-0.20
Llanymynech	0.55	486.35	13.70	29.00	41.67	143.69	3.36	15.23	0.25	-0.37
Montford	3.04	473.42	28.20	51.50	58.05	112.71	2.21	5.98	0.21	0.74
Pen-y-coed	1.20	91	6.5	9.815	9.571	97.51	2.31	8.03	0.19	-1.20
Rhos-y-Pentref	0.00	46.99	2.15	2.13	3.33	156.54	3.78	22.30	0.26	0.37
Welshpool	1.20	51.50	4.00	5.82	5.32	91.37	2.74	11.95	0.20	-0.98

Prior to analysis, prewhitening of the flow time-series was conducted following methods described in Chapter 3. Some research has questioned the need to prewhiten time-series records when using the MK test, particularly that of daily time-series. Yue and Wang (2002a) and Modarres and Silva (2007) conclude that their findings for AM daily flow analysis showed little difference when accounting for serial correlation or not, and Yue and Wang (2002b) state that "when a sample size and magnitude of a trend are large enough, serial correlation does not significantly influence the MK test. In such a case, it is more accurate to use the MK test on the original data rather than after prewhitening." In light of these recommendations, testing for serial correlation and prewhitening of flow data was performed solely on *annual* flow records. The Durbin-Watson test was implemented to identify serial correlation. Significant autocorrelation was present in only two records at a significance of $\alpha < 0.05$ with critical bounds $d_L = 1.35$ and $d_U = 1.49$ (see Appendix 1 for test results). These time-series records exhibiting significant serial correlation were prewhitened prior to trend analysis using the sequential regime shift detection software.

5.3 PRECIPITATION AND FLOW TIME-SERIES ANALYSIS

To contextualise, hydrological extremes analyses using the Mann-Kendall (MK) test for trend detection have been performed by researchers in studies from around the world. Examples of extreme precipitation analyses using the MK test are numerous, ranging from Italy (Bonaccorso *et al.*, 2005; Buffoni *et al.*, 1999) to India (Kothyari and Singh, 1996; Pal and Al-Tabbaa, 2009) and Japan (Yue and Hashino, 2003) to Australia (Suppiah and Hennessy, 1998). Particular rainfall variables investigated for changes in extremes include annual maxima (Adamowski and Bougadis, 2003), intensity (Brunetti *et al.,* 2000), percentiles, *n*-day maxima (Lázaro *et al.*, 2001; Qian and Lin, 2005) and measures of spatial variability (Modarres and Silva, 2007). Flow analysis using the MK test has also been implemented at locations around the world with annual maxima, flood volume and flood duration extremes being analysed (e.g. Koutsoyiannis and Baloutsos, 2000; Burn and Hag Elnur, 2002; Nadarajah and Shiau, 2005). Some studies have endeavoured to incorporate trend analysis of the temporal and spatial aspects of both extreme rainfall and flow within specific river basins. Examples include the Yangtze River Basin (Jiang *et al.*, 2007), Rio Puerco Basin, New Mexico (Molnár and Ramírez, 2001) and the Mackenzie River Basin, Canada (Aziz and Burn, 2006). With numerous researchers using the MK

non-parametric method to test hydrological variables, and in particular those representing extremes, it was deemed appropriate for use in analysing extremes within this research, especially given the nature of the hydrological variables in question.

The MK technique described in Chapter 3 was used to test for the presence of trends. Positive values of the MK test statistic Z indicate increasing trends and negative values of Z indicate decreasing trends. Z was deemed significant at a confidence level $\alpha < 0.05$. Three variables were investigated to cover a range of possible changes in extremes; (i) individual maximum values which are representative of the *extreme intensity* of various temporal data series, (ii) the number of events falling above long-term percentile thresholds which refers to the *extreme frequency*, and (iii) the *n*-day maxima which looks at maximum totals for *extreme persistence*. Both precipitation and flow time-series were analysed for extremes in intensity and frequency. Only the precipitation time-series were tested for trends in extreme persistence.

5.3.1 Extreme intensity

The daily maxima time-series records were analysed for extreme flows. Maxima are useful for identifying changes in the magnitude of variables. The yearly maximum of the daily maximum flow record was used to define the annual maxima (AM) series, which corresponds to the largest flow peak on record per year. In addition to trend analysis of the AM time-series, exceedence of the discharge median threshold was considered for the flow records. The median annual maximum flow, QMED, is the middle-ranking value in the ordered AM series. This is commonly used as a flood index estimate that represents a flood which is exceeded on average once every two years (Reed and Robson, 1999). Annual flood counts were calculated as the number of times the QMED was exceeded by the daily flow series. This gives an indication of the temporal frequency of flood events and whether the two-year flood threshold is exceeded throughout the time-series record above the average rate. Statistical trend analysis was performed on monthly, seasonal and annual maximum values of precipitation and flow time-series.

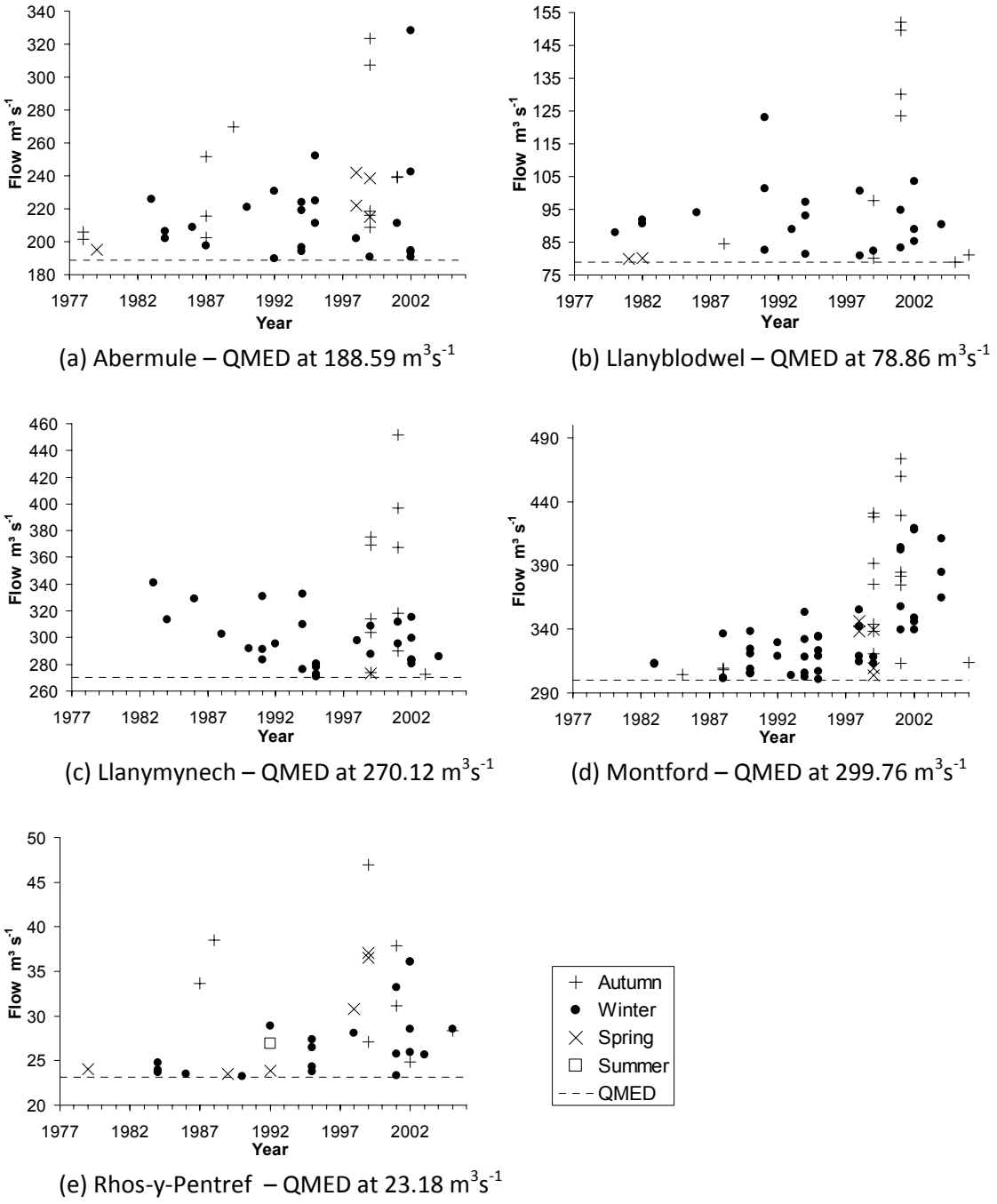

Figure 5.2 Daily maxima flows (water years) which exceeded the long-term QMED threshold at each gauging station

5.3.1.1 QMED exceedence

Figure 5.2 indicates daily flow values which exceeded the QMED flood threshold at individual gauging locations per year. The long-term flood threshold has evidently been exceeded more, both in frequency and magnitude, in the latter part of the time-series for most sites, particularly during the winter and autumn seasons. Magnitude changes are

greatest at Montford, with winter indicating a steady linear increase over time. Rhos-y-Pentref also exhibits a slight increase in QMED exceedence during winter, whereas Llanymynech shows a decrease. Autumn frequency is high at both Llanymynech and Montford for 1998 and 2000, reflecting the occurrence of the nationwide autumn 1998 and 2000 floods. These annual extremes seem fairly isolated in comparison to the remaining extremes in each record. Spring increases are evident at Abermule, Montford and Rhos-y-Pentref with the Easter 1998 floods revealed in the records. These three sites are all located on the main River Severn branch of the Upper Severn catchment; an environmental factor affecting runoff into this sub-catchment of the Severn Uplands is likely to be influencing spring flows. The only exceedence of the long-term QMED threshold in the summer occurred in 1992 at Rhos-y-Pentref. This reflects a particularly wet August, where total precipitation at Dolydd (closest precipitation gauge) was recorded at approximately 265% of the average 30-year monthly total. All gauge station annual maxima indicate that in more recent years the QMED threshold has been exceeded at least once a year by daily maxima flood events (more than the statistical average).

5.3.1.2 Precipitation Maxima

No significant trends exist in the AM precipitation records (Table 5.3). Seasonally, Pen-y-Coed shows significant signs of increase in spring whereas Welshpool has decreasing spring precipitation. Summer precipitation has decreased at Dolydd. Some monthly maxima analyses, as highlighted in Table 5.3, revealed significant increasing trends but the only significant monthly trend to concurrently occur at more than one gauge was an increase in April precipitation at Cefn Coch and Llangynog.

5.3.1.3 Flow Maxima

MK test results indicate significant increasing AM trends at Llanyblodwel, Montford and Rhos-y-Pentref for flow maxima (Table 5.3). The trend at Montford is even significant at $\alpha < 0.01$ which re-emphasises the substantial increase in magnitude above the QMED threshold previously described. Significant increases in winter flows are present at Montford and Rhos-y-Pentref, but no other seasonal trends are apparent at any of the

gauges. At all gauges except Llanymynech, the maximum flow value for July has increased significantly over the last 30 years. No other monthly trends were detected.

Table 5.3 Annual, seasonal and monthly maxima analysis where *Z* is the Mann-Kendall test statistic and α is the significance of the trend for (i) precipitation and (ii) flow. Bold indicates significance at $\alpha < 0.05$.

(i) Precipitation

	Cefn Coch		**Dolydd**		**Llanfyllin**		**Llangynog**		**Pen-y-Coed**		**Welshpool**	
	Z	*α*	*Z*	*α*	*Z*	*α*	*Z*	*α*	*Z*	*α*	*Z*	*α*
Annual												
Ann	-1.218	0.112	0.021	0.492	0.563	0.287	0.257	0.399	0.234	0.408	-0.459	0.323
Seasonal												
Aut	0.079	0.468	0.688	0.246	1.099	0.136	0.720	0.236	1.589	0.056	1.125	0.130
Win	-0.742	0.229	0.125	0.450	0.132	0.447	-0.678	0.249	0.508	0.363	-1.104	0.135
Spr	-0.447	0.327	0.104	0.458	-1.032	0.151	0.670	0.251	**1.789**	**0.037**	**-2.045**	**0.020**
Sum	-0.969	0.167	**-2.232**	**0.013**	-0.304	0.381	0.845	0.199	-1.142	0.127	-1.523	0.064
Monthly												
Nov	0.978	0.164	1.588	0.056	0.000	0.500	0.521	0.301	0.397	0.346	1.029	0.152
Dec	0.556	0.289	-1.146	0.126	-0.423	0.336	-0.496	0.310	-0.979	0.164	-0.771	0.220
Jan	-1.111	0.133	-0.332	0.370	-0.327	0.716	**-1.960**	**0.025**	-0.344	0.365	-1.587	0.056
Feb	**-1.799**	**0.036**	0.000	0.500	0.745	0.228	-0.149	0.441	-1.185	0.118	-0.265	0.396
Mar	0.900	0.184	1.106	0.134	0.861	0.195	0.958	0.169	**1.788**	**0.037**	-0.188	0.426
Apr	0.000	0.500	-0.667	0.252	-1.403	0.080	0.050	0.480	-0.529	0.298	**-1.755**	**0.040**
May	**1.789**	**0.037**	1.147	0.126	1.123	0.131	**1.764**	**0.039**	0.529	0.298	0.730	0.233
Jun	0.969	0.166	1.168	0.121	0.492	0.311	0.968	0.166	0.186	0.426	-0.042	0.483
Jul	-1.044	0.148	-0.856	0.196	-0.514	0.304	-0.273	0.392	-0.317	0.376	-0.627	0.265
Aug	0.821	0.206	0.309	0.379	0.468	0.320	0.571	0.289	0.238	0.406	0.375	0.354
Sep	-0.555	0.289	-1.612	0.054	0.257	0.399	**-2.159**	**0.014**	0.132	0.447	-0.155	0.439

(ii) Flow

	Abermule		**Llanyblodwel**		**Llanymynech**		**Montford**		**Rhos-y-Pentref**	
	Z	*α*	*Z*	*α*	*Z*	*α*	*Z*	*α*	*Z*	*α*
Annual										
Ann	0.749	0.227	**1.713**	**0.043**	0.844	0.199	**2.498**	**0.006**	**1.713**	**0.043**
Seasonal										
Aut	0.244	0.464	0.882	0.189	0.281	0.389	0.094	0.463	0.394	0.347
Win	0.963	0.168	1.332	0.091	0.678	0.249	**1.891**	**0.029**	**2.212**	**0.013**
Spr	0.393	0.348	0.678	0.249	1.288	0.106	-0.131	0.448	-0.214	0.415
Sum	-0.357	0.361	0.107	0.457	-1.142	0.127	0.469	0.320	-1.231	0.109
Monthly										
Oct	1.178	0.120	1.747	0.142	1.570	0.058	0.807	0.210	1.089	0.138
Nov	-0.071	0.472	-0.071	0.472	-0.500	0.309	-0.582	0.280	0.143	0.443
Dec	0.000	0.500	0.431	0.333	-0.356	0.361	-0.094	0.463	0.821	0.206
Jan	-0.464	0.321	0.356	0.639	-0.642	0.260	-0.019	0.493	-0.071	0.472
Feb	0.286	0.388	0.582	0.280	0.000	0.500	0.000	0.500	0.500	0.309
Mar	0.071	0.472	0.206	0.418	0.500	0.309	-0.206	0.418	-0.286	0.388
Apr	0.678	0.249	1.499	0.067	1.035	0.150	0.169	0.433	1.320	0.093
May	1.534	0.063	1.213	0.113	1.463	0.072	1.519	0.064	0.856	0.196
Jun	-0.678	0.249	-1.106	0.134	-0.928	0.177	-0.657	0.226	-1.214	0.113
Jul	**1.748**	**0.040**	**1.713**	**0.043**	0.821	0.206	**1.820**	**0.034**	**1.891**	**0.029**
Aug	-0.642	0.260	-0.607	0.272	-0.928	0.177	-0.657	0.256	-0.928	0.177
Sep	-0.678	0.249	-0.482	0.334	-0.749	0.227	-0.582	0.280	-1.213	0.113

5.3.2 Extreme frequency

Daily precipitation and daily maximum flow magnitudes were categorised into several classes. Rather than splitting the data using arbitrary numerical thresholds (e.g. Karl *et al.*, 1995), the time-series record was divided into frequency percentiles (e.g. Karl and Knight, 1998) with the largest percentiles indicative of infrequent extreme events. In this way, spatial variation resultant from inconsistent variables (i.e. the west-east rainfall gradient observed across the study site) can exist without being constrained by fixed catchment thresholds. As extreme events are of interest, only the extreme upper tail of the distributions was analysed. Above the 90th percentile is usually taken to signify very wet periods or periods of high-flows, and above the 95th percentile is generally allocated as a threshold for extreme frequencies (Haylock and Nicholls, 2000). Therefore, data were analysed for counts of days that exceeded the long-term 90th, 95th and 97th percentiles (top 10%, 5% and 3%, respectively).

Statistical analysis of rainfall percentiles was performed on a filtered time-series record which incorporated "rain-days" only, thus, avoiding days with minimal or zero rainfall skewing long-term percentile values. A rain-day was classed as a day when rainfall exceeded 1 mm. This produced a two-fold distribution, where (i) rainfall was either present or absent, and (ii) given rainfall presence, a frequency distribution was obtained according to the specified percentile threshold.

5.3.2.1 Precipitation Percentiles

Analysis of precipitation percentile exceedence indicates that at Dolydd there was a significant negative trend in the number of days exceeding the summer 97th percentile (Table 5.4). All other significant precipitation trends were detected at Pen-y-Coed station where the annual 95th and 97th, autumn 95th and winter 90th percentile exceedence have all increased throughout the time-series records.

Table 5.4 Annual and seasonal percentile analysis where *Z* is the Mann-Kendall test statistic and *α* is the significance of the trend for (i) precipitation and (ii) flow. Bold indicates significance at $\alpha < 0.05$.

(i) Precipitation

	Cefn Coch		**Dolydd**		**Llanfyllin**		**Llangynog**		**Pen-y-Coed**		**Welshpool**	
	Z	*α*	*Z*	*α*	*Z*	*α*	*Z*	*α*	*Z*	*α*	*Z*	*α*
Annual												
90th	0.125	0.450	0.251	0.401	0.845	0.199	-0.141	0.444	1.548	0.067	-0.253	0.400
95th	0.528	0.299	0.211	0.417	0.567	0.285	-0.758	0.224	**1.998**	**0.023**	-0.549	0.291
97th	0.000	0.500	0.339	0.367	0.085	0.466	0.734	0.232	**1.766**	**0.039**	0.000	0.500
Autumn												
90th	1.380	0.084	-0.882	0.189	0.029	0.386	0.825	0.205	1.320	0.093	-0.237	0.406
95th	0.856	0.196	-0.211	0.416	0.433	0.333	0.195	0.423	**1.699**	**0.045**	0.437	0.331
97th	0.501	0.308	-0.213	0.416	0.215	0.415	0.838	0.201	0.271	0.393	0.334	0.369
Winter												
90th	-0.882	0.189	-0.063	0.475	1.005	0.158	-0.710	0.239	**1.842**	**0.033**	-1.349	0.089
95th	-0.785	0.216	-0.935	0.148	0.429	0.338	-1.559	0.060	1.529	0.063	-1.051	0.147
97th	-0.221	0.413	-0.892	0.186	-0.348	0.364	0.078	0.531	0.584	0.280	-1.171	0.121
Spring												
90th	1.106	0.134	0.000	0.500	0.522	0.301	0.605	0.273	1.047	0.148	0.513	0.304
95th	0.691	0.245	-0.043	0.483	0.000	0.500	1.315	0.094	1.357	0.087	-0.792	0.786
97th	0.980	0.163	0.328	0.372	-0.077	0.531	0.237	0.407	1.272	0.102	-1.349	0.089
Summer												
90th	-1.164	0.122	-0.791	0.214	0.429	0.334	-1.259	0.104	-1.423	0.077	0.000	0.500
95th	-0.838	0.201	-1.171	0.121	0.000	0.500	-0.598	0.275	-0.460	0.323	-0.333	0.370
97th	0.000	0.500	**-1.666**	**0.048**	0.672	0.251	-0.319	0.375	-0.184	0.427	-1.232	0.109

(ii) Flow

	Abermule		**Llanyblodwel**		**Llanymynech**		**Montford**		**Rhos-y-Pentref**	
	Z	*α*	*Z*	*α*	*Z*	*α*	*Z*	*α*	*Z*	*α*
Annual										
90th	-0.608	0.272	0.787	0.216	-0.429	0.334	0.732	0.232	-0.375	0.354
95th	-0.197	0.422	1.312	0.095	0.000	0.500	0.804	0.211	0.769	0.221
97th	0.902	0.184	0.896	0.185	0.521	0.301	0.879	0.190	1.152	0.125
Autumn										
90th	0.592	0.277	0.555	0.290	0.502	0.308	1.379	0.084	0.323	0.374
95th	0.990	0.161	1.028	0.152	0.613	0.270	1.168	0.121	0.792	0.214
97th	0.888	0.187	1.300	0.097	0.549	0.291	0.786	0.216	0.401	0.344
Winter										
90th	0.627	0.265	0.658	0.255	-0.054	0.479	0.323	0.373	1.457	0.073
95th	1.237	0.131	0.855	0.196	0.522	0.301	0.942	0.173	**1.827**	**0.034**
97th	1.330	0.092	0.287	0.387	0.989	0.161	0.965	0.167	0.941	0.173
Spring										
90th	-1.199	0.115	-0.301	0.382	-0.591	0.302	0.251	0.401	**-0.172**	**0.043**
95th	-0.881	0.189	0.245	0.403	0.000	0.500	-0.271	0.393	-0.142	0.078
97th	**-0.198**	**0.023**	0.749	0.227	0.146	0.442	-0.729	0.233	-0.381	0.352
Summer										
90th	-0.467	0.320	-0.717	0.237	-0.501	0.308	-0.415	0.339	-0.252	0.401
95th	-0.379	0.346	-0.415	0.339	-0.721	0.235	-0.055	0.478	-0.848	0.198
97th	0.110	0.456	0.018	0.493	-0.602	0.245	-0.353	0.362	-0.682	0.248

Table 5.5 Annual and seasonal *N*-day precipitation maxima analysis where *Z* is the Mann-Kendall test statistic and α is the significance of the trend. Bold indicates significance at $\alpha < 0.05$.

	Cefn Coch		**Dolydd**		**Llanfyllin**		**Llangynog**		**Pen-y-Coed**		**Welshpool**	
	Z	*α*	*Z*	*α*	*Z*	*α*	*Z*	*α*	*Z*	*α*	*Z*	*α*
3-day max												
Ann	0.199	0.421	0.417	0.338	1.545	0.061	0.771	0.220	1.448	0.074	-0.063	0.475
Aut	0.344	0.366	-0.792	0.214	0.402	0.337	0.769	0.221	**1.729**	**0.042**	0.949	0.171
Win	-0.344	0.366	**1.252**	**0.011**	0.772	0.220	-0.327	0.372	0.701	0.242	-0.861	0.195
Spr	1.588	0.056	0.521	0.301	0.000	0.500	0.894	0.186	**1.960**	**0.025**	-0.690	0.245
Sum	0.844	0.199	-1.315	0.094	-0.304	0.381	-0.646	0.259	-1.564	0.059	-1.302	0.096
7-day max												
Ann	0.500	0.304	0.521	0.301	1.500	0.067	0.701	0.242	**2.104**	**0.018**	0.730	0.233
Aut	0.000	0.500	-1.105	0.135	0.421	0.337	0.471	0.319	1.004	0.158	**1.743**	**0.041**
Win	-0.053	0.479	0.584	0.280	1.478	0.070	0.958	0.169	1.589	0.056	0.044	0.482
Spr	1.588	0.056	0.667	0.252	-0.117	0.453	0.223	0.412	**1.762**	**0.039**	-1.440	0.075
Sum	-1.192	0.117	**-2.107**	**0.018**	0.327	0.372	-1.440	0.075	**-2.407**	**0.008**	-1.434	0.076
10-day max												
Ann	-0.174	0.431	0.292	0.385	**1.940**	**0.026**	1.191	0.117	**2.265**	**0.012**	0.250	0.401
Aut	0.317	0.376	-1.459	0.072	0.397	0.346	0.496	0.310	0.608	0.272	0.772	0.220
Win	-0.238	0.406	0.042	0.483	1.279	0.100	0.771	0.220	**1.892**	**0.029**	-0.022	0.491
Spr	1.490	0.068	0.688	0.246	-0.842	0.200	-0.223	0.412	**1.662**	**0.048**	**-1.774**	**0.038**
Sum	-0.092	0.137	-1.606	0.054	-0.049	0.481	-0.745	0.228	-1.389	0.082	-0.419	0.338
30-day max												
Ann	0.199	0.421	0.313	0.377	1.433	0.076	0.164	0.435	**2.219**	**0.013**	0.814	0.208
Aut	0.423	0.336	-0.667	0.252	-0.140	0.444	0.447	0.328	1.563	0.059	1.146	0.126
Win	-0.660	0.254	0.146	0.449	0.992	0.161	0.187	0.426	1.495	0.067	-0.177	0.430
Spr	0.521	0.301	-0.083	0.467	-1.098	0.136	-1.091	0.138	0.968	0.167	**-2.023**	**0.022**
Sum	-1.564	0.059	-0.459	0.323	-0.561	0.288	-1.614	0.053	-0.943	0.173	-0.093	0.177

5.3.2.2 Flow Percentiles

Trend analysis of flow percentiles revealed significant increases for winter 95th percentile exceedence at Rhos-y-Pentref (Table 5.4). Significant decreases were found for spring 90th percentile exceedence at Rhos-y-Pentref and the spring 97th percentile at Abermule. Overall trends in the *Z*-values showed a general increase in autumn percentile exceedence for all gauges and a majority increase in winter and decrease in summer.

5.3.3 Extreme persistence

In addition to individual extreme values exceeding a certain threshold, maximum 3-day, 7-day, 10-day and 30-day rainfall totals were calculated to determine whether periods of prolonged rainfall indicate increased rainfall persistence. *N*-day totals were assigned to the central value of the *N*-day period. The maximum of the *N*-day totals was then calculated for seasonal and annual time periods.

5.3.3.1 Precipitation *N*-day maxima

Pen-y-Coed exhibited many significant trends in the *N*-day maxima; autumn (3-day), spring (3-, 7- and 10-day), winter (10-day) and annual (7-, 10- and 30-day) maxima have all increased and summer (7-day) has decreased (Table 5.5). Changes in precipitation persistence at Dolydd show increases in 3-day winter maxima and reductions in 7-day summer maxima. For Welshpool, 7-day autumn maxima have increased and both 10-day and 30-day spring maxima have decreased. This spring reduction for precipitation persistence coincides with the decrease in spring flow percentile exceedence and maxima at Welshpool. Finally, Llanfyllin shows an increase in the annual 10-day maxima series.

5.4 CLIMATE VARIABILITY

The characteristics of flood magnitudes and frequencies are highly sensitive to climatic variations, in particular to changes in atmospheric circulation regimes (Lamb, 1972), as well as changes in physical catchment properties. The relationship between climate variables, physical land characteristics and the hydrological cycle is complex. To predict future changes it is useful to look at the past to understand how such interactions have evolved. Precipitation is important for predicting changes in flow regimes, but a simple increase in precipitation will not necessarily result in increased flooding. The influence of climate variables on river flow regimes is complex with intricate interactions between evaporation losses, soil moisture conditions, catchment geology, land use and artificial changes to watercourses. As the relationship between rainfall and runoff is not straightforward, which is evident given the MK trend analysis results, patterns in climate variability were examined to identify common underlying meteorological characteristics and provide possible causal triggers with which to explain the observed trends in the precipitation and flow extremes.

5.4.1 Weather Patterns

Sumner (1996) highlights two major climate factors as important in producing or enhancing precipitation in the UK (i) the interaction between near-surface airflow and

topography and (ii) the position, degree of development and movement of precipitation-producing systems. Large-scale atmospheric circulation is an important climate factor determining dominant airflow systems (Post *et al*., 2002). Regional weather patterns are important in determining interannual variations in precipitation, which are often directly, or indirectly, linked to climatic changes on a wider scale (Harrison *et al.*, 2001). Sumner (1996) investigated daily precipitation patterns over Wales and concluded that stable and humid weather systems, with a tropical maritime flow, yielded the most precipitation in upland areas. Yet research by Howe *et al.* (1967) found that widespread floods were most commonly related to the occurrence of intense depression systems and sequences of storms, and were enhanced in areas with changing elevation. Orographic uplift is important in these upland regions and may occur even under fairly high pressure. As convective, frontal and orographic rainfall can have an impact on flow extremes, weather types were further investigated to determine if particular weather systems correlated with increases in extreme flow intensities.

Weather typing constitutes a useful tool for understanding certain dynamical aspects related to precipitation regimes (Trigo and DaCamara, 2000). A subjective long-term record of daily weather types and spells in the British Isles was produced by Lamb (1950). Long weather spells marked by the persistence of specific weather types are a familiar feature of the British climate and commonly determine the prevailing character of a particular season. Jenkinson and Collison (1977) advanced Lamb's weather types by producing an objective catalogue of numerical values representing pressure, airflow and vorticity prepared from surface pressure grid point data. The new system was developed to match classification types with Lamb's previous research. Table 5.6 lists the numerical values assigned to daily weather conditions prevalent across the British Isles and their corresponding weather types. These are explained by Jenkinson and Collison (1977) as (i) if vorticity is greater than two-times the airflow then the weather pattern is strongly anticyclonic or cyclonic (0 and 20), (ii) if vorticity is less than airflow then airflow is essentially straight (11-18), (iii) if vorticity lies between one- and two-times airflow then airflow is moderately anticyclonic or cyclonic (1-8 and 21-28), and (iv) if vorticity and airflow are both less than 6 units there is light indeterminate airflow (-1).

Table 5.6 Lamb Weather Types

-1	U				
0	A			20	C
1	ANE	11	NE	21	CNE
2	AE	12	E	22	CE
3	ASE	13	SE	23	CSE
4	AS	14	S	24	CS
5	ASW	15	SW	25	CSW
6	AW	16	W	26	CW
7	ANW	17	NW	27	CNW
8	AN	18	N	28	CN

The links between weather types and river flows were investigated to determine if extreme flows coincided with particular airflow types. Most weather types corresponding to days where flow exceeded the long-term QMED threshold at Montford, the site with the most significant increasing AM trend ($\alpha < 0.01$), were found to be cyclonic and/or with S-SW-W-NW-N airflow components (Figure 5.3). There are a few occurrences of high-flows during anticyclonic SW-W-NW conditions, yet these are found to occur at the lower-value flows of the high-flow series. These weather characteristics are also mirrored in the AM flow for all gauges (Figure 5.4a). Svensson *et al.* (2002) found that the most likely weather types to result in extreme flows are cyclonic conditions with SE-S-SW-W airflow. Their research, focused across Scotland, found that in winter cyclones are more vigorous and orographic enhancement is pronounced with cyclonic direction airflows. However, in the summer extreme flows occur mainly under purely cyclonic conditions. With high-flows occurring on days where weather types are predominantly cyclonic and air flows originate over the Atlantic Ocean, it can be inferred that frontal or orographic rainfall is most likely the strong driving force behind extreme flow intensity in the Severn Uplands.

Time-series analysis results indicate changes in both magnitude and frequency of precipitation records, yet the largest number of significant trends is found in the *N*-day maxima persistence analyses. In this upland region, the seeder-feeder mechanism is important, where moist low-level air is forced to rise over a range of hills in strong maritime winds and is cooled to its saturation point as it rises, forming a capping feeder cloud (Sibley, 2005). This is reflected in trend observations as the gauge with the largest number of significant persistence trends, Pen-y-Coed, is one of the highest elevated and receives the second highest annual rainfall (approximately 1600 mm annum^{-1}). For summer precipitation, trend analysis results indicate significant decreases in the two highest elevation rain gauges, Dolydd and Pen-y-Coed. Both gauges show significant reductions in

summer precipitation persistence, and additionally, Dolydd shows decreasing trends in extreme intensity and frequency.

The July-maxima upward trends for the flow gauges are an interesting feature of the trend analysis. These significant flow trends are present concurrently in the precipitation record, with all July maxima rainfall *Z*-values indicating an increase, but not at a statistically significant level. Wood (1987) states that there has been a slight increase in the frequency of very heavy summer events since the late 1960s. Beven (1993) hypothesises that any increases in summer rainfall may well be in the form of convective storms of increasing frequency or intensity. Pitt (2008) claims that there is insufficient evidence of an increase in the frequency of intense summer storms which trigger extreme convective rainfall. However, some research findings have found this to be the case; McEwen (1989) found evidence in Scotland suggesting that the most extreme precipitation was associated with high recurrence interval summer frontal storms.

Exploring the larger high-flows in accordance to weather types, a predominant cyclonic or SW-S-SE airflow component was observed (Figure 5.4b). Lamb (1950) states that southerly airflows are very rare in the summer. However, when they do prevail, they are characteristic of warm, thundery weather. It would seem the July-maxima under SW-S-SE airflow conditions coincides with locally warmer summers as evident in the temperature record for the Severn Uplands, including the three warmest years on record (1977-2005; see section 5.4.3). During these years convective rainfall is more likely to be influencing high-flows in the Severn Uplands, given the higher land temperatures and stable air masses. Wood (1987) makes a valuable statement that a flood-causing situation in the uplands may not necessarily appear as a major factor on hydrograph shape. For example, localised summer convective storms may have more important consequences in the headwaters, whereas frontal situations may be more important at the catchment outlet. This seems to have some truth for flood events in the Severn Uplands. Weather type analysis shows that flow AM occurred at Montford (outlet) mainly under cyclonic conditions. At Rhos-y-Pentref (headwaters), although high-flows under cyclonic conditions were frequent between 1977-2006, AM flows under anticyclonic conditions were more common at the upstream location.

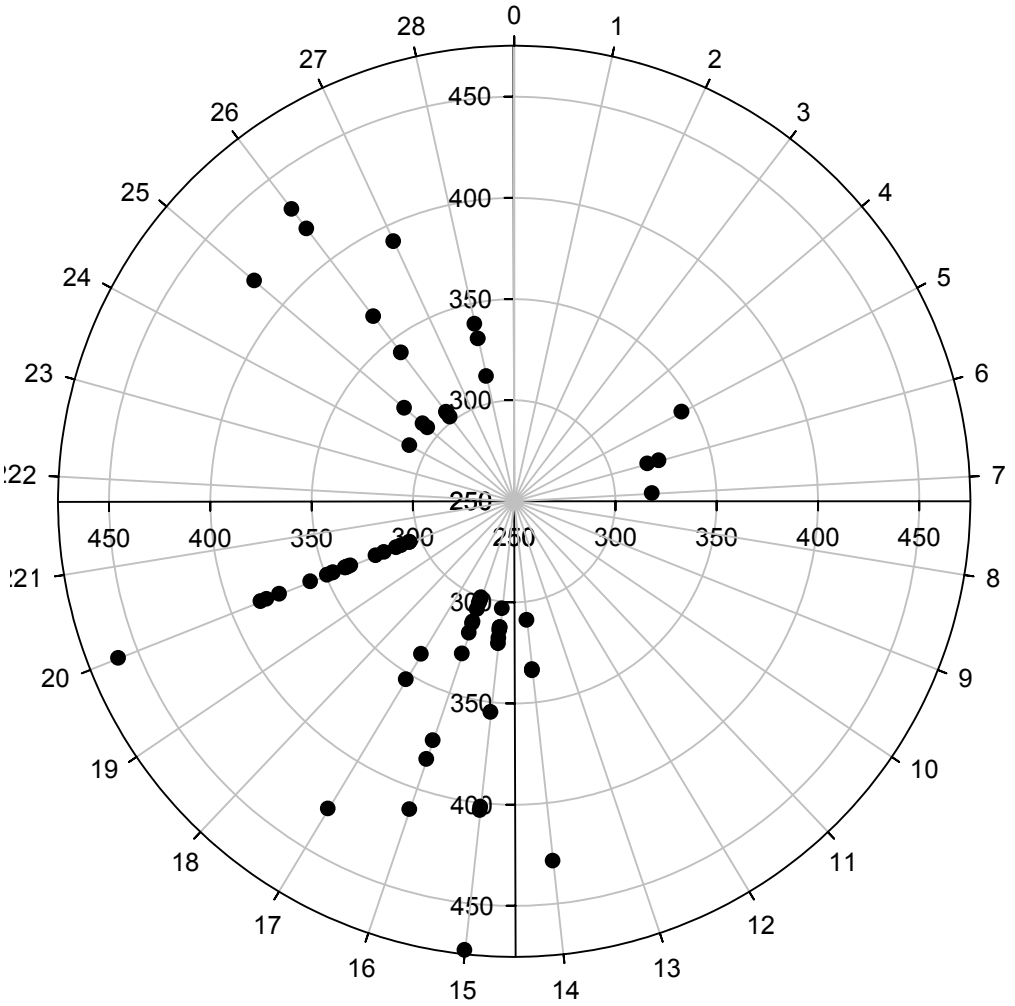

Figure 5.3 Lamb Weather Type (angular axis) for days where flow (radial axis) exceeded the long-term QMED threshold at Montford

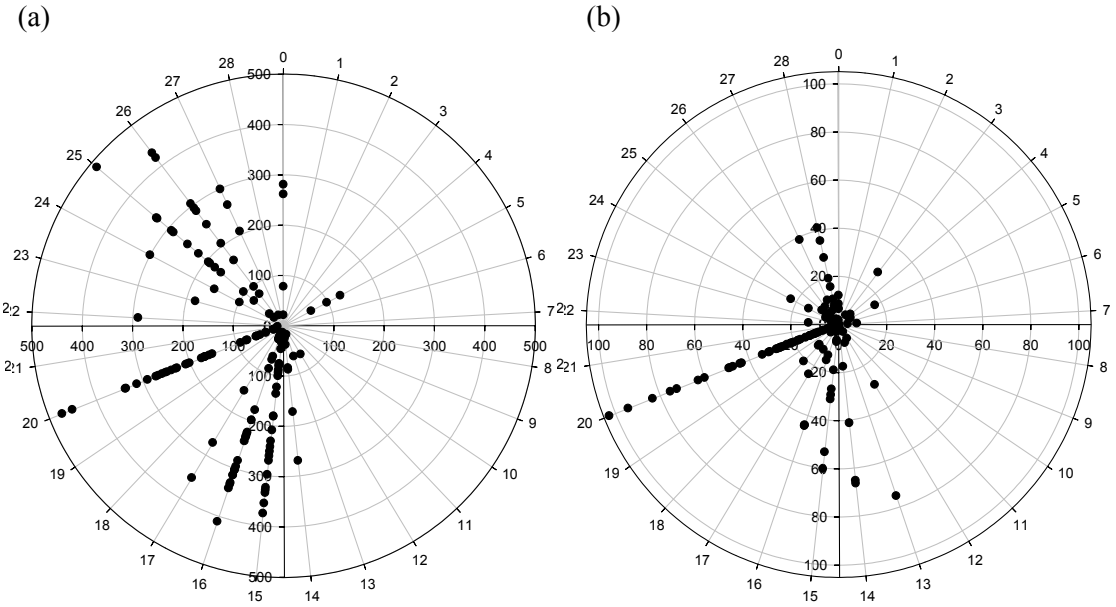

Figure 5.4 Lamb Weather Types (angular axis) for (a) annual maxima flow and (b) July maxima flow (radial axis) both for all flow gauge sites (1977-2006)

In terms of seasons, analysis of 50 extreme precipitation events across the UK by Collier *et al.* (2002) found that only a very small proportion occurred during spring, which they attributed to relatively low sea surface temperature and colder air temperatures preventing rain producing systems due to less moisture. Relating this to flow intensities in the Severn Uplands, a catchment average of all gauges indicates that 62.2% of AM flows occurred during winter, 27.6% during autumn, 9.6% during spring and 0.6% during summer. Therefore, air temperature and SST, which characteristically differ on a seasonal basis, may be influencing extreme events across the Severn Uplands (these are subsequently analysed in sections 5.4.2 and 5.4.3). Collier *et al.* (2002) also found that a number of the frontal cases of extreme precipitation had convective elements, with wholly convective events most likely to occur in June, July and August, and orographic events more likely in December, January and February.

Frontal rainfall is classed as widespread with continuous rainfall over a large area and clearly associated with a synoptic scale frontal system. Convective events are localised and less continuous in nature which result from unstable airflows during uplift, horizontal flow convergence or due to hill surfaces acting as elevated heat sources relative to the surrounding environment (Lewis and Harrison, 2007). Orographic enhancement is mainly a wintertime phenomenon where a change in airflow during forced ascension over higher topography induces the displacement of rain droplets. Topographic changes can also trigger convection which may result in the generation of rainfall. Additionally, convective and synoptic activities are not separate processes. For example, convection often occurs along strong cold fronts (McSweeney, 2007). Hand *et al.* (2004) investigated extreme events in the UK and out of the events they analysed, all of the winter induced rainfall events were orographic in nature; autumn events were mainly frontal, orographic or frontal with a convective component, spring events were sparse but convective in nature and summer events were mainly convective or convective with frontal component. For rainfall and flow extremes analysis in the Severn Uplands from 1977-2006 it can be concluded that rainfall events resulting in extreme flow intensities are generally likely to agree with these observations, with most extremes (outside the summer months) occurring due to frontal and orographic weather systems. These events are likely to be influenced by large-scale circulation patterns and SSTs, whereas summer convective events are more likely to be linked to over-land air temperatures.

5.4.2 Sea Surface Temperature

At approximately 30 km inland from the Irish Sea, sea surface temperature (SST) influences the climate characteristics of the Severn Uplands due to prevailing westerly winds feeding moisture into both frontal and orographic precipitation systems. Both global and northern hemisphere SSTs have shown signs of increase over the 20th century (Rayner *et al.*, 2003; Brohan *et al.*, 2006) and previous studies have identified a warming of the Irish Sea over the latter part of the 20th century (Young and Holt, 2007), particularly during winter over the last 20 years of the century (Hardman-Mountford and Leaper, 2003). SST data for the Irish Sea were extracted from the HadISST1 global coverage at 1º latitude by 1º longitude grid resolution (see Rayner *et al.* (2003) for dataset details). The Irish Sea was deemed to encompass an area of 4º by 4º of which three cells are classified as land cells (Figure 5.5). Figure 5.6 shows 5-year averages for SSTs in the Irish Sea. Annual average SST has increased by 0.58 ºC since 1977.

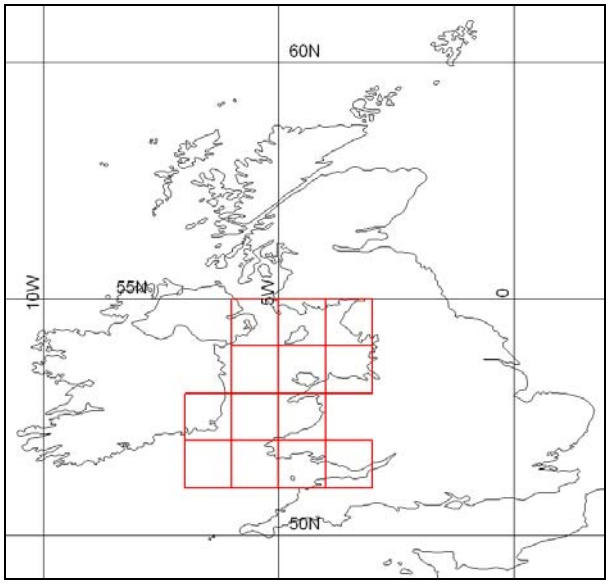

Figure 5.5 Location of HadISST1 'water' cells for the Irish Sea

Correlation coefficients were calculated between SSTs and flow and precipitation extremes on an annual and seasonal basis (Appendix 2). No significant correlations were present at the annual scale. SST showed significant negative correlation with summer flow intensity extremes at Llanymynech for winter, summer and autumn and Rhos-y-Pentref for autumn. Flow frequency extremes have increased in autumn correlating with an increase in autumn

SSTs at Llanyblodwel, and increased autumn SSTs are significantly correlated with a decrease in summer frequencies at Llanyblodwel, Llanymynech, Montford and Rhos-y-Pentref. Precipitation extremes also indicated significant negative correlations between autumn SSTs and summer rainfall frequency (Llangynog) and persistence, mainly for the 30-day maxima (Dolydd, Llangynog and Pen-y-Coed). The relatively low SST and colder air during spring means less available moisture for rain-producing systems. So, even though atmospheric instability can be high in spring months, Hand *et al.* (2004) suggested that although shower events can give short bursts of very heavy rain at that time of year, they are not capable in themselves of providing extreme rainfalls. No correlation exists between SST and spring extremes for the Severn Uplands. However, SST increases in autumn and spring were significantly correlated with a reduction in summer rainfall intensity at Dolydd and Llanfyllin respectively.

5.4.3 Air Temperature

Central England temperature records show air temperature rises of almost 1ºC over the 20th century (Parker *et al.*, 1992), with all UK regions experiencing rapid warming since the late 1970s (Perry, 2006) and unprecedented warming during the 1990s (Jones and Hulme, 1997). Temperature data for the Severn Uplands were extracted from Met Office archives at a 5 km^2 spatial resolution. Figure 5.7 shows temperature change for the catchment over the last 30 years. Average catchment temperature has increased by 1.7 ºC between 1977 and 2005, with warming occurring at a rate of approximately 0.06 ºC annum^{-1}. As expected, due to the influence of maritime airflow across the catchment, air temperatures show significant correlation with SSTs (Figure 5.8), with both variables tightly mimicking peaks and troughs in the time-series record.

Unlike the SST record, air temperature shows significant positive correlation with flow intensity at Rhos-y-Pentref, precipitation frequency at Cefn Coch and Pen-y-Coed, and precipitation persistence at Cefn Coch (Appendix 2). These stations are the highest flow gauge and the two highest precipitation gauges, indicating that flow extremes at higher altitudes may have been affected more by annual air temperature increases than at lower elevations. Seasonally, air temperature increases are correlated with a general decline in summer and an increase in winter extreme flow intensities and frequencies. Precipitation

shows seasonal increases in winter frequency, winter and spring persistence, and a reduction in summer frequency and persistence, particularly for 30-day maxima. Changes in precipitation given increased air temperature are most evident at gauges located in the most western part of the Severn Uplands, the part of the catchment which receives the greatest rainfall. Wilby *et al.* (1997) found significant positive correlations between air temperatures and the Lamb westerly weather type; as warmer weather systems traversing the country from the west usually bring waves of wet weather a correlation between temperature and precipitation would be expected.

5.4.4 North Atlantic Oscillation

Positive values of the NAO are associated with higher winter temperatures and recently the NAO Index (NAOI) has been showing trends towards the positive phase, which may be partly due to increasing atmospheric temperatures (Gillett *et al.*, 2003). NAO indices were retrieved from the Climatic Research Unit (CRU) database (after Jones *et al.*, 1997). The NAOI shows larger correlation with air temperatures than SSTs with emphasis in the winter and spring seasons. To some extent, the previous analyses of weather type and air temperature act as a proxy record for changes in the NAO by monitoring the strength of westerly airflows. This indicates that given a positive NAO value westerly airflow patterns are stronger and air temperatures are higher. This is observed in the record for the Severn Uplands (Figure 5.9). Higher winter NAO values are associated with significantly higher air temperatures ($p < 0.001$) and slightly higher SSTs. As the NAO is linked to increased westerly airflow this itself is a proxy for precipitation, as greater rainfall is prevalent originating from westerly-driven frontal systems in the UK.

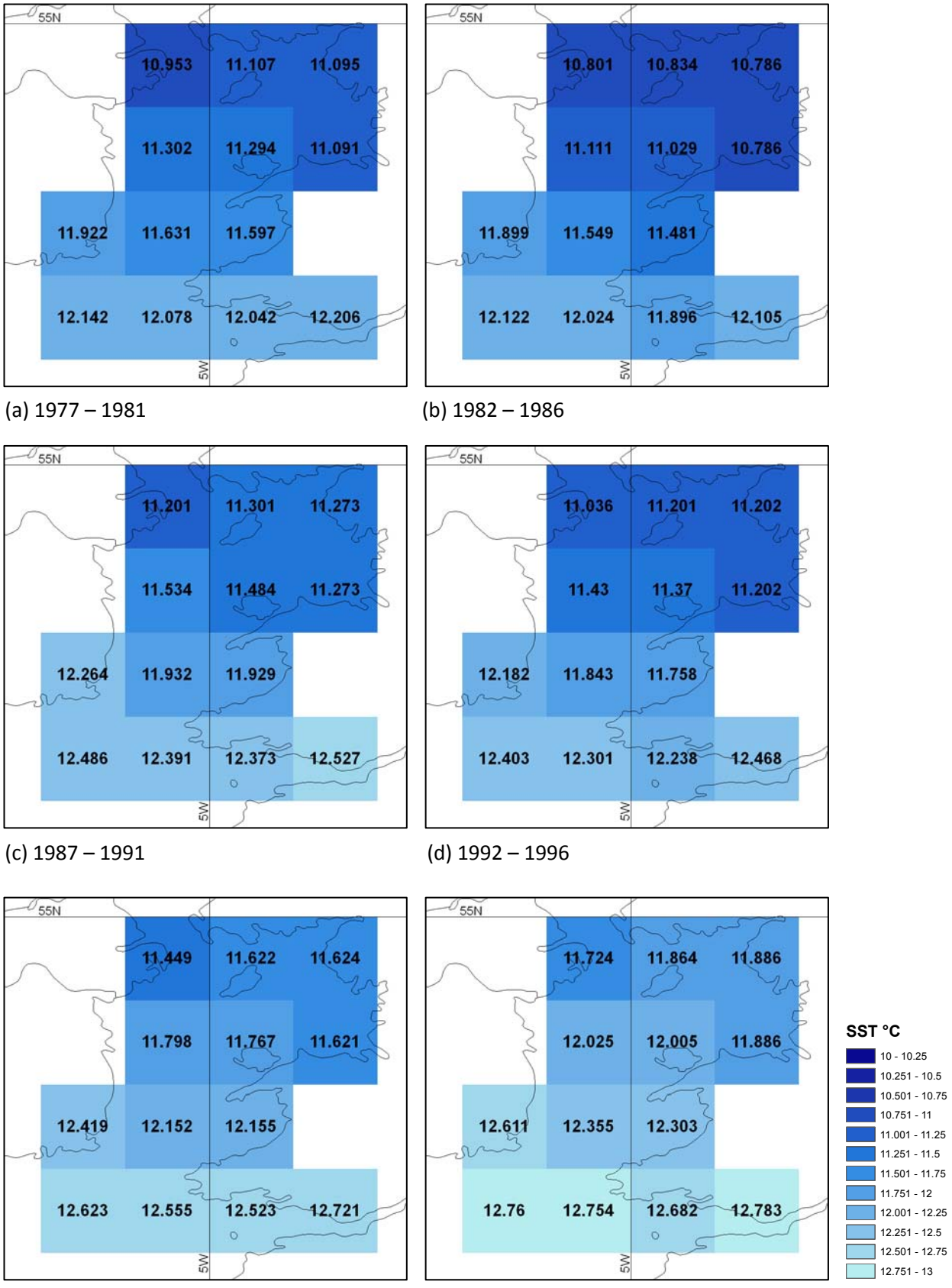

Figure 5.6 Average annual sea surface temperatures for the Irish Sea over 5-year periods at 1° grid resolution

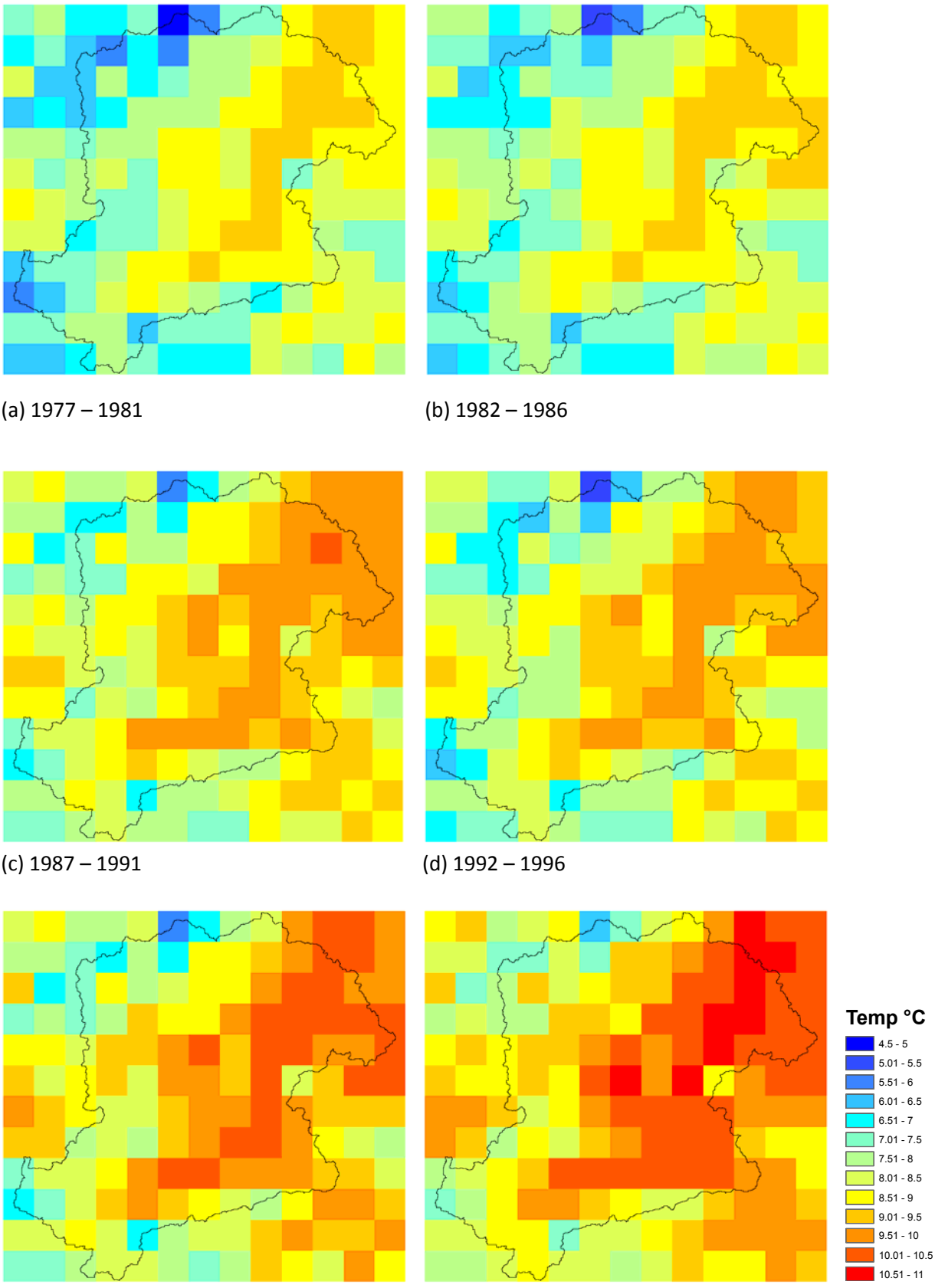

(a) 1977 – 1981

(b) 1982 – 1986

(c) 1987 – 1991

(d) 1992 – 1996

(e) 1997 – 2001

(f) 2002 – 2005

Figure 5.7 Average annual land surface temperatures for the Severn Uplands over 5-year periods (except 2002-05) at 5km² grid resolution

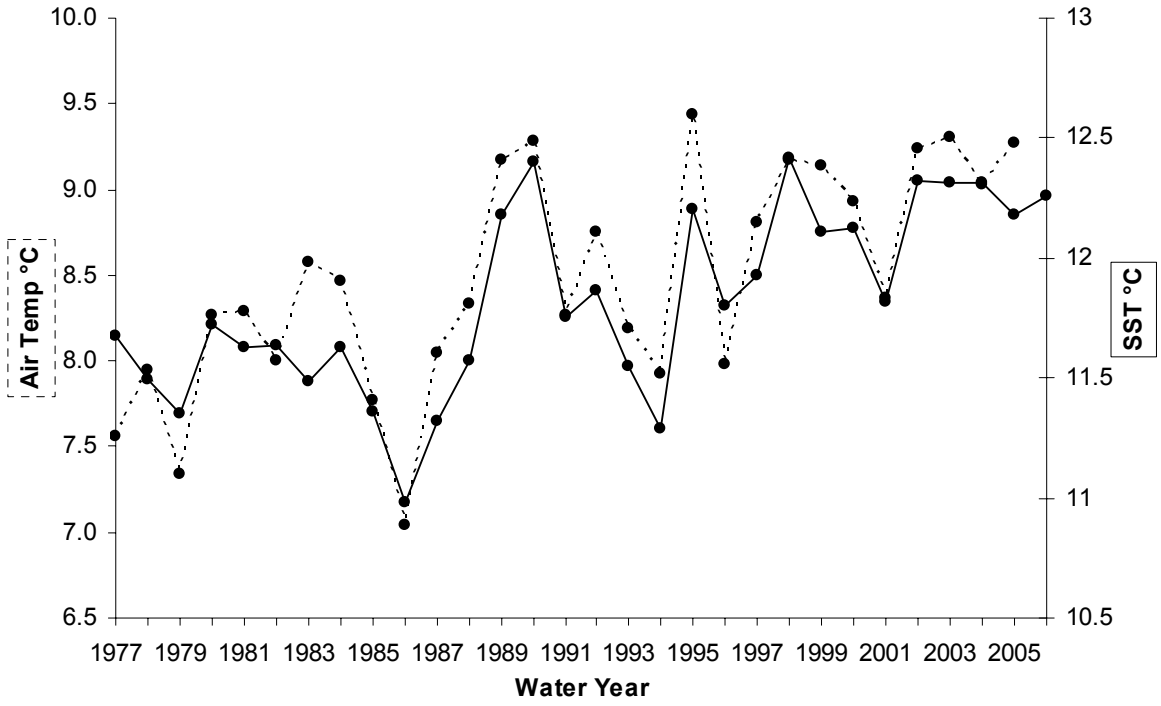

Figure 5.8 Air temperature and SST time-series from 1977 to 2005/6.

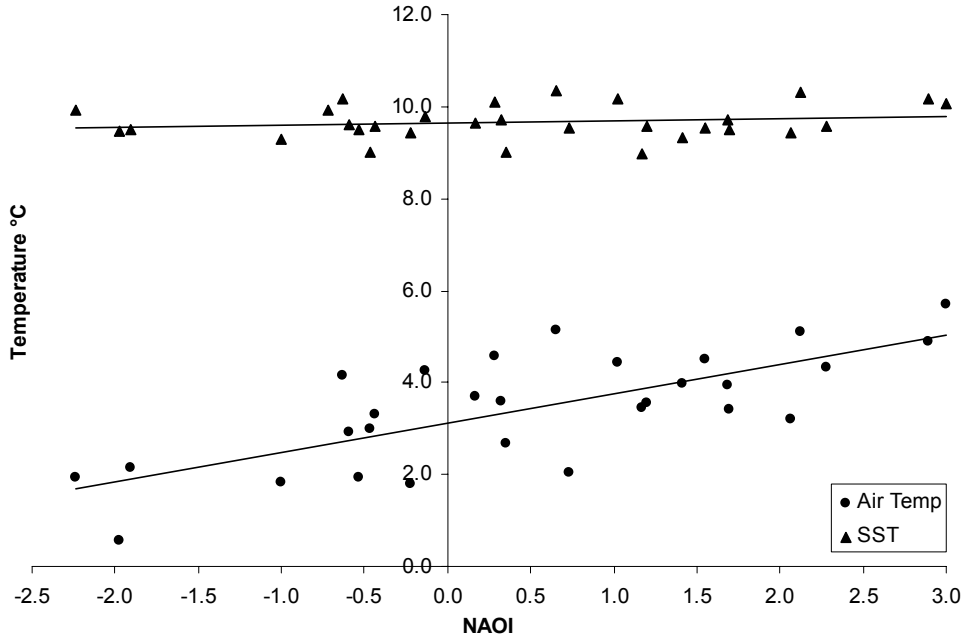

Figure 5.9 A comparison between winter NAO Index and winter air and sea surface temperatures

The NAO has been found to be correlated with winter precipitation and winter runoff in the UK due to enhanced westerly airflows and a more northerly storm track (Hannaford and Marsh, 2003; Wilby *et al.*, 1997; Shorthouse and Arnell, 1997; McElwain and Sweeney, 2003). The strength of the NAO is greatest in winter so this was the season predominantly analysed. No significant correlation coefficients between annual changes in the NAO and annual precipitation and annual flow extremes were found (Appendix 2). The winter NAOI, however, supporting evidence from the literature seems to have a significant influence over extremes in the Severn Uplands. All flow gauge locations experienced an increase in extreme winter flow frequencies relative to higher values of the NAOI, and extreme winter rainfall frequencies and persistence increased in the same manner. Similar to correlated changes between precipitation persistence and air temperature, significant positive correlations with the NAOI were found for the maxima of the longer 30-day rainfall series. This suggests that the larger the positive values of the NAOI in the winter phase, the more likely extreme flows and precipitation will resultantly occur during this season.

In addition to correlations of the NAO in winter with hydrological extremes, the July NAOI was compared with July extremes to determine whether North Atlantic circulation affects summer extremes. No significant correlation was detected between the July NAOI and July precipitation maxima, but significant negative correlations were present with the July flow maxima at Llanyblodwel and Llanymynech ($p<0.05$), where large flow maxima coincided with large negative values of the NAOI. In the summertime, negative values of the NAO are usually associated with high geopotential height across the high latitudes of the North Atlantic, with westerly winds consequently weakened and less persistent over the British Isles. This would suggest a convective component to precipitation formation and physical catchment characteristics having increased influence on flow regimes.

5.4.5 Snow cover and depth

A warming climate is thought to be the main reason behind decreasing snow accumulation in northern Europe. Since the late 1970s the UK has experienced a substantial reduction in the average number of days with snow lying which is most evident during spring (Harrison *et al.*, 2001). Snowfall has previously been linked directly with the NAO due to changes in Atlantic low pressure systems and the subsequent strength and persistence of westerly

airflows (Osborn *et al.*, 2000). Higher temperatures and moisture content of airflows originating from the North Atlantic, associated with the positive phases of the NAOI, has resulted in increased ephemeral snow cover during winter and spring (Harrison *et al.*, 2001). The UKCIP02 scenarios predict 80-90% reductions in snowfall coverage over Wales and western England by the 2080s (Hulme *et al.*, 2002); this could severely change upland hydrological systems where snow packs have traditionally influenced flow regimes.

Across Wales, the number of days recorded where snow cover was more than 50% (5 km² grid-based) has declined severely since 1977 (Figure 5.10). Snow has decreased from a maximum of 61-70 days cover (1997-1981) to less than half, at approximately 21-30 days (2001-2005). Heavier snow cover has retreated from widespread national coverage to small clusters along the central mountainous spine. For the Severn Uplands snow cover has reduced from an average of 30 days cover in 1977 down to 12 days in 2005 (Figure 5.11). Cumulative winter season snow depth records for Northern Snowdonia also indicate a significant snow pack decline (Figure 5.11). The Countryside Council for Wales predicts that Snowdon may lose its winter snow cover by 2020, and with a peak height approximately 330 m below Snowdon, the Cambrian mountain range, which borders the Severn Uplands, will certainly become snow-free before Snowdonia. Snowdon's snowline has moved from 100 m above sea level to 500 m since the mid-1990s (Williams, 2007). If these thresholds for snow depth are crudely extrapolated to the Severn Uplands catchment, a 500 m snowline presently covers a mere 3.9% of the catchment; a reduction from 86.6% when the snowline previously reached 100 m (based on catchment elevation data; CEH Wallingford, 2005).

In many mid to high latitude regions the freeze-free season has lengthened and rising temperatures have reduced substantially the influence of snowmelt and frozen ground in UK flood events. In the past, flood events in the UK were often induced by snowmelt, but the frequency of these event types has declined in recent years (Hudson, 1998). Snowmelt floodwaters may not be extreme in quantity, but in terms of timing they are rapidly transferred to the channel network by frozen ground and less restricting vegetation. Temperature increases are also likely to trigger an earlier temporal release of spring meltwater. Burn and Hag Elnur (2002) state that earlier snowmelt is expected due to increased winter temperatures and Christensen *et al.* (2007) speculate that over the course of the 21st century the duration of the snow season is likely to shorten by potentially one to three months in Northern Europe and snow depth will decrease by 50 to 100% across most

of Europe. Increasing winter temperatures will result in a growing proportion of rainfall at the expense of snowfall, which will lead to acceleration in runoff formation processes (Frei *et al*., 2000). Changes in snowmelt amounts within the Severn Uplands may be having an influence on flow regimes, particularly in the mountainous western part of the catchment. Additionally, the high basin impermeabilty over much of the catchment area may enhance such processes. Arnell (1999) found that a changing climate with rising temperatures strongly affects the spatial distribution and amount of snow cover which has an affect on the timing of flows throughout the year, with a reduction in spring flow and an increase in winter flow.

Comparison of snow cover with both SST and air temperature indicates a significant negative correlation between snow cover and temperature (Figure 5.12). Additionally, as snow cover has decreased, AM flows have generally increased, as illustrated by a comparison with Llanyblodwel, Montford and Rhos-y-Pentref, the three flow gauges with increasing AM trends (Figure 5.13). The largest correlation between these two variables is at Rhos-y-Pentef, a gauge which is located relatively close to the Cambrian Mountains, where snowmelt rates will likely be the most influential. Correlations between precipitation values and snow cover in snow-influenced regions are also present for the Severn Uplands; Dolydd, Llangynog and Pen-y-Coed all have moderate correlations with winter rainfall (Appendix 2).

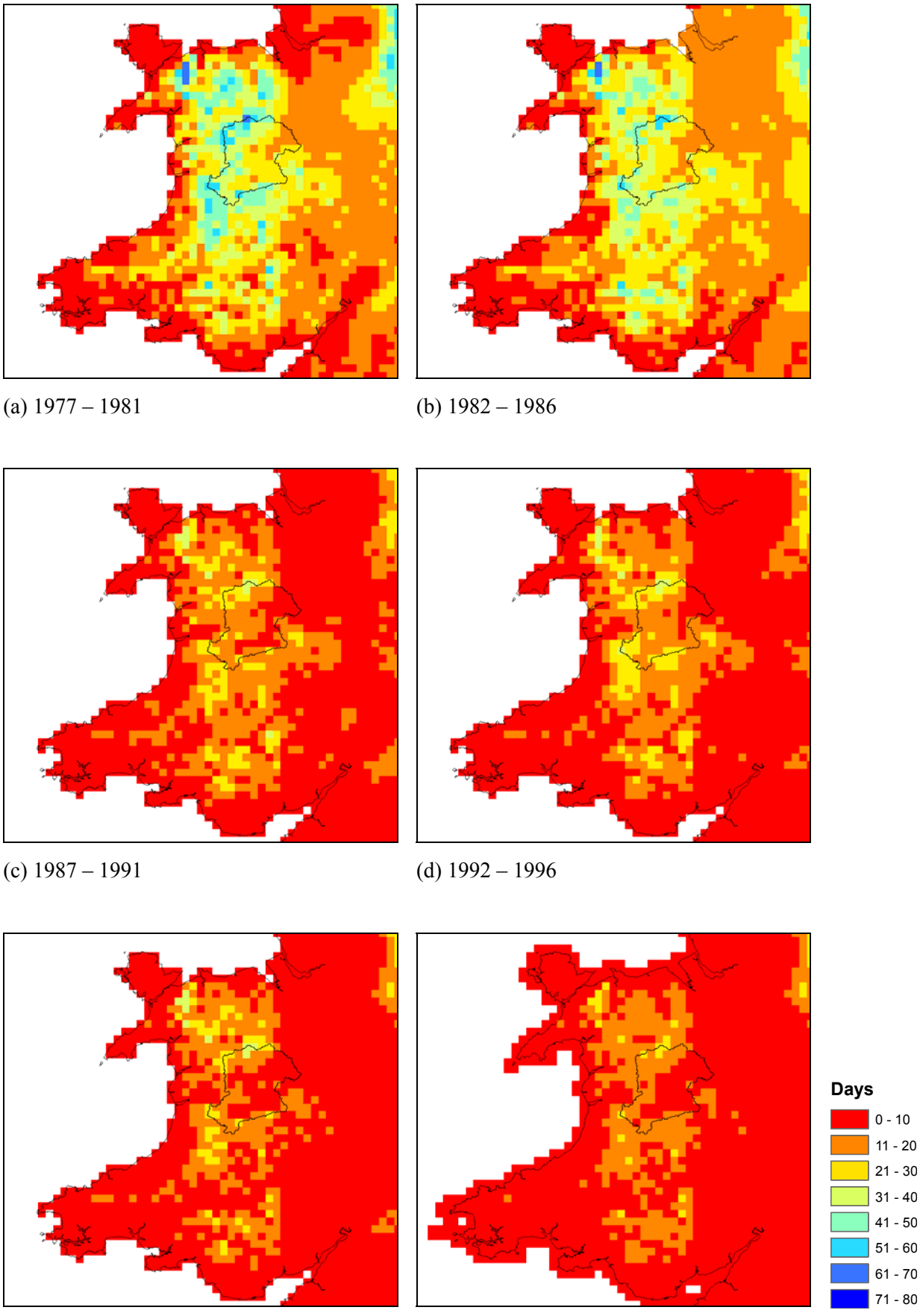

(a) 1977 – 1981

(b) 1982 – 1986

(c) 1987 – 1991

(d) 1992 – 1996

(e) 1997 – 2001

(f) 2002 – 2005

Figure 5.10 Average annual number of days where percentage snow cover is > 50% over 5-year periods (except 2002-05) at 5km² grid resolution. Severn Uplands catchment is outlined.

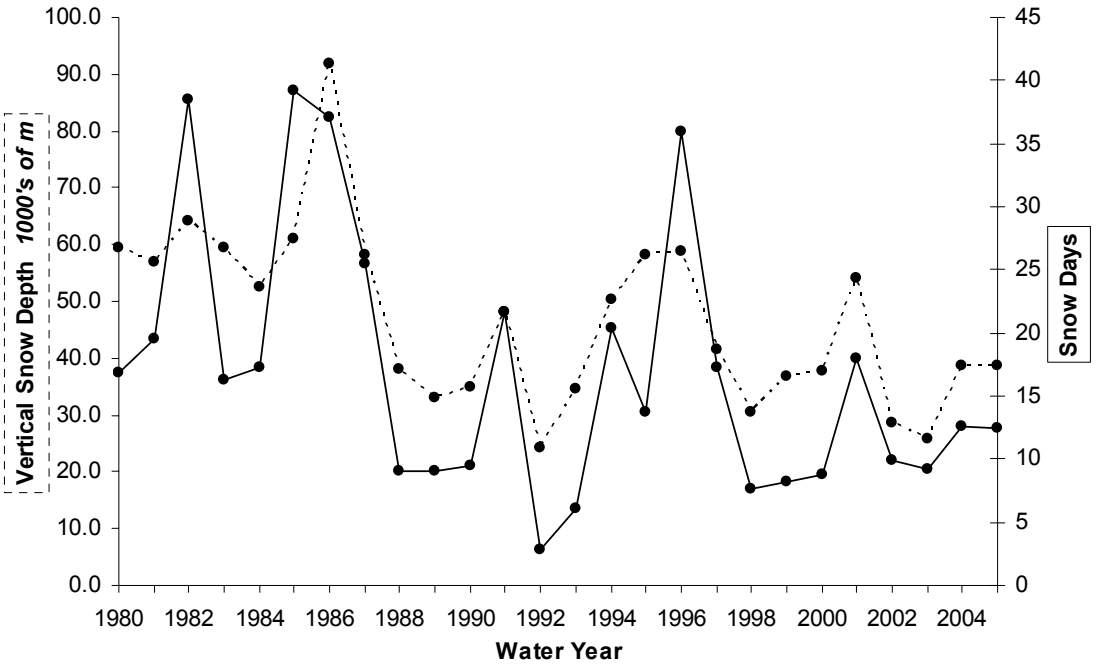

Figure 5.11 Time-series of winter season vertical snow depth for northern Snowdonia and average annual number of snow days where snow cover > 50% for the Severn Uplands.

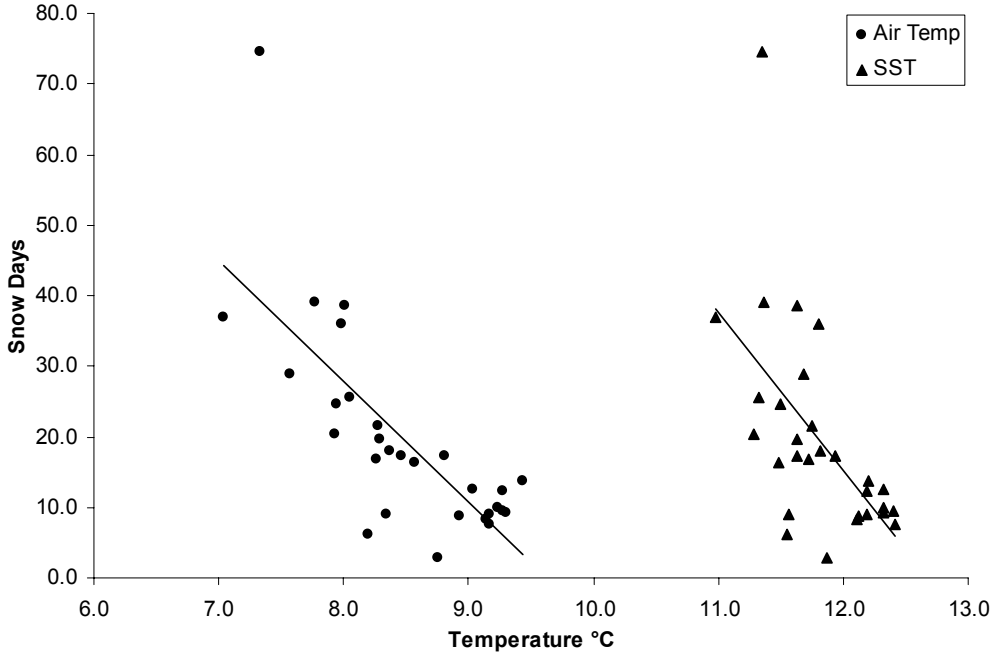

Figure 5.12 A comparison of annual snow days where snow cover > 50% with annual average temperature; both air and sea surface.

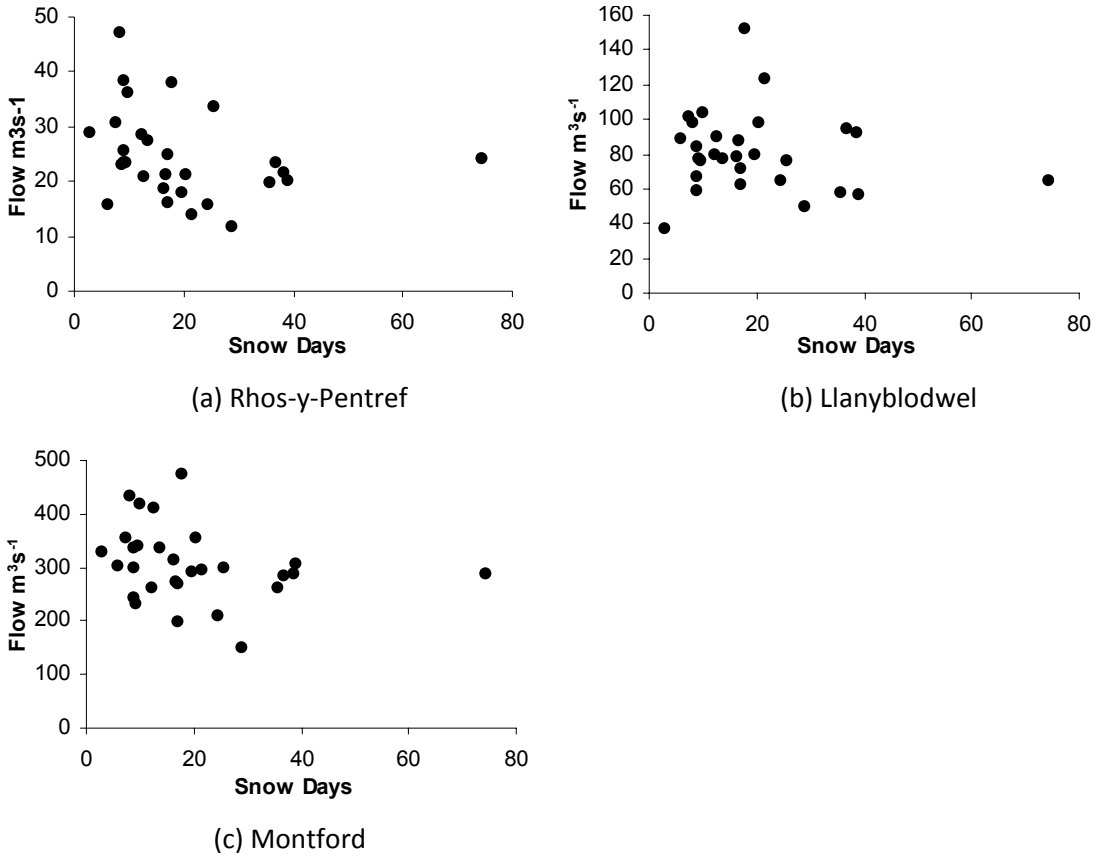

Figure 5.13 A comparison of the number of snow days where snow cover > 50% and AM flows at (a) Rhos-y-Pentref (b) Llanyblodwel and (c) Montford.

5.4.6 Teleconnections

Even further afield than the NAO, the El Niño Southern Oscillation (ENSO) has been found to influence climate regimes across the globe on a cyclical scale and worldwide climate anomalies could be influencing local weather patterns in the Severn Uplands. Fraedrich and Muller (1992) and Fraedrich (1994) found evidence linking El Niño events to weather over the North Atlantic and Europe, and Wilby (1993) provided evidence for correlation between El Niño events and rainfall over the British Isles. Oceanic Niño Index (ONI) data were retrieved from the NOAA online archives. This is a 3 month (seasonal) running mean of SST anomalies in the Niño 3.4 region (central equatorial Pacific) based on the 1971-2000 base period. Cold and warm episodes, indicative of La Niña and El Niño episodes, are defined when the ± 0.5 °C threshold is sustained for a minimum of five consecutive overlapping seasons. Strong events are observed at ± 1.5 °C. Figure 5.14 shows the time-series of the ONI and ENSO years. Strong El Niño occurred in 1982-83, 1991-92 and 1997-98 and strong La Niña was apparent in 1988-89 and 1998-2000. The

annual total number of times the QMED was exceeded across the basin at the five flow gauges is also indicated. There does not seem to be any clear connection between ENSO events and flood events. And there are no significant correlations between the ONI and precipitation and flow AM for the Severn Uplands (Table 5.7). Furthermore, research by Benner (1999) finds no convincing relationship between central England temperatures and NINO 3 SST (a measure of the amplitude of ENSO). El Niño may be indirectly affecting flow and precipitation extremes in the Severn Uplands through its influence on global circulation regimes, but no strong link between the variables can be identified.

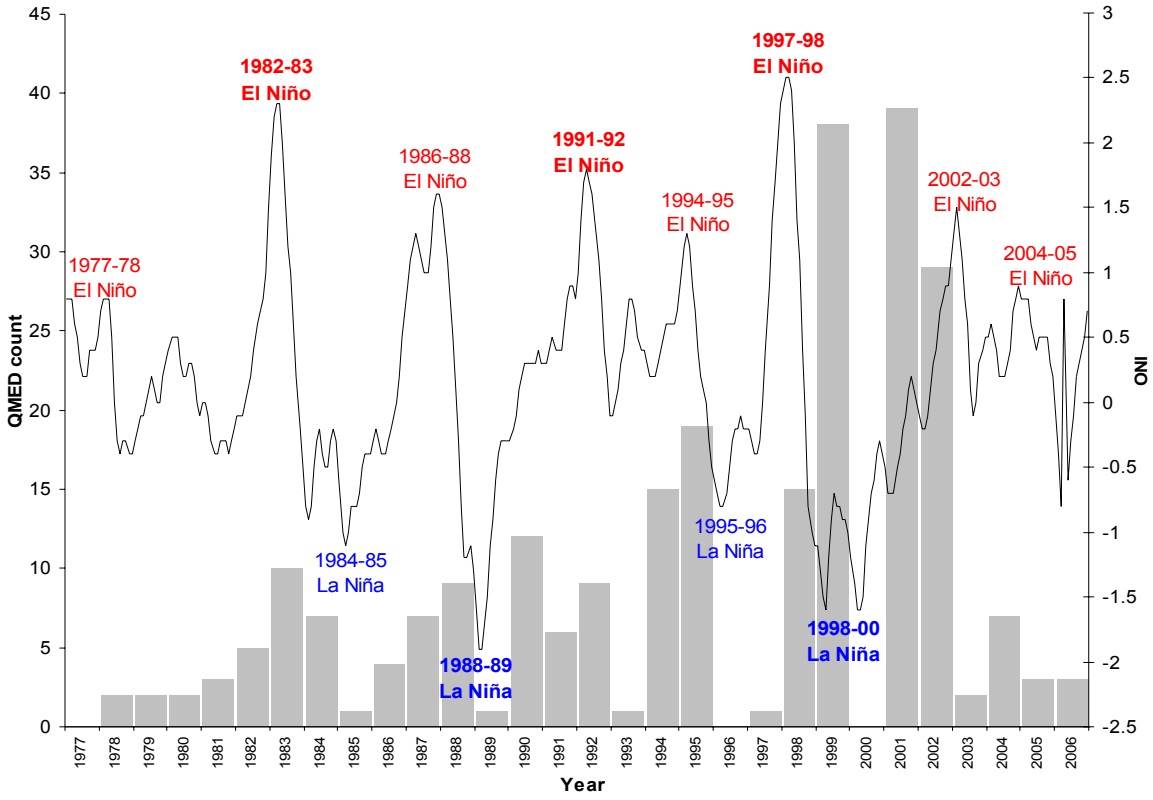

Figure 5.14 Total number of times the QMED threshold was exceeded for all gauges. ONI with ENSO years labelled. Bold indicates strong El Niño/La Niña events.

5.5 Discussion

UK National trends as discussed in chapter 2 reveal an increase in flood frequency and a change in seasonality over the last 30 years. It has to be emphasised that every river system is unique, each having a different multitude of factors which influence fluvial processes. Therefore, trends observed in the Severn Uplands may not be comparable directly to those on a national scale as local changes in climate are not well understood and may be vastly

different to those observed on a national scale (Svensson *et al.*, 2006). Nonetheless, a loose comparison can be made. Changes in high-flow frequency for the Severn Uplands suggest that a seasonal shift may have occurred, with higher extreme flows evident in winter and lower extreme flows in spring. Trend analysis revealed increasing trends in intensity but not frequency, and July maxima have increased.

In terms of precipitation, national trends in the literature recognised increases in precipitation intensity, frequency and multi-day heavy rain, as well as an increase in winter wetness. Findings for the Severn Uplands have identified similar trends. Seasonal changes are summarised in Figure 5.15. Changes in precipitation intensity, frequency and persistence are all apparent, with seasonal increases not only in winter but also autumn. Spring has conflicting trends with some sites showing decreases and others experiencing an increase. Annual trends are prevalent for increases in precipitation persistence, but not in intensity or frequency. This would imply that longer periods of heavy rain are contributing to changes in flow, but probably via intermediary changes such as catchment saturation levels (this is further discussed in Section 5.5.2).

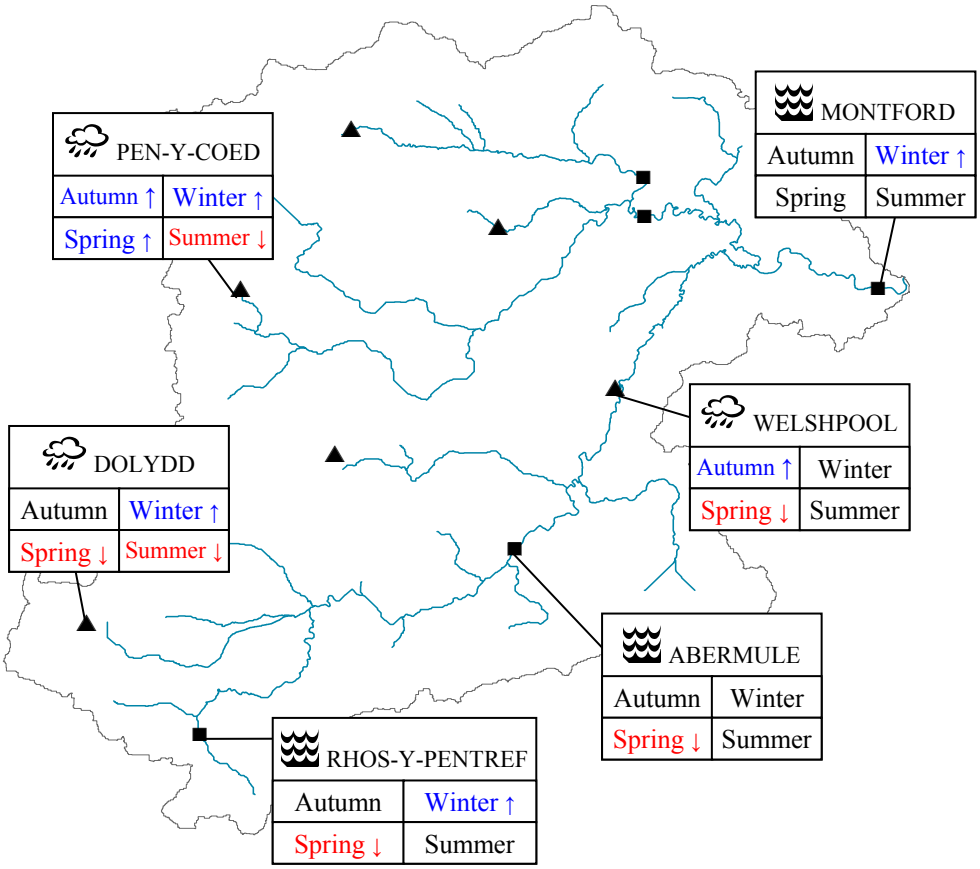

Figure 5.15 Seasonal increases (blue) and decreases (red) in precipitation and flow based on statistically significant trends at $\alpha < 0.05$.

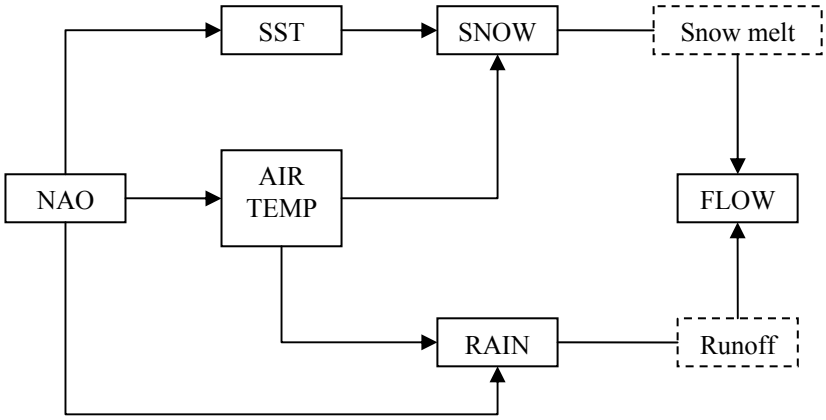

Figure 5.16 Links between climate variables and hydrology

Climate variables have revealed some interesting patterns and have provided an explanatory basis for changes in precipitation and flow extremes. Multiple links between variables have been identified and are represented schematically in Figure 5.16. This figure summarises the climate analysis of Section 5.4. All climate variables explored were found to be interlinked, with the NAO, air temperature, rainfall and snow cover all directly influencing flow extremes, and SST having an indirect effect. Research by Hand *et al.* (2004) implied that all extreme rainfall events are highly likely to cause flooding and supports findings by Collier and Fox (2003) that flooding will be exacerbated if the rain falls in sensitive catchments, over steep orography or over already saturated ground. Even though climate variability explains some underlying patterns in the Severn Uplands extremes analyses, there are still two other important factors which need to be considered: (i) changes in climate over the years which have shifted the occurrence of extremes temporally and (ii) any other physical catchment changes, such as human-induced modifications to land cover, which have influenced changes in flow extremes directly.

5.5.1 Temporal climatic shifts

Changes in rainfall and flow time-series for the Severn Uplands may be attributable to a change in climate regime over the last 30 years, with rainfall extremes of both magnitude and intensity shifting from the winter-spring months to the autumn-winter months. Spatial changes in precipitation amounts may also coincide with seasonal shifts. Analysis of Irish precipitation records by McElwain and Sweeney (2003) revealed that the autumn and

winter seasons showed the greatest increases in precipitation, an observation which is mimicked in the Severn Uplands. Summer rainfall shows general decline and may be related to the influence of global climatic changes on regional warming. However, analyses of extremes conducted indicated an upward trend in July flow extremes. A viable explanation may be that a warmer climate will not only affect rainfall regimes, but also influence catchment characteristics, such as evapotranspiration and soil porosity, which will simultaneously act in changing flow regimes.

By comparing precipitation changes with streamflow, it is plausible to suggest that a shift in rainfall towards autumn-time may be resulting in the more extreme flows observed in autumn and winter. Multiple factors could be influencing this shift, yet one climate variable which has changed drastically over the last 30 years and appears to be influencing catchment changes is temperature. Increases in temperature are unlikely to be directly influencing changes in flow patterns, but are probably having an indirect effect through snowmelt changes (as described above) and alterations in catchment physical properties. Bower *et al.* (2004) found that regional patterns in flow regime shape appear to be driven by rainfall seasonality and modified by geology.

Increases in summer temperatures have elevated evaporation demands and could result in substantial soil moisture deficits extending through a longer portion of the spring and autumn seasons (Reynard *et al.*, 2001). The wetter the initial state of the catchment the higher the proportion of incident rainfall that will contribute to the flood peak (Beven, 1993). Periods with larger than average annual rainfall may be associated with fluctuations in soil moisture deficits which contribute to variation in the hydrological response of a catchment, especially in the summer months (McEwen, 1989). Drier soil conditions may reduce the length of the flood season or cause a temporal shift in high-flow occurrence.

5.5.2 Physical catchment properties

Changes in land cover and land use have direct implications on hydrological processes through evapotranspiration, soil stability and the timing and quantity of surface runoff. Changes in runoff generation are affected by soil compaction, the efficiency of land drains and the connectivity of flow paths. Land use is found to have the greatest influence on the

middle range of flow events (Gilman, 2002), although Prudhomme *et al.* (2001) found the impact of land use change was mainly significant for the low flow regime. For upland areas in the UK flow generally follows major rainfall events (or snowmelt) and hydrological extremes are more impacted by climatic and physiographic changes than land use management (Newson, 1997; Fohrer *et al*., 2001; Gilman, 2002). Higgs (1987) concludes that irrespective of catchment size, the frequency of heavy rainfall, presumed to be independent of land use, is generally the most important variable defining flood frequency. Howe *et al*. (1967) made the point that intense storm event frequency is thought to be the triggering mechanism for increased flooding, but that land use changes further aggravate the problem.

O'Connell *et al.* (2007) claimed that agricultural change may cause local flooding, but stated that there is an almost complete lack of evidence that local-scale effects aggregate, causing larger scale impacts downstream. Gilman (2002) also expressed that little direct and incontrovertible evidence exists detailing the effects of extensive land use changes on the flood hydrology of catchments, particularly in rural areas. A number of studies investigating land use change and hydrology in the Severn Uplands have all concluded that isolating anthropogenic effects from climate variability is very difficult (e.g. Hudson and Gilman, 1993; Kirby *et al.*, 1991). Analysis for the Severn Uplands has indicated numerous relationships between climate variables and precipitation and flow extremes within the catchment. Nonetheless, land cover and land use change may also be affecting extremes by altering land characteristics which could be enhancing the impacts of changing climate variables.

Land *cover* change in the Severn Uplands has been fairly minimal in recent years. Map differencing of the 1990 and 2000 Corine land cover maps (Figure 5.17) indicates that change for that period occurred in the forest and scrub land classification categories, with a predominant increase in forest to the north-west of the catchment and an increase in scrub to the south-west. However, during the mid-20th century changes in forestry were observed. From the 1930s onwards, large areas in the Severn were planted with fast-growing conifer species (Brandt *et al.*, 2004) and many trees in the catchment are now managed on a forest rotation cycle of about 40 years. Mature forest reduces peak flows due to large evaporation levels of canopy interception and an increase in water storage capacity of soils beneath trees. Afforestation can increase precipitation interception, transpiration and soil moisture deficits (Fohrer *et al.*, 2001), but Jones (1997) speculates that a modest

change in vegetation has more impact on soil infiltration capacity than through modified interception of rainfall. Felling of the forest since the 1980s has resulted in an increase in flows and reduced evapotranspiration losses due to replantation in smaller coupes (Marc and Robinson, 2007).

Even though some of the upland catchments are all heavily forested, the regulating effect of reservoirs in upstream areas obscures the impact that tree cover has on river flows. Yet despite the presence of the Vyrnwy and Clywedog dams, these upstream catchments are still capable of generating very high flows, with flood peak magnitudes similar to those recorded downstream at Montford, where the catchment is much larger but slower to respond (Gilman, 2002). Reservoirs and other human-induced impacts on catchments appear to affect trends in the low-flow series rather than the flood series (Kundzewicz *et al.*, 2005). Gilman (2002) also states that a quickening in the upstream hydrograph response is due to the recent increase in rate of surface runoff cause by tile drainage and improved agriculture.

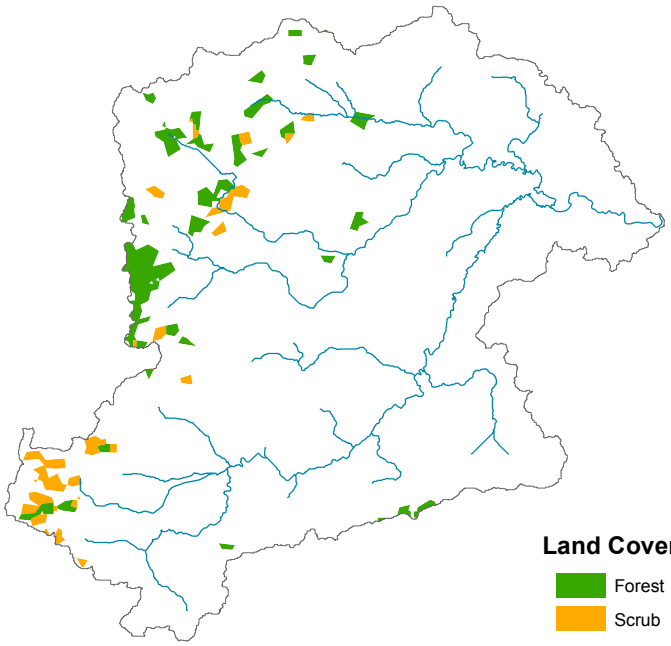

Figure 5.17 Corine land cover change in the Severn Uplands from 1990 to 2000

Changes in land *use* can also contribute to changes in runoff regimes. Modern agricultural practices in the UK may be causing a reduction in soil water storage capacity and infiltration rate leading to overland flow and rapid runoff of water into rivers (Marshall *et*

al., 2006). Over the last century there has been an increase in agricultural intensification due to economic pressures, with an increase in stocking rates and the amount of land under improved grassland production. This, combined with hedgerow and woodland buffer strip removal, has enhanced runoff generation, at least at the local scale (Marshall *et al.,* 2009; Wheater, 2006). Physical properties of soil are affected by intensive grazing of livestock (Marshall *et al.,* 2009) and Marshall *et al*. (2006) found that infiltration rates in tree-planted areas were up to 60 times higher in comparison to adjacent grazed areas.

Observed land use changes are likely to affect soil characteristics and subsequent susceptibility to climate induced changes. Desiccation cracking of soils and resistance to re-wetting (hydrophobicity) can induce rapid lateral movement of runoff over unsaturated soils (Doerr *et al.*, 2000). In the summer months, given the high land temperatures, flash flooding from convective storms may arise. Soil properties are quite sensitive to summer drought, especially the effect of hydrophobicity and macroporosity in the peat and peaty podzols in upland Wales. These factors are likely to increase overland flow and shallow through-flow and with them the risk of severe high-flow events in the autumn (Pilling and Jones, 2002). Increased convective precipitation from a westerly maritime source could also be occurring during autumn, as SSTs have climbed and increased evaporation may have caused increased convective storms (Fowler and Kilsby, 2002). The alternative extreme soil state is that of complete saturation. Pilling and Jones (2002) state that heavier precipitation events are expected to coincide with times when the soil is close to or fully saturated. Saturated soils can result in rapid runoff as was the case during the summer 2007 floods across the UK. In this case, a series of precipitation events can lead to ground waterlogging and once the saturation level is reached, any further rainfall will be directly transformed into runoff at a rapid rate of response.

Currently, major uncertainty surrounds the impact of land management practices especially in upland regions (Marshall *et al.*, 2009). Jackson *et al.* (2008) highlighted the potential significance of small-scale land management changes for reducing runoff, although results were inconclusive due to substantial variation and uncertainty in the model parameterisation. Water-balance effects of afforestation can be modelled relatively accurately but the impacts of drainage change can not be easily predicted (Wheater, 2002). If drainage changes are of sufficient spatial extent they may significantly alter fluvial hydrology, but the effects are not known at present (Wheater, 2006). The relative effects of land use management interventions decrease with an increasing event magnitude (Jackson

et al., 2008). Therefore, although land cover and land use change is important, the affects these changes have on runoff regimes during extreme high-flow events are yet to be adequately quantified, particularly in the short- and medium-term, due to a lack of relevant data (Wheater 2002).

5.6 SUMMARY

The application of the Mann-Kendall trend detection test identified some significant trends in rainfall and flow particularly in time-series data in the Severn Uplands. Rainfall showed signs of having increased in winter and autumn and decreasing in summer. Spring rainfall has increased in the Vyrnwy catchment but decreased in the main Severn basin. Flows were found to have increased in winter and July, and decreased in spring. Overall, trends are not particularly strong as there is little temporal consistency across the extremes for intensity, frequency and persistence, and they could have occurred by chance. Nonetheless, the trend test statistics show some significant results which may be explained by a recent shift in climate variability of the Severn Uplands, as inferred by snow and temperature proxies, which is likely to be explained by an underlying global temperature rise. The most likely changes directly influencing flow regimes are soil desiccation and evapotranspiration which are linked to temperature changes and minor alterations in land use. Changes in precipitation extremes are mainly controlled by the positive and negative phases of the NAOI, with a large positive influence during the winter months. Some caution has to be extended when interpreting the time-series extremes analysis results due to constraints of the test statistic used and the length of the record analysed. This is further discussed in Chapter 9.

Previous hydrological data collated for the Severn Uplands catchment indicates that upland streamflow generation is not just a simplistic rainfall-runoff process, as a more complex system actually exists (Haria and Shand, 2004). Analysis undertaken in this chapter seems to support this statement. Trends in extremes have been identified in flow records but cannot be readily coupled to trends in extreme precipitation. A somewhat complex underlying structure of interlinking variables exists between basin runoff, physical catchment properties and climate characteristics. It terms of the literature reviewed in

Chapter 2, significant trends in flow extremes found in the Severn Uplands generally followed a similar pattern to those observed on a national scale.

With climate variability envisaged to increase over the coming century, as identified in the literature, it is essential that changes in extremes are modelled as accurately as possible. Chapter 9 looks at future climate changes in the Severn Uplands and the effect of hydrological extremes. However, to model effectively the impacts of climate change on flow characteristics an intermediary stage is required, as research in this chapter has emphasised. Physical basin properties need to be represented virtually by parameter sets, and physical processes hydrologically modelled using various mathematical equations. Thus, a catchment hydrological model was selected to enable rainfall inputs to drive flow outputs. Chapter 6 presents the hydrological model analysis for the Severn Uplands looking at data and model accuracy, as well as model development for a baseline to investigate future changes in hydrological extremes.

CHAPTER 6

Modelling the Severn Uplands

This chapter presents the HEC-HMS model of the Severn Uplands. A rainfall-runoff model was selected to simulate flows in the catchment as, being an upland area, precipitation is rapidly translated into river flows. The necessary pre-processing stages of model development are described and calculated parameters are listed. An extreme precipitation event was then used to drive the model and generated results are presented. Flow observations coinciding with this time period were used to calibrate the model and validation was achieved using an additional extreme event. Prior to calibration a sensitivity analysis was performed to locate model-sensitive parameters and following validation, uncertainty analysis was undertaken to quantify uncertainty bounds.

6.1 DATA SELECTION

To model the Severn Uplands topographic data were pre-processed with a river network file to create a virtual representation of the catchment. A digital elevation model (DEM) was acquired from the United States Geological Survey (Figure 6.1). The elevation data were derived from the Shuttle Radar Topography Mission using synthetic aperture radar (SAR) data to define the topography of the region. Altitude readings were conveyed as a digital raster grid with 20 m absolute horizontal accuracy and 10 m relative vertical height accuracy (USGS, 2002). The input shapefile of the stream network (Figure 6.2) was obtained from the Environment Agency. Parameters were then calculated within a GIS, using mathematical formulae, or extracted from the literature. Time periods of extreme precipitation and flow data were selected to drive, calibrate and validate the model.

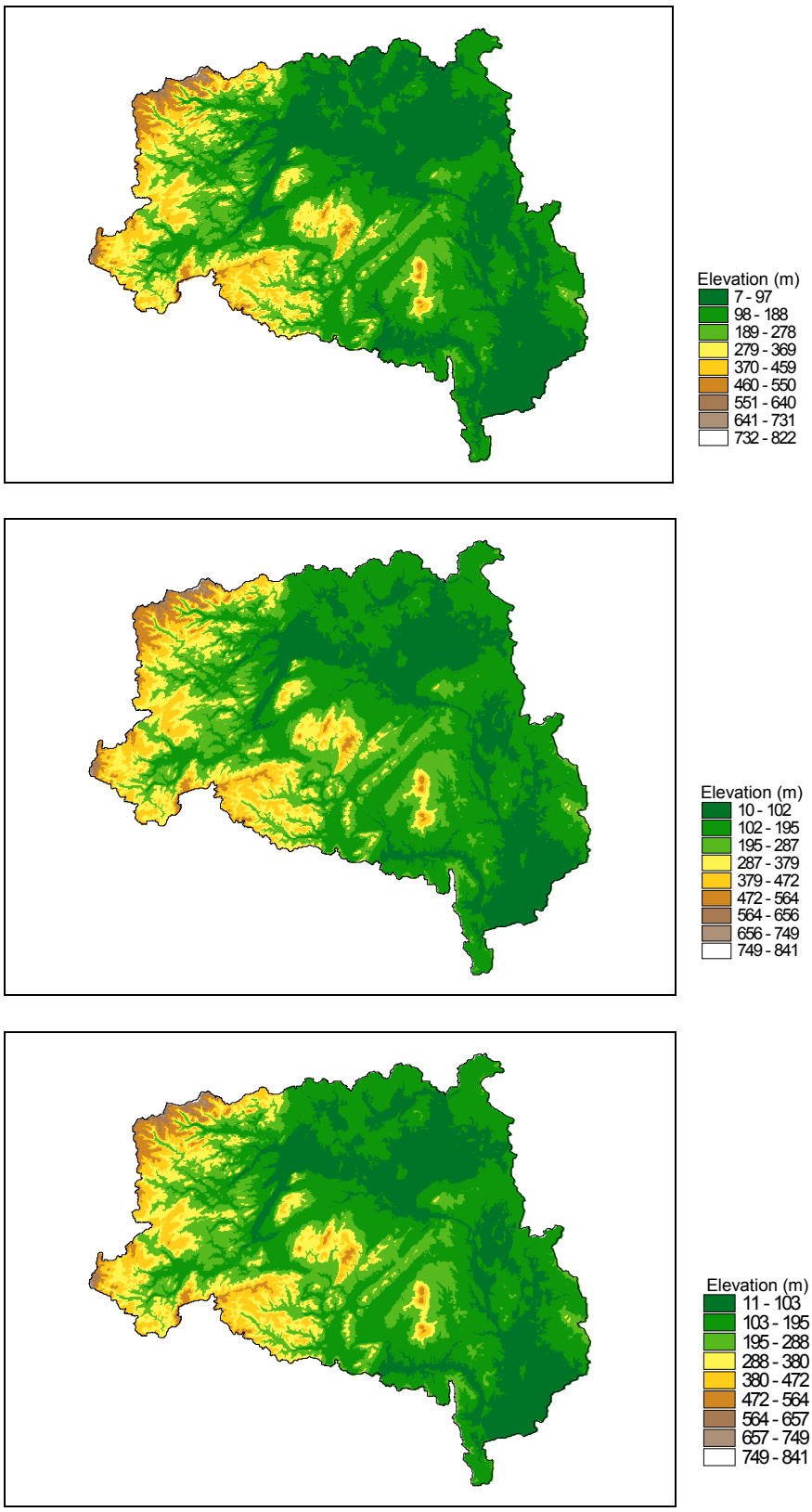

Figure 6.1 The initial pre-processing stages of HEC-GeoHMS using the original DEM (top), the reconditioned DEM (middle) and the DEM with sinks filled (bottom).

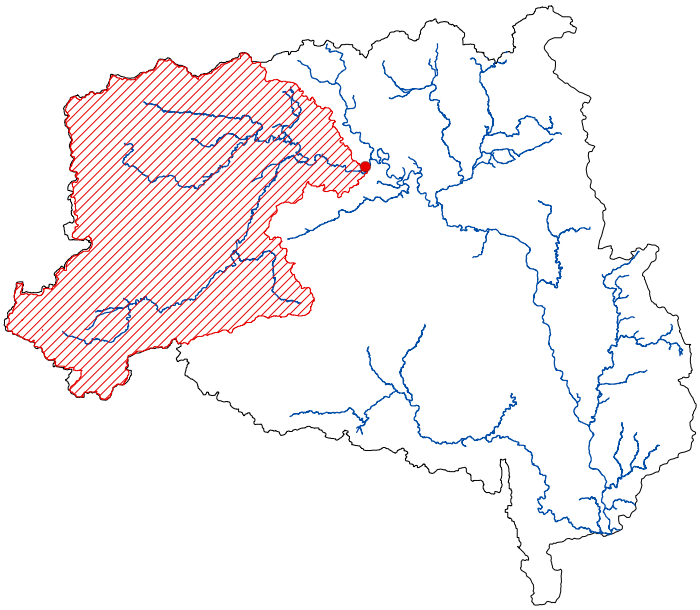

Figure 6.2 Stream network for the entire Severn basin and the Severn Uplands project area and catchment outlet point highlighted

For model calibration, data from the November-December 2006 floods (1st November to 31st December) were extracted from Environment Agency archives. These data are at 15-minute temporal resolution for both precipitation and flow gauges. The autumn 2000 event (23rd October 2000 to 23rd December 2000) was selected for model validation and weather events resulting in this flood inundation period were described in Chapter 1. The 2006 floods were of a lower magnitude than the autumn 2000 floods, but they resulted in substantial inundation around Shrewsbury and Bridgnorth; downstream of the Severn Uplands catchment. Long duration rainfall prevailed throughout the first half of December due to a series of Atlantic frontal systems driving gale-force winds and unsettled weather conditions.

6.2 HEC-GeoHMS

The HEC Geospatial Hydrological Modelling Extension (HEC-GeoHMS; USACE, 2003) provides a geospatial hydrology tool kit for use in ArcGIS. The program extension was used to process terrain data, estimate basin characteristics and approximate hydrologic parameters. Results generated were then imported into HEC-HMS as boundary conditions for the hydrologic modelling process. HEC-GeoHMS pre-processing is split into three stages: (i) terrain pre-processing; (ii) basin processing; and (iii) hydrologic parameter estimation.

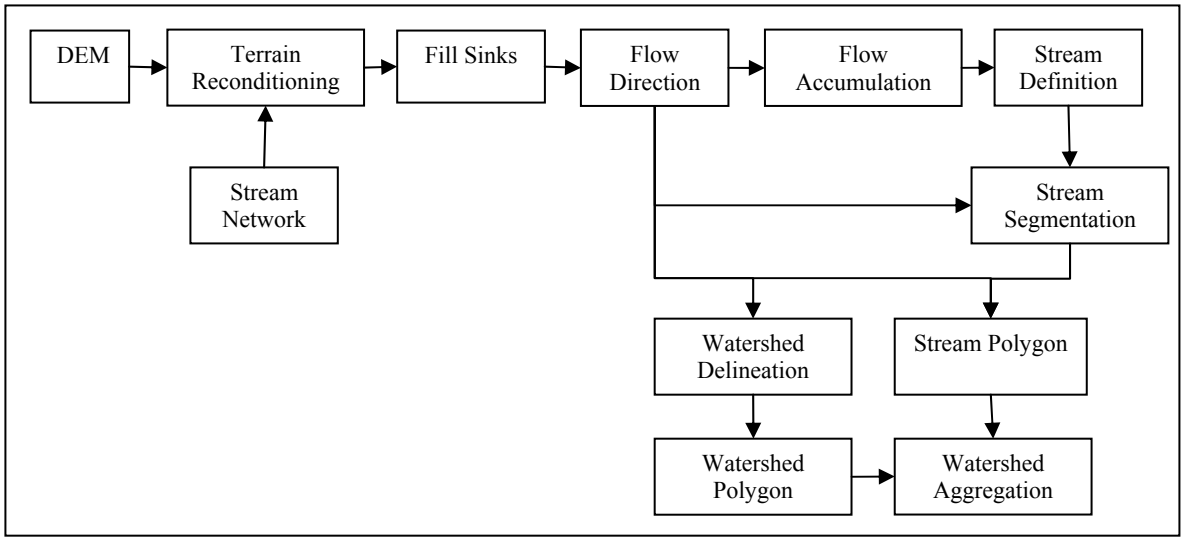

Figure 6.3 HEC-GeoHMS terrain pre-processing

6.2.1 Terrain pre-processing

The initial stage of HEC-GeoHMS is to pre-process the terrain data (Figure 6.3). Terrain reconditioning was undertaken by utilising the DEM and flow network files and imposing the line features of the stream network onto the DEM grid by lowering ('burning') and raising ('fencing') grid cell elevation along the line feature. Paz *et al.* (2008) found that stream burning increases the quality of the results for constructing a stream network in all subbasins. The method creates a gradual transition from the overbank to the stream centreline in the DEM for water to enter the stream. The subsequent reconditioned grid produced (Figure 6.1) was then transformed into a depressionless DEM by increasing the elevation of pit cells to the level of surrounding terrain (Figure 6.1). This removed any potential sinks and allowed water to flow freely across the landscape.

Flow direction was calculated from the depressionless DEM by defining the direction of the steepest descent for each terrain cell using the eight-point pour algorithm (Jensen and Domingue 1988). A single downstream cell out of the eight neighbouring cells was defined for each topographic cell. The resulting flow direction grid file (the reach network, in the shape of a spanning tree) was used as an input to determine flow accumulation; the number of upstream cells draining into a given cell. Accordingly, all cells with flow accumulation greater than the defined threshold (default value at 1% of total catchment size; 22372 cells or 20.13 km²) were classified as cells belonging to the stream network. The union of the threshold and user defined cells delineated the DEM cells that formed the reaches and a unique identification number was assigned to each stream segment.

An important aspect of the drainage network is that it partitions the drainage basin into fast response (channels) and slow response (hillslope) components (Giannoni *et al.*, 2003). Subbasin outlets were created where two sets of grid cells were united at reach junctions. Outlet locations such as those associated with flow gauges were added manually. The catchment was then delineated into areas draining into each subbasin outlet, firstly as a grid file which was then transformed into a polygon file. Subbasins were assigned an identification number which related to both the corresponding reach segment and outlet. Finally, to complete the HEC-GeoHMS pre-processing procedure, the polygon vector file was merged with the stream segmentation vector file to amalgamate upstream subbasins at every stream confluence within the catchment.

6.2.2 Basin processing

A project area within the catchment was selected by indicating the desired flow outlet location. For the Severn Uplands the selected outlet point was Montford Bridge (the catchment output location used routinely in other research focusing on the Upper Severn River e.g. Gilman *et al.*, 2002). The project catchment then comprised of all the subbasins contributing to flow upstream of Montford (Figures 6.4). Basin processing allows user-defined basin alteration by subdividing or merging subbasins. Some subbasins in the Severn Uplands catchment were subdivided and merged to create a catchment boundary layout similar spatially to that of the Environment Agency's Midland's catchment rainfall-runoff model (MCRM; see Section 6.3 for description) to obtain suitable initial parameter sets. Basin characteristics depicting river length, river slope, basin centroids, flow path length and centroidal flow path were generated once the basin processing was completed satisfactorily.

6.2.3 Hydrologic Parameter Estimation

Hydrologic parameters were estimated from the terrain, surveys and precipitation data. For the Severn Uplands, Muskingum-Cunge routing parameters (including reach lengths and slopes which were determined automatically in the reach vectorisation process), time of concentration and lag times for the hydrograph transform method and subbasin areas were all estimated within the GIS. Reach length modelling within HEC-HMS needs to be accurate so that the timings of the hydrograph peaks are accurate.

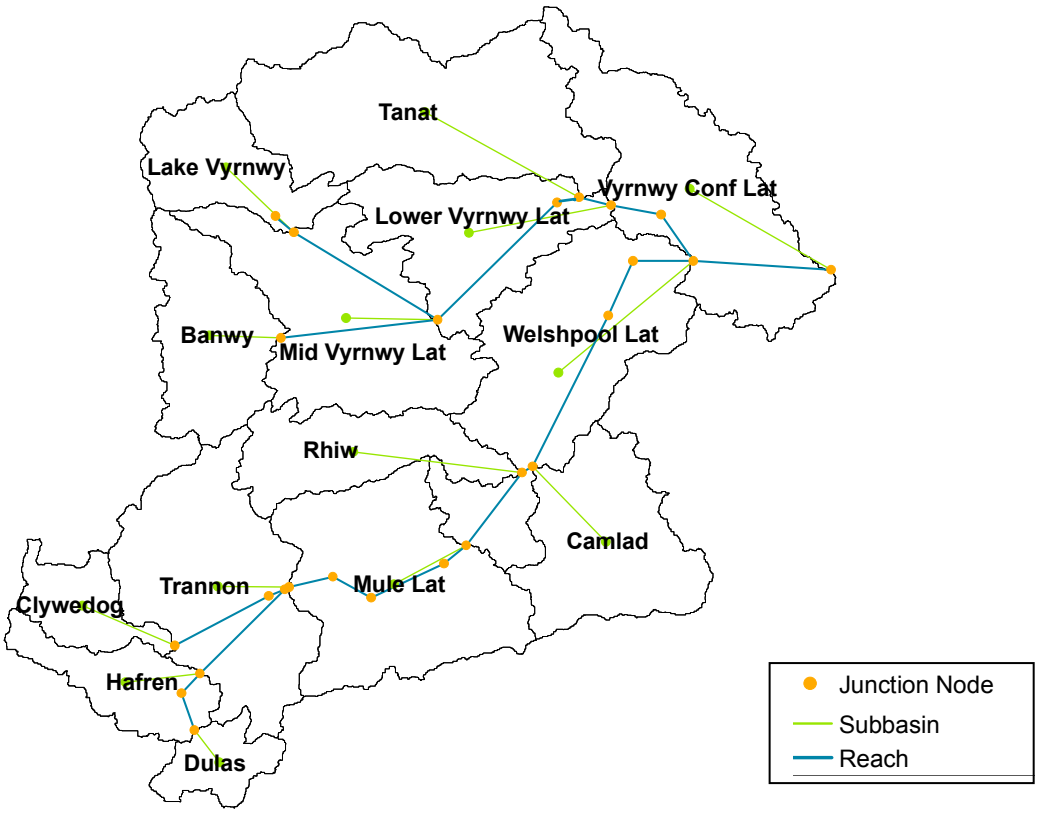

Figure 6.4 Subbasin delineation with names and HEC-HMS schematic representation of the Severn Uplands

6.3 Model Parameters

Parameters used to model the Severn Uplands using HEC-HMS are listed in Table 6.1, along with the sub-model they were nested within and their origin. Parameters were estimated in a GIS, formulated from mathematical equations or extracted from existing archives. The MCRM is a pre-existing model used previously by the Environment Agency in the Midlands region. Parameters which could not be estimated due to data deficiencies were retrieved from those used in the MCRM. Cross-sections of the channel and immediate floodplain were extracted from Ordnance Survey maps at the mid-point of each reach. All initial parameters (prior to model calibration) for each subbasin are listed in Table 6.1 and cross-sections for each reach are tabulated in Appendix 3. A schematic diagram depicting how the HEC-HMS reach, subbasin and junction components were linked together is illustrated in Figure 6.4.

Sub-model	Parameter	Parameter Description	Units	Source
Area	A	Subbasin area	km²	GIS
Routing	L	Length	m	GIS
	S	Slope	m/m	GIS
	n_C	Channel Manning's n	-	Cowan's method
	n_{LB}	Left Bank Manning's n	-	Cowan's method
	n_{RB}	Right Bank Manning's n	-	Cowan's method
	-	Channel Cross-sections	m	Ordnance Survey
Loss	D_i	Initial Deficit	mm	MCRM
	S_{Max}	Maximum Storage	mm	MCRM
	Q_R	Constant Rate	mm/hr	MCRM
	I	Percent Impervious	%	GIS
Transform	T_C	Time of Concentration	hr	Kent method
	R	Storage Coefficient	hr	Kent method
Baseflow	Q_i	Initial Discharge	mm	Time-series data
	C_R	Recession constant	-	MCRM
	P_R	Ratio to Peak	-	MCRM

Subbasin	A	D_i	S_{Max}	Q_R	I	T_C	R	Q_i	C_R	P_R
Banwy	115	11	150	0.4	2.74	4.82	3.94	0.52	0.45	0.8
Camlad	140	23.1	150	0.5	3.01	7.87	2.62	1.27	0.25	0.5
Clywedog	50.1	12.8	400	0.4	2.72	3.88	3.18	0.21	0.45	0.75
Dulas	38.9	10	150	1	3.1	2.88	1.92	0.18	0.4	0.7
Hafren	68.1	7.8	400	0.3	3	4.00	4.89	0.18	0.55	0.75
Lake Vyrnwy	85.1	9.4	400	0.3	2	3.37	5.05	0.52	0.6	0.95
Lower Vyrnwy Lat	138	12.8	150	0.5	2.89	6.95	2.98	0.52	0.3	0.5
Mid Vyrnwy Lat	197	12.1	150	0.4	2.96	6.12	5.01	0.52	0.45	0.7
Mule Lat	206	12.8	150	0.5	3.16	5.44	2.33	0.18	0.3	0.5
Rhiw	98.9	13.5	150	0.4	3.05	6.50	3.5	1.27	0.35	0.6
Tanat	240	6	150	1	2.87	6.41	7.22	0.96	0.53	0.65
Trannon	200	13.5	150	0.4	2.97	4.66	2.51	0.18	0.35	0.7
Vyrnwy Conf Lat	203	23.1	160	0.6	2.8	30.02	10	3.51	0.25	0.5
Welshpool Lat	234	23.1	160	0.6	2.93	12.81	4.27	1.27	0.25	0.5

Table 6.1 Parameter description and source (top left) and initial subbasin (bottom left) and reach (right) values for HEC-HMS modelling of the Severn Uplands

Reach	L	S	n_C	n_{LB}	n_{RB}
R11910	3163	0.017	0.110	0.150	0.150
R11920	2299	0.004	0.109	0.149	0.149
R11940	2869	0.008	0.070	0.142	0.142
R11950	5238	0.001	0.074	0.089	0.089
R7830	2233	0.000	0.074	0.092	0.092
R7840	7617	0.001	0.070	0.053	0.053
R7870	75	0.000	0.070	0.142	0.142
R7890	8138	0.000	0.070	0.053	0.053
R7900	9213	0.000	0.070	0.053	0.053
R7910	16427	0.000	0.070	0.053	0.053
R7920	6154	0.000	0.070	0.053	0.053
R7940	19517	0.007	0.070	0.142	0.142
R7950	15800	0.001	0.074	0.092	0.092
R8010	19786	0.004	0.090	0.150	0.150
R8040	17916	0.001	0.070	0.053	0.053
R8060	1843	0.000	0.083	0.072	0.072
R8080	10017	0.002	0.074	0.072	0.072
R8100	2309	0.000	0.079	0.092	0.092
R8150	5122	0.001	0.069	0.096	0.096
R8160	375	0.000	0.142	0.149	0.149
R8170	7206	0.003	0.079	0.092	0.092
R8180	1558	0.001	0.109	0.149	0.149
R8190	4124	0.000	0.069	0.096	0.096
R8230	9188	0.005	0.109	0.149	0.149
R8250	14514	0.002	0.109	0.149	0.149

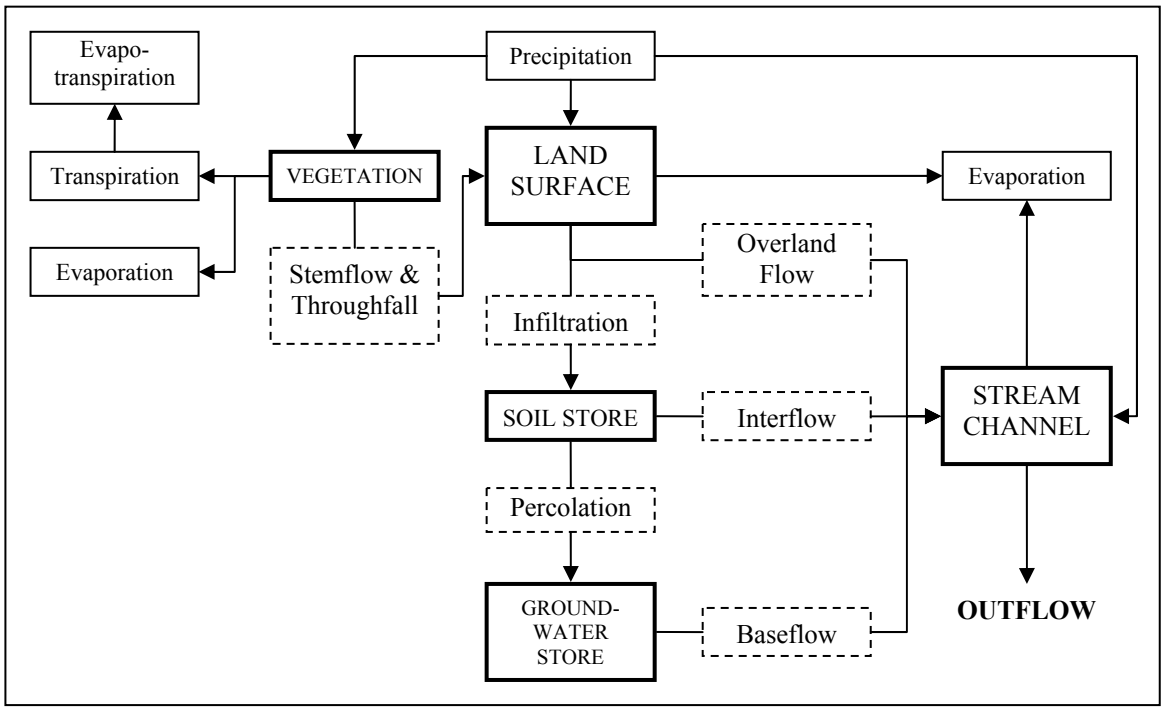

Figure 6.5 Components of HEC-HMS. Water stores are outlined in bold, ground processes in hashed and atmospheric processes in solid (adapted after Feldman, 2000)

Table 6.2 Evapotranspiration values; pan coefficient and monthly averages

Subbasin	Pan	Jan	Feb	Mar	Apr	May	Jun	Jul	Aug	Sep	Oct	Nov	Dec
Banwy	0.66	8	12	16	32	48	64	80	80	56	36	24	16
Camlad	0.72	10	15	20	40	60	80	100	100	70	45	30	20
Clywedog	0.66	4	6	8	16	24	32	40	40	28	18	12	8
Dulas	0.67	4	6	8	16	24	32	40	40	28	18	12	8
Hafren	0.64	4	6	8	16	24	32	40	40	28	18	12	8
Lake Vyrnwy	0.62	4	6	8	16	24	32	40	40	28	18	12	8
Lower Vyrnwy Lat	0.73	10	15	20	40	60	80	100	100	70	45	30	20
Mid Vyrnwy Lat	0.72	8	12	16	32	48	64	80	80	56	36	24	16
Mule Lat	0.69	10	15	20	40	60	80	100	100	70	45	30	20
Rhiw	0.69	8	12	16	32	48	64	80	80	56	36	24	16
Tanat	0.69	6	9	12	24	36	48	60	60	42	27	18	12
Trannon	0.69	8	12	16	32	48	64	80	80	56	36	24	16
VyrnwyConf Lat	0.77	12	18	24	48	72	96	120	120	84	54	36	24
Welshpool Lat	0.75	12	18	24	48	72	96	120	120	84	54	36	24

6.4 TIME-SERIES INPUTS

Observed flow and precipitation were input to the HEC-HMS meteorological model via HEC-DSSVue. Also stored in the meteorological model were evapotranspiration data (Table 6.2), gauge depth and time weights as well as an index assigned to gauges and subbasins which adjusts for regional bias in precipitation (Table 6.3). Flow and precipitation gauges are mapped in Figure 6.6.

Table 6.3 Depth and time weights of precipitation gauges for each subbasin

Subbasin/Gauge	Bagley	Bishop's Castle	Cefn Coch	Dolydd	Llanfyllin	Langynog	Nantgwyn	Pen-y-Coed	Rorrington	Sarn	Vyrnwy	Welshpool
Banwy	-	-	0.2	-	-	-	-	0.8	-	-	-	-
	-	-	0.09	0.02	-	-	-	0.89	-	-	-	-
Camlad	-	0.15	-	-	-	-	-	-	0.35	0.45	-	0.05
	-	0.131	-	-	-	-	-	-	0.465	0.283	-	0.121
Clywedog	-	-	-	1	-	-	-	-	-	-	-	-
	-	-	-	1	-	-	-	-	-	-	-	-
Dulas	-	-	-	-	-	-	1	-	-	-	-	-
	-	-	0.01	0.02	-	-	0.97	-	-	-	-	-
Hafren	-	-	-	0.7	-	-	0.3	-	-	-	-	-
	-	-	0.05	0.75	-	-	0.2	-	-	-	-	-
Lake Vyrnwy	-	-	-	-	-	0.25	-	-	-	-	0.75	-
	-	-	-	-	-	0.27	-	0.25	-	-	0.48	-
Lower Vyrnwy Lat	-	-	-	-	0.9	0.05	-	-	-	-	0.05	-
	0.01	-	0.02	-	0.92	-	-	-	-	-	-	0.05
Mid Vyrnwy Lat	-	-	0.3	-	0.3	-	-	0.2	-	-	0.1	0.1
	-	-	0.287	-	0.248	-	-	-	-	-	0.386	0.079
Mule Lat	-	-	0.35	-	-	-	0.15	-	-	0.5	-	-
	-	-	0.356	-	-	-	0.099	-	-	0.436	-	0.109
Rhiw	-	-	0.9	-	-	-	-	-	-	0.05	-	0.05
	-	-	0.8	0.04	-	-	-	-	-	0.08	-	0.08
Tanat	0.15	-	-	0.05	0.8	-	-	-	-	-	-	-
	0.04	-	-	0.5	0.46	-	-	-	-	-	-	-
Trannon	-	-	0.3	0.35	-	-	0.35	-	-	-	-	-
	-	-	0.3	0.48	-	-	0.22	-	-	-	-	-
Vyrnwy Conf Lat	0.842	-	-	-	-	0.105	-	-	0.053	-	-	-
	0.55	-	-	-	-	0.1	-	-	0.13	-	-	0.22
Welshpool Lat	-	-	-	-	0.05	-	-	-	0.05	0.1	-	0.8
	-	-	-	-	0.01	-	-	-	0.03	0.01	-	0.95

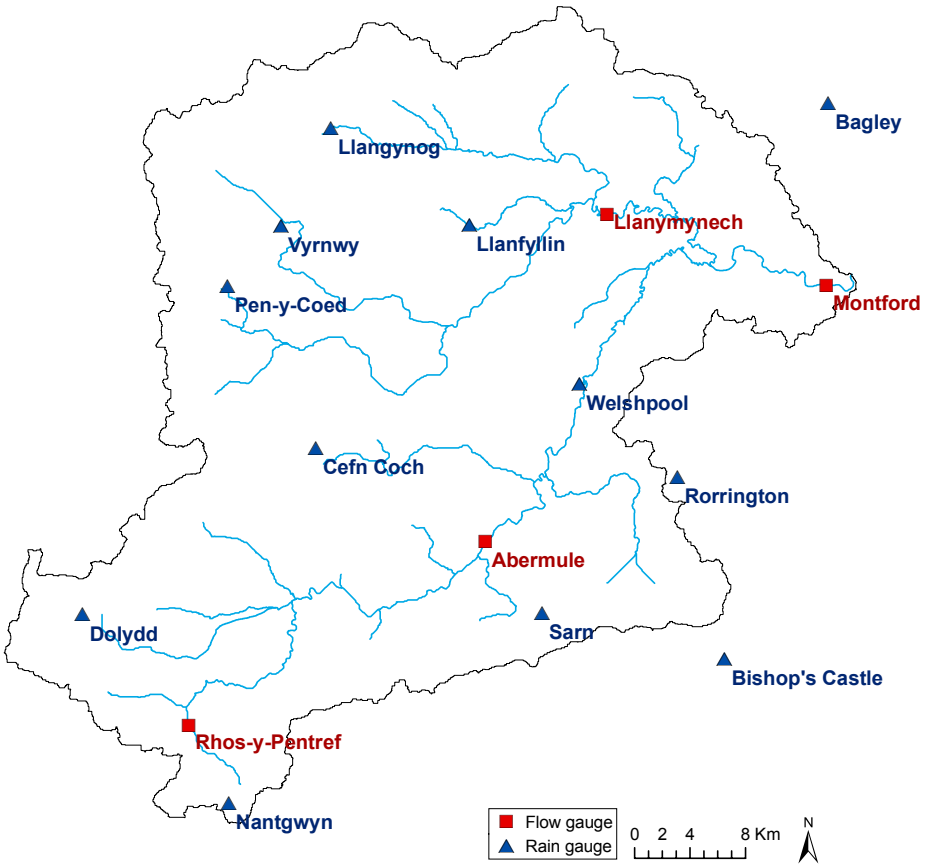

Figure 6.6 Location of precipitation and flow gauges used for hydrological modelling and calibration

6.5 PRE-CALIBRATION RESULTS

HEC-HMS modelling predictions were compared to observational data for four locations across the catchment – Abermule, Llanymynech, Montford and Rhos-y-Pentref (Figures 5.1 and 6.4). Large correlations can be achieved by mediocre or poor models. Therefore, Legates and McCabe (1999) recommend the use of more conservative measures such as efficiency coefficients which use absolute values rather than squared differences. They also advise that the mean, standard deviation and MAE or RMSE of observed and simulated time-series be reported (as reported in Chapter 3). Flow simulation accuracy was tested using the Nash-Sutcliffe efficiency index, E_f, the Pearson-product moment correlation coefficient, ρ, the coefficient of determination, R^2, the mean absolute error, *MAE,* and the root mean squared error, *RMSE* (Table 6.4). The mean and standard deviation σ were also reported.

Pre-calibration results indicated that simulated flows match the overall pattern to that of observed flows (Table 6.4). The accuracy between predicted and observed flow at

Llanymynech was particularly large with a high E_f of 0.80. Efficiency at Rhos-y-Pentref and Montford was moderate with E_f values of 0.48 and 0.58 respectively. Flow prediction at Abermule was unsatisfactory as the E_f value was negative (-2.19) which constituted model performance below that of a "no-knowledge" model. The correlation and R^2 values between simulated and observed time-series were large for all sites, with Abermule having slightly smaller values than the other three locations. However, there are quite large discrepancies between observed and predicted means and standard deviations, and errors are quite large.

To increase the predictive power of the model, model-sensitive parameters were selected then calibrated to extreme conditions using the November-December 2006 flow data. Wilby (2005) stated that the transferability of model parameters depends on the representation of the calibration period. The ability to identify optimal parameters can often be significantly increased by selecting the wettest period of data for calibration (Yapo *et al.*, 1996). As extreme wet periods were of interest for this research, extreme hydrological periods of two months were selected for calibration and validation which ensured that both the precipitation and flow extremes would be well represented in the data records. The quality of information contained in the data is often more important than the length of the record, as after a certain length the use of additional data will only marginally increase the accuracy of parameter estimates. All precipitation and flow gauge data used for hydrological modelling consisted of complete records.

6.6 PARAMETER SELECTION FOR MODEL CALIBRATION

Prior to calibration, sensitive subbasin model parameters were identified by testing sensitivity across each of the parameter spaces for three selected subbasins (Dulas, Tanat and Welshpool Lat). Sensitivity analysis was adopted to determine which parameters were the most sensitive to the model and within what range. Fleming and Neary (2004) found it necessary to determine a practical range of parameters before using the HEC-HMS automated calibration functions. Local sensitivity analysis constituted determining the effect of each input parameter whilst the remaining parameters were held constant. Sensitivity analysis results using the Nash-Sutcliffe efficiency index, which compared flow outputs of values across each parameter space to that of initial parameter values, are illustrated in Figure 6.6. From these plots it is evident that the maximum storage parameter

has no effect on the model output and the percentage impervious parameter has little impact. Variation across the parameter space for total discharge, total baseflow, peak discharge and total loss are illustrated as cumulative distributions (Figures 6.7-6.11). Some variables showed clear variation across the parameter space whereas others seemed to show little or no change. Welshpool Lat showed a higher sensitivity to model parameters which may be explained by its downstream location exhibiting floodplain characteristics in contrast to Dulas and Tanat which are characteristic of upstream headwater basins. Results indicated that the constant loss rate parameter is highly sensitive as shown by the large variation in all variables. Additionally, total baseflow and peak discharge were affected by the time of concentration, storage coefficient, recession constant and ratio to peak.

One of the major problems in rainfall-runoff modelling is dealing with over-parameterisation (Jakeman and Hornberger, 1993). Perrin *et al.* (2001) demonstrated that very simple models can achieve a level or performance almost as accurate as models with more parameters. These complex models are subject to over-parameterisation and so the number of free parameters is usually restricted to between 3 and 5, a number also indicated by Beven (1989), who stated that 3 to 5 parameters should be sufficient to reproduce most of the information in a hydrological record.

Table 6.5 summarises the parameters that were the most influential on model outcomes, ranked according to importance. Of the nine subbasin parameters tested, five parameters seemed to influence sensitivity more than the remaining four. Based on the Nash-Sutcliffe and variable sensitivity analyses, these five important parameters (constant loss rate, time of concentration, storage coefficient, recession constant and ratio to peak) were subsequently selected for use in calibrating the hydrological model. These selected parameters have been found by other researchers to be of high calibration importance. For example, Knebl *et al.* (2005) used HEC-HMS to model regional scale flooding driven by distributed rainfall and they deemed the time of concentration, storage coefficient, initial baseflow and initial abstraction ratio as parameters important for calibration.

Table 6.4 HEC-HMS modelling results between observed and simulated time-series at four gauge locations for the observed-calibrated (November-December 2006) and observed-validated (October-November-December 2000) periods using gauge rainfall

		Observed (ND 2006)	Uncalibrated (ND 2006)	Calibrated (ND 2006)	Observed (OND 2000)	Validated (OND 2000)
Rhos-y-Pentref	Mean	3.545	3.908	3.214	5.116	5.144
	σ	2.971	4.519	3.488	4.632	5.044
	ρ	-	0.924	0.939	-	0.840
	R^2	-	0.850	0.885	-	0.705
	MAE	-	0.544	0.442	-	0.462
	RMSE	-	5.341	4.099	-	6.479
	E_f	-	0.477	0.818	-	0.643
	Peak *Q*	16.6	25.8	20.8	37.9	32.6
	Volume	479.7	528.9	434.9	703.8	707.7
Abermule	Mean	36.956	70.057	27.867	54.503	45.117
	σ	31.232	69.067	30.656	38.510	43.343
	ρ	-	0.866	0.880	-	0.888
	R^2	-	0.747	0.775	-	0.788
	MAE	-	1.070	0.491	-	0.396
	RMSE	-	92.163	35.980	-	56.210
	E_f	-	-2.191	0.680	-	0.673
	Peak *Q*	173.2	307.1	150.7	279.6	273.4
	Volume	294.1	557.5	221.7	440.9	364.9
Llanymynech	Mean	54.391	42.661	58.369	90.523	139.095
	σ	52.229	46.395	56.625	76.516	89.441
	ρ	-	0.922	0.945	-	0.894
	R^2	-	0.850	0.893	-	0.799
	MAE	-	0.489	0.407	-	0.754
	RMSE	-	51.983	68.845	-	147.078
	E_f	-	0.799	0.867	-	0.321
	Peak *Q*	264.5	186.0	253.5	451.4	512.5
	Volume	370.3	290.4	397.7	629.4	962.5
Montford	Mean	102.651	114.861	88.668	182.730	194.043
	σ	84.046	115.712	87.686	97.639	134.608
	ρ	-	0.908	0.951	-	0.941
	R^2	-	0.825	0.906	-	0.885
	MAE	-	0.523	0.385	-	0.221
	RMSE	-	144.673	106.616	-	205.547
	E_f	-	0.584	0.870	-	0.680
	Peak *Q*	359.8	437.6	327.3	473.4	751.1
	Volume	268.7	300.6	232.1	486.2	516.3

Table 6.5 Sensitivity analysis of parameter performance

Rank	Parameter	Total Direct Runoff	Total Baseflow	Peak Discharge	Total Loss
1	Constant Loss Rate	Yes	Yes	Yes	Yes
=2	Time of Concentration	No	Yes	Yes	No
=2	Storage Coefficient	No	Yes	Yes	No
=4	Recession Constant	No	Yes	Some	No
=4	Ratio to Peak	No	Yes	Some	No
6	Initial Deficit	Some	No*	No*	No
7	Initial Baseflow	No	No*	Some	No
8	Impervious	No*	No*	No	No
9	Maximum Storage	No	No	No	No

* except slight variation at Welshpool Lat

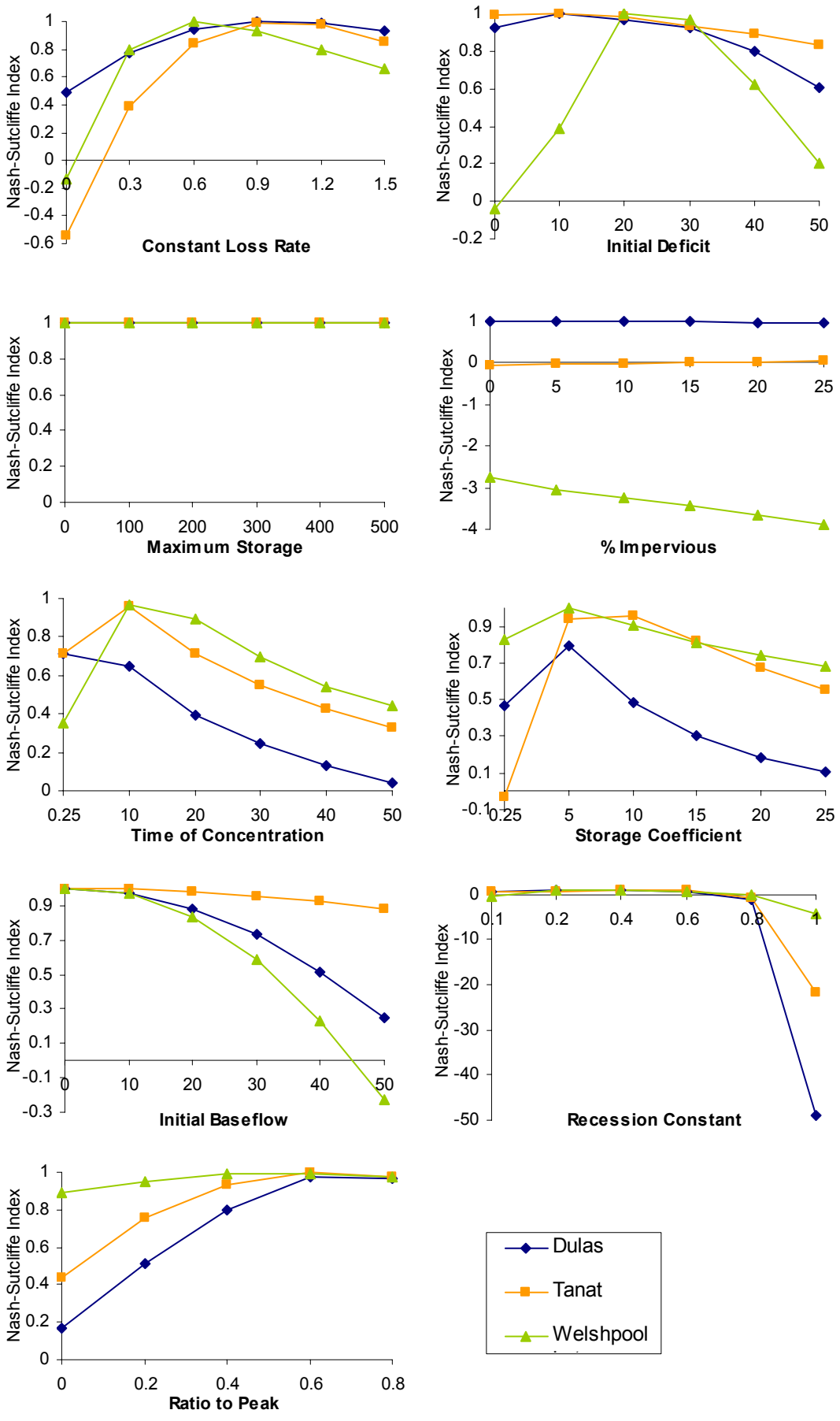

Figure 6.7 Nash-Sutcliffe efficiency index comparing the initial model parameter simulation to simulations strategically sampling the parameter space.

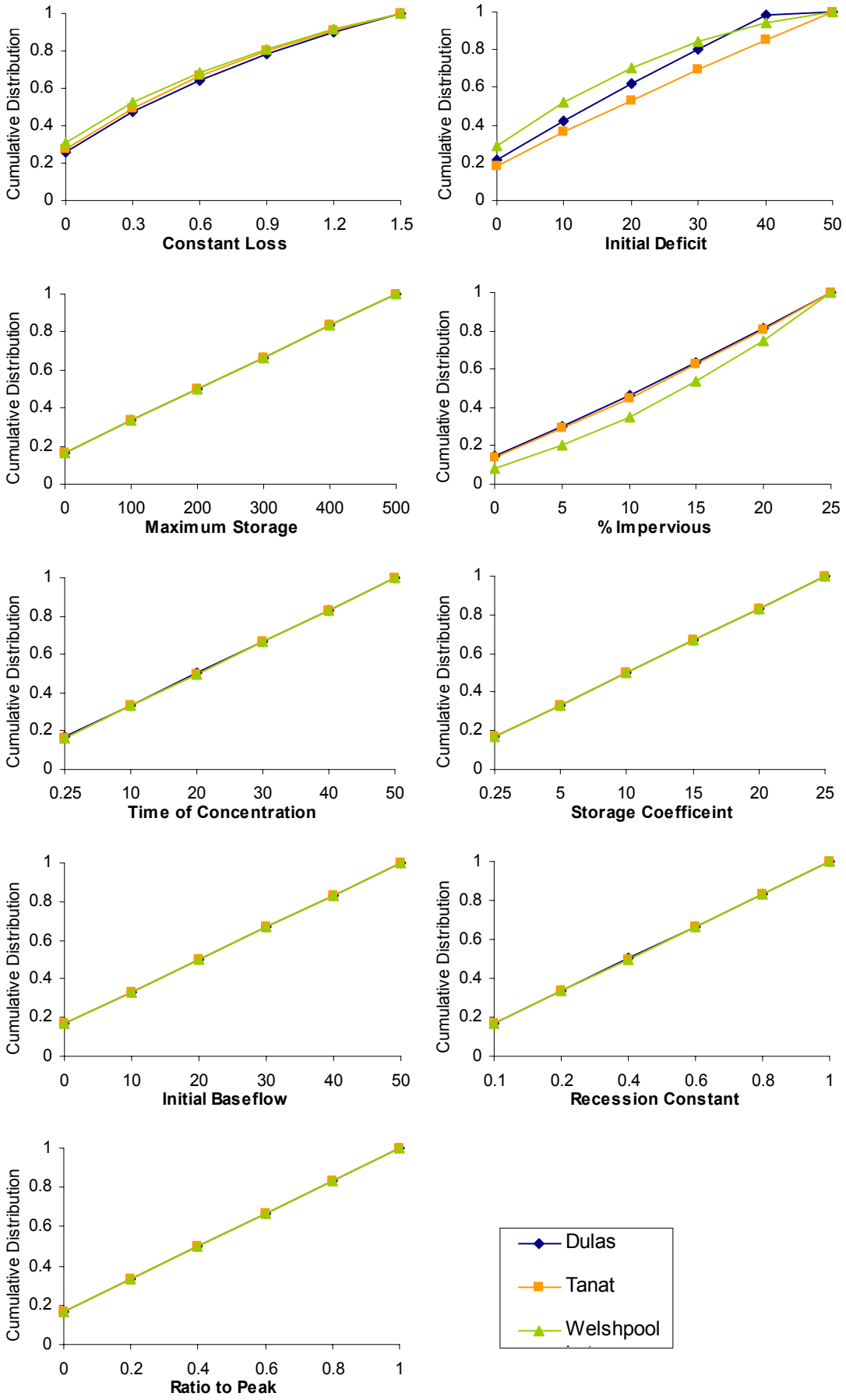

Figure 6.8 Cumulative changes in total direct runoff across the sampled parameter space.

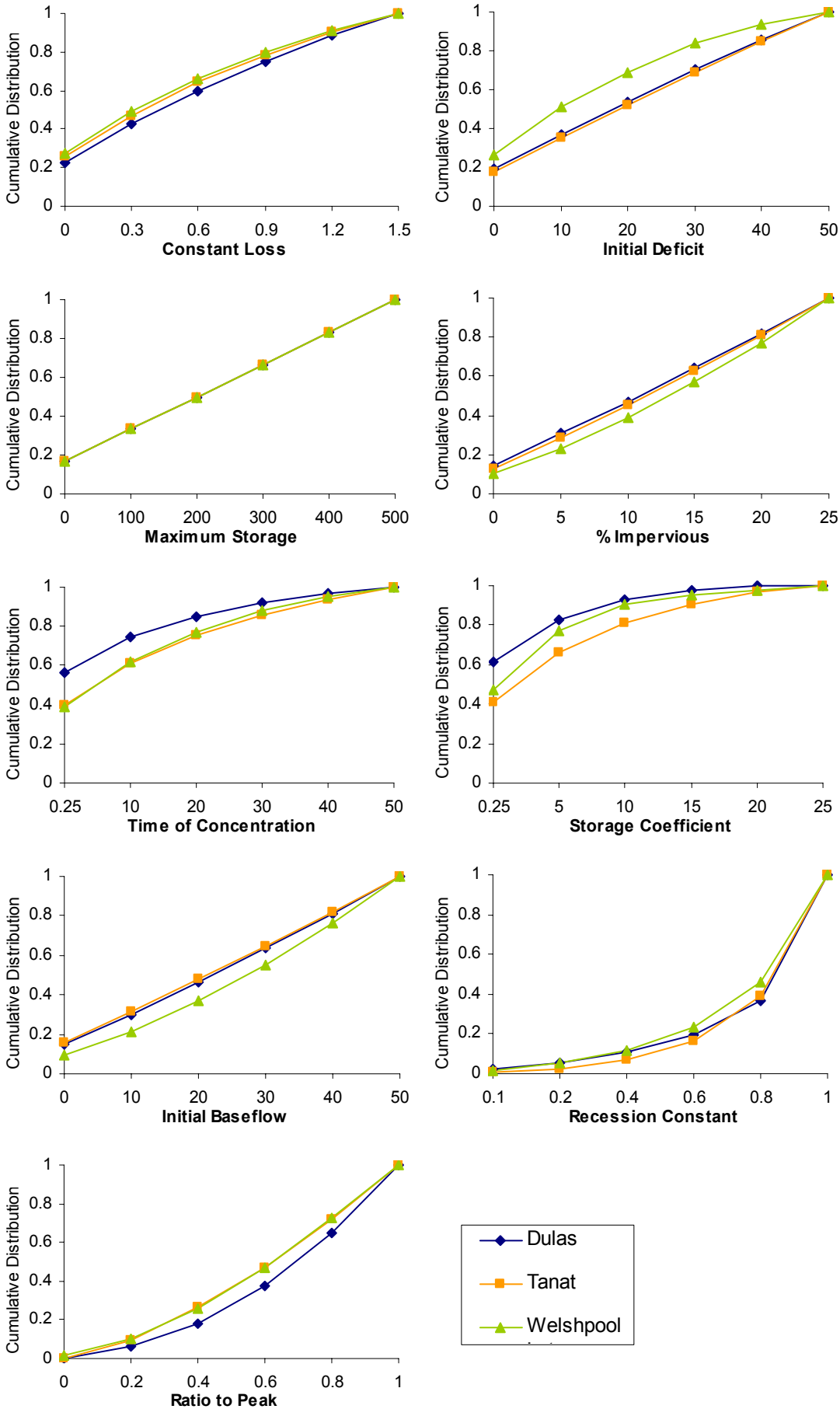

Figure 6.9 Cumulative changes in total baseflow across the sampled parameter space.

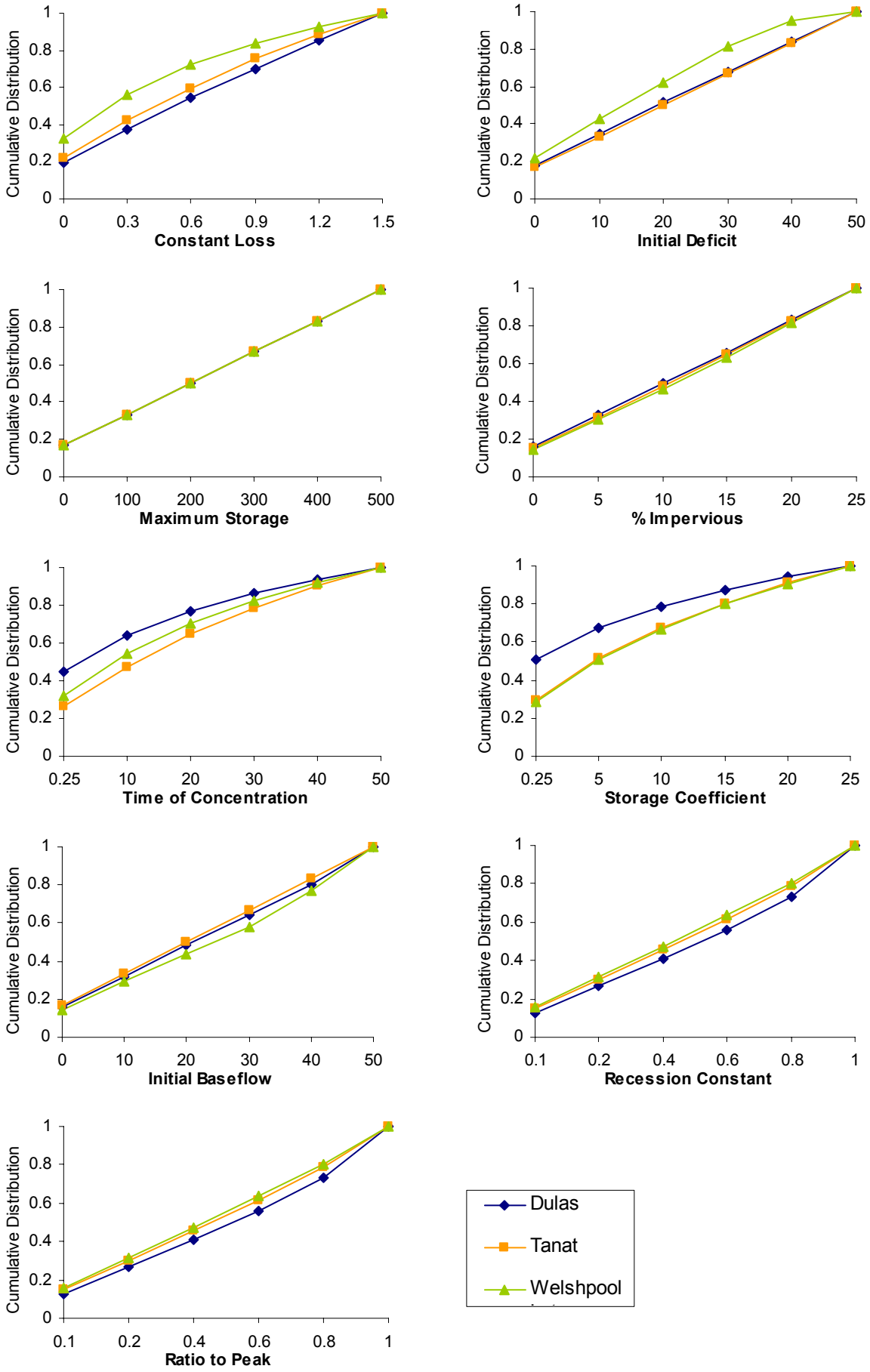

Figure 6.10 Cumulative changes in peak discharge across the sampled parameter space.

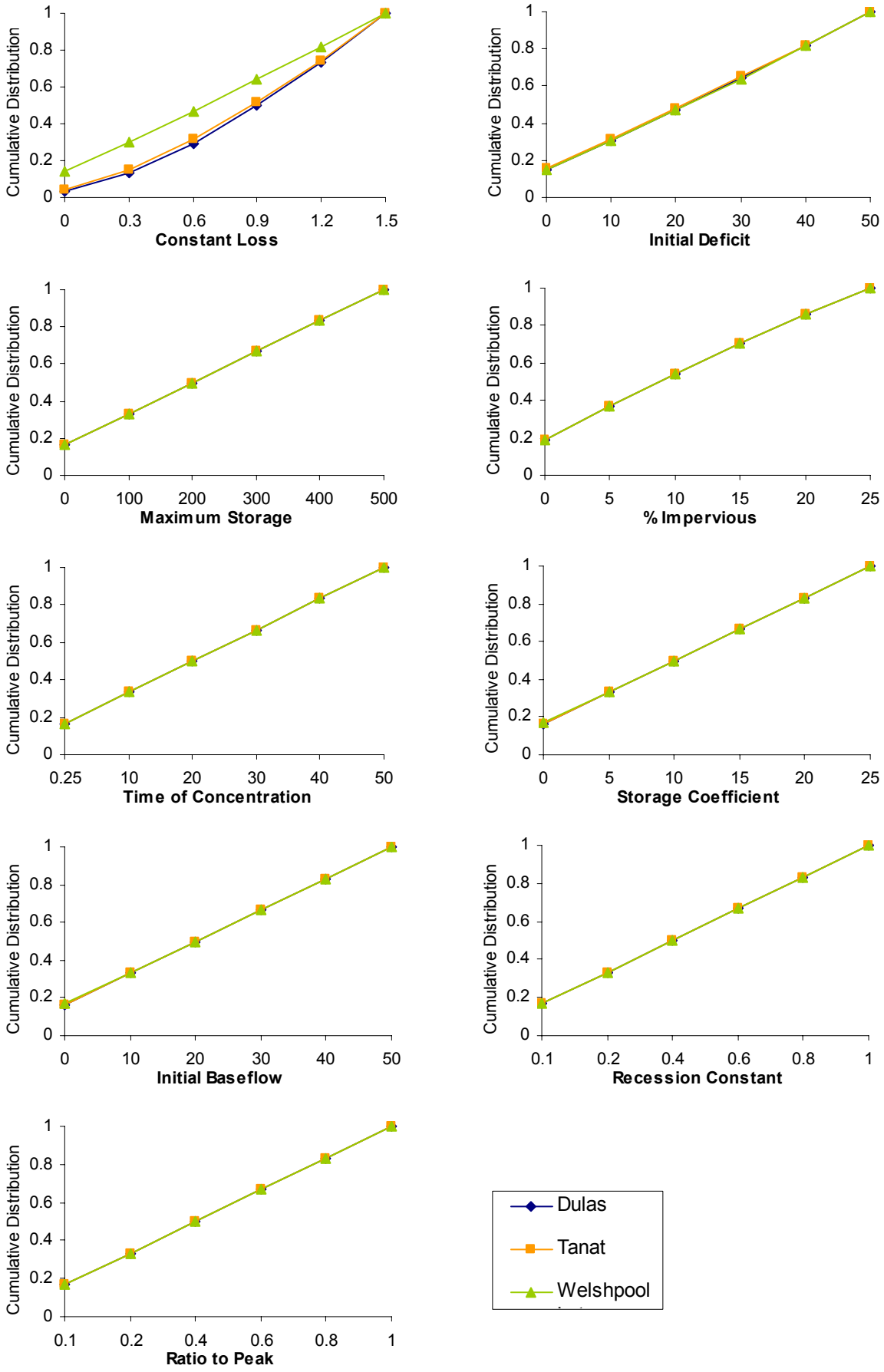

Figure 6.11 Cumulative changes in total loss across the sampled parameter space.

6.7 CALIBRATION

The same observation stations, as used in the pre-calibration procedure, were used to assess simulated versus observed flow. Four optimisation methods, as described fully in Chapter 3, were used to identify optimal parameters sets. A combination of the parameters which resulted in the most efficient simulations was then used for the final calibration stage. Following calibration the model accuracy increased as the correlations between simulated and observed flows significantly increased and error was substantially reduced (Table 6.4). This increase in accuracy is visualised in Figure 6.12 for the four gauge locations. The plots show that error in predicted values is substantially larger for larger flow values at Rhos-y-Pentref and Abermule. Prediction errors at Llanymynech and Montford appear to be more uniform and consistent. Prior to calibration the model seemed to under-predict flows at Llanymynech and over-predict at all other locations. Calibrating the model parameters resulted in less bias.

Subsequent to calibration, the means and standard deviations of the predicted time-series more closely resembled those of the observed data; a significant increase in accuracy compared to that predicted prior to calibration. Correlation and R^2 values increased marginally at all sites. The MAE was reduced at all sites following calibration as did the RMSE, with the exception of Llanymynech where there was an increase. Model calibration significantly increased the efficiency of the predictions with E_f values ranging from 0.68 to 0.87. The predictive efficiency at Abermule remained the lowest, but model accuracy was substantially more accurate post-calibration.

Referring to the literature, Sharma *et al.* (2007) used HEC-HMS to model river flows in the Ping River Basin, Thailand. The Nash-Sutcliffe value obtained in this study post-calibration was 0.65. Muleta and Nicklow (2005) obtained E_f values for streamflow simulation of -0.38 prior to calibration and 0.74 following calibration. Knebl *et al.* (2005) found that the average subbasin calibrated correlation coefficient for runoff simulation in their study was 0.78, increased from a subbasin average of 0.64 prior to calibration. Wilby (2005) stated that E_f values in excess of 0.6 indicate a satisfactory fit between observed and simulated hydrographs. Given the calibrated Severn Uplands modelling results, the HEC-HMS model was deemed sufficient in reproducing the November-December 2006 extreme event. To test the model independently, data from an alternative extreme event were used to assess the model.

(a) Rhos-y-Pentref

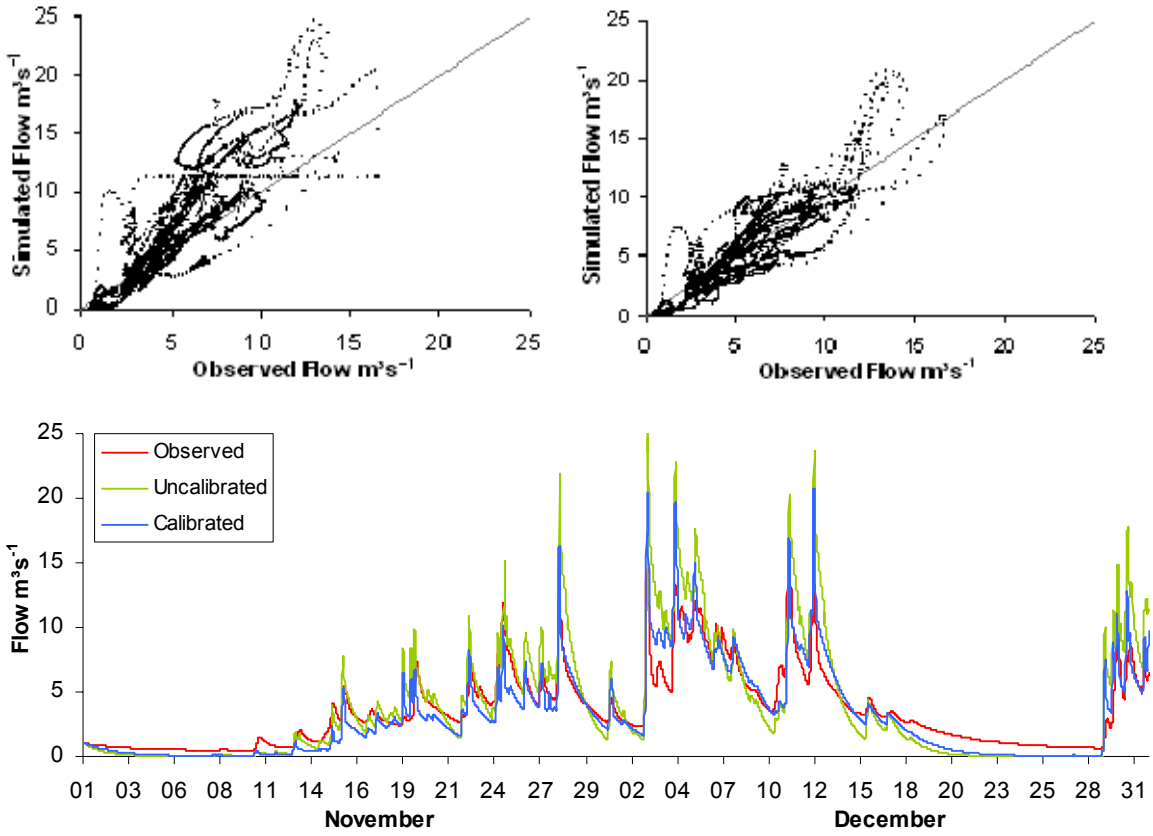

(b) Abermule

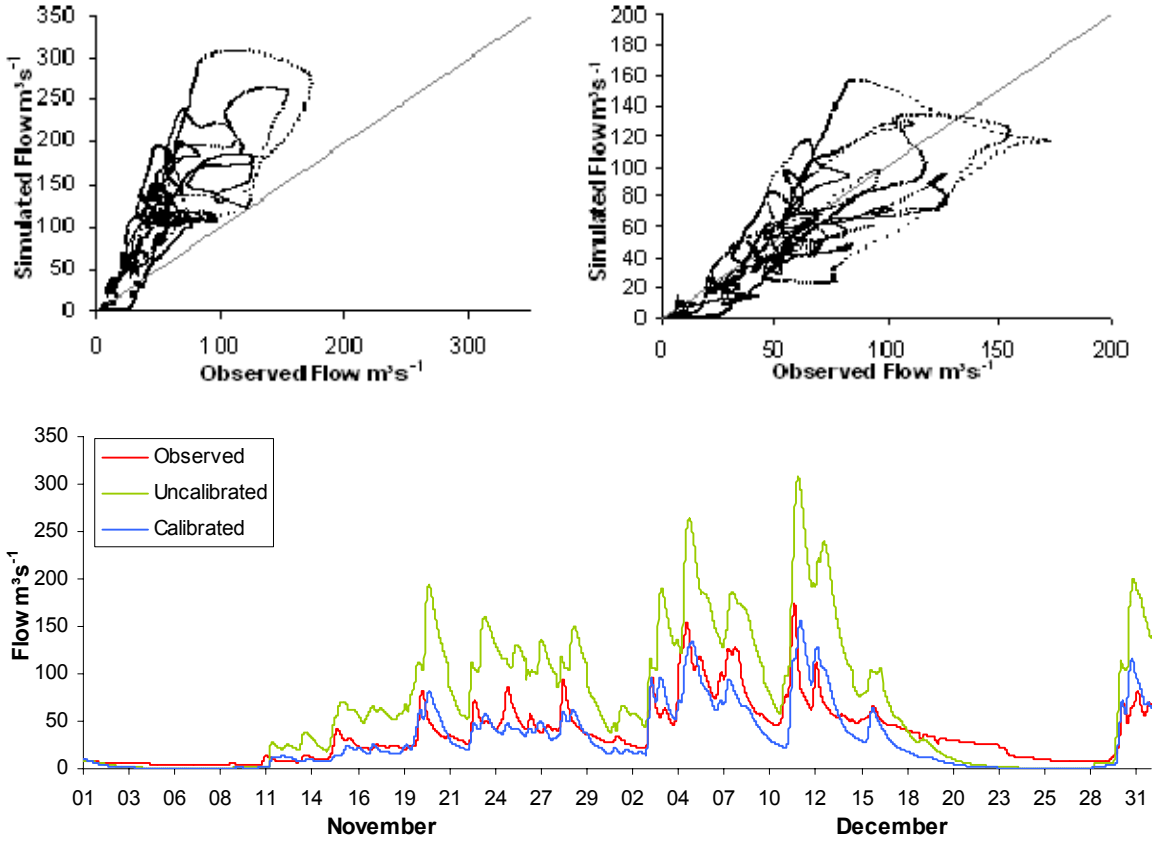

(c) Llanymynech

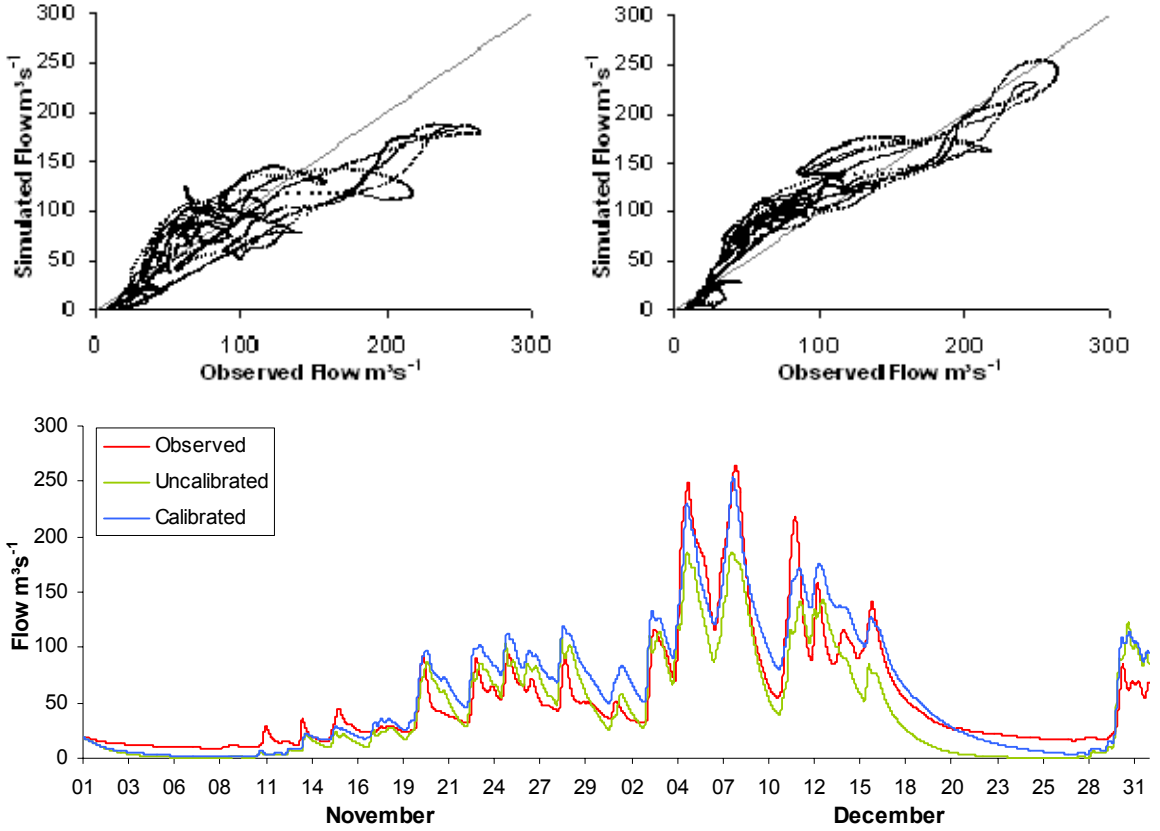

(d) Montford

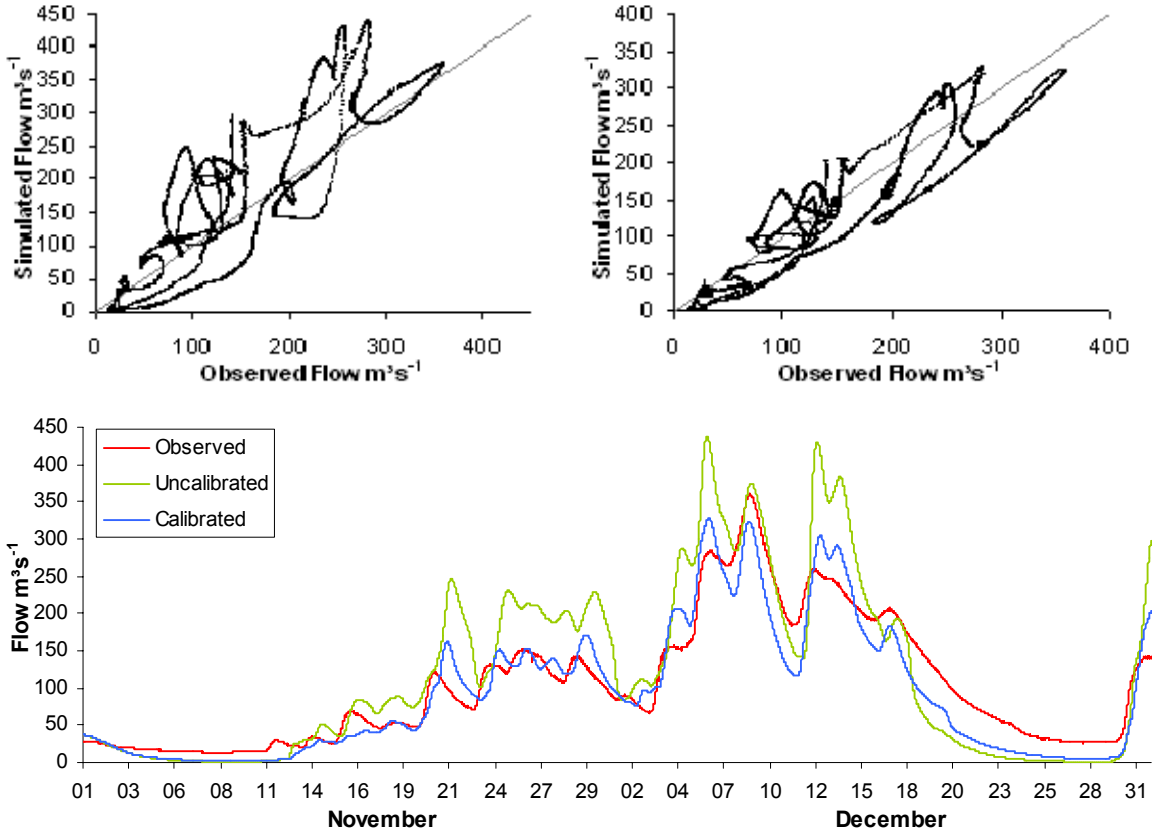

Figure 6.12 Observed flows versus uncalibrated (top left) and calibrated (top right) flow predictions; hydrograph of model output and observed flow values (bottom), for each gauging station

6.8 VALIDATION

Even after calibration there is a great deal of uncertainty in simulation results simply because error-free observational data are very unlikely and no model simulation is an entirely true reflection of the physical process being modelled (Muleta and Nicklow, 2005). If model parameter estimates are unique and realistic the estimated parameters should be independent of the calibration data (Gan *et al.*, 1997). The accuracy of this can be tested by assessing model parameter efficiency using a validation period. By using an alternative extreme event as input the HEC-HMS model could be validated to ensure accurate calibration was achieved. Cunderlik and Simonovic (2004) found that during manual calibration one set of model parameters could not be used to simulate different seasonal event types well. Therefore, the winter 2000 extreme hydrological event was chosen for validation as this occurred at roughly the same time of year as the calibration extreme event.

All parameters except initial conditions (e.g. initial discharge) which were unique to the event periods were kept constant. Cunderlik and Simonovic (2004) deemed the Clark T_c to be event-dependent since large, intensive storms can quickly saturate the basin, which then acts as if it is impervious. Following this finding, the T_c was calibrated for the validation period which resulted in only a slight increase in model accuracy. Validation results along with observed means and standard deviations are listed in Table 6.4. The same comparison measures were used as when testing the calibration accuracy. Results indicate adequate modelling accuracy at Rhos-y-Pentref, Abermule and Montford with means and standard deviations well matched, large correlations and E_f values of 0.64, 0.67 and 0.68, respectively. Model accuracy at Llanymynech is fair, with large discrepancies in the mean and standard deviations and a lower E_f value at 0.32.

The above accuracy measures can be put into context by assessing other values achieved in the literature. Sharma *et al.* (2007) found that the Nash-Sutcliffe measure in their research increased to 0.77 when validating the model. Pilling and Jones (2002) used the Nash-Sutcliffe performance measure to compare simulated and observed flows and achieved a value of 0.86 during the validation period and Cunderlik and Simonovic (2005) achieved an identical E_f value for validation using HEC-HMS, but over ten-year time periods.

Table 6.6 Percentage errors for peak discharge and total volume predictions

		Pre-calibration	Calibration	Validation
% error peak flow	Rhos-y-Pentref	55.0	25.3	-14.0
	Abermule	77.3	-13.0	-2.2
	Llanymynech	-29.7	-4.2	13.5
	Montford	21.6	-9.0	58.7
% error output volume	Rhos-y-Pentref	10.3	-9.3	0.6
	Abermule	89.6	-24.6	-17.2
	Llanymynech	-21.6	-7.3	52.9
	Montford	11.9	-16.3	6.2

Percentage errors of pre-calibration, calibration and validation simulation results are indicated for the peak event flow and flood volume in Table 6.6 (derived from the figures listed in Table 6.5). Donigian (2002) advises that percentage differences between observed and simulated flows indicate a very good modelling procedure if < 10%, good if 10-15% and fair if 15-25%. Butts *et al*. (2004) indicate that a reasonable estimate of the uncertainty in measured discharge for normal flows is about 10%. However, larger uncertainties can be expressed for peak events. Differences for the Severn Uplands indicate generally inaccurate results for prediction of peak flows and total output volumes of the November-December 2006 extreme event prior to calibration. Post-calibration peak discharge prediction is very good at Llanymynech and Montford, good at Abermule and fair at Rhos-y-Pentref. In terms of total volume calibrated predictions are very good at Rhos-y-Pentref and Llanymynech, good at Montford and fair at Abermule. Pre-calibration results mainly overpredict peak flow and total volume at sites, whereas following calibration, variables are generally underpredicted.

Validation prediction results are variable. Percentage errors are large at Montford for peak flow at 58.7% and Llanymynech for output volume at 52.9%. As with calibration errors, this may be attributable to error in input data, output data or due to modelling inaccuracy. Quantifying output error in observational flows is difficult unless more than one gauge is operational at a specific location. The EA does not have these resources, yet, upon investigation of the UK HiFlow series data (online archive at http://www.environment-agency.gov.uk/hiflows/91727.aspx) there were discrepancies of between 0 and 4.3 % when comparing peak flow values to those obtained from EA archived 15-minute records. This may explain some of the uncertainty in the flow simulations. Further uncertainty may be derived from the model-specific nature of each extreme event. As previously discussed, Cunderlik and Simonovic (2004) stated that the time of concentration parameter needed independent calibration for event simulation, but calibration for autumn 2000 validation

period provided limited accuracy increase to model simulations. Therefore, the amount of water stored in the system may be affecting accuracy (this is further discussed in the research limitations in Chapter 7 in reference to radar-gauge prediction accuracy). The autumn 2000 flood spatial extent indicates that the Llanymynech and Montford gauging stations were both located in areas where out-of-bank flow occurred. Event-specific floods often result in flood peaks higher at Abermule than Montford, with a considerable time delay between the two due to bank and channel storage (Howe *et al*., 1967). Independent flood conditions may have influenced recording accuracy, and could significantly affect optimal model parameter values for individual events. Finally, flow prediction inaccuracies may be attributable to errors in the input precipitation data. This is further investigated in detail in Chapter 7.

Although precipitation explains most of the variation in modelling flows, other factors will explain the remaining variation. Differences in predicted and observed flows are likely explained by changes in physical catchment characteristics. Error in volume amounts will be larger at floodplain locations due to storage of floodwaters and an inability to predict the area under the hydrograph so accurately. Contrastingly, error in peak discharge predictions is likely to be larger where runoff is more erratic. This occurs in the headwater subbasins of the catchment. The lower E_f values during validation for the Severn Uplands are likely to be attributable to differences in parameter values resultant from catchment characteristics unique to the event period such as ground saturation.

6.9 UNCERTAINTY

Marsh (2002) stated that "modest flows and limited river depths, combined with technical and logistical difficulties of refining the stage-discharge relation above bankfull, imply that the accuracy bands which characterise the medium flow ranges can seldom be approached in the extreme flow ranges." The extreme events modelled in this Chapter for the Severn Uplands imply that simulating extreme flows accurately during periods of extreme precipitation is not a straightforward process. Despite fairly accurate results following calibration of the HEC-HMS model for the Severn Uplands, issues still remain regarding sources of uncertainty.

Three main forms of uncertainty associated with model results exist and are derived from firstly, the precipitation data input; secondly, uncertainty inherent in the modelling process and thirdly, the robustness of the parameter sets defining the model and the calibration procedures. There is a plethora of conflicting research whereby data and model uncertainty are questioned. Yapo *et al.* (1996) suspected that model errors in many hydrological models may actually be as large as, if not larger, than the errors in the measurement data. Perrin *et al.* (2001) formed the same opinion and believed that the quality of a rainfall-runoff modelling methodology resides essentially and primarily in the model structure. In contrast, although modelling of the rainfall-runoff process is a problem in its own right, Dinku and Anagnostou (2002) believed error in rainfall input to be a major factor in flood simulation uncertainty. Butts *et al.* (2004) also stated that variation due to uncertainty in rainfall estimation can be significantly larger than the uncertainty due to model structure and parameter variations; however, this depends on catchment size and response time. Also linking to uncertainty in data measurements, Bradley *et al.* (2002) found that previous studies have shown that gauge density is the most important factor in estimating uncertainty. Uncertainty is further discussed in Chapter 9.

6.11 SUMMARY

This chapter has provided the model setup for further analysis in chapters 7 and 8. The gauge-driven runoff predictions simulated the extreme hydrological event of November-December 2006 relatively accurately compared to observed flows. Chapter 7 further investigates the possibility of reducing inaccuracy associated with the HEC-HMS model of the Severn Uplands by using spatially-distributed precipitation inputs to increase accuracy of predictions over gauge sampling. By increasing sampling density, and testing measurement error within gridded precipitation data, a conclusion can be determined as to whether uncertainty derived from measurement error has a large impact on model prediction accuracy, or whether greater sources of uncertainty lie within the modelling structure.

CHAPTER 7

The Comparison, Correction and Performance of Precipitation Data

At present the linkage between radar systems and hydrological forecasting models (e.g. rainfall-runoff models) is not exploited fully. Problems remain in discriminating hydrological model error from that in the forecasts and issues of missing data (Tilford *et al.*, 2003). Nonetheless, literature reviewed in Chapter 2 indicated that radar data have generally increased the accuracy of hydrological forecasts over purely utilising interpolated gauge networks. In the Severn Uplands, the Environment Agency (2003) states that weather radar is not used to its optimum extent and advise further exploration of its use as a forecasting tool. Complex topography, combined with complex meteorological and orographic effects and inadequate gauge representation make accurate predictions of extreme rainfall difficult. Radar images provide spatially and temporally enhanced rainfall data. Nonetheless, it is widely recognised that radar-rainfall algorithms predict rainfall with a high degree of uncertainty (Anagnostou and Krajewski, 1999). Radar rainfall is subject to large amounts of error and often leads to biased prediction compared to reference values from gauge records.

This chapter investigates the difference in accuracy of distributed precipitation grids at high temporal and spatial frequency, compared to an interpolated gauge network as inputs to a hydrological model to simulate an extreme event. Gauge and radar rainfall predictions are compared and geostatistical interpolation is used to generate a reference rainfall surface using gauge data and secondary variables. This reference surface is then used to correct radar rainfall predictions to try to increase accuracy during the hydrological modelling process.

7.1 PRECIPITATION DATA COMPARISON

7.1.1 Gauges

Tipping bucket gauges give the most accurate point measurements of rainfall (Cole and Moore, 2008). A network of 12 precipitation tipping bucket gauges covers the Severn Uplands with complete datasets for the time periods in question (Table 6.4 and Figure 6.6). The accuracy of the rain gauge network is deemed sufficient if it accurately measures and is representative of rainfall over the selected area (Vieux, 2004). USACE (1996) recommend a minimum number of rain gauges N_g for catchment modelling using HEC-HMS. This is calculated as

$$N_g = \left(\frac{A}{2.59} \right)^{0.33} \tag{7.1}$$

where A is the catchment area in square kilometres. For the Severn Uplands, N_g equates to approximately 9 (A is 2014.1 km²). Therefore, a total of 12 gauges situated across the catchment is an estimated third larger than the recommended minimum number of gauges. Even so, spatial resolution with an average density of one gauge per every 169 km² (a square coverage of 13 km by 13 km) may result in localised precipitation being unaccounted for in the gauge records. A solution to this issue is provided by radar rainfall imagery which offers a data source of both increased spatial and temporal resolution.

7.1.2 Radar

Generally, rainfall radar images are used in nowcasting mode, which utilises rainfall forecasts to run through a calibrated model in order to predict river flow values and alert the relevant authorities to possible flood inundation. However, archived imagery is available, enabling historical extreme hydrological periods to be recreated. Weather radar emit pulses of microwave radiation and samples the received backscattered power which is converted to reflectivity (Z), a measure for the total cross-section of the particles within the measurement volume. The reflectivity is then converted to a radar precipitation estimate (R) using an empirical relationship (Gjertsen *et al.*, 2003).

Radar data for the UK are available at a maximum temporal resolution of 5-minutes and a spatial resolution of 1 km^2, a much finer spatial and temporal sampling resolution than the gauge network. These radar data, known as Nimrod image files, are collated by the Met Office and are freely available for academic use via the British Atmospheric Data Centre (BADC). Nimrod radar images are derived from the Radarnet IV system. Across the UK, a network of 19 ground-based radar dishes scan at four elevations (angles to the horizontal) and have a beam width of 1 degree. Nimrod incorporates data from the weather radar network, Mesosat satellite observations, lightning location systems and Met Office and some Environment Agency gauges to generate as complete an observation of areal precipitation as possible. A combination of radar and limited gauge data utilising kriging with an external drift is used to produce the final precipitation estimate produced by the UK Met Office. The product is a corrected composite of radar rainfall data. Corrections are made for errors to account for (after Tilford *et al.*, 2003; Golding, 1998):

- Overshooting of precipitation by beam at long ranges
- Low-level orographic and other growth, drift or evaporation of rainfall below the radar beam
- Intersection by the radar beam of the melting layer in which snow flakes acquire a layer of melted water enhancing reflectivity (the so-called “bright-band”)
- Attenuation of the radar beam as it passes through precipitation leading to a reduction in reflected energy
- Distortion of the beam due to strong gradients in temperature and moisture at low levels leading to the beam intersecting the ground which causes false returns of precipitation (the so-called “anomalous propagation” or “anaprop”)
- Any remaining anomalous echoes due to hills and other ground clutter
- Occultation (hiding) of the radar beam(s) due to topography

Nimrod images are processed by the Met Office to produce three radar-based rain rate composites at 1 km, 2 km and 5 km gridded resolution. At each point the grid represents the highest quality and spatial resolution data available. The quality of the composite product is dependent on both the quality and spatial resolution of the source data, which in turn is highly reliant on distance from the nearest radar site. Hydrological applications need radar data as near to the source as possible and, therefore, ranges beyond 100 km usually give results of reduced quality. The furthest point from a radar source in the Severn

Uplands is approximately 85 km (Table 7.1). All Nimrod files are projected in the Cartesian National Grid.

Radar signals originating from non-meteorological sources need to be detected and removed before bias adjustment. With the Nimrod data this is performed by the Met Office to produce the Nimrod composite output files. Gauge adjustment has been performed operationally in the UK for around two decades (Gjertsen et al., 2003). However, Tilford *et al.* (2003) state that in recent years, radar measurements are not adjusted in real time but are in fact only corrected on a weekly basis to remove systematic bias due to hardware calibration errors and variation in radar sensitivity. For accurate forecasting of hydrological extremes using radar rainfall these temporal adjustments may be too infrequent, particularly in areas with complex topography, where residual errors are likely to be large. Nonetheless, the horizontal spatial variability of rainfall in upland areas makes radar measurements particularly useful for hydrological modelling in upland catchments (Lewis and Harrison, 2007). The operational use of radar rainfall in hydrological applications spans around 15 years (Krajewski and Smith, 2002).

7.1.3 Data selection and pre-processing

UK radar composite images at 1 km^2 spatial resolution are only available from April 2004 which limits the period of data availability to approximately four years. Within this time period an extreme winter-time precipitation event occurred during November-December 2006 (matching the gauge data used for model calibration in Chapter 6). This event was selected to compare gauge and radar rainfall data capabilities. Stellman *et al.* (2001) stated that it is important to compare mean areal precipitation with grid-distributed precipitation during heavy rain events when river response will be greatest.

Radar products are not frequently delivered in a way that they can be used directly (Einfalt, 2004). This is true with the UK Nimrod radar data supplied by the Met Office. For high temporal and spatial resolutions, images covering the entire UK generate in the order of 2GB of data per day. Furthermore, radar imagery is supplied in a format that is not recognised by most hydrological models. To reduce data capacity the Nimrod cells encompassing the Severn Uplands were extracted from the UK composite files (Michaelides, 2008). Nimrod ASCII files were converted into data storage system (DSS)

files (stored in the HEC-DSSVue program) using a batch file (Evans, 2008) so that the resulting DSS files were readable by HEC-HMS.

7.1.4 Comparison measures

Radar imagery was compared to gauge readings for the November-December extreme event. Time-series data were extracted from each radar cell that the 12 rain gauges were located in. To create time-series records that were temporally comparable to those of the gauges, groups of three 5-minute values from the radar images were summed to give 15-minute total precipitation values. The time-series were compared using the methods described in Chapter 3. Error detection is crucial for the accurate application of rainfall predictions. Errors in gauge readings are mainly caused by wind effects and tipping bucket gauges are known to under-report during heavy rainfall (Vieux, 2004; Wilson and Brandes, 1979). As weather radar measures the reflectivity of precipitation particles aloft, they normally report precipitation earlier than rain gauges on the ground. Some particles may melt or evaporate before ground contact and in such cases the radar reports precipitation where ground-based recording devices observe no rainfall. These noisy images generally result in an overestimation of rainfall by radar fields (Teschl *et al.,* 2006). A complete statistical characterisation of these gauge-radar rainfall uncertainties must be performed such as to account for all error possibilities (Mandapaka *et al.*, 2008).

7.1.4.1 Prediction accuracy

The Gilbert Skill score (GS) was used to determine at which threshold values the radar data were predicting more accurately in comparison to the rain gauge readings. The higher the GS score the higher the predictive accuracy of the radar prediction compared to the corresponding gauge values. GS scores for the November-December 2006 extreme event suggest greater predictive accuracy at a 0.2 mm threshold (Figure 7.1). This can be explained by the incremental way in which the gauges record rainfall every 0.2 mm. The prediction of rainfall between 0.01 and 0.1 mm, and that between 0.4 and 0.8 have a similar success rate. At 1.6 mm and above, the accuracy of the radar to predict rainfall at the gauge locations reduces. These findings suggest that larger error values will coincide with higher radar rainfall values (above 0.8 mm) when compared to corresponding rain gauge readings.

Table 7.1 Radar and gauge comparison properties and statistics

							Total (mm)			Average (mm)		
Station	**Elevation (m)**	**Distance from radar (m)**	**Correlation**	**RMSE**	**RMSF**	**MFB**	**Radar**	**Gauge**	**BIAS**	**Radar**	**Gauge**	**BIAS**
Bagley	83	58500	0.74	0.31	1.20	0.808	192.64	155.60	-37.04	0.033	0.027	0.006
Bishop's Castle	243	26500	0.78	0.31	1.22	0.993	227.01	225.40	-1.61	0.039	0.038	0.000
Cefn Coch	310	59700	0.76	0.36	1.28	0.981	381.38	374.20	-7.18	0.065	0.064	0.001
Dolydd	294	70200	0.78	0.42	1.42	1.187	530.18	629.40	99.22	0.091	0.107	-0.017
Llanfyllin	156	62300	0.72	0.47	1.30	0.769	431.49	332.00	-99.49	0.074	0.057	0.017
Llangynog	166	74000	0.77	0.38	1.34	0.966	535.92	517.80	-18.12	0.092	0.088	0.003
Nantgwyn	306	56700	0.67	0.44	1.34	0.892	438.77	391.60	-47.17	0.075	0.067	0.008
Pen-y-Coed	306	71700	0.74	0.43	1.40	0.978	624.42	610.80	-13.62	0.107	0.104	0.002
Rorrington	205	38500	0.80	0.42	1.21	0.650	276.73	179.80	-96.93	0.047	0.031	0.017
Sarn	194	39200	0.66	0.37	1.22	0.710	291.22	206.80	-84.42	0.050	0.035	0.014
Vyrnwy	264	71500	0.78	0.40	1.39	1.082	570.91	617.80	46.89	0.098	0.106	-0.008
Welshpool	74	48300	0.69	0.47	1.24	0.760	310.94	236.20	-74.74	0.053	0.040	0.013

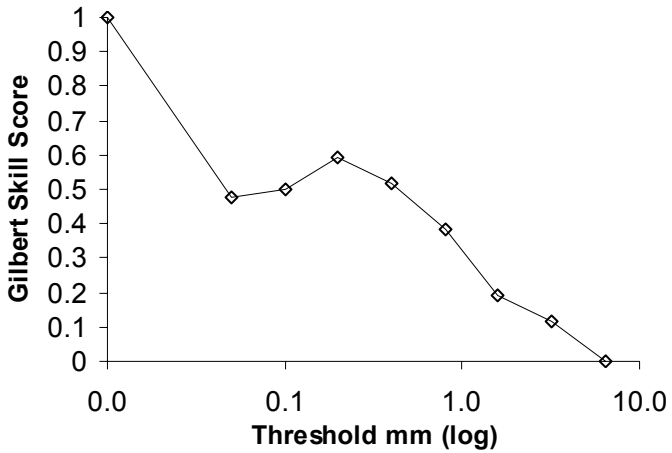

Figure 7.1 Gilbert Skill scores for incremental precipitation threshold values

7.1.4.2 Coefficient of correlation

Correlation values are large for all radar-gauge site comparisons, ranging from 0.66 to 0.8 (Table 7.1). To provide context, comparisons of radar and gauge event rainfall by Haberlandt (2007) found coefficient of correlations of between 0.59 and 0.89. No spatial pattern is present for the correlation values across the catchment. Even though correlation coefficients are large, there still may be large error discrepancies between radar and gauge observations.

7.1.4.3 Bias

The difference between the predicted and corresponding measured value is the experimental error. The recorded bias for the November-December 2006 extreme event indicates systematic errors of approximately ± 100 mm for precipitation totals (Table 7.1). Radar time-series over-predict ground observations at most of the gauging station locations. Two stations (Dolydd and Vyrnwy) show large under-predictions by the radar and five stations (Llanfyllin, Rorrington, Sarn, Welshpool and Nantgwyn) show large over-predictions by the radar for precipitation totals. In terms of absolute error the most accurate radar predictions in accordance to gauge reference data are Bishop's Castle and Cefn Coch. Additionally, the mean average error was calculated for the station time-series. Only values above a 0.05 mm threshold were included such as to minimise discretisation errors and the influence of anomalous propagation (Cole and Moore, 2008). Average precipitation (15-minute interval) bias for November-December 2006 indicates systematic errors with a range of ± 0.017 mm (Table 7.1). The largest biases were located at Dolydd for radar under-prediction and Llanfyllin and Rorrington for radar over-prediction. The smallest absolute error for average precipitation was at Bishop's Castle and Cefn Coch.

7.1.4.4 Root mean squared error (RMSE)

Time-series precipitation residuals indicate a mean RMSE of approximately 0.40 mm across the Severn Uplands catchment for rainfall with a range of 0.31 to 0.47 mm (Table 7.1). Again, these were calculated for values ≥ 0.05 mm. No obvious spatial pattern is

apparent for RMSE values. Gauging stations with the smallest error are Bagley and Bishop's Castle; those with the largest error are Llanfyllin and Welshpool.

7.1.4.5 Root mean squared factor (RMSF)

RMSF typically uses hourly rain gauge data above a threshold as ground reference. This threshold was held at 0.2 mm, equal to the incremental values of tipping bucket gauges. As the time-series analysed here are sampled at 15-minute intervals, a quarter of the standard hourly threshold was used. Values above the 0.05 mm threshold were used for error calculations (this also avoids division by zero when computing the RMSF). The multiplicative error ranges in scale from 1.2 to 1.42 across the Severn Uplands (Table 7.1). RMSF values are generally smaller towards the east of the catchment and larger in the west.

In comparison to findings in the literature, RMSF values for the Severn Uplands are relatively small. For example, Trapero *et al.* (2006) estimated RSMF values of between 3.62 and 7.89 for rainfall above a 0.2 mm threshold and Golding (1998) compared hourly precipitation accumulations with point rain gauge observations, obtaining a RMSF of 3.62. Harrison *et al.* (2000) found that sampling difference alone can account for a RMSF difference of between 1.26 and 2.51 for hourly radar data at a 5 km² spatial resolution. Recent Met Office figures suggest an RMSF of 2 is now obtained for rainfall values for quality controlled and corrected Nimrod radar data under most conditions except at extreme range (Harrison *et al.*, 2000). With respect to these guidelines, RMSF values for the Severn Uplands indicate less error between precipitation residuals at analysed sites than expected. This is probably due to the higher spatial and temporal resolution of radar data used in this study compared with those routinely used by the Met Office for weather forecasting.

7.1.5 Explanatory factors

Differences between the gauge and radar precipitation time-series are likely to have arisen from capabilities of radar devices to represent rainfall accurately. Several sources of uncertainty are present when processing radar data. Although many uncertainty issues are

corrected for at a nationwide level, as discussed in Section 7.1.2, error still remains at a local scale. Three main spatially varying factors seem to correlate with error in the Severn Uplands. These factors are described below and are explored in relation to the RMSF values.

(i) Topography

Given the smaller prediction accuracy for larger rainfall amounts, as indicated by the GS scores, radar readings over areas of high elevation, where rainfall is generally greater, are likely to be the most erroneous. Predicting extreme rainfall in mountainous terrain is challenging and radar-rainfall prediction in complex terrain is complicated by ground returns and signal loss associated with beam blockage (Krajewski and Smith, 2002). The occultation and echoes of the radar beam due to topographic changes and issues arising from orographic enhancement may have resulted in larger inaccuracies in the higher elevations to the north and west of the Severn Uplands. Correlation between site elevation and RMSF shows a significant positive correlation of 0.61 ($p < 0.05$). Figure 7.2 illustrates the relationships between these two variables; radar-gauge comparisons over higher elevations generally have larger RMSF values.

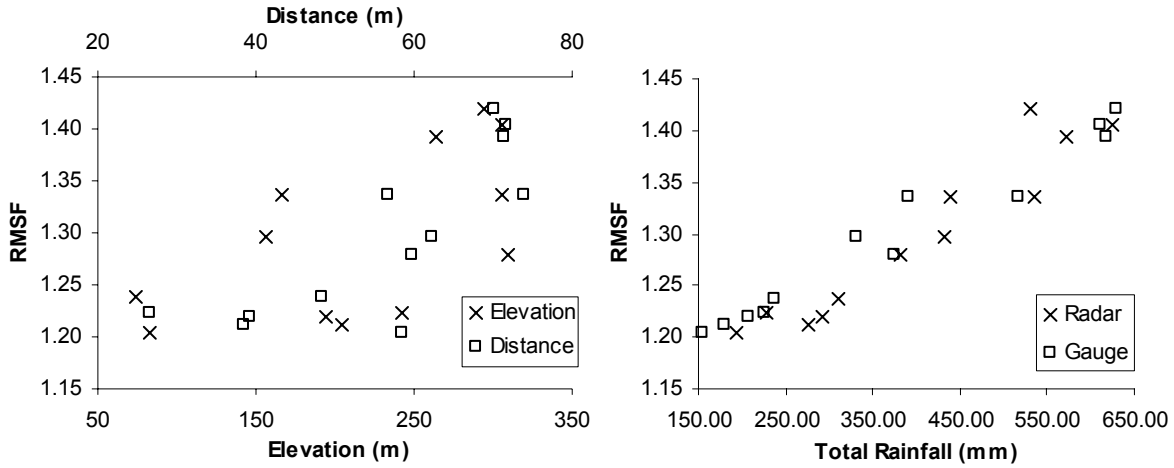

Figure 7.2 RMSF values between radar and gauge precipitation for elevation, distance from the radar source, and radar and gauge precipitation totals

(ii) Radar range

The greater the distance from the radar source the greater the error, which can result from the overshooting of precipitation by the radar beam at long ranges (Tilford *et al.*, 2003). The nearest ground-based radar dish, named Clee Hill, is located to the south-east, outside the Severn Uplands catchment boundary. Multiplicative error is greater further away from the radar source, towards the north-west of the catchment (Figure 7.2). Correlation between distance from the radar and RMSF is significantly positive at 0.80 ($p < 0.01$). At close ranges both overestimation and underestimation can occur due to the interaction of mean-field and range-related biases, whilst at further ranges (>50 km) range-related bias dominates and causes significant underestimation of rainfall (Borga *et al.*, 2000). It is difficult to distinguish whether this is the case in the Severn Uplands as the sites furthest away from the radar also happen to be those at the highest elevations.

(iii) Rainfall amount

The amount of precipitation may have an effect on gauge-radar residuals. Multiplicative error is larger given higher rainfall totals for the November-December 2006 event. Significant positive correlations are evident between RMSF values and the radar rainfall totals (0.95; $p < 0.001$) and the gauge rainfall totals (0.98; $p < 0.001$). Larger error values at sites in the west of the Severn Uplands are likely to have resulted from greater rainfall totals which are evident given higher elevations which in turn result in increased radar distortion. These locations also happen to be furthest away from the nearest radar source.

Given the significant correlation of error with these contributing factors, the variation of the elevation and radar surfaces were subsequently used to correct radar imagery and enhance distributed precipitation predictions. Radar distance was not used for correction as although it may be a contributing factor to radar error, it does not provide any direct useful spatial variation information, as it lacks a causal relationship between rainfall and physical catchment characteristics, to predict a rainfall surface.

7.2 INDEPENDENT CALIBRATION

Prior to correcting the radar data the HEC-HMS model of the Severn Uplands was re-calibrated for the new radar precipitation data. Bradley and Kruger (1998) discuss the importance of model recalibration when switching precipitation products, particularly when an observed bias in precipitation is found between the two products. Their study confirmed that recalibration was required to increase the accuracy of the radar-driven simulation. Sun *et al.* (2000) also found that prior to the calibration of radar data larger amplitude errors were evident in the hydrograph. Therefore, an optimal parameter set was located using the peak-weighted objective function using the univariate search algorithm optimisation procedure, as detailed in Chapters 3 and 6 (only one was selected due to the computational and time intensive process of optimising the model using gridded precipitation data). The model prediction statistics are detailed in Table 7.2. Prior to independent dataset calibration (i.e. using the calibrated parameters from the gauge-driven model) the model was not predicting accurately. Efficiency values were very low (all negative) and error was large. Hydrograph volume was substantially over-predicted; by as much as 150% at Llanymynech. Peak flows were also over-predicted at all gauge locations. Following model recalibration predictive accuracy significantly increased. E_f values ranged from 0.51 to 0.72, with both Llanymynech and Montford predicting sufficiently ($E_f > 0.6$), Abermule was border-line in terms of acceptability at 0.6 and Rhos-y-Pentref was below criterion of 0.6. Errors were smaller than those of the uncalibrated radar model and the descriptive statistics were more closely matched to those of the observed flow time-series.

In comparison to modelling using the gauge time-series, the radar data provided no increase in accuracy in terms of efficiency. As with the gauge-driven simulations, Abermule was found to report the lowest predictive accuracy. Nonetheless, the RMSE and MAE were substantially smaller for most gauging stations using the radar precipitation as input. As the radar data were not found to increase accuracy during the modelling procedure, the possible influence of error within the precipitation data itself was investigated to determine whether corrected radar inputs provided an increase in accuracy for model simulations.

Table 7.2 HEC-HMS modelling results between observed and simulated time-series at four gauge locations for the observed-calibrated (November-December 2006) and observed-validated (October-November-December 2000) periods using radar rainfall

		Observed (ND 2006)	Uncalibrated (ND 2006)	Calibrated (ND 2006)	Corrected Elevation	Corrected Radar
Rhos-y-Pentref	Mean	3.545	8.510	3.909	3.627	3.469
	σ	2.971	8.591	3.754	3.496	3.362
	ρ	-	0.883	0.839	0.839	0.839
	R^2	-	0.780	0.705	0.704	0.704
	MAE	-	1.222	0.406	0.383	0.379
	RMSE	-	5.048	2.333	2.147	2.058
	E_f	-	-6.045	0.510	0.590	0.618
	Peak *Q*	16.6	53.0	27.5	25.7	24.7
	Volume	479.7	1161.4	529.1	490.8	469.45
Abermule	Mean	36.956	49.293	29.118	27.866	27.710
	σ	31.232	51.279	30.308	28.455	28.320
	ρ	-	-0.190	0.825	0.833	0.877
	R^2	-	0.036	0.681	0.694	0.769
	MAE	-	0.701	0.524	0.515	0.503
	RMSE	-	38.615	22.487	20.494	20.544
	E_f	-	-7.510	0.597	0.603	0.681
	Peak *Q*	173.2	185.8	119.0	113.6	113.4
	Volume	294.1	401.4	231.7	221.8	220.0
Llanymynech	Mean	54.391	134.539	50.933	51.827	50.894
	σ	52.229	117.273	54.692	55.145	54.306
	ρ	-	0.896	0.868	0.868	0.868
	R^2	-	0.803	0.753	0.753	0.753
	MAE	-	1.632	0.537	0.535	0.530
	RMSE	-	72.749	30.604	29.922	29.662
	E_f	-	-3.374	0.716	0.715	0.719
	Peak *Q*	264.5	487.1	259.1	272.1	265.6
	Volume	370.3	937.2	346.8	352.8	346.5
Montford	Mean	102.651	198.696	92.438	87.222	86.490
	σ	84.046	182.381	92.456	87.027	86.291
	ρ	-	0.904	0.857	0.860	0.858
	R^2	-	0.817	0.735	0.740	0.737
	MAE	-	1.027	0.488	0.470	0.471
	RMSE	-	94.553	43.131	37.978	38.475
	E_f	-	-2.092	0.661	0.676	0.671
	Peak *Q*	359.8	667.9	368.6	365.4	359.4
	Volume	268.7	536.6	242.0	228.3	225.4

7.3 RADAR DATA CORRECTION

It is expected that, for a well-calibrated hydrological model that represents adequately the important runoff processes within the catchment, the major factor contributing to the uncertainty in the predicted flows is the uncertainty in rainfall (Butts *et al.*, 2004). Despite the high spatial resolution of radar data there is often a large space-time variable bias in radar rainfall estimates and data are subject to various sources of random and systematic

error. Random errors tend to average out at large spatio-temporal scales of aggregation, yet systematic errors remain. This makes the direct use of radar rainfall data in quantitative hydrologic forecasting extremely difficult (Seo *et al.*, 1999). These errors have been quantified and discussed in section 7.1.4. Using radar imagery for accurate hydrological predictions is not possible unless the uncertainties that are associated with radar-derived precipitation are quantified and corrected. Radar by itself has not been demonstrated to be a consistent predictor of the actual rainfall amounts, but by merging gauge and radar data, strengths from each measurement system can be used whilst minimising their respective weaknesses (Hoblit and Curtis, 2001). The basic assumption underlying radar correction is that gauge precipitation is correct and radar data only provide extra information. Gauge adjustment is a widely used approach for increasing the quantitative accuracy of radar precipitation predictions (Gjertsen *et al.*, 2004). This is achieved at a national level, as described in Section 7.1.2, however, the gauge network density is insufficient to account for accurate adjustments in areas of complex topography. Gauge adjustment combines the individual strengths of both the gauge and radar measuring systems; the radar provides spatial distribution information while a gauge reading provides a point measure of relatively high quantitative accuracy. Elevation data are also useful in providing information concerning spatial information where topography largely influences rainfall regimes. To correct the radar imagery, the gauge point data were interpolated to create a reference distribution of average precipitation using the spatial variability of the radar precipitation and elevation fields. The process is represented schematically in Figure 7.3.

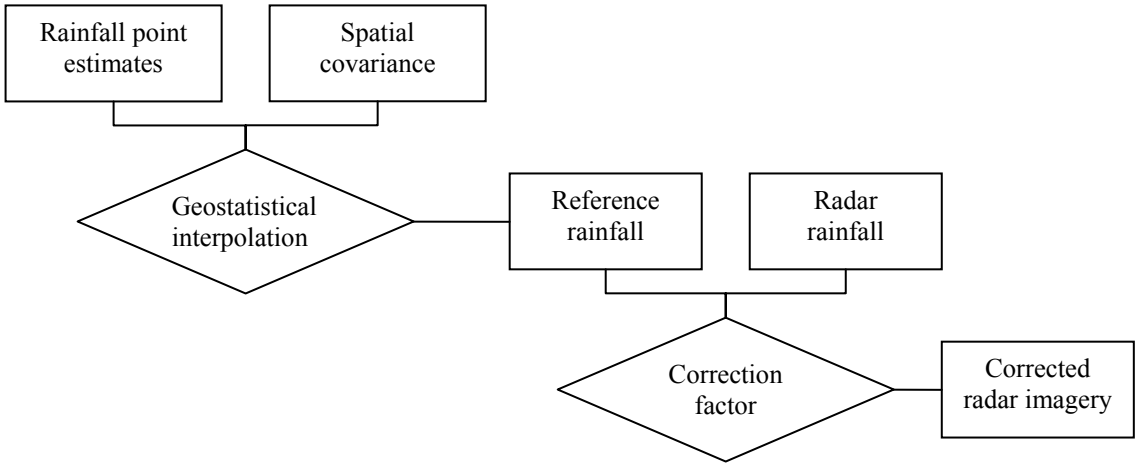

Figure 7.3 Schematic diagram illustrating the correction stages of radar imagery using geostatistical interpolation and a correction factor

7.3.1 Geostatistical interpolation

There are many types of interpolation methods which interpolate between point values to create a continuous surface. Basic deterministic interpolation procedures include Thiessen polygons and inverse-distance weighting (IDW). The downfall of these simple objective analysis schemes is that they ignore important spatial variation in secondary variables. Consequently, over-smooth representations of the spatial distribution of rainfall are produced; an adverse effect which is further intensified when the network of rain gauges is sparse. More complex interpolation techniques include multiple regression and kriging (geostatistics). Creutin and Obled (1982) showed that in a region with intense and greatly varying rainfall events, sophisticated techniques predict more accurately than any of the more commonly used techniques.

Multiple regression is a straightforward approach for incorporating the most relevant predictors into the spatial interpolation of rainfall. Rainfall can be predicted from collocated variates, such as elevation, through (non)linear regression. Multiple regression is very common in the mapping of climatic variables because it adapts to almost any space and usually generates adequate maps (Vincente-Serrano *et al.*, 2003). However, Prudhomme and Reed (1999) state that there is an evident lack of accuracy in using multiple regression analysis to map precipitation in mountainous areas, which many authors have undertaken. The major disadvantage of multiple regression is the disregard for information provided by surrounding climatic stations, which is critical when the correlation between the two variables is small and the residuals are spatially correlated (Ricart, 2004; Bacchi and Kottegoda, 1995). Given the topographic variability in the Severn Uplands, regression and simpler interpolation methods were rejected and geostatistical interpolation was adopted. Many authors have found geostatistical methods to out-perform regression methods as the covariance of secondary variables drastically reduces prediction errors (e.g. Goovaerts, 2000; Kyriakdis *et al.*, 2001; Sun *et al.*, 2000; Kelly and Atkinson, 1993). The average event rainfall (15-minute interval) was used to create an average precipitation reference surface through interpolation using the covariance of elevation and radar precipitation fields which are generally largely correlated with gauge rainfall over an event period.

7.3.1.1 Covariates

The advantage of using geostatistics is the ability to use covariates as secondary information, which provides detailed spatial distributions given higher sampling densities, to aid interpolation of the predicted variable (Earls and Dixon, 2007). For rainfall, secondary information usually takes the form of elevation or weather-radar observations, both of which have frequently been used as covariates to increase gauge interpolation accuracy (Goovaerts, 2000; Krajewski, 1987; Seo *et al.*, 1990a; Sinclair and Pegram, 2005; Sun *et al.*, 2000; Earls and Dixon, 2007). The interactions between atmospheric and topographic structure within high relief areas make interpolation methods which do not consider these features unrealistic from a meteorological point of view (Lang and Grebner, 1998). Both elevation and radar rainfall were used independently as covariates to interpolate gauge rainfall across the Severn Uplands.

(i) Elevation

Elevation is the most frequently used variable for enhancing interpolation, especially over mountainous regions. It is used as a surrogate as detailed temperature information is often lacking, given that precipitation is heavily influenced by temperature, especially by its vertical lapse rate, which dictates the local level (height) and rate of condensation (Kyriakdis *et al*., 2001). Prudhomme and Reed (1999) found that estimated errors are one third smaller when taking into account topographical information. Agnew and Palutikof (2000) found elevation to be one of the most powerful predictors of local climate and within the UK Lloyd (2005) discovered that for most months (March to December) the use of elevation data to inform estimation of monthly precipitation was beneficial.

Broad-scale topographic features have been found to correlate highly with precipitation. Where precipitation amount and elevation are related linearly (in this case, precipitation amounts tend to be small at low elevations and large at high elevations), estimates informed by elevation data are often more accurate than those made using the precipitation data alone (Lloyd, 2005). To determine the scale of interaction between precipitation and elevation the Pearson product-moment correlation coefficient was calculated between rain gauge precipitation and varying spatial averages of elevation (Kyriakdis *et al.*, 2001). These low-pass filters were used to measure the wider influence of elevation. Results indicate that a filter of 2 km produced optimum correlation with gauge rainfall with a

correlation value of 0.78 (Figure 7.4). Goovaerts (2000) and Guan and Wilson (2005) recommend a Pearson correlation coefficient threshold of 0.75 for useful precipitation-elevation cokriging. As correlation exceeded this threshold for the Severn Uplands elevation was deemed as a suitable covariate for geostatistical interpolation.

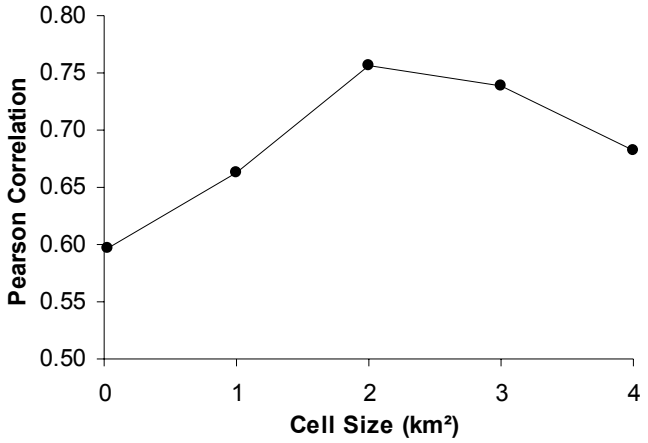

Figure 7.4 Pearson correlation of elevation and gauge rainfall for varying grid cell sizes

(ii) Radar rainfall

Interpolation methods more often than not fail to represent the variability of the rainfall pattern. In addition to elevation, alternative spatial information such as radar precipitation data may increase the accuracy of estimates (Lloyd, 2005). In the Severn Uplands, spatial rainfall information was predicted using radar rainfall as a covariate, given that radar rainfall retains the general covariance structure of the true precipitation field (Sinclair and Pegram, 2005). Average radar and gauge rainfall (radar pixels at gauge locations) for the Severn Uplands have a correlation coefficient of 0.96 (p <0.001). As the average radar field should retain a similar covariance structure to that of the gauge data, average radar rainfall was selected as a suitable covariate to interpolate gauge rainfall using cokriging.

7.3.1.2 Data distributions

A Gaussian distribution is desired for geostatistical interpolation because kriging and cokriging assume that the data are multivariate normally distributed and given normality,

the most accurate results will be obtained. The distributions of the three variables (gauge rainfall, elevation and radar rainfall) were interpreted visually using histograms and normal QQplots. Visual inspection revealed that all the data sets were non-Gaussian distributed. As radar rainfall data were skewed towards small values, a natural logarithm was applied in order to fit a Gaussian distribution more closely. Skewness was reduced from 0.32 to -0.05 and kurtosis remained the same at 1.56. The logarithmic transformation was also applied to the gauge data, reducing the skewness value from 0.55 to subsequently match that of the transformed radar. Kurtosis was slightly reduced from 2.70 to 2.12. Elevation was slightly skewed towards smaller values and a Box-Cox transformation with a parameter value of 0.59 resulted in an approximately Gaussian distribution. The transformation of the elevation data resulted in a skewness value of 0.003 (0.4 untransformed) and a kurtosis value of 2.21 (2.59 untransformed).

7.3.1.3 Trends

The non-random (deterministic) component of the variation across a surface can be represented by a mathematical formula (trend). For example, a gently sloping hillside can be represented by a linear plane. Trend analysis was performed within a GIS to determine the trend surfaces required for the universal cokriging (cokriging with a trend) method. The term ‘universal’ for kriging and cokriging indicates the presence of trend terms (Stein and Corstern, 1991). Drift is a systematic change in the *Z* value. The radar, gauge and elevation data all exhibited linear trends in the *XZ* plane (Figure 7.4). Data in the *YZ* plane were relatively trend-free; the slight trends present in the gauge data (linear) and elevation (U-shaped) were not modelled as repetition of the Cokriging procedure showed that ignoring these minor trends resulted in increased predictive performance of the variogram model. As the radar and elevation covariates exhibited similar trend properties to that of the gauge data, they were considered suitable for use as secondary variables. Due to the presence of trends, universal cokriging interpolation was applied and first-order trend functions were fitted to model each variate globally.

7.3.1.4 Cokriging

Universal cokriging was performed to interpolate the gauge mean precipitation surface, independently using the two covariates, elevation and radar. As the Severn Uplands covers

a large area, with complex topography and a fairly sparse gauge network, there is likely to be an increase in accuracy using cokriging compared to simpler interpolation methods (Prudhomme and Reed, 1999). Cokriging is most effective when the covariates are highly correlated with the dependent variable (Apaydin *et al.*, 2004). This was confirmed for the radar and elevation covariates for the Seven Uplands in Section 7.2.1.1 and by visually inspecting the projected data as the projected trends follow a similar pattern (Figure 7.5).

Common practice consists of inferring and modelling the semivariogram rather than the covariance function (Goovaerts, 1997). Consequently, the model was predominantly fitted to the semivariogram. However, the covariance was also considered. The spherical model was found to be the best fitting model for both methods and resulted in the smallest error. The largest distance between points for both the covariates was approximately 90 km. Half of the maximum distance was set as the maximum model range at 45,000 m, which equates to an approximate lag size of 4500 m with 10 lags. Anisotropy was not present in any of the semivariogram or covariance surfaces.

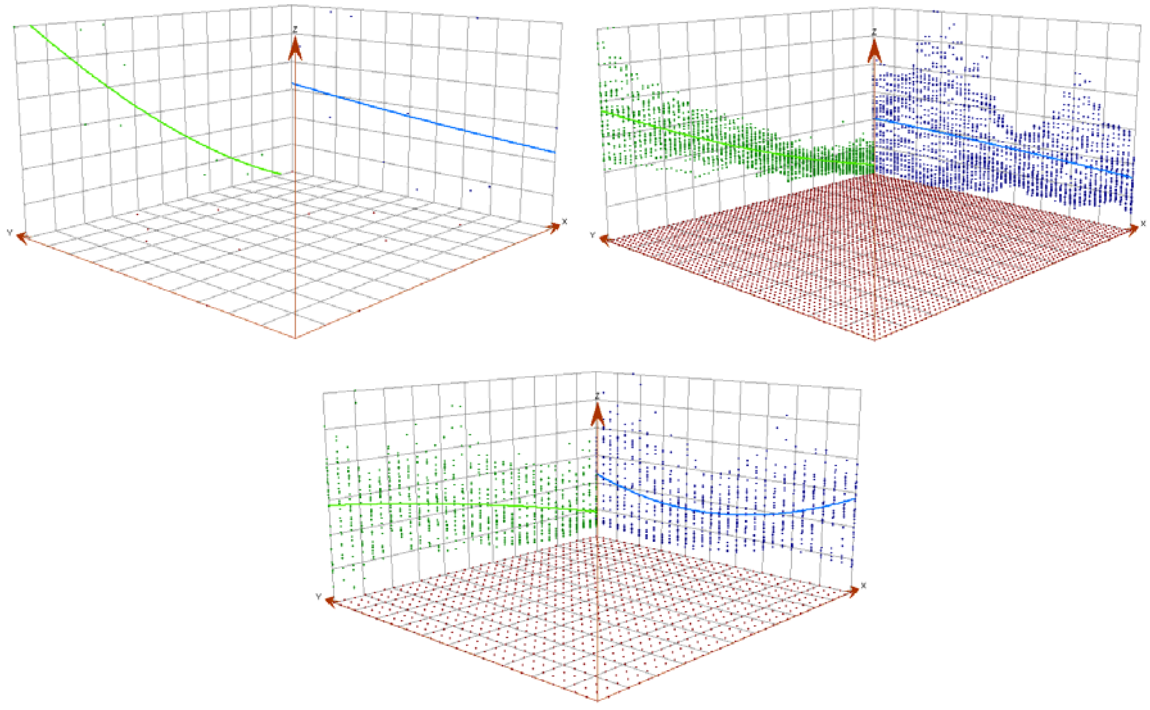

Figure 7.5 Trends in projected data for gauge (top left), radar (top right) and elevation (bottom)

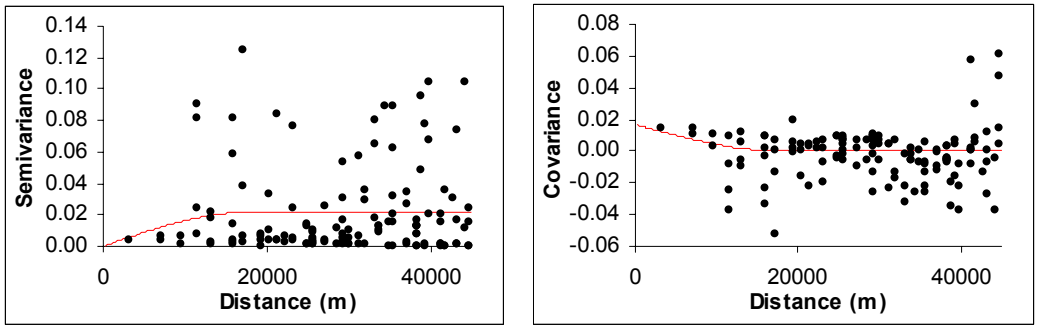

(i) Gauge semivariogram and covariance (nugget: 0; partial sill: 0.15687 and 0.050425)

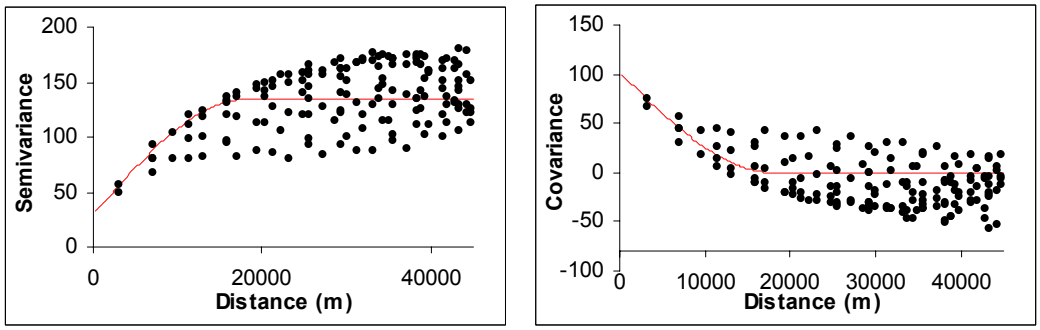

(ii) Elevation semivariogram and covariance (nugget: 37.093; partial sill: 104.39 and 101.51)

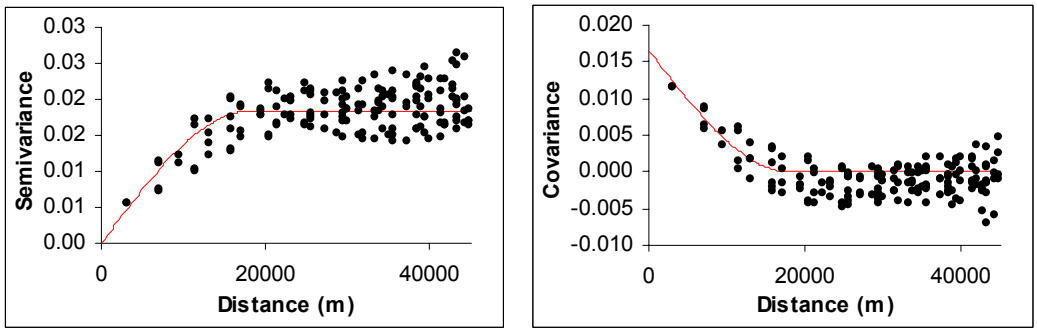

(iii) Radar semivariogram and covariance (nugget: 0.0022539; partial sill: 0.15901 and 0.016521)

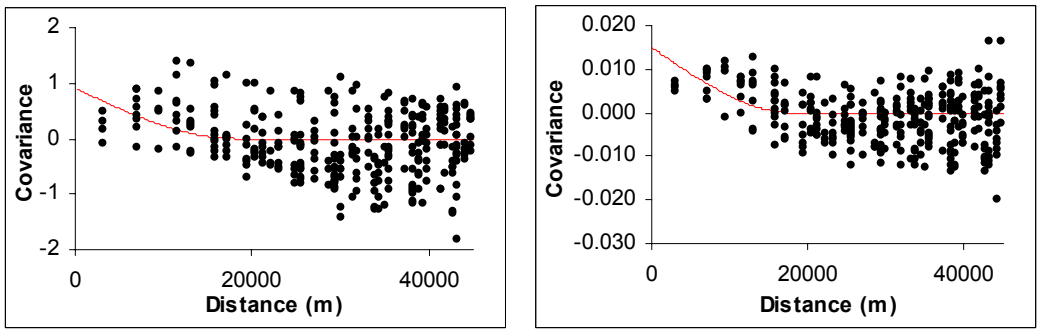

(iv) Cross-covariance of gauge and elevation (partial sill: 2.8572) and gauge and radar (partial sill: 0.019591)

Figure 7.6 Spherical semivariogram models for gauge prediction using elevation and radar as independent covariates

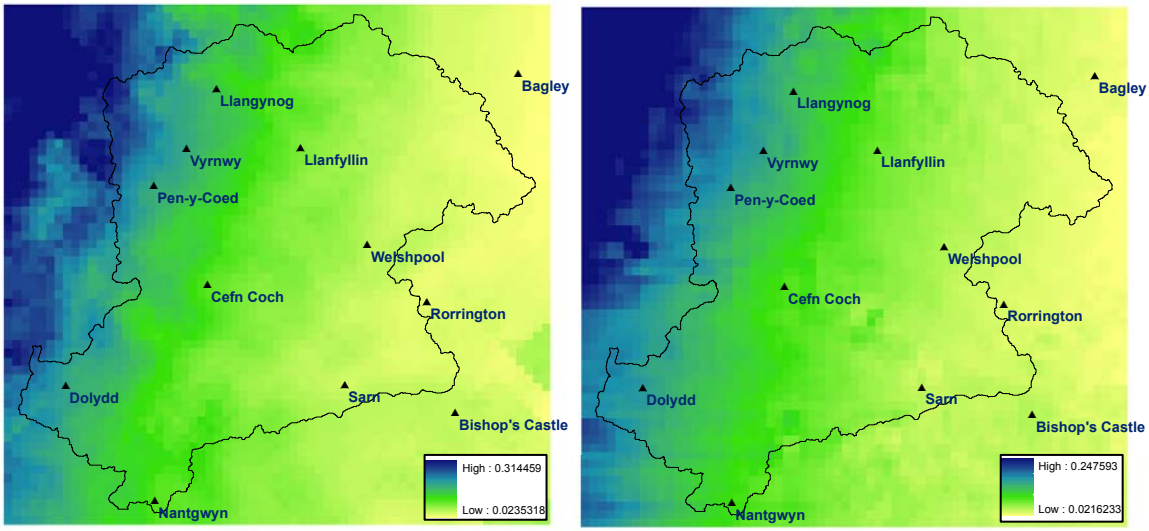

Figure 7.7 Geostatistical interpolation of mean gauge precipitation using the universal cokriging method using the elevation (left) and radar (right) covariates

Table 7.3 Prediction errors and cross-validation results for universal cokriging using elevation and radar as covariates

	Elevation	**Radar**
Prediction errors		
Mean	0.000008306	-0.002235
RMS	0.0135	0.012
Average SE	0.04159	0.039
Mean standardised	-0.099	-0.037
RMS standardised	1.080	1.084
Cross Validation results		
Measured	Predicted	
0.107	0.106	0.087
0.104	0.102	0.109
0.067	0.081	0.079
0.106	0.089	0.093
0.064	0.071	0.069
0.088	0.115	0.095
0.057	0.061	0.058
0.035	0.042	0.046
0.040	0.038	0.042
0.031	0.035	0.034
0.038	0.022	0.023
0.027	0.002	0.002
Correlation	0.924	0.926

Visually, the radar covariate indicates a better model fit to the data than that of the elevation covariate (Figure 7.6). The nugget and partial sill values are stated in Figures 7.6 for each model. No nugget or near-zero nugget values of the gauge and radar data may indicate minor instrumental measurement error (Longley *et al.*, 2005). In contrast, the elevation semivariogram has a relatively large nugget value indicating a possible error

source from the measuring instrument. This may be attributable to satellite sensor imaging error of elevation or the selected spatial resolution of the data.

The final cokriged gauge surfaces are illustrated in Figure 7.7. Predicted average precipitation values range from a minimum of 0.02 mm to a maximum of 0.31 mm using the elevation covariate and 0.25 mm using the radar covariate. Average rainfall is large towards the north-west of the catchment which is expected given the mountainous terrain. The two images are similar in terms of spatial variation. The accuracy of the two predictive methods was tested using cross-validation at gauge locations.

7.3.1.5 Cross-validation

Cross-validation aids the assessment of prediction errors. For the most accurate results the RMSE needs to be small, the RMS standardised prediction error close to 1 and the mean prediction error close to 0. Results for cokriging across the Severn Uplands indicate fairly low prediction errors and high correlations for cross-validation (Table 7.3). Elevation produced a smaller mean prediction error than the radar field, but radar had slightly smaller RMS, average standard error and standardised mean error values. The correlation coefficients between observed gauge averages and those predicted during cross-validation using the radar and elevation covariates were nearly identical and correlations were large at approximately 0.92 – 0.93. Nonetheless, the search strategy that produced the most accurate cross-validation results may not yield the most accurate predictions at unsampled locations (Goovaerts, 1997). The accuracy at ungauged locations will become apparent later in this chapter when corrected radar images are tested for their hydrological modelling predictive accuracy.

7.3.1.6 Standard error surface

Error surfaces associated with kriging interpolation may be used to understand the propagation of errors through spatial models (Burrough, 2001). Uncertainty can be accounted for by using kriging to predict rainfall spatially (Borga *et al.*, 2000). Predicting mean-areal rainfall from point measurements is subject to sampling error. With the prediction standard error surface, the true value of the surface will be within the interval formed by the predicted value ± two times the prediction standard error around 95% of the

time if the data are normally distributed. Locations near sample points generally have smaller error. Error surface maps illustrate minimal error buffering the gauge locations (Figure 7.8). The maximum error for cokriging with elevation is 0.11 mm and with radar is 0.06 mm. Errors are lower in the south-east of the catchment for cokriging with elevation.

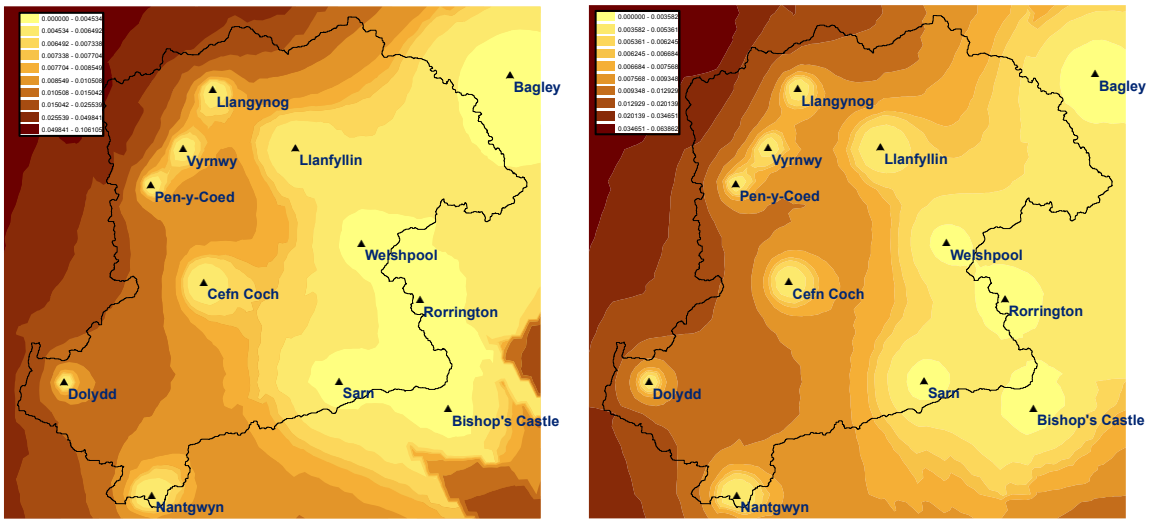

Figure 7.8 Prediction standard error maps using elevation (left) and radar (right) as covariates

7.3.2 Mean field bias

Simple standard correction of radar rainfall imagery uses an estimate of the mean field bias which is applied to produce bias-adjusted radar rainfall data. Gauge adjustment is performed on radar precipitation to remove the residual random bias (Kitchen *et al.*, 1994). Some previous research has investigated the use of interpolation to create a bias field for adjusting radar data (e.g. Wilson and Brandes, 1979). Correcting for multiplicative error over larger areas has a large impact, particularly on volumetric estimation of rainfall. To increase the accuracy of radar forecasts, and subsequently increase modelling predictive capabilities, the radar data were corrected using bias fields. A static method for merging radar and rain gauge data was undertaken following a technique by Wood *et al.* (2000). This technique aims to increase the accuracy of the radar data by identifying the long-term average bias of a radar dataset and then correcting for it uniformly by applying a mean bias correction to all images. Instead of using an individual average bias catchment value (e.g. Cole and Moore, 2008) distributed bias values were determined. This was achieved by dividing the optimally interpolated gauge surface of average rainfall by the average radar

rainfall for each individual pixel (1 km² spatial resolution). The calculated mean field bias (MBF) surface (Figure 7.9) was then used to correct each radar image.

The MFB surface kriged using elevation as the covariate shows a clustering effect and MFB values range from 0.43 to 4.60. In contrast, the MFB surface predicted from radar-gauge cokriging is smoother and values range from 0.42 to 3.13. These values indicate that radar estimates may be overestimated (red areas mainly to the south-east) by up to 60% and underestimated (blue areas mainly to the north-west) by as much as 315%. Discrepancies in the bottom right corner of the MFB surfaces are attributed to interference error in the radar recording which can clearly be seen when viewing the entire UK radar imagery (likely to be attributable to beam shadow or blockage from the radar dish). However, the few cells affected are outside the catchment boundary and do not affect rainfall-runoff processes in the hydrological catchment.

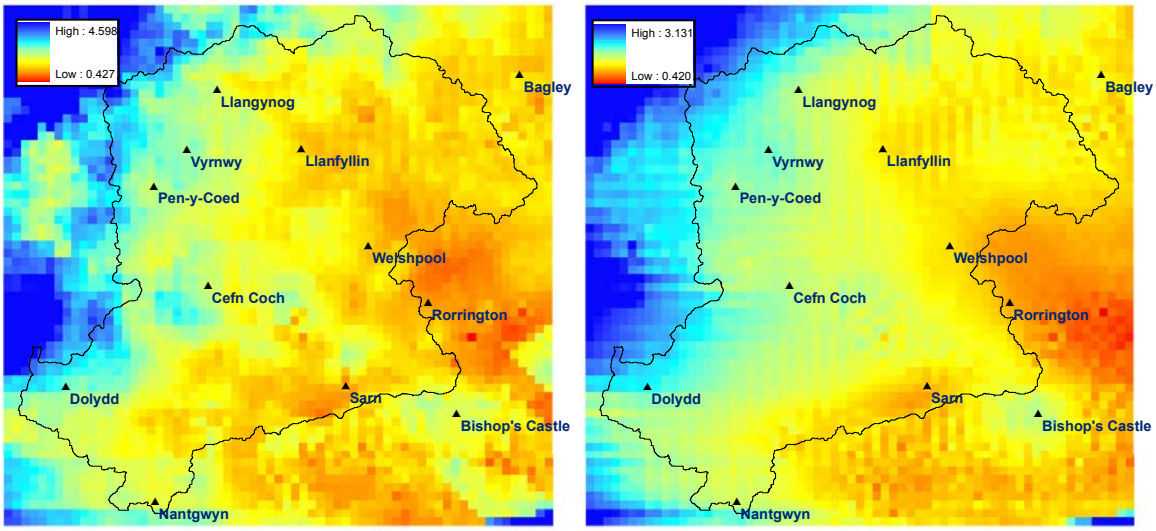

Figure 7.9 Mean-field bias between average precipitation of gauge interpolated surfaces (using elevation (left) and radar (right) covariates) and radar rainfall

7.3.3 Corrected radar rainfall

Differences between the average gauge interpolated and average corrected radar surfaces are depicted in Figure 7.10. Using the geostatistical interpolation technique, error at gauge locations was minimised using the MFB correction method with maximum absolute errors of 0.21 mm using the elevation covariate and 0.14 mm using the radar covariate. Nonetheless, error between the gauge and radar average precipitation surfaces still

remains, predominantly around areas of higher elevation where rainfall is still slightly underestimated and across lower elevations rainfall has some overestimation. Wilson and Brandes (1979) found that radar tended to over-predict light rainfall and under-predict heavy rainfall. This is likely to be pronounced in the Severn Uplands as heavy rainfall generally occurs over higher elevations, and so will be under-predicted. Prudhomme and Reed (1999) echo these findings, showing that there was general systematic underestimation for gauges higher than 100 m and overestimation lower than 100 m (kriging). These over- and under-estimations reflect the difficulty in modelling the complex relationships between topography and rainfall extremes.

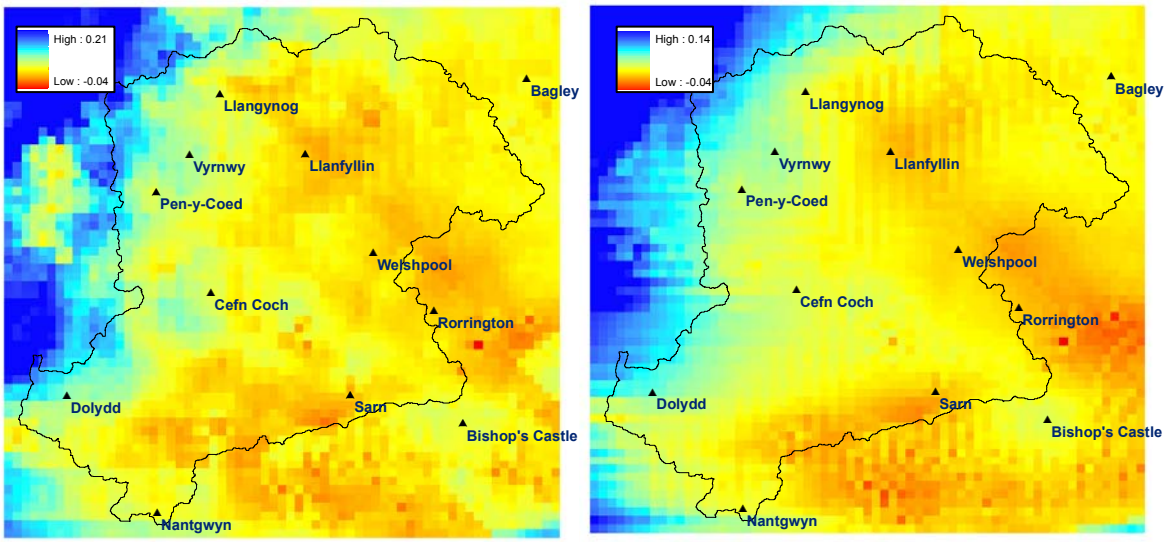

Figure 7.10 Bias between average precipitation from gauge interpolated surface (using elevation (left) and radar (right) covariates) and radar rainfall

The MFB bias surfaces were applied to the radar time-series data by multiplying each 5-minute time slice by the MFB. Corrected radar time series were then inputted to HEC-HMS and changes in the hydrological forecasts were analysed to determine which cokriging technique produced the greatest accuracy in terms of hydrograph predictions.

7.4 Improvements in Hydrological Modelling

To determine which covariate provided the most accurate method for interpolating gauge rainfall and corrected radar imagery, both sets of corrected radar imagery for the November-December 2006 event were run through the HEC-HMS model. Results indicate

that using the MFB created from the spatial variability of the radar field provides a greater increase in predictive accuracy of the hydrological model than that created from the elevation variability (Table 7.2). Increases in E_f values were largest at Rhos-y-Pentref and Abermule with slight increases observed at Llanymynech and Montford for both methods. Simulations using the corrected radar data provided a near-perfect match of peak discharge values at Llanymynech and Montford. Minor increases in accuracy were noted in slight RMSE and MAE reductions. Generally, all descriptive statistics indicated an increase in accuracy when using the corrected radar time-series. The gauge interpolation method using the spatial variability of the radar data resulted in slightly more accurate results than that corrected using the elevation interpolation method. Therefore, even though both correction methods provided increases in accuracy over simply using the uncorrected radar data, from this point on in this research, radar data corrected using the spatial variability of the radar are used for all subsequent processing and analyses.

In terms of increased accuracy, using gauge-corrected radar data to drive the HEC-HMS model, compared to using the gauge network, results were variable. All correlation coefficients and R^2 values were larger using gauge precipitation. E_f values were all larger for gauge simulations except at Abermule where the corrected radar data offered a slight increase in accuracy. Nonetheless, corrected radar data provided substantial reductions in RMSE at all sites and the standard deviations of the simulated time-series data more accurately matched to that of the observed records at Rhos-y-Pentref, Llanymynech and Montford. Peak flows were also predicted with increased accuracy at Llanymynech and Montford using the radar precipitation data as input. Results suggest that HEC-HMS is capable of using both gauge and radar sources to replicate November-December extreme flows with suitable accuracy, albeit, the Nash-Sutcliffe efficiency measure used indicated that gauge-driven simulations offer no real significant difference to those using the gauge-corrected radar data.

7.5 RADAR VALIDATION

The radar-driven HEC-HMS model was validated by splitting the November-December 2006 event time period; modelling for November and December independently. This method was adopted due to a lack of an alternative wintertime extreme precipitation time period, as radar records began only in April 2004 and the only event which existed

occurred in 2006. Validation results indicate variable model efficiency for both time periods. All validation E_f values are positive ranging from 0.18 to 0.7. These validation results are not as accurate as those achieved using the gauge data alone to model extreme periods in the Severn Uplands. The November validation period produced relatively accurate predictions of the data means, whereas the standard deviations were more closely matched during the December validation period. Correlation coefficients and R^2 values were generally large for all sites for both validation periods, with Montford the largest. The MAE was similar for all locations and the RMSE was much smaller for the November validation period. This was likely a reflection of the greatest precipitation and flow peaks occurring during December and greater error was associated with these values as predicted by the GS scores (as described in Section 7.1.4.1).

Table 7.4 HEC-HMS radar-driven validation results for two time periods; November 2006 and December 2006

		Observed (Nov 2006)	Validation (Nov 2006)	Observed (Dec 2006)	Validation (Dec 2006)
Rhos-y-Pentref	Mean	2.739	2.734	4.325	2.856
	σ	2.300	3.294	3.319	2.509
	ρ	-	0.796	-	0.858
	R^2	-	0.633	-	0.736
	MAE	-	0.231	-	0.202
	RMSE	-	2.058	-	2.539
	E_f	-	0.229	-	0.529
	Peak Q	24.7	12.2	16.6	14.1
	Volume	181.9	182.2	297.5	196.4
Abermule	Mean	24.200	22.827	49.304	29.148
	σ	20.519	23.740	34.664	30.058
	ρ	-	0.842	-	0.851
	R^2	-	0.709	-	0.724
	MAE	-	0.256	-	0.287
	RMSE	-	20.622	-	30.852
	E_f	-	0.605	-	0.385
	Peak Q	97.8	94.6	173.2	111.8
	Volume	89.3	64.7	199.4	117.9
Llanymynech	Mean	31.327	36.768	76.715	59.102
	σ	22.051	35.449	62.316	62.630
	ρ	-	0.878	-	0.888
	R^2	-	0.770	-	0.789
	MAE	-	0.273	-	0.269
	RMSE	-	29.562	-	75.482
	E_f	-	0.176	-	0.695
	Peak Q	157.0	94.5	264.5	257.7
	Volume	123.1	104.9	265.4	204.5
Montford	Mean	59.697	64.919	144.225	94.915
	σ	46.017	62.471	91.292	93.127
	ρ	-	0.904	-	0.899
	R^2	-	0.818	-	0.809
	MAE	-	0.233	-	0.257
	RMSE	-	38.114	-	97.132
	E_f	-	0.600	-	0.502
	Peak Q	200.4	152.8	359.8	334.7
	Volume	83.6	76.8	191.6	126.2

7.6 DISCUSSION

"Models are simplifications of reality and no matter how sophisticated they may be models undergo some aspect of conceptualisation or empiricism, and their results are only as realistic as model assumptions and algorithms, detail and quality of inputs and parameter estimates. For most models, it is imperative that a mechanism that improves accuracy of model estimates, based on observed information available to the modeller, be implemented before using models for their intended purposes."

(Muleta and Nicklow, 2004)

Following the preceding statement by Muleta and Nicklow (2004), the HEC-HMS model of the Severn Uplands was improved upon as outlined in this chapter, accounting for data error and model optimisation. However, limitations still remain and error is inherent when replicating real-world physical processes, which inevitably leads to issues regarding uncertainty in data resources and model development.

7.6.1 Radar capabilities

Generally, the literature reviewed in Chapter 2 found that the integration of rain gauge data into radar forecasts produced increases in accuracy, particularly in mountainous terrain. Nonetheless, exceptions exist and some researchers have found that radar data offered no increase in accuracy over gauge data for hydrological modelling. Borga *et al.* (2000) found that although gauge-based simulations provided a more accurate fit than radar-based simulations, as expected, the efficiency of (corrected) radar-driven simulations is close to that obtained for gauge-based simulations for a number of events. Neary *et al.* (2004) also concluded that radar-driven HEC-HMS simulations were generally less accurate in prediction of streamflow volume as compared to gauge-driven simulations and, although comparable to the gauge-driven simulation in predicting the magnitude and time to peak, offered no increase in accuracy in predicting these quantities either.

Vehvilainen *et al.* (2004) stated that the potential of spatially distributed precipitation depends on the ratio of the amount of water in the rainfall event compared to the water already in the dynamic part of the catchment i.e. rivers, lakes, soil surface. It may be that

the November-December event in question does not conform to such a ratio. Borga (2002) states that the high spatial and temporal resolution and large areal coverage of radar rainfall observations provides detailed information on precipitation events previously unattainable from ground-based rain gauges. However, this research implies that the gauge network density seems adequate for modelling an extreme wintertime rainfall event in the Severn Uplands (using HEC-HMS) and the radar data provided no improvement on flow prediction accuracy. Seo *et al.* (1990b) stated that under a range of rain gauge network densities, the margin of improvement by gauge-radar estimation using cokriging is greatest over gauge-only estimations when the gauge density is lowest. It would seem that the gauge density in the Severn Uplands is independently sufficient for accurately modelling flows under the conditions investigated. Precipitation events during autumn and winter are generally uniform in spatial and temporal precipitation variability; events are usually prolonged with a west (greatest) – east (least) precipitation gradient. During these conditions the gauge network was able to sufficiently characterise the spatial variability of the event. However, during localised short convective events, which are more common during summer, the enhanced spatial and temporal resolution of radar may increase predictive accuracy. Additionally, catchment saturation levels also vary throughout the year with saturation levels reduced during summer, which affects the translation rates of rainfall into runoff, and may affect modelling accuracy due to an indirect rainfall-runoff translation.

7.6.2 Gauge rainfall as reference

Even though gauge measurement errors are assumed to be significantly smaller than the radar bias (Gjertsen *et al.*, 2003), rain gauge rainfall measurement can significantly deviate from the true mean-areal rainfall (Anagnostou and Krajewski, 1999). Automated rain gauge records rely on human inspection for quality checking. Sources which may be associated with errors in the rain gauge record are outlined by Upton and Rahimi (2003) as problems arising from blockages, wetting, evaporation, high rain rates, wind effects, position and shelter. When strong winds are present the under-prediction by rain gauges can exceed 20%, and error is even larger when other factors such as exposure and topography are considered (Seo *et al.*, 1990a). Typically, only a few point observations are used for ground reference. Nationally, 381 Environment Agency and Met Office owned precipitation gauges are used for radar correction, equating to approximately 1 gauge per

640 km² of UK land coverage. Of these selected gauges, only two, Lake Vyrnwy and Sarn, are located within the Severn Uplands catchment. Given the topographical complexities and high rainfall variability of mountainous areas, it may be necessary to use more gauges to increase the accuracy of forecasts.

Results using the HEC-HMS model of the Severn Uplands offered some indication that doing so resulted in a slight increase in the accuracy of predictions. Remaining insufficiency in the model predictions, as indicated by the imperfect E_f values, could be inherent to rain gauge errors, where rainfall is slightly different to that recorded and this error then propagates when making a comparison to flow observations. This is explained by the differences in data recording procedures and differing physical processes at surface and atmospheric levels. Uncertainty due to the difference in sampling areas when comparing rainfall estimates from radar (pixels) to that of gauges (near-point) is referred to as the point-area difference (Neary *et al.*, 2004). This error will be greater the coarser the spatial resolution of the radar images.

7.6.3 Modelling constraints

Complexities such as dependence on model type (lumped versus distributed or semi-distributed), catchment size, runoff-generation mechanism, and quality of radar data and its prediction algorithms make it difficult to draw any general conclusions about the value of radar data to increase the accuracy of the hydrological model (Neary *et al.*, 2004). Cunderlik and Simonovic (2004) discovered computational restraints when modelling using HEC-HMS, with the program being unable to run increasingly complex model set-ups. The same problems were encountered during this research, and even with relatively simple model components selected, model optimisation procedures were still highly computationally intensive.

Due to its semi-distributed structure, the continuous model may lack the ability to capture subbasin-specific features, but as more subbasins become included in the contributing area, the ability of the model to reproduce observed hydrographs increases (Cunderlik and Simonovic, 2004). This was indicated by results in the Severn Uplands, with simulation efficiency greatest at the three gauging locations further downstream (Abermule, Llanymynech and Montford) where an increasing number of subbasins were integrated

into the modelling process. Both the gauge- and radar-driven models exhibit these characteristics.

7.6.4 Method limitations

Cole and Moore (2008) found that their hydrological model performed most accurately when using rain gauge-only data as input. This was prior to any radar calibration. Their model simulations provided compelling evidence supporting the need for frequent and spatially varying gauge-adjustment of radar rainfall. An improvement on the cokriging method to determine the average MFB might be to correct radar imagery over smaller temporal averages rather than using the event average. This was not investigated in this research due to computational and time constraints. All of the selected hydrological modelling and data processing methods have limitations, primarily due to limitations experienced collating data and parameterising the model.

7.6.5 Equifinality

The main problem associated with model parameterisation is that of equifinality. Even though automated optimisation procedures, as used by HEC-HMS in this research, offer a marked increase in accuracy compared to manual calibration, the issue still remains that only one set of optimal parameters were defined. Equifinality follows the concept that multiple optimum parameter sets can produce similar simulation accuracy. Some researchers have used more complex calibration methods where equifinality is considered. Wilby (2005) used Monte Carlo analysis of the parameter space to locate optimal parameter combinations for a rainfall-runoff model and the E_f values obtained ranged from 0.45 to 0.82. Hossain *et al.* (2004) achieved optimal parameter values with an E_f efficiency of approximately 0.8 using the GLUE framework. However, these calibration methods are computationally intensive and given that E_f values obtained using automated calibration for the Severn Uplands sites ranged from 0.68 to 0.87 using gauge data and 0.61 to 0.72 for using gauge-corrected radar data, it was not considered beneficial enough to investigate equifinality further in this research, particularly given the exhaustive parameter sets of the HEC-HMS hydrological model.

Beven (1993) stated that "the transformation of the magnitude/frequency distribution of rainstorms to the magnitude/frequency distribution of floods is complex and not well understood". Research in these analysis chapters has investigated this process by trying to link periods of extreme rainfall to that of extreme flows in a historical context. Results indicate agreement with Beven's statement; the rainfall-runoff process is not simple and there are many interplaying factors which affect the transformation of extreme precipitation into extreme flow. This chapter has highlighted how error originating in both data sources and the modelling processes results in a complex transition between rainfall and flow.

7.7 SUMMARY

It has to be reiterated that neither rain gauge nor weather radar measurements can be taken as 'truth' (Tilford *et al.*, 2003). Despite differences in the gauge and radar time-series records, both point-interpolated and grid-distributed (radar) precipitation produced comparable results when using HEC-HMS to model extreme hydrological events in the Severn Uplands. Overall, although some error remains, the extreme hydrological events were modelled adequately using both gauge and radar precipitation inputs, although radar provided no increase in accuracy over gauge-driven hydrological predictions. The geostatistical method used for correcting the MFB did, however, increase radar prediction accuracy, particularly at sites of higher elevation where an underestimation of rainfall was evident. This provides encouragement for using the HEC-HMS in further research on how future precipitation extremes will influence fluvial extremes given current climate change predictions. Despite the similarities between radar- and gauge-driven hydrological predictions, radar data do offer the advantage of being grid-distributed, a valuable structure for climatic assessment given the gridded nature of the climate change scenario projections.

CHAPTER 8

Future Hydrological Extremes

Research conducted in Chapter 5 showed that hydrological extremes of flow and precipitation intensity, frequency and persistence have changed over the last 30 years in the Severn Uplands. The literature suggests that these changes are likely to increase in variability into the future. The purpose of this chapter is to determine the extent to which extremes will become accentuated in the future given predicted changes in precipitation and temperature. In addition, given the creation and calibration of a hydrological model which accurately simulated an extreme event in the Severn Uplands (Chapters 6 and 7), the performance of the model for simulating future conditions will be examined. In particular, the difference in predicted flow outputs when using gauge-interpolated or radar-distributed rainfall as data input will be quantified. This will enable the consequences of using different data inputs to be explored.

8.1 DATA SELECTION

Despite radar data offering no increase in accuracy over modelling the November-December extreme rainfall event in the Severn Uplands compared to using the gauge network, it was decided that both radar and gauge precipitation data should to be used with the UKCIP02 predictions of future conditions. The HadRM3 RCM was used to generate the UKCIP02 scenarios and as reviewed in Chapter 2, problems with climate scenarios generated from RCMs are predominantly suggested to arise from rainfall issues related to topography. Therefore, it seems sensible to continue the investigation of using the finer spatial resolution of precipitation data, which may more accurately account for topographical changes during the modelling stage. Consequently, both precipitation

datasets were selected to determine how the flow predictions would differ given the difference in transform methods used for point and gridded precipitation data. A comparison was then made between the hydrological modelling results produced using the different input precipitation datasets to predict future percentage changes in fluvial peak flows and outflow volume for the time period in question. Peak flow was chosen to investigate future changes in flow intensity and outflow volume was chosen to indicate the translation of precipitation totals to flow totals. The November-December 2006 event was selected to monitor changes as the hydrological model was calibrated accurately for this period. From the findings of the extremes analyses in Chapter 5, autumn and winter flows were observed to be increasing, and the UKCIP02 scenarios predict increases in precipitation for these months, in particular large increases for the month of December. Additionally, literature discussed in Chapter 2 revealed that extremes in the winter season are associated with warmer periods, in particular, a connection with positive phases of the NAOI. Changes in event magnitude, rather than frequency or persistence, were considered so that relative proportional changes could be applied to determine changes in event intensity. As discussed in section 2.2.3, small changes in the mean can result in large changes in the intensity and frequency of extremes. It was possible to look at changes in intensity using the hydrological model at an event-level. Continuous simulation would have been required to investigate changes in frequency and was not possible with the radar precipitation data due to intensive computational requirements. All UKCIP02 scenarios predict temperature and precipitation increases over the 21st century for November and December (a summer period could not be selected due to predicted reductions in monthly precipitation). By selecting this two-month period the combined effect of both precipitation and temperature increases could be investigated.

8.2 PRECIPITATION CHANGES

Percentage precipitation changes were determined for the Severn Uplands using monthly mean UKCIP02 averages projected for future time-slices and the baseline mean monthly average for November and December. The UKCIP02 scenarios were introduced and described in Chapter 2. Percentage changes in precipitation are depicted in Figure 8.1 for the 2020s, Figure 8.2 for the 2050s and Figure 8.3 for the 2080s all relative to the baseline average (1961-1991). Projected changes in precipitation indicate an increase over the 21st Century for both November and December under all emissions scenarios. Percentages

range from 1.12 - 5.26% for the 2020s, 2.00 - 9.90% for the 2050s and 2.84 - 21.71% for the 2080s. The greatest precipitation increases are predicted in the southern part of the Severn Uplands catchment, particularly in the south-west near the Dolydd and Nantgwyn precipitation gauges. The smallest increases are predicted for the north of the catchment near the Llangynog, Llanfyllin and Vyrnwy precipitation gauges. The monthly percentage changes from the baseline value to that of the projected UKCIP02 precipitation were calculated. Baseline values, sourced from the Met Office online archives, were taken as average observed precipitation for the standard 1961-1990 baseline period. Predicted percentage changes were used to alter the extreme event (November-December) precipitation time-series and subsequently input into the HEC-HMS model. Index values of average annual precipitation (for each rain gauge) stored in HEC-HMS were also altered for future conditions based on UKCIP02 annual precipitation change predictions.

8.3 EVAPORATION CHANGES

Results from analyses in Chapter 5 suggest that extreme precipitation can influence extreme flows indirectly. Catchment characteristics mediate the translation of extreme precipitation into extreme runoff and these processes are influenced by climate variability. One of the most important climate variables found to correlate with the occurrence of extremes was air temperature, which also influences catchment properties such as soil porosity and evaporation rates. Given the importance of air temperature, future predicted changes in temperatures were incorporated into the hydrological modelling process. This was achieved by calculating future evaporation rates, given that monthly average temperatures are positively linearly correlated with evaporation rates. Kay and Davies (2008) state that evaporation processes are an important part of the catchment water budget, and as such, they are essential to incorporate into a hydrological model. Unfortunately, data required to calculate gridded evapotranspiration rates were not available for this research. Therefore, subbasin averages were used.

Walsh and Kilsby (2007) derived empirically the coefficients of the Blaney-Criddle equation for a catchment in northwest England where α was 0.456 and β was 0.416. These coefficients were used to estimate future potential evaporation using the Penman-Monteith formulation as discussed in Chapter 6. As there is little difference in the historic potential evapotranspiration-temperature relationship for different upland catchments in NW

England (Fowler and Kilsby, 2007), the equation used by Walsh and Kilsby (2007) was used for the Severn Uplands (see Chapter 3). Mean daily percentages (for month) of total annual daylight hours were calculated using daylight values extracted from tables in List (1949) for latitude 52° north. Average daily daylight was approximated at 8.86 hours for November and 7.85 hours for December. Daylight values will change slightly over the 21st century due to orbital changes in the Earth's eccentricity, obliquity and precession. However, data projecting future daylight hours were not available and were considered unnecessary given such minor alterations over a century time-scale. Future temperature values were extracted from the UKCIP02 scenarios for the 2020s, 2050s and 2080s for each of the four emissions scenarios (see Appendix 4). Evaporation values calculated for November and December for each time-slice are listed in Table 8.1. These were derived as subbasin averages using temperature projections under each of the UKCIP02 scenarios. The altered evaporation rates were then used in the HEC-HMS meteorological model to calculate future evapotranspiration.

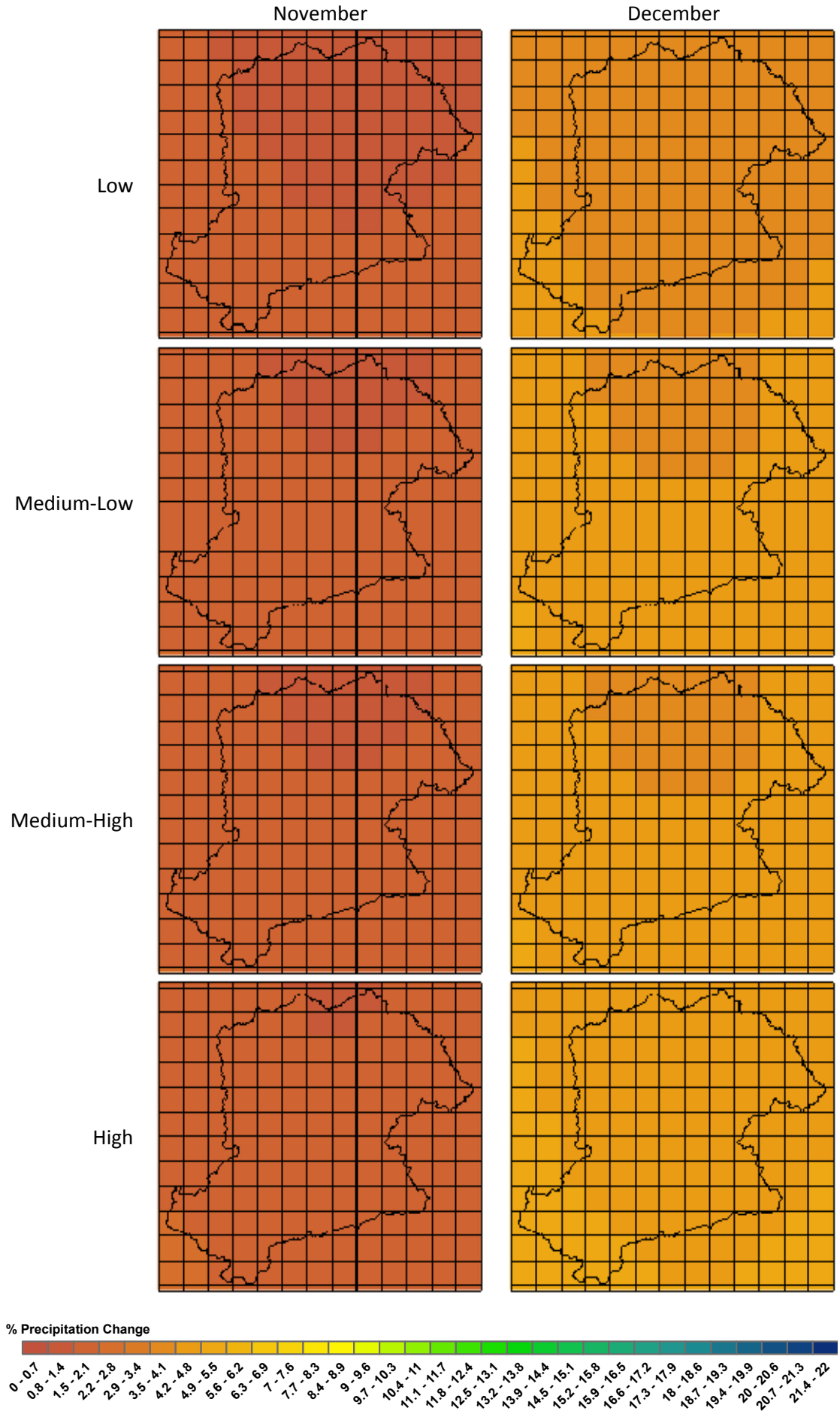

Figure 8.1 Precipitation change scenarios for the 2020s in the Severn Uplands

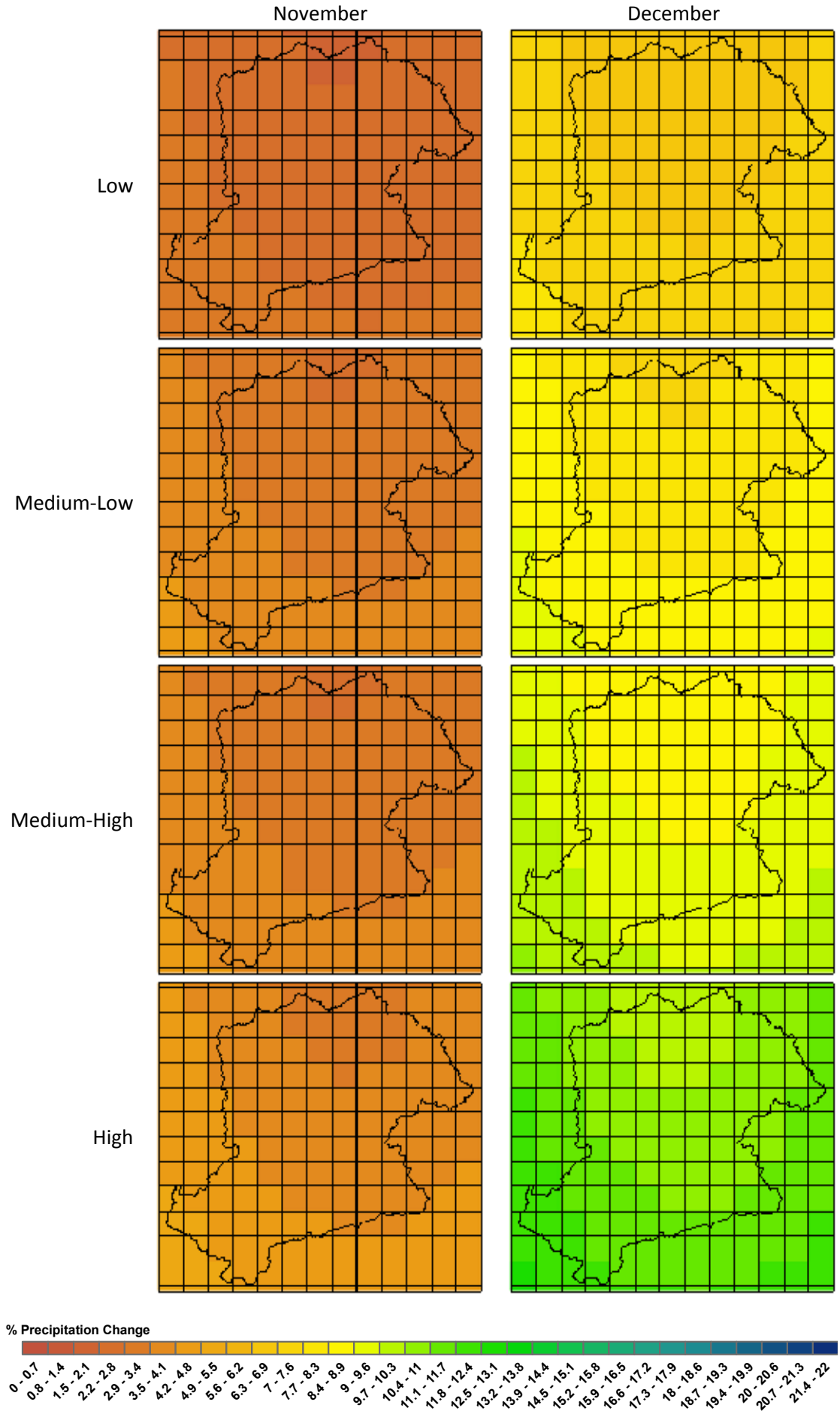

Figure 8.2 Precipitation change scenarios for the 2050s in the Severn Uplands

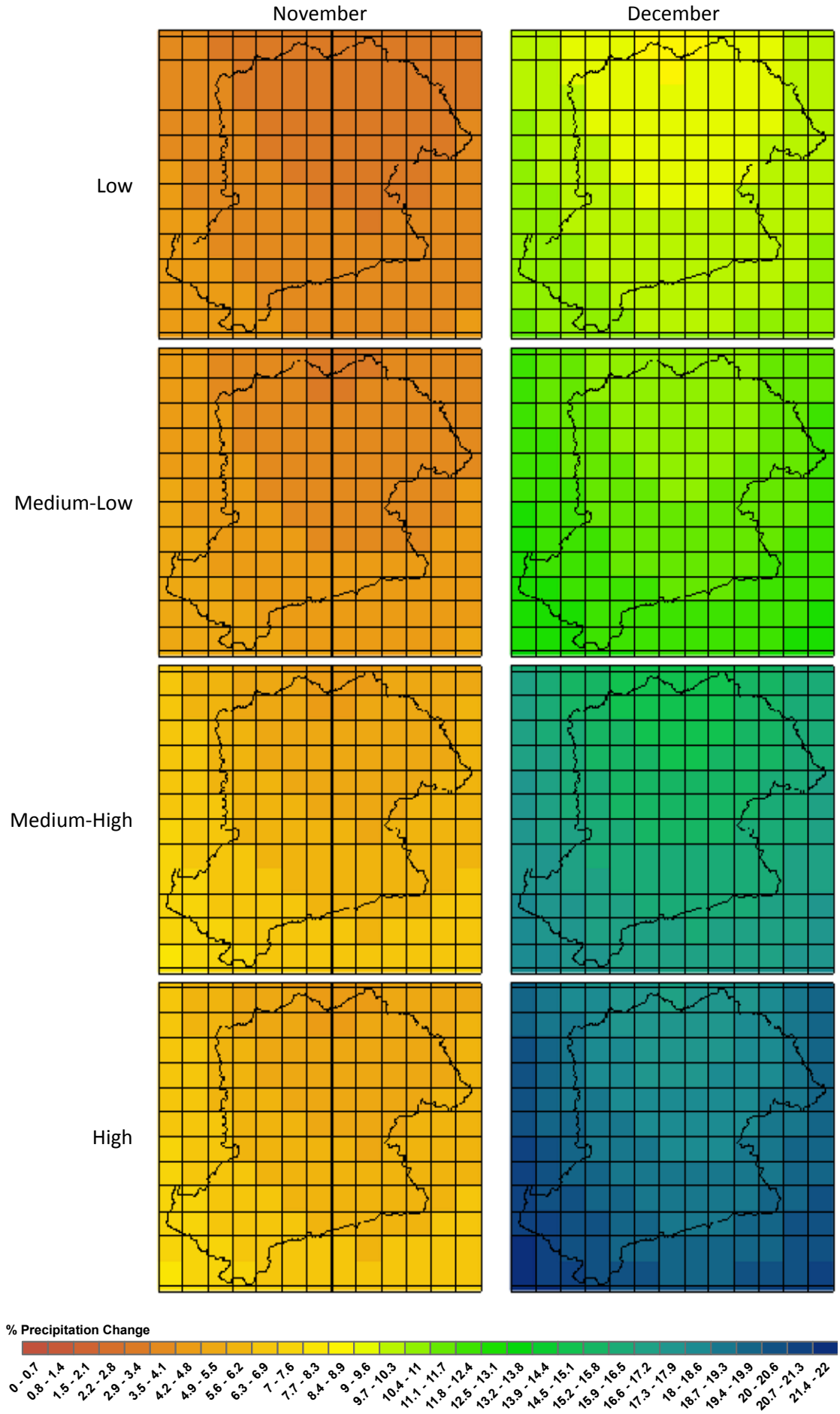

Figure 8.3 Precipitation change scenarios for the 2080s in the Severn Uplands

Table 8.1 Evaporation values for November and December

November		Low			Medium-Low			Medium-High			High		
Subbasin	**Present**	**2020**	**2050**	**2080**	**2020**	**2050**	**2080**	**2020**	**2050**	**2080**	**2020**	**2050**	**2080**
Banwy	17	19	21	22	20	22	23	20	22	26	20	23	27
Camlad	19	21	23	24	21	23	25	21	24	28	21	25	29
Clywedog	16	18	20	21	18	20	22	18	21	25	18	22	26
Dulas	16	18	20	22	19	21	23	19	21	25	19	22	27
Hafren	14	16	18	19	16	18	20	16	19	23	16	20	24
Lake Vyrnwy	17	19	21	22	19	21	23	19	22	26	20	23	27
Lower Vyrnwy Lat	19	21	23	24	21	24	25	21	24	28	22	25	29
Mid Vyrnwy Lat	19	21	22	24	21	23	25	21	24	27	21	25	29
Mule Lat	20	22	24	25	22	24	26	22	25	28	22	26	30
Rhiw	19	21	22	24	21	23	25	21	23	27	21	24	29
Tanat	17	19	21	22	19	21	23	19	22	26	19	23	27
Trannon	17	19	21	23	20	22	23	20	22	26	20	23	28
Vyrnwy Conf Lat	20	23	24	26	23	25	27	23	25	29	23	26	31
Welshpool Lat	20	22	24	25	22	24	26	22	25	29	23	26	30

December		Low			Medium-Low			Medium-High			High		
Subbasin	**Present**	**2020**	**2050**	**2080**	**2020**	**2050**	**2080**	**2020**	**2050**	**2080**	**2020**	**2050**	**2080**
Banwy	12	13	15	16	14	15	17	14	20	18	14	16	20
Camlad	13	14	16	17	15	16	18	15	22	19	15	17	21
Clywedog	11	12	13	15	12	14	15	12	19	17	12	15	18
Dulas	11	13	14	15	13	14	16	13	19	18	13	16	19
Hafren	9	10	12	13	11	12	14	11	17	16	11	13	17
Lake Vyrnwy	12	13	15	16	14	15	17	14	20	18	14	16	20
Lower Vyrnwy Lat	13	15	16	17	15	17	18	15	22	20	15	18	21
Mid Vyrnwy Lat	13	14	16	17	15	16	18	15	22	20	15	17	21
Mule Lat	14	15	16	18	15	17	18	15	23	20	15	18	21
Rhiw	13	14	16	17	15	16	17	15	21	19	15	17	21
Tanat	12	13	14	16	13	15	16	13	20	18	13	16	19
Trannon	12	13	15	16	13	15	16	13	20	18	14	16	20
Vyrnwy Conf Lat	14	16	17	18	16	17	19	16	23	21	16	19	22
Welshpool Lat	14	15	17	18	16	17	19	16	23	21	16	18	22

8.4 CHANGES IN EXTREME FLOWS

Changes in peak discharge and outflow volume were calculated for the same four gauging stations as used in Chapters 6 and 7; Rhos-y-Pentref, Abermule, Llanymynech and Montford. Future changes in these two variables were calculated relative to the simulated values (see Tables 6.4 and 7.2 for model simulation values) and percentage differences were calculated. Simulated values were selected over observational data such as to allow a relative comparison between model outputs and reduce error propagation.

8.4.1 Gauge changes

Changes in gauge data indicate an increase in all peak flows (Table 8.2). Increases were greatest for the 2080s with Montford experiencing the greatest increase of up to 27.6%. Outflow volumes increased for all future time periods under each emission scenario with Rhos-y-Pentref predicted to receive the largest percentage change up to 21.9% by the 2080s. Volumetric increases were greater the higher the emissions scenario and the further into the future. Summary results (Table 8.4) indicate catchment-wide increases in peak discharge of between 4.7 and 6.6% for the 2020s, 8.9 and 16.0% for the 2050s and 12.6 and 27.6% for the 2080s. Increases in volumes ranged from 3.8 to 4.8% for the 2020s, 6.7 to 12.9% for the 2050s and 6.9 to 21.9% for the 2080s across the catchment.

8.4.1 Radar changes

Percentage changes in precipitation using radar data indicate increases in all peak flows and outflow volumes (Table 8.3). Results reflect changes in the emission scenarios with higher emissions inducing larger changes in peak flows and outflow volumes. Summary results (Table 8.4) indicate catchment-wide increases in peak discharge of between 2 and 7.5% for the 2020s, 4 and 17.6% for the 2050s and 5.7 and 30.5% for the 2080s. Increases in outflow volumes ranged from 3.3 to 5% for the 2020s, 6 to 11.9% for the 2050s and 8.6 to 20.2% for the 2080s across the catchment. The largest changes were predicted for Abermule.

Table 8.2 Percentage changes in peak flow and outflow volume between November-December 2006 gauge event precipitation and that altered for the 2020s, 2050s and 2080s across the four emissions scenarios

	Low			Medium-Low			Medium-High			High		
	2020	2050	2080	2020	2050	2080	2020	2050	2080	2020	2050	2080
Peak Flow												
Rhos-y-Pentref	4.71	8.90	12.57	5.24	10.47	14.66	5.24	11.52	21.47	5.76	14.14	25.13
Abermule	5.14	9.08	12.88	5.72	10.81	15.09	5.72	12.11	20.81	6.15	14.46	24.75
Llanymynech	5.30	9.08	13.08	5.91	10.87	15.37	5.91	12.20	21.74	6.33	14.72	25.82
Montford	5.55	10.03	14.27	6.19	11.93	16.73	6.17	13.35	23.12	6.62	16.04	27.57
Volume												
Rhos-y-Pentref	4.65	8.18	11.49	5.03	9.97	13.46	5.03	10.89	18.84	5.40	12.91	21.91
Abermule	4.00	7.10	10.03	4.46	8.67	11.77	4.43	9.47	16.23	4.77	11.31	19.42
Llanymynech	3.83	6.72	9.62	4.25	8.19	11.23	4.24	8.95	15.74	4.52	10.76	18.74
Montford	3.79	6.70	9.57	4.19	8.25	11.20	4.18	8.99	15.66	4.49	10.78	18.67

Table 8.3 Percentage changes in peak flow and outflow volume between November-December 2006 radar event precipitation and that altered for the 2020s, 2050s and 2080s across the four emissions scenarios

	Low			Medium-Low			Medium-High			High		
	2020	2050	2080	2020	2050	2080	2020	2050	2080	2020	2050	2080
Peak Flow												
Rhos-y-Pentref	2.02	4.05	5.67	2.43	5.26	6.48	2.43	5.26	8.91	2.43	6.07	8.91
Abermule	6.35	11.2	15.78	7.05	13.23	18.52	7.05	14.73	25.93	7.50	17.64	30.51
Llanymynech	5.04	9.07	12.95	5.65	10.76	15.17	5.56	16.06	21.38	6.02	14.49	25.22
Montford	4.20	7.54	10.74	4.70	8.93	12.57	4.70	10.05	20.61	5.01	12.04	21.42
Volume												
Rhos-y-Pentref	3.34	6.00	8.57	3.73	7.57	9.99	3.73	7.71	14.19	3.98	9.74	15.45
Abermule	4.19	7.47	10.66	4.66	9.15	12.48	4.66	10.25	17.69	4.99	11.92	20.17
Llanymynech	3.64	6.44	9.20	4.02	7.86	10.74	4.02	9.07	15.11	4.30	10.29	17.27
Montford	3.78	6.69	9.55	4.18	9.19	14.10	4.19	10.01	15.71	4.46	10.68	17.86

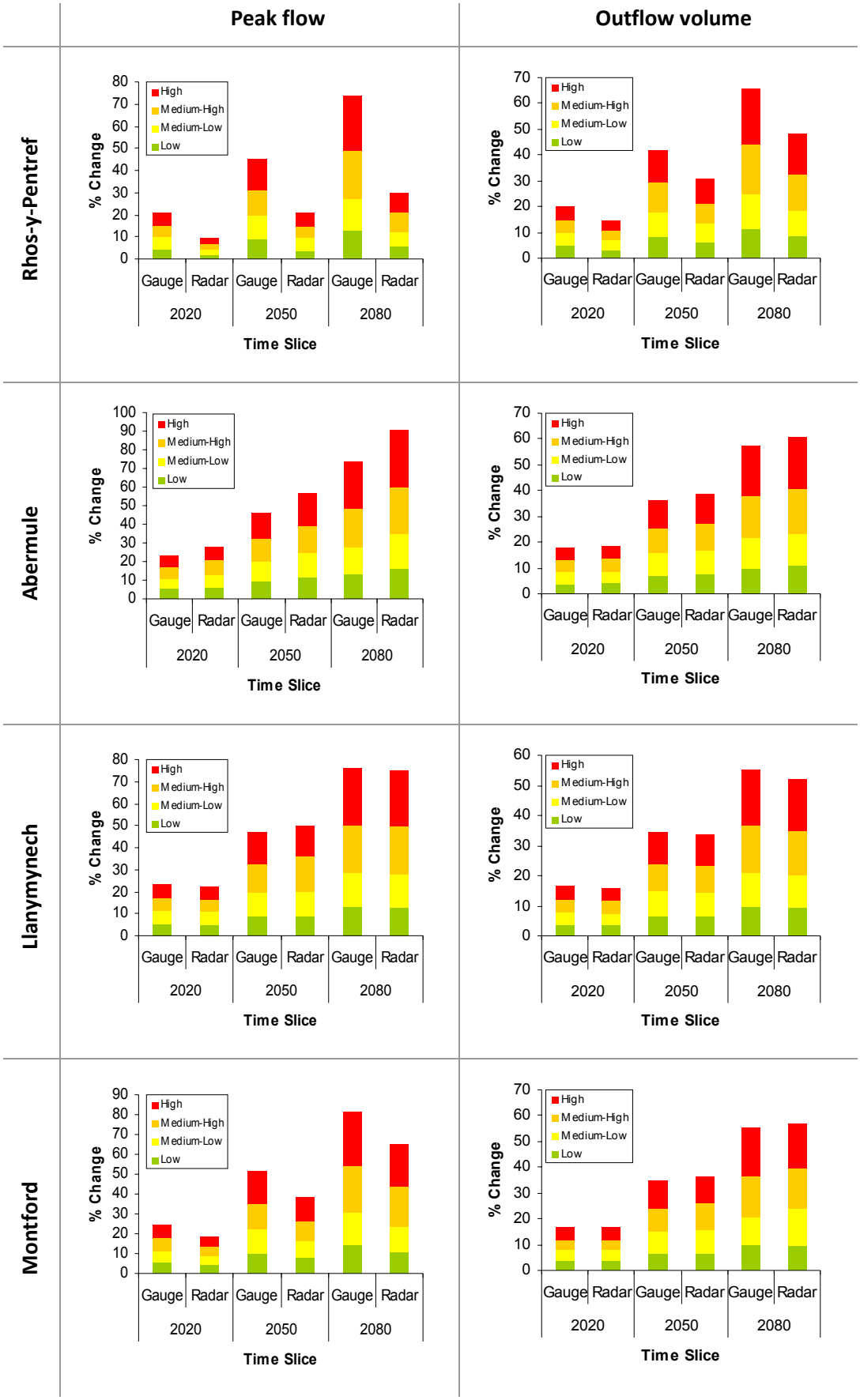

Figure 8.4 Predicted percentage changes in peak flow and outflow volume across the four emissions scenarios at four gauging locations using the gauge- and radar-driven hydrological models.

Table 8.4 Summary percentage changes in peak flow and outflow volume for the 2020s, 2050s and 2080s

	Gauge			Radar		
	2020	2050	2080	2020	2050	2080
Peak Flow						
Rhos-y-Pentref	4.7 to 5.8	8.9 to 14.1	12.6 to 25.1	2.0 to 2.4	4.1 to 6.1	5.7 to 8.9
Abermule	5.1 to 6.2	9.1 to 14.5	12.9 to 24.8	6.4 to 7.5	11.2 to 17.6	15.8 to 30.5
Llanymynech	5.3 to 6.3	9.1 to 14.7	13.1 to 25.8	5.0 to 6.0	9.1 to 14.5	13.0 to 25.2
Montford	5.5 to 6.6	10.0 to 16.0	14.3 to 27.6	4.2 to 5.0	7.5 to 12.0	10.7 to 21.4
Outflow volume						
Rhos-y-Pentref	4.7 to 5.4	8.2 to 12.9	11.5 to 21.9	3.3 to 4.1	6 to 9.7	8.6 to 15.5
Abermule	4.0 to 4.8	7.1 to 11.3	10.0 to 19.4	4.2 to 5	7.5 to 11.9	10.7 to 20.2
Llanymynech	3.8 to 4.5	6.7 to 10.8	9.6 to 18.7	3.6 to 4.3	6.4 to 10.3	9.2 to 17.3
Montford	3.8 to 4.5	6.7 to 10.8	9.6 to 18.7	3.8 to 4.5	6.7 to 10.7	9.6 to 17.9

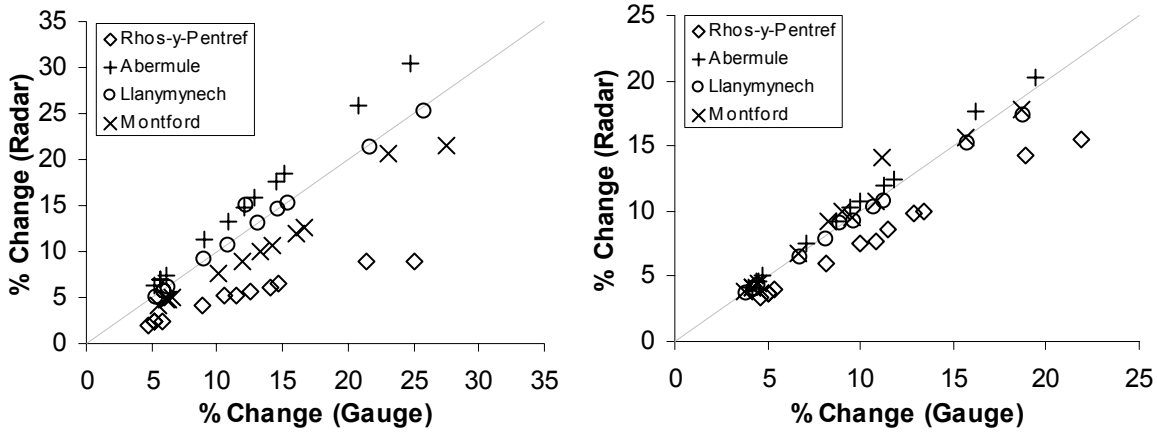

Figure 8.5 Comparison of predicted percentage changes from gauge- and radar-driven models for (a) peak flow and (b) outflow volume

8.4.3 Comparing gauge and radar predictions

There are discrepancies between gauge- and radar-driven future predictions, as can be interpreted from the summary statistics in Table 8.4. A comparison of percentage changes between the gauge- and radar-driven predictions is indicated in Figure 8.4 for each emissions scenario and time period. Predictions which have minimal discrepancies are those at Llanymynech for peak flow and Abermule, Llanymynech and Montford for changes in outflow volume. The greatest difference between predictions is observed at Rhos-y-Pentref. Differences attributed to the emissions scenarios indicate a subtle divide between the low and medium-low predictions and those of the medium-high and high predictions, with similar percentage changes attained for each time slice. A comparison of gauge- and radar-driven modelled flow residuals indicates large precision and overall correlation coefficients of between 0.97 and 1 for each station location (Figure 8.5).

Correlation between predictions is larger for outflow volumes compared to peak flow, with Llanymynech achieving the greatest correlation and Rhos-y-Pentref the smallest.

Discrepancies between the gauge- and radar-driven flow predictions are likely to be attributed to differences in the rainfall-runoff transformation processes in the modelling stage. The Clark unit hydrograph transform process uses precipitation time-series with annual indexing totals for each rain gauge and subbasin. This adjusts for regional bias in the monthly precipitation. The ModClark transformation process depends solely on gridded rainfall as an input without any indexing. The smallest prediction comparison correlation at Rhos-y-Pentref are likely to be attributed to precipitation inputs reflecting large elevation values.

The gauge-driven percentage change predictions are more uniform across the catchment than results generated using the radar-driven model. The bias-correction of the gauge-driven predictions from the indexing would imply an increased accuracy, however, the distributed composition of the radar data should in itself provide a more realistic representation of the spatial pattern of precipitation. Even though the gauge precipitation time-series are bias-corrected the index is still a point average for the gauge or the subbasin and lacks spatial variation. It is difficult to determine which set of predictions possess the largest accuracy.

8.4.4 Comparing precipitation and flow

A comparison between the November-December 2006 simulated average daily flows and those simulated under the high emissions scenario for the 2080s, along with daily precipitation totals, was made (Figure 8.6). The greatest difference in river flows occurred during December. Flow patterns are similar for both time periods and average daily peak flows occur on the same day, indicating no temporal shift in flows (beyond a day). The greatest daily precipitation totals fall in the west of the catchment as indicated by the Dolydd gauge. The rainfall-runoff transform at Rhos-y-Pentref is rapid, occurring on the same days as peak precipitation totals. There are no observed temporal differences between peak precipitation totals and peak daily average flows for the simulated November-December 2006 event and those simulated for the 2080s.

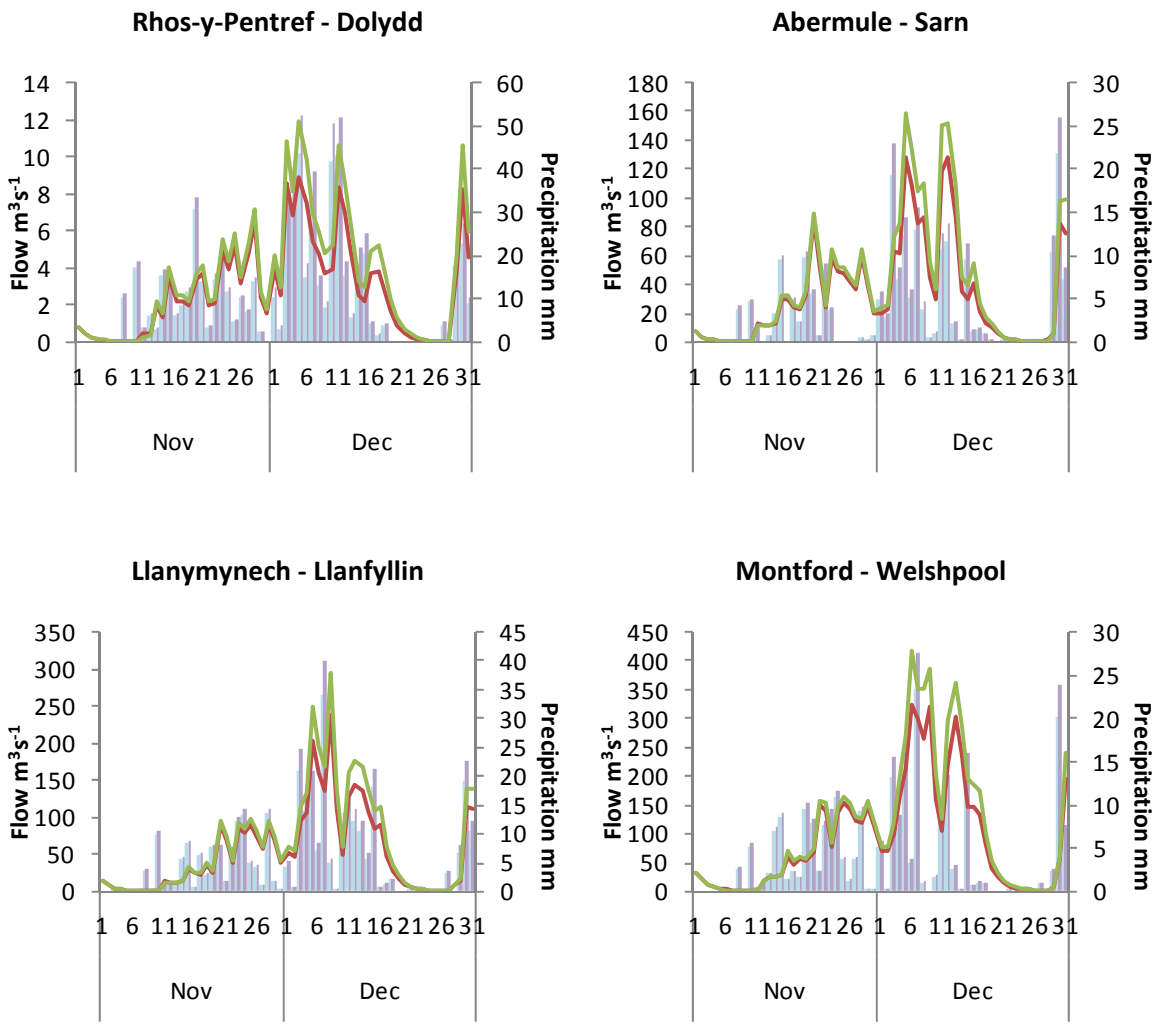

Figure 8.6 A comparison of daily precipitation totals for the nearest rain gauge located to the flow gauge and average daily flows simulated for the November-December event (blue-red) and the same event under the high emissions scenario for the 2080s (purple-green)

8.5 CLIMATE MODELLING UNCERTAINTY

Uncertainty is an inherent part of climate modelling and as the UKCIP02 scenarios are based on only one climate model uncertainty needs to be stringently accounted for as there are many scientific uncertainties which affect the ability to predict climate change. The future remains as uncertain as ever, and much uncertainty is inherent with the prediction of future conditions. Integrated into the creation procedure for the UKCIP02 scenarios are a multitude of factors concerning uncertainty bounds for the future and these are discussed in Chapter 9, where a thorough description of uncertainty surrounding climate modelling is given. However, the uncertainty concept is introduced here to provide a context for undertaking sensitivity analysis of hydrological extreme predictions. For the UKCIP02

scenarios, uncertainty can be accounted for by modelling the uncertainty margins surrounding the future precipitation and temperature predictions.

8.6 SENSITIVITY ANALYSIS

RCMs are currently unable to completely reproduce baseline climate accurately and therefore, results of impact studies using RCM series directly must be treated with caution (Environment Agency, 2003). Hulme *et al.* (2002) recommend the use of guided sensitivity analysis when using the UKCIP02 scenarios. They provide suggested uncertainty margins for temperature and precipitation changes based on the comparison of model results to those computed by a suite of GCMs (Table 8.5). Given these guidelines, changes in flow characteristics should be treated with vigilance.

To account for the uncertainty margins surrounding future flow and outflow volume calculations in the Severn Uplands, the UKCIP02 figures (Table 8.5) were used to perform sensitivity analyses. The maximum and minimum winter margins were applied to the future precipitation and temperature UKCIP02 scenarios. For example, under the high emissions precipitation scenario the projected future precipitation values were increased by 20% to determine the high precipitation margins. The same methods as described in sections 8.1.1 and 8.1.2 were applied to calculate the evaporation values and percentage changes in precipitation. All four possible combinations of (i) high precipitation; low evaporation, (ii) high precipitation; high evaporation, (iii) low precipitation; high evaporation, and (iv) low precipitation; low evaporation were then input to the HEC-HMS model and the uncertainty margins surrounding the peak flow and outflow volume were predicted. Results for the gauge- and radar-driven sensitivity analyses are summarised below.

Table 8.5 Suggested uncertainty margins for application with the UKCIP02 scenarios

	Low Emissions	Medium-Low Emissions	Medium-High Emission	High Emissions
Average Temperature				
Winter (°C)	± 0.5	± 1.0	± 1.5	± 2.0
Summer (°C)	± 0.5	± 1.0	± 1.5	± 2.0
Average Precipitation				
Winter (%)	± 5	± 10	± 15	± 20
Summer (%)	+ 10	+ 15	+ 30	+ 40

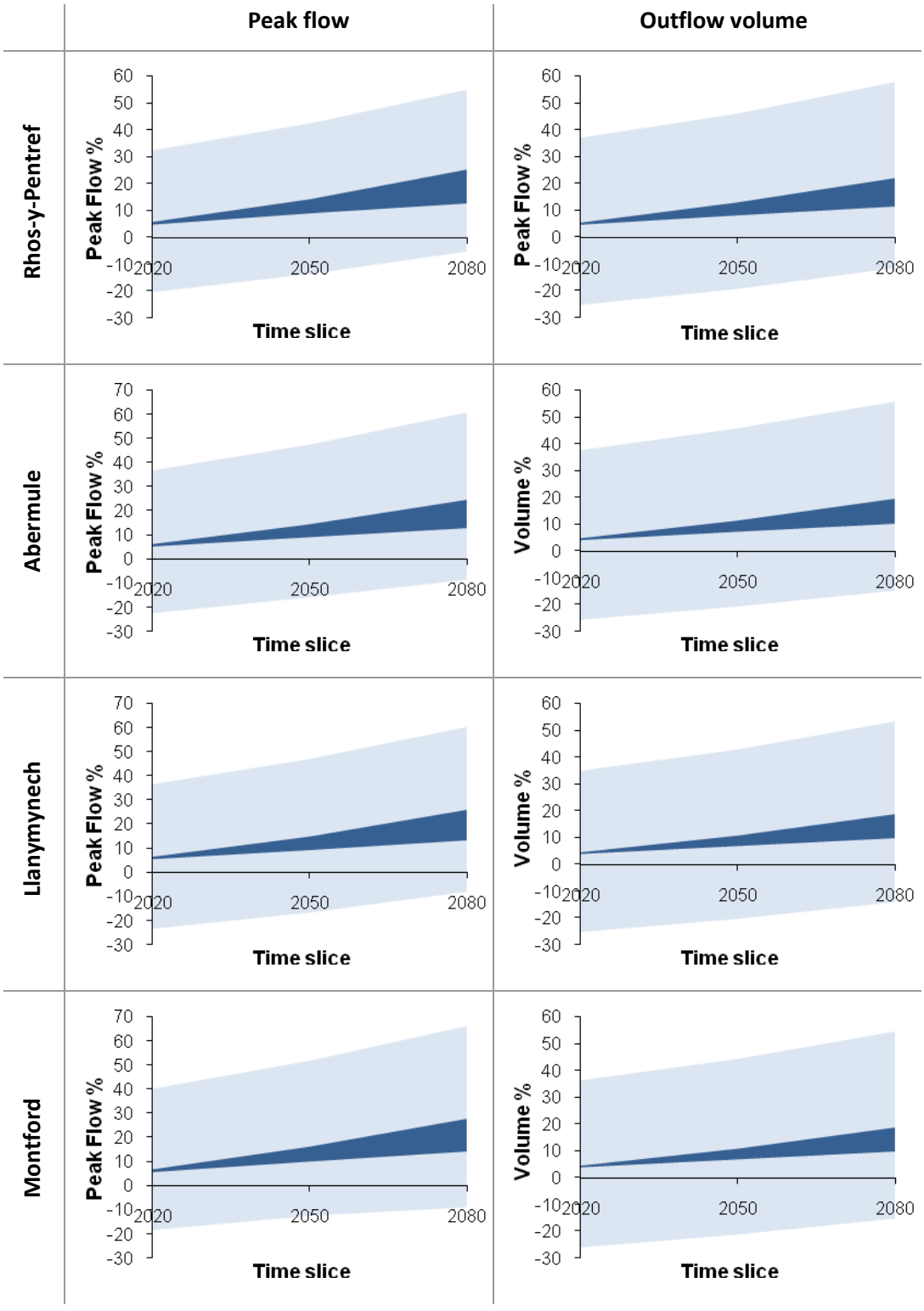

Figure 8.7 Predicted percentage changes in peak flow and outflow volume at four gauging locations using the gauge-driven hydrological model, indicating the predicted range (dark blue) and uncertainty margins (light blue).

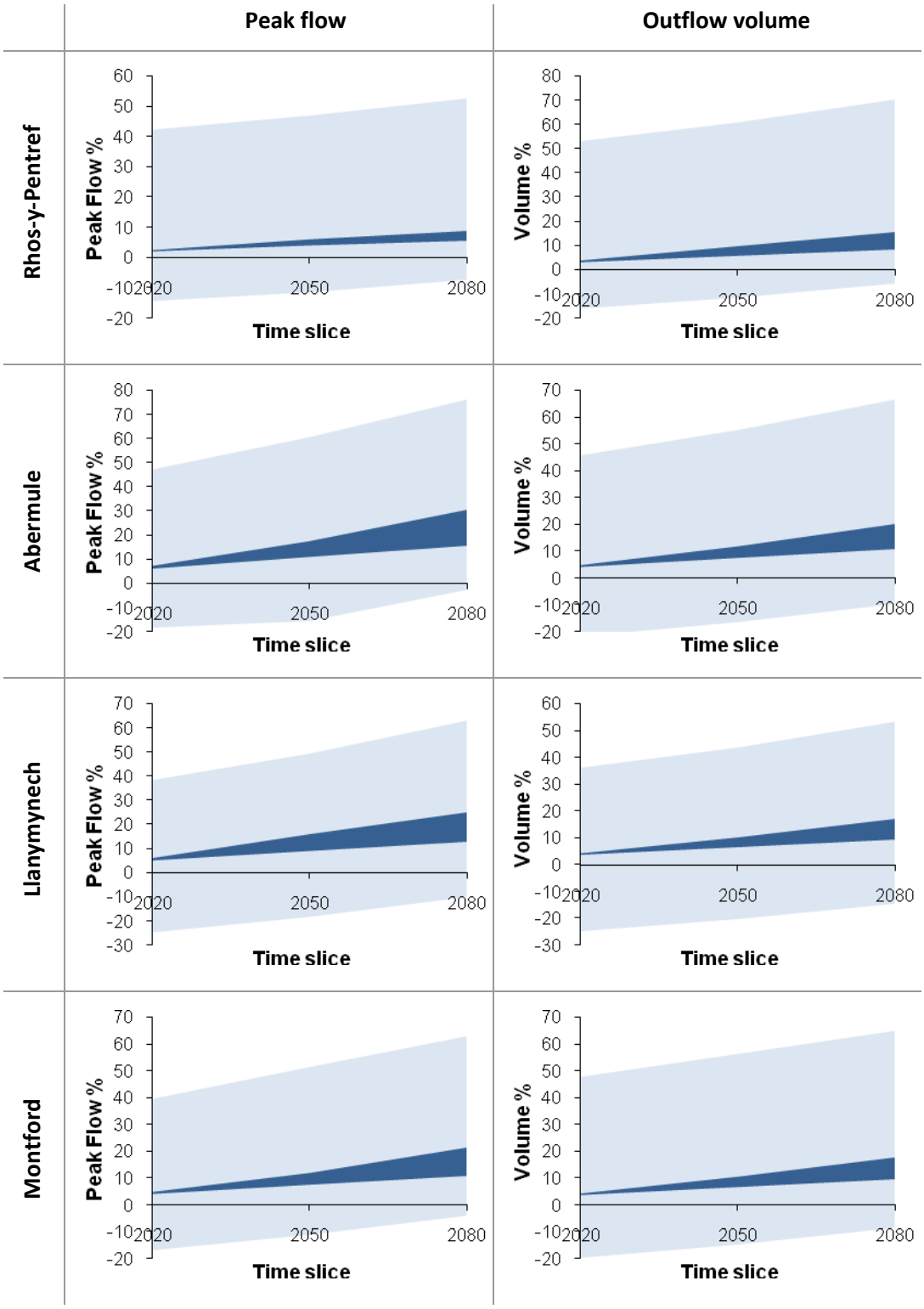

Figure 8.8 Predicted percentage changes in peak flow and outflow volume at four gauging locations using the radar-driven hydrological model, indicating the predicted range (dark blue) and uncertainty margins (light blue).

The maximum uncertainty margins for the three time slices are illustrated in Figure 8.7 and Figure 8.8 for changes in peak discharge and outflow volume using the gauge- and radar-driven model, respectively. These plots represent changes across all emissions scenarios. The mid-range indicates the range of predicted percentage changes across the emissions scenarios (the minimum and maximum predictions for each time slice, as tabulated in Table 8.4). These values were described earlier in Section 8.4.

8.6.1 Gauge uncertainty margins

Predicted changes in peak flows and outflow volumes indicate similar uncertainty margins for all four gauging locations (Figure 8.7). Additionally, both low and high uncertainty margins remain fairly constant for each time slice relative to the range of predicted values. High uncertainty margins range from a percentage increase in peak flow and outflow volume of approximately 35% in the 2020s to 60% by the 2080s. Low uncertainty margins predict reductions in both peak flow and outflow volume of approximately 25% for the 2020s and lessening to a maximum reduction of around 15% by the 2080s.

8.6.2 Radar uncertainty margins

Radar uncertainty margins are large for all gauges (Figure 8.8). The lower uncertainty bounds record reductions in peak flow and outflow volume of up to approximately 25% for the 2020s and to a lesser extent of approximately 10% by the 2080s. The upper uncertainty bound reaches increases of over 75%. The uncertainty bounds remain relatively constant in value throughout the 21st century. Changes in peak flow and outflow volume follow a similar pattern for all three time slices.

8.6.3 Comparing uncertainty margins

Uncertainty margins are similarly matched between gauge- and radar-driven percentage change predictions with correlation coefficients ranging between 0.98 and 1 (Figure 8.9). Percentage changes in outflow volumes are most accurate at Llanymynech with the other three stations showing larger inaccuracies between predictions, with radar-driven

percentage changes consistently larger than those produced from the gauge-driven models. Peak flow predictions show less diversity in prediction comparisons and Llanymynech and Montford produce the largest accuracy in matching predictions. All four stations indicate high precision between predictions. Any contrast between predicted flow uncertainty margins for gauge- and radar-driven hydrological modelling is likely to be attributed to the same inconsistencies which led to the discrepancies in the range of predictions as discussed in Section 8.4.3.

(a) Peak flow

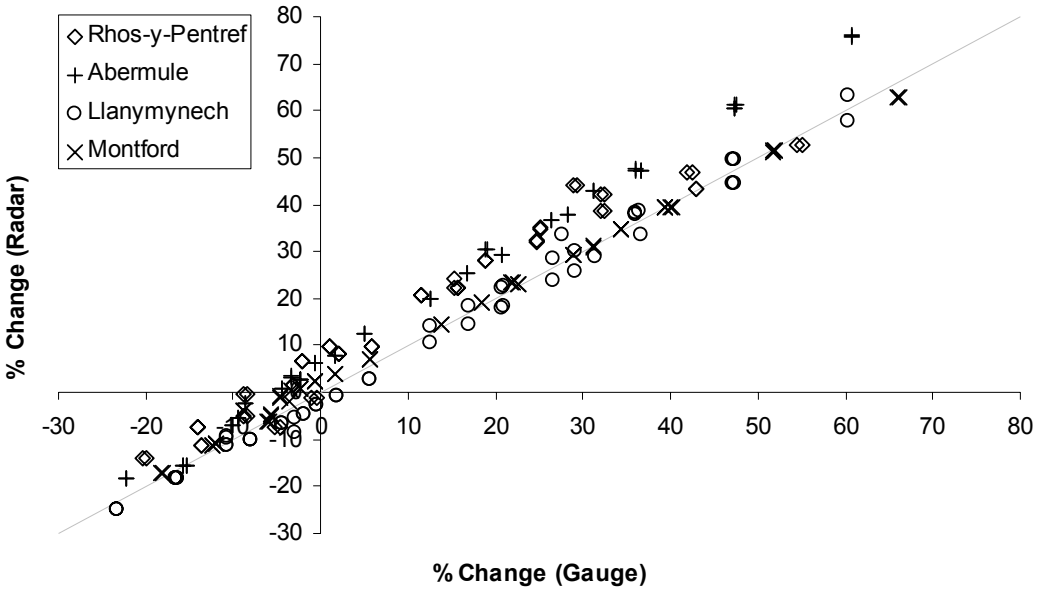

(b) Outflow volume

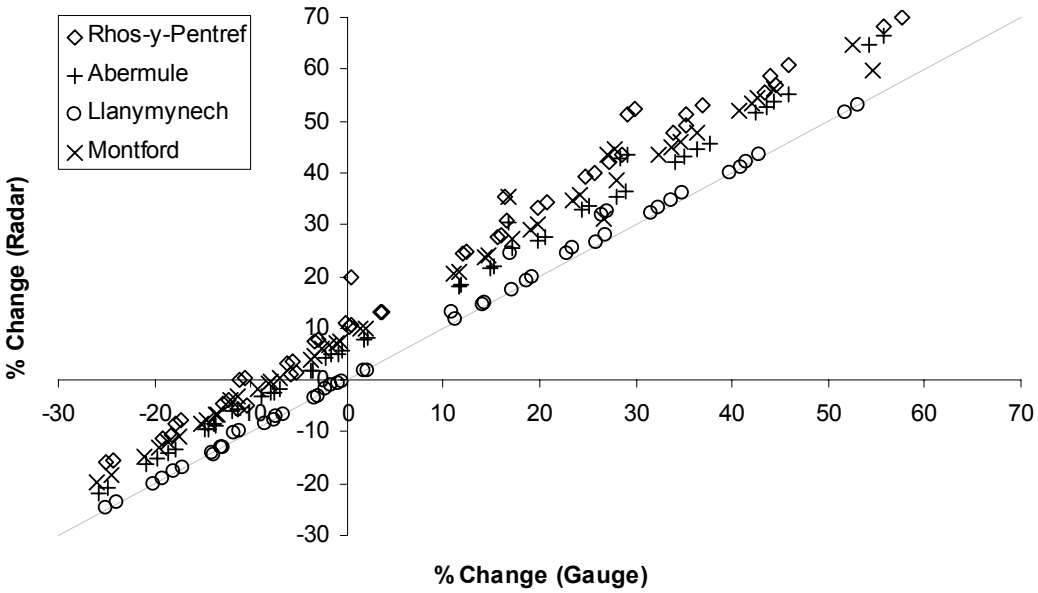

Figure 8.9 Comparison of predicted percentage changes from gauge- and radar-driven models for (a) peak flow and (b) outflow volume

Table 8.6 Global climate change estimates relative to the 1961-1990 baseline (Source: Hulme *et al.*, 2002)

	2020s		2050s		2080s	
	ΔT (°C)	CO_2 (ppm)	ΔT (°C)	CO_2 (ppm)	ΔT (°C)	CO_2 (ppm)
Low	0.79	422	1.41	489	2.00	525
Medium-Low	0.88	422	1.64	489	2.34	532
Medium-High	0.88	435	1.87	551	3.29	715
High	0.94	437	2.24	593	3.88	810

8.7 FUTURE CATCHMENT CONDITIONS

Flow magnitude and volume have been predicted to increase over the 21st century for the Severn Uplands during the months of November and December given projected changes in evapotranspiration and precipitation. Arnell (2003b) states that there is minimal variation in the pattern of change in global runoff between the four SRES emission scenarios up to the 2080s. For the Severn Uplands results indicate variation in predictions of approximately 15% from baseline values by the 2080s. These comparisons could detrimentally affect local inundation; for example, peak flow at Abermule could be up to 16% greater under the low emission scenario for the 2080s, or as much as 31% under the high emissions scenario. The contrast between these predictions is vast and temperature and precipitation predictions under the emissions scenario are evidently important for indicating future flows in the Severn Uplands. Although these two variables have an important direct affect on flow regimes, there are additional catchment characteristics that will likely contribute to future changes in flow extremes, and may either enhance flow or suppress it. All are discussed below.

8.7.1 Temperature

Temperature is a primary climate variable controlling future changes in hydrological regimes, which, in turn, is largely dependent on the concentration of atmospheric CO_2. The UKCIP02 emissions scenarios reflect this with higher global temperatures occurring under larger CO_2 concentrations (Table 8.6). As discussed in Chapter 2, this is linked to the intensification of the hydrological cycle under a warming climate, where changes in precipitation result in changes in fluvial discharge. Simulations for the Severn Uplands indicate an increasing range in flow predictions relative to the emission scenarios (Figure 8.4). Differences in future fluvial flow regimes can be indirectly attributed to projected

atmospheric CO_2 concentration, with the underlying emissions scenarios reflecting changes in technology, population, sustainability and the economy (Table 2.1). CO_2 influences global temperatures which influences changes in flow characteristics through alterations in precipitation regimes and physical catchment properties. Future changes in the Severn Uplands flow regimes will depend on an ability to mitigate the impact of climate change and slow the rate of CO_2 emissions.

Despite quite large differences in emissions between the four UKCIP02 scenarios, there is relatively little difference in global temperature changes until after the mid-21st Century (Hulme *et al.*, 2002). This implies that changes for approximately the next 40-years have already been predetermined. This could infer that predicted changes in flow extremes for the Severn Uplands are likely to be less uncertain up to this time. Such probability is indicated for future flows, particularly for each of the emissions scenarios for the 2020s, with a small range of predictions apparent, as interpreted from Table 8.4 and illustrated in Figures 8.4, 8.7 and 8.8. Nonetheless, uncertainty surrounding predictions remains fairly constant throughout the 21st century.

8.7.2 Evaporation

Despite increases in winter precipitation, higher temperatures and reductions in relative humidity indicate that winter evaporation will increase and soil moisture levels will decrease relative to the present (Hulme *et al.*, 2002). This is reflected in the evaporation rates across the Severn Uplands. Average catchment evaporation (average of subbasins) rates increase by 57% for November and 63% for December from present day rates to those under the high emissions scenario for the 2080s (Table 8.1). Despite such large increases in evaporation, which can be attributed to temperature changes, the effect of evaporation rates on flow simulations is relatively minimal. Evaporation changes can be evaluated from future flows calculated under the uncertainty margins. For example, a difference in predictions between high precipitation/low evaporation and high precipitation/high evaporation were around 2% (Appendix 5). This suggests that evaporation has little relative effect on future flow regimes, and precipitation is the dominant variable driving change.

8.7.3 Precipitation and weather patterns

Precipitation had the greatest effect on future flow predictions for the Severn Uplands. This is illustrated from the uncertainty margin calculations where a *reduction* in precipitation of 20% (corresponding to the 2080s) resulted in peak flow reductions up to 24% and volume reductions up to 25% (Appendix 5). In contrast, an *increase* in precipitation of 20% resulted in peak flow increases up to 76% and outflow volume increases up to 70%. These values relate to an increase in extreme precipitation from modelling the November-December 2006 event, and subsequently relate to extreme flows. It is envisaged that changes in flow extremes in the Severn Uplands will largely depend on changes in the variability and type of precipitation, as well as the response of catchment properties to a changing climate (see Section 8.7.5). Some climate models (e.g. Gordon *et al.*, 1992; Hennessy *et al.*, 1997; Chen *et al.*, 2005) have indicated that under a warmer climate, an increased proportion of rainfall might be caused by convective processes, and less by large-scale dynamical processes. If this occurs within the Severn Uplands then the trend in extreme summer flows (see Chapter 5), when convective processes are more common due to higher temperatures, may well propagate into the future. There is also the possibility that the seasonal aspect of convective storms may change; with higher temperatures throughout the year, rainfall from convective processes may occur more frequently.

Other climate variables to consider which will affect weather patterns in the Severn Uplands are the NAO and the path of storm tracks. These are dependent on factors such as convective processes at the equator and Atlantic SSTs. Again, uncertainty surrounds these variables and how they will change in future, let alone how they will affect hydrological extremes in the Severn Uplands. It is beyond the scope of this research to investigate the future influence of weather patterns and related climate variables, yet it is something to consider when drawing conclusions.

8.7.4 Snowmelt

Given that snow cover has declined over the last 30 years (Section 5.4.5) a snowmelt model was not incorporated into producing flow predictions for the Severn Uplands. Arnell (2004) found that future runoff maxima occur during winter and early spring and although some winter precipitation falls as snow in UK upland catchments, snowmelt is not a

dominant feature and is becoming even less so given trends in increasing temperature. Snow decline over recent years (Figure 5.11) across the Severn Uplands implies that snowmelt will not be a major component of future climate-hydrology regimes, and, as such, is unlikely to considerably contribute to trends in future hydrological extremes.

8.7.5 Land use

Land use change is another uncertainty which will affect future flow regimes of the Severn Uplands. Land use change has a direct effect on hydrologic processes through its link with evaporation and the type of ground cover which greatly affects surface runoff (Foher *et al.*, 2004). Given that evapotranspiration rates have been found to have little impact on future flow predictions it is likely that land use changes will have a greater impact through surface runoff processes. Approximately 131.1 km² (6.4%) of the Severn Uplands falls under statutory environmental legislation, 184.6 km² (8.9%) is designated as Environment Agency flood zone and 19.9 km² (1.0%) is classified as built-up areas (Table 8.7). This renders approximately 320.8 km² (15.5%) of the catchment unsuitable for urban development, assuming that construction within these areas is prohibited. In addition, slope can be accounted for and if inclines greater than 15° are discounted then approximately 493.0 km² (23.9%) of the catchment becomes unsuitable for urban development, or if slopes above 10° are disregarded then this leaves 730.0 km² (35.4%) of the catchment unsuitable for urban development. Strategic guidance on the level and location of urban growth is provided by Regional Spatial Strategies and the latest end date of this is 2026. It is, therefore, difficult to predict accurately long term urban development beyond this date. Major urban areas (brownfield sites) will accommodate the majority of designated growth and development in rural areas will be limited. In the Welsh Severn Uplands the CFMP identifies several riverside towns (Llanyllin, Llanidloes, Newtown, Welshpool) for an increase in housing provision (Environment Agency, 2008). As the Severn Uplands is a predominantly rural catchment and is fairly isolated from large urban centres, building construction and expansion of existing urban areas is unlikely to occur at a scale that will impact severely upon flow extremes. A more likely scenario is that of land use change, predominantly from agricultural and forestry practices (Environment Agency, 2008). Alterations in vegetation cover and land management can impact significantly upon soil stability and water storage, which in turn can affect flow regimes. There is a significant link between land use and land management practices and runoff generation at the plot or

individual field scale (Environment Agency, 2008). Land cover within the Severn Uplands which is not constrained by legislative protection, is external to the flood zone and is not already classified as urban is listed in Table 8.8. Land cover in these remaining areas comprises predominantly of grassland and woodland. Figure 8.10 illustrates the spatial distribution of the land cover. Arable agricultural land (tilled) constitutes 4.9% of the Severn Uplands and is concentrated in low-lying areas, with a particular presence in the eastern part of the catchment. Climate change may instigate the need for land cover change as land degradation may drive a shift in land productivity (Environment Agency, 2008). There is vast potential for land use change to occur to meet future demands such as water resources, fuel and food security. For example, grassland, including that which is presently used for pastoral farming, may need to be converted to arable agriculture to meet future crop demands. Uncertainty surrounding future requirements propagates into the hydrological modelling as land use changes which will impact on flow extremes need to be modelled using a series of 'what-if' scenarios.

A direct impact on future flow extremes will occur from channel modifications. These may arise from natural geomorphological changes or as a result of flood engineering schemes to mitigate inundation. As described in Section 4.8 flood protection on the Severn Uplands is limited and if urban expansion was to occur then more investment would be required to protect properties from flooding. The low-level defences at the Severn-Vyrnwy confluence are often overtopped during extreme flood events as they are designed to do. Properties across the floodplain can be inundated from main river sources, ordinary watercourses and surface water. A recent report published by the Environment Agency (2009b) outlines the long-term investment strategy to manage flood risks between 2010 and 2035. One of the major components discussed is the investment required to adapt to climate change and associated risks over this time period. The report states that in England alone, spending will need to increase from the £570 million asset maintenance and construction budget in 2010-2011 to around £1040 million by 2035, plus inflation. In the 2001 Environment Agency report detailing the October/November flooding in Wales there was no mention of the Agency to take action on the threat of climate change. And even without these impacts being considered the cost of an improved level of service to flood defence works in the Severn Uplands was estimated at £1.9 million (Environment Agency, 2001b). The Association of British Insurers has stated that its members will not necessarily offer to insure new properties sited in areas of flood risk (Environment Agency, 2009a). Building property and locating other assets away from the floodplain is the best way to reduce risk (Environment Agency, 2009a).

There are currently two large reservoirs with dams controlling flow in the upper reaches of the Severn Uplands. Changes in flow extremes may affect reservoir storage capacity and may impact upon downstream locations should more water require release during times of peak storage. Construction or expansion of existing reservoirs could also impact upon flow regimes. However, reservoirs in the Severn Uplands have limited impact on general flood alleviation, as indicated during the 1998 and 2000 floods when overspill occurred and little change in downstream flow was observed compared to flows prior to the spillage (Environment Agency, 2001b). Reservoirs were not included in the hydrological model, due to a significant lack of data for parameterisation, but for water resources management, detailed hydraulic models including reservoir storage will be needed to investigate the impact that climate change will have. Given their limited impact on past flood events, reservoir omission from the hydrological model should not greatly impact upon future river flow predictions at this catchment scale, especially as reservoirs have less impact on high-flow extremes compared to low-flow extremes (Gilman, 2002).

The Severn catchment flood management plan (Environment Agency, 2008) states that likely land management changes may include (i) an increase in environmentally sensitive farming which may lead to a reduction in agricultural drainage, (ii) an increase in the quality of the rural environment which may lead to a decrease in runoff from agricultural areas, (iii) an increase in woodland to meet forestry market demands, and (iv) a requirement for more land for mineral extraction, but this is thought to be positive as will provide pits for increased drainage. Research by Gilman (2002) states that modelling land use impacts can only be accounted for fully when using a complete distributed model. However, a more intensive hydrometric database than currently exists for the Severn will need development to conduct such research.

Table 8.7 Land deemed unsuitable for further urban development

Designation	Area km^2
Urban Areas	19.9
National Park	5.3
RAMSAR	0.04
National Nature Reserve	48.1
Special Area of Conservation	100.2
Site of Special Scientific Interest	130.7
Special Protected areas	114.7
EA Designated Flood Zone	184.6

Table 8.8 Land cover within areas of which could likely experience future change based on LCM2000 land cover map data

Land cover	Area *km²*	% of catchment
Grass	934.1	45.2
Moor/heath	202.9	9.8
Orchard/Bog	15.9	0.8
Woodland	326.9	15.8
Tilled	100.6	4.9
Bare Ground	2.9	0.1

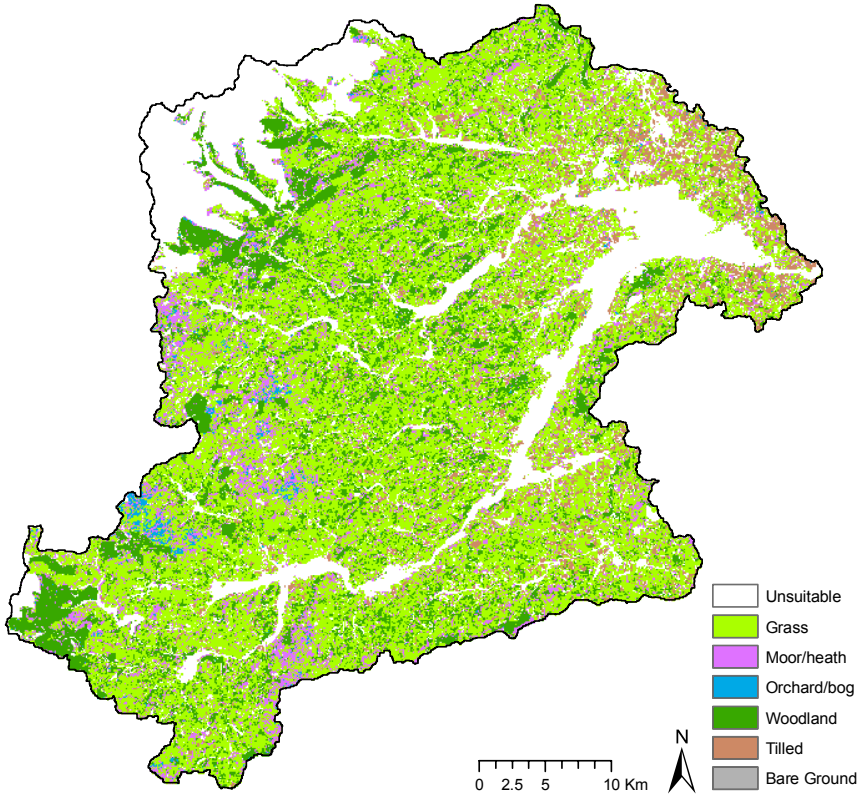

Figure 8.10 Land cover which is more likely to urbanisation and land use changes in the future

8.8 FLOOD IMPLICATIONS

Relative to future changes in an extreme wintertime hydrological event under the high emissions scenario, percentage changes in peak flows may be 30% larger and outflow volume may increase by 20% for some locations in the Severn Uplands. These increases will have a substantial effect on flooding within the region, and effects will propagate, combined with a likely enhancement, with distance downstream. Inundation is already a severe problem along the Severn watercourse, and reflecting on policy issues raised in

Chapters 1 and 2 from previous flood incidents, it is likely that vast amounts of investment will be required to mitigate for such changes.

The Environment Agency's aim is to "minimise the harm caused by flooding. This involves reducing the likelihood of flooding and reducing the impacts when flooding occurs. At the same time there are underlying pressures that are increasing risk, such as climate change, housing development or changes in land use" (Environment Agency, 2009a). These factors have been discussed in Section 8.7 and are hard to predict as the future is unknown and any number of combinations could be plausible; uncertainty increasing with the number of factors considered. This gives rise to the extensive uncertainty surrounding all future predictions which is further discussed in Chapter 9. The solution to protecting against flood inundation is to ensure successful adaptation to climate change, mitigate impacts and monitor risks on a continual basis. The UK climate change act instigated in 2008 requires the risks from climate change and adaptation to such changes, to be assessed every five years. This Act enables the government to impose demands on public bodies and statutory organisations to report how they are adapting to climate change. This is important for all river catchments and in the Severn Uplands the Environment Agency and local water authorities are now under a legal obligation to comply with regulations to monitor the ongoing affects of climate change.

8.9 SUMMARY

This chapter has investigated what will happen to future extremes under the UKCIP02 climate scenarios for the November-December 2006 case study. Extreme river flows are predicted to increase in terms of both peak flow and outflow volume given an increase in winter precipitation, despite an accompanying increase in temperature resulting in increased evaporation rates. Differences in flow predictions were obtained from using different precipitation inputs which emphasises the need to remain cautious when making predictions, especially as uncertainty in the data, model and parameters will propagate to predicted outputs. It is uncertain to what extent the Severn Uplands will respond to predicted climate change, particularly given that influential factors such as land cover cannot be accounted for accurately. These uncertainties have been quantified for the precipitation and temperature predictions. However, a plethora of additional uncertainties are inherent in data, assumptions and the modelling processes, and are subsequently discussed in detail in the following chapter.

CHAPTER 9

Uncertainty and Further Research

The four analysis chapters in this research have (i) investigated trends in hydrological extremes in an upland catchment of the UK, (ii) quantified the ability of a rainfall-runoff model to adequately simulate past hydrological extreme events, (iii) identified the differences in model output when using point and gridded precipitation inputs, and (iv) attempted to predict future flow changes for an extreme winter-time event. This chapter considers the error and uncertainty inherent in all four of the analysis stages relative to the Severn Uplands. The latter part of the chapter reviews the limitations associated with the research undertaken and suggests possible improvements and ideas for future research.

9.1 UNCERTAINTY

Uncertainty is a constant companion of scientists and decision-makers involved in global climate change research and management. It is an issue of crucial importance which has not yet been properly dealt with. There are multiple sources of uncertainty in climate science, some of which are endemic (Dessai and Hulme, 2001). A phrase frequently associated with climate change science is *the only certainty is uncertainty* and as Khatibi (2005) points out "there is uncertainty about uncertainty". Future predictions are riddled with uncertainty. Estimates of future environments are made given current understanding of how systems operate and how they have operated in the past. Calibrating future predictions is impossible given that the future has not yet occurred, hence the uncertainty. When making predictions, uncertainty is introduced through a multitude of sources including natural randomness, data inputs, scale issues relating to the level of aggregation, variability, model parameters, model structure (boundary conditions and representations of

physical processes), use of non-optimal parameters and error in measurements used for model calibration. The quantification of the different uncertainty sources is still a major concern (Timbe and Willems, 2004). Uncertainties relevant to the analyses conducted in this research are further discussed below; a comprehensive review of uncertainty sources in hydrological modelling is provided by Melching (1995) and uncertainties attributed to the UKCIP02 scenarios are described in detail by Hulme *et al.* (2002) and Jenkins and Lowe (2003).

9.1.1 Data inputs

Measurement error, constituting both random (precision) and systematic (bias) errors, arises when attempting to measure an unknown physical constant. These errors normally result from measurement discrepancies in input data and can arise from missing data, faulty recordings due to equipment failure or natural phenomena such as flooding out-of-bank, and changes in equipment used. All data sources were subject to measurement errors which lead to inherent uncertainty in the outputs. Time-series data used in Chapter 5 had a maximum record length of 30-years. If longer records were used then different trend results might be detected dependent on the preceding behaviour of the time-series variables. If time-series were extended further into the past, it could be that significant trends detected over the last 30 years may be part of a longer trend in climate variability, may contradict previous trends and therefore be statistically insignificant, or might be part of a cyclical component.

The records used contained missing data and although gauge measurements were checked routinely for inconsistencies by the recording authorities, errors could still be present. This is also true for time-series data used in the other three analysis chapters. The radar rainfall time-series constitute calculated rainfall amounts, yet radar measures microwave radiation back-scattered from particles in the atmosphere, and not actual rain amounts, so there is uncertainty in the calculation of precipitation rate. Data used to estimate parameters may also contain errors. For example, terrain variables were derived from a DEM which can contain measurement errors (e.g. satellite malfunctions). Processing data inputs also introduces uncertainty, such as pre-processing of terrain data or the geostatistical correction of radar rainfall. In the latter example, radar bias correction using gauge data was applied to overcome the error of discontinuities in change which were evident from

using sampled measurements with no interpolation. However, by interpolating values at unsampled locations a false geographical precision is introduced to the predictions and can generate an increase in associated inaccuracies regarding predicted precipitation amounts (Engen-Skaugen *et al.*, 2005).

9.1.2 Model simplifications

Simplifications applied when representing reality induce uncertainty in both the hydrological and climate modelling stages. Increasing the size and complexity of a model can result in either a reduction or increase in associated uncertainty (Katz, 2002). A more complex model may be more accurate at representing reality and reducing the uncertainty of replicating physical processes, but the more parameters used, the more uncertainty is introduced to the modelling boundaries. Uncertainty in the model structure can arise from the omission of parameters and the mathematical simplification of physical processes. However, the number of model parameters often needs to be restricted in order to avoid over-fitting. Hydrological modelling by nature is generally quite parameter-intensive, and a large number of parameters (a total of 14, plus additional boundary conditions) constituted the HEC-HMS model of the Severn Uplands, along with the use of some complex data inputs (use of distributed precipitation). No increase in accuracy was observed using the distributed precipitation inputs to predict flow and similar conclusions have been made in other research, as reviewed in Chapter 7. Therefore, it seems an unnecessary complexity to use gridded rainfall in the Severn Uplands where the gauge network can predict flows with increased accuracy, especially as using gridded precipitation data in the hydrological model increases computational requirements and processing time. However, the advantage of using spatially distributed precipitation is that the climate projections could be applied on a distributed basis, reducing the uncertainty associated with using datasets of different formats. Given an alternative location, where the gauge network inadequately represents precipitation, using radar rainfall inputs may be highly beneficial and could substantially increase the accuracy of predictions.

9.1.2.1 Hydrological models

Uncertainties in basin runoff predictions occur due to the inadequacies of the mathematical model used to approximate a highly complex physical system and an inability to perfectly observe and predict rainfall conditions (Smith and Kojiri, 2003). Simplifications are made when representing reality but models are generally satisfactory at replicating hydrological processes. Murphy and Charlton (2006) state that model parameter uncertainty is more important than the uncertainty due to emissions scenarios. Therefore, the more accurate the hydrological model, the more accurate future predictions will be. In rainfall-runoff modelling both for real-time forecasting and for prediction of peak flows of a certain return period the uncertainty is quite large (Blazkova and Beven, 2004). Model structure and parameterisation errors are assumed to be of the same magnitude under current and future conditions when using the same model so can, therefore, be ignored (Prudhomme, 2003). This was applied in Chapter 8 of this research, where future predictions were calculated relative to the simulated (not observed) baseline values, and further to this, no predictions were made outside the calibration range.

9.1.2.2 Climate models

Climate models cannot account explicitly for every process at the smallest of scales; therefore, many processes are modelled at a scale unresolved by the resolution of the model. The main theoretical limitation of using an RCM are the effects of systematic errors in driving the large scale fields provided by GCMs and the lack of mutual interaction between regional and global models (Mearns *et al.*, 2003). UKCIP02 projections are available at 5 km² spatial resolution, derived from a 50 km² RCM and dynamically downscaled from a GCM. The pattern-scaling method which applies the GCM results to RCM results to interpolate the UKCIP02 scenarios is uncertain as the dynamic downscaling process results in terrain being smoothed within the RCM and local processes are not accurately represented. Consequently, the UKCIP02 future precipitation and temperature changes may have increased error margins as the Severn Uplands catchment is at a local rather than national or even regional scale. Additionally, the UKCIP02 scenarios rely on SRES emissions scenarios which are uncertain in themselves as they do not take into account direct climate polices aimed at GHG mitigation or climate change adaptation polices (Nakicenovic *et al*., 2000). Until the second half of the next century, in terms of global temperature changes, it will be impossible to differentiate between which SRES world we are inhabiting (Dessai and Hulme, 2001).

Different climate models generate different climate change scenarios. UKCIP02 is based on just one climate model developed by the Hadley Centre. At the time of producing these scenarios no other RCM of 50 km spatial resolution for Europe was in existence so there was no means of comparison (Hulme *et al.*, 2002). However, using a different GCM as a driver, and/or a different nestled RCM could have resulted in very different results. Xu (1999) provides a comprehensive overview of issues surrounding the downscaling climate model methods for applying to hydrological model output.

9.1.2.3 Physical representation

Some scientific processes, such as radiative forcing of changes in atmospheric aerosol concentrations and their indirect cooling effect, are poorly understood. Uncertainties such as these are merely represented by median values in simple climate models (Jones, 2000). A step beyond this is that the fundamentals of science can even be misunderstood. A recent article in the *New Scientist* (23rd May 2009) reported that forecasters could be miscalculating how much it rains due to a fundamental flaw in the physical representation of rainfall. Weather radar has become an indispensable tool in weather forecasting and its quantitative use in hydrometeorology relies on the accurate measurement of rainfall rates. The article, based on research by Montero-Martinez *et al.* (2009), states that some raindrops defy the conventional theory that all raindrops fall at their terminal velocity, and may be falling at "super-terminal" speeds (up to 10 times faster) upon fragmentation. If rainfall rates are being calculated incorrectly then rainfall may be overestimated by as much as 20% and subsequently the risks of flooding could be being overstated. This may help explain discrepancies in flow extremes calculated from radar rainfall driving hydrological model as opposed to the gauge driven predictions. Additionally, uncertainty derived from mathematical inconsistencies can be further augmented by errors sustained during data collection and parameterisation. For example, Romanowicz and Beven (1998) identified that many combinations of roughness parameters may exist that are consistent with downstream water level prediction, but can produce very different inundation predictions.

9.1.3 Future conditions

Future emissions of greenhouse gases and how the climate system will respond to these emissions are the two main sources of uncertainty that influence descriptions of potential future climates (Hulme *et al.*, 2002). GCMs use numerous different algorithms for describing physical processes and vary in their modelling approaches. Various emissions scenarios also incorporate uncertainties, reflecting the uncertainties associated with modelling economic growth, societal implications and energy demands. The UKCIP02 scenarios provide likely projections of future environmental conditions based on predictions of relevant variables. These particular emissions scenarios were developed based on predicted changes in technology, population, sustainability and the economy. Emissions scenarios are only likely projections of future climate and are not exact science.

The climate system is uncertain and estimated increases in global temperature in line with radiative forcing may waver from predicted projections. Accounting for every possible change in the future hydrological environment is impossible and models increase in complexity with the number of included environmental variables. Error can be introduced in maintaining the same parameterisation for the hydrological simulation for all time horizons (baseline and future). Assumptions were made to retain model simplicity, but in reality the majority of model parameters will deviate from fixed values under future conditions. For example, parameters representing water losses reflect changes in ground characteristics such as soil porosity and these changes, which are likely to be significantly impacted upon by increasing temperatures, were not projected for future conditions. Changes in physical properties of the catchment were identified in Chapter 5 as having an influential role on changes in flow regimes alongside climatic alterations. There are numerous interplaying factors, and subsequently the uncertainty associated with future predictions is large. Inevitably, the prediction of future flows is dependent on a multitude of possible outcomes, not just precipitation and evapotranspiration. Future climates can only be envisaged and changes in hydrological extremes are speculative.

9.1.4 Feedback

The Earth is an intricate system and many complex relationships exist between factors such as the atmosphere, oceans and biosphere. Therefore, it is often impossible to create a complete and accurate replication of reality. Feedback is an important source of

uncertainty and system interactions may enhance or counteract global warming processes, as well as affecting each other's response to a warming climate. The modelling of greenhouse gas and aerosol concentrations requires feedback mechanisms to monitor processes such as absorption, deposition and chemical metamorphosis which are difficult to predict. In addition, the response of large-scale climatic processes within global and regional models can vary greatly to changes in radiative forcing. Furthermore, natural climate variability could enhance or diminish current climate change. It is difficult to incorporate feedback mechanisms, such as interactions between climate, vegetation and soil properties, into future conditions. All factors are interlinking and there are infinite possibilities when it comes to assessing positive and negative feedback processes. Ensemble runs within models and multiple runs of climate models can be used to produce a range of plausible projections which attempts to capture some of the uncertainty which feedback presents.

9.1.5 Uncertainty propagation

The process whereby uncertainty accumulates throughout the process of climate change prediction and impact assessment has been variously described as a *cascade of uncertainty* or the *uncertainty explosion* (Jones, 2000). This is where the upper and lower limits of projected ranges of uncertainty are applied to impact models and the range of possible impacts becomes too extensive. As the number of initial conditions increases and the range of associated uncertainties increases with these initial values, the more uncertainty will propagate to model outputs. The more model stages that are included, particularly with the introduction of additional uncertain variables or boundary conditions, the larger the uncertainty will be in the final outputs. Mearns *et al.* (2001) describes the cascade of uncertainty when using climate modelling for impact studies and if the relative importance of the various sources of uncertainty is measured in terms of the effect on the final range of possible impacts, then their importance will likely vary from one impact to another (Mearns *et al.*, 2003). An example of uncertainty propagation within climate change modelling is provided by Zapert *et al.* (1998). Research conducted found that the stochastic fluctuations in variables contribute more to uncertainty than the initial state measurements, and that CO_2 concentration and temperature change were the climate variables more likely to experience uncertainty magnification. Within this research, the error and uncertainty sources for modelling changes in hydrological extremes in the Severn Uplands, as

discussed throughout Section 9.1 are illustrated in Figure 9.1. Uncertainty at any stage of the modelling process will propagate to affect the final output results; changes in hydrological extremes.

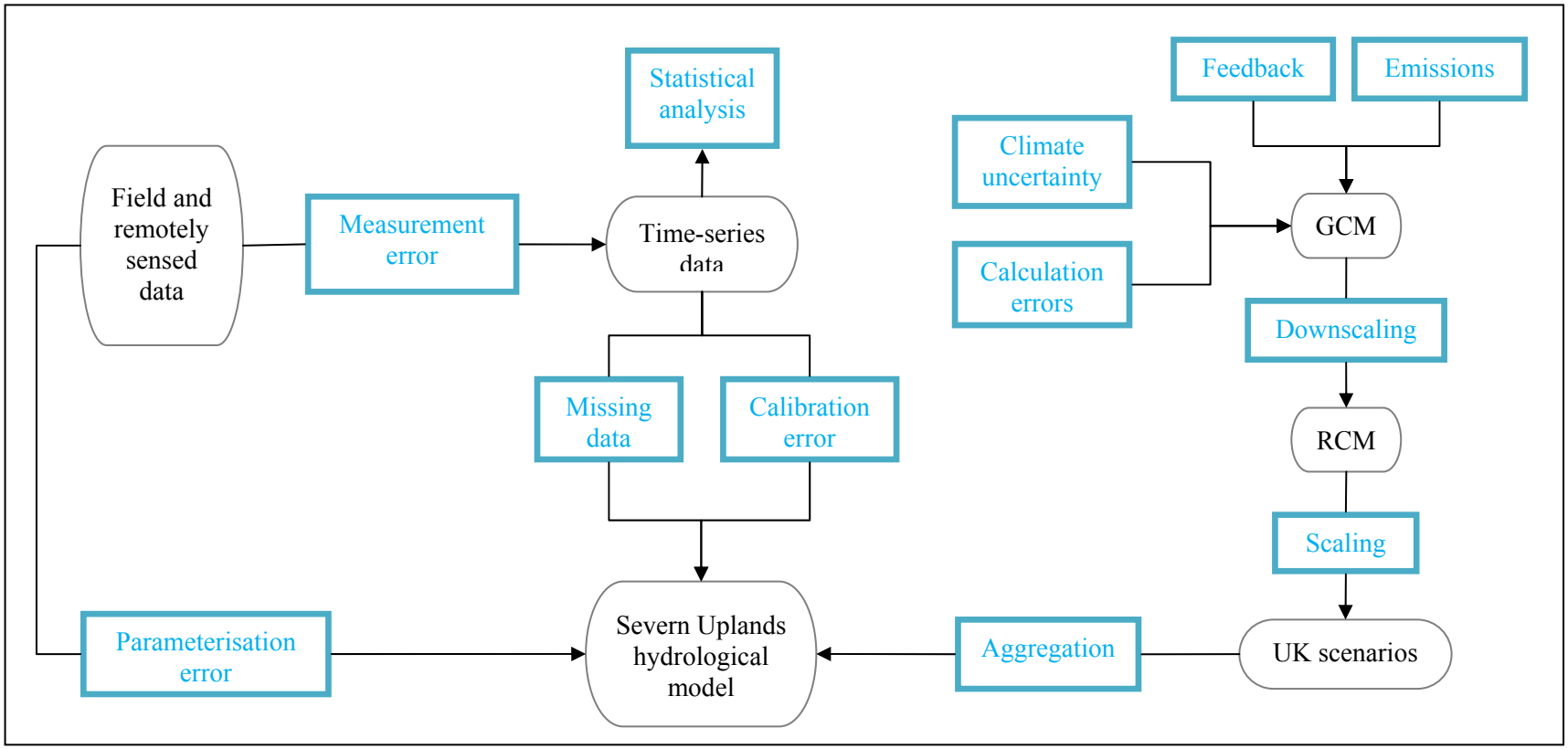

Figure 9.1 Sources of error and uncertainty in modelling the hydrology and climate of the Severn Uplands

9.2 LIMITATIONS AND IMPROVEMENTS

Research undertaken was site specific and all results refer directly to hydrological extreme changes in the Severn Uplands catchment. Consequently, results are interpreted on a local scale, as it is hard to extrapolate results beyond the local area because both climate and physical catchment conditions will differ elsewhere. Similar results might be expected at other upland sites in the UK where climate and environmental conditions are similar. However, each hydrological catchment is unique and has distinctive process interactions. Therefore, any extrapolations should be made with caution. As with all research, there are several limitations associated with the hydrological modelling of the Severn Uplands and the following suggested improvements could be made.

9.2.1 Hydrological model

Parts of the hydrological modelling were limited for simplicity and due to a lack of available data for accurate parameterisation. Most components of the HEC-HMS model were lumped models with parameters accounted for at the subbasin level (semi-distributed). More sophisticated parameterisation could be adopted where all components are modelled on an entirely distributed basis. However, simple hydrological models often outperform the more complex ones, and using simple lumped data inputs can be just as accurate in predicting flows. This was illustrated by the gauge-radar comparison research in Chapter 7. Therefore, a key question to pose is 'are more detailed hydrological models necessary?' If all model components were distributed at a fine spatial resolution processing time would increase, and more uncertainty in the input data would enhance error propagation to model outputs. Alternatively, a different hydrological model may increase accuracy without requiring extensive parameterisation and would provide a comparison to HEC-HMS outputs. A UK-built hydrological model which could directly utilise Nimrod radar rainfall data would be ideal. However, the advantage of HEC-HMS is that its freeware, which appeals to a wide user base, and is compatible directly with other HEC modelling suites which eases the transferability of data if undertaking additional research such as hydraulic or reservoir modelling. Different hydrological models might give different absolute magnitudes for the changes in flow under future conditions, but the broad direction and range of change is likely to be robust (Arnell, 2004).

9.2.2 Climate change projections

Numerous projections in climate change have been developed and applying outputs of changes in predicted climate variables to hydrological modelling has many limitations. In reality, percentage changes in precipitation and temperature under the UKCIP02 scenarios would not occur in such a structured way; a more smooth transition would be apparent at the 5 km² grid boundaries. An improvement to the method could be to focus on using interpolated climate variable surfaces which match the spatial resolution of the radar rainfall data. In addition, regional changes due to topographical and altitudinal effects would have more influence over climate characteristics in the Severn Uplands, particularly precipitation and temperature. Only climate outputs from one RCM have been considered for the purpose of this research. There is a plethora of climate modelling suites which have produced a range of outputs detailing the predicted future climate changes. Ensemble climate predictions would assist in reducing the uncertainty associated with the prediction of future hydrological extremes, and would lead to increased certainty in the probability of outputs. Global and regional climate modelling are not the only methods of projecting hydrological data into the future; a weather generator could be used which bases predictions on statistical distributions. This would also allow a finer temporal resolution to be studied. Cunderlik and Simonovic (2007) used a weather generator to model flood risk under a changing climate and adopted an inverse modelling approach. If the socioeconomic impacts of changes in flow extremes were to be investigated in the Severn Uplands this approach may provide a more suitable method.

9.2.3 Time-series analysis

Two scales of time-series analysis were adopted in this research; firstly, statistical analysis of extremes over a 30-year time period, and secondly, extreme event analysis over a temporal period of two months. Various extreme event-types were selected for time-series analysis in Chapter 5. The extreme distributions investigated were limited to the time period and also the statistical methods applied. Other extreme variables such as river stage and volume could return further information about different aspects of extremes. By using stage measurements instead of the flow, the uncertainties related to stage-flow conversion could be avoided (Romanowicz *et al.*, 2004). Another statistical limitation is that only one

trend detection technique was employed (the Mann-Kendall test); the use of alternative statistical methods to analyse the time-series may yield similar or different results. Yue *et al.* (2002a) compared the power of the Mann-Kendall test to that of the Spearman's rho test for detecting trends in hydrological series and found that both statistical methods produced similar results. Whereas Bonaccorso *et al.* (2005) used the Mann-Kendall and Students *t* tests to analyse trends in rainfall time-series. Results from this study indicated that some gauges had statistically significant trends in annual maxima time-series using one trend detection test, whereas trends went undetected using the alternative test. Statistics can also produce results to a varying degree of significance. For example, research by Robson *et al.* (1998) identified no long-term significant trends in flow extremes, but stated that yearly variations in flood occurrences and annual maxima were found to be statistically significant. However, Pilon and Yue (2002) point out that Robson *et al.*'s (1998) research made no effort to select pristine or stable basins. This is just one example which highlights the need to choose wisely a trend analysis test compatible with the data in question and not to draw too much from the results.

Future time-series predictions were restricted to changes that will occur in November and December, and the UKCIP02 projected changes that were applied to temperature and precipitation changes are limited to a monthly temporal period. These predicted changes were applied uniformly across the months and no account of daily, or even hourly, variability in climate variables was made. Future improvements could look at extreme distributions and how these will change in the future, as well as extreme events during different seasons.

9.3 FURTHER RESEARCH

Additional research possibilities into the future climate of the Severn Uplands are copious. Within this research changes in future extremes relative to one event have been investigated. The recent release of the new climate change scenarios from the UK climate impacts programme provides scope for climate scenario comparison. Aside from the main research topic of hydroclimatology in the Severn Uplands, an additional side project has evolved in relation to obtaining the gridded precipitation datasets. This project has commenced and is investigating the use of computer technology tools to assist geographical science. Possible further research topics are described in more detail below.

9.3.1 Aspects of extremes

Different aspects of future hydrological extremes, such as alternative extreme events and continuous annual simulation of extremes would provide a clearer idea of how extremes are predicted to change on a longer term basis. Aside from extreme high-flows and precipitation events, extreme low flows may become a problem for the River Severn system. Predicted warmer summers will be accompanied by precipitation reductions and water management will require strict monitoring regulations to ensure adequate water supplies are sustained. During low flows the reservoirs in the upper reaches of the Severn Uplands are essential for maintaining regular river flows. Investigating reservoir response to extremes, groundwater modelling and surface water systems are additional aspects of hydrological extremes that could be researched in addition to rainfall-runoff modelling. Further to this, the optimal parameterisation of the HEC-HMS model could be investigated under low-flow extremes to compare to optimum parameters obtained for the high-flow extreme period.

9.3.2 Updated climate scenarios

Throughout the duration of this research the UK climate impacts programme (UKCIP) has been developing an updated set of climate scenarios for the UK. These UKCP09 scenarios (also titled UKCIP08 – renamed due to rebranding to UK climate projections and the postponement of the release date) use the most recent HadGEM1 GCM outputs produced by the Hadley Centre, as briefly described in Chapter 2 (Section 2.3.1) and were released in June 2009. The main improvements to the scenario formulation include a finer RCM spatial (25 km²) and temporal resolution (decadal) where scenarios are based on a large ensemble of Hadley Centre climate model runs. Information from other IPCC climate model runs is also incorporated into the scenario production and a statistical distribution of each emissions scenario is provided as an output. The advancements in science and computing power since the UKCIP02 scenarios release has enabled some of the uncertainties associated with climate modelling to be more accurately quantified (Jenkins *et al.*, 2009). To further the research of predicted climate change impacts on future river flows it would be interesting to see how results from hydrological modelling of extreme future flows using the UKCP09 scenarios differ to those generated using the UKCIP02 scenarios for the Severn Uplands.

9.3.3 Workflow

Hydrologists continually require distributed models to use increasingly large amounts of spatial data. Modelling capabilities have developed simultaneously with advancements in computing processing power, data collection and data distribution though media such as the Internet (Whiteaker *at al.*, 2006). One development which has allowed these advances to be applied to external fields such as geography is the concept of workflow systems and *grid* computing. The composition of workflow is such that an enabling technology can distribute components and compile them into an end-to-end executable process. Workflow allows for the synthesis of large amounts of complexly structured data and enables intricate applications to be made simple for the user. This aims at appealing to a wider audience as it is unnecessary for the end user to understand the complex underlying structure of the workflow. Due to the high computing power required by many workflow systems, grid computing has emerged as a key enabling infrastructure for a wide range of disciplines in science and engineering. Grid provides a solution to the requirement for high-processing capabilities by supplying fundamental mechanisms for resource discovery, management and sharing. This gives scientists tremendous connectivity across traditional organisations and encourages cross-disciplinary, large-scale research (Gil *et al.*, 2004). Grid provides more than just computing power as it allows many resources to be assembled on demand to solve large problems. “grid workflows” consist of a number of components and are interconnected in a dynamic and flexible way to give the appearance of a single application (Abramson *et al.*, 2005).

Information technology frameworks are used to streamline hydrological modelling processes. Many hydrological researchers create their own workflow systems for processing large quantities of data by generating batch files to save time and complete mundane repetitive tasks. Some research involves creating a system whereby an executable program is the required outcome, published for general public use to aid research in that specific subject area. Given the data issues of size and model compatibility encountered with the radar data, as detailed in chapter 3, an additional research element was founded. In addition to the research presented here, work has been ongoing for the development of a workflow system to aid the processing of Nimrod radar images for hydrological model integration. The research on climate change in the Severn Uplands has provided a case study application for the School of Electronics and Computer Science (ECS) at the University of Southampton to create workflow systems which combat data problems in the

applied disciplines such as Geography. The final workflow will aim to process radar data into a number of compatible files for a range of hydrological models, but for now, research is focusing on radar use with HEC-HMS.

Some research has been undertaken using the HEC modelling suite as a workflow applicator. Robayo *et al.* (2004) and Whiteaker *et al.* (2006) used a workflow system which automatically executes both HEC-HMS and HEC-RAS and geospatially integrates them into a GIS to produce flood inundation maps. This application, called "Map-to-map", starts with rainfall radar images, which then go through hydrologic and hydraulic modelling procedures and finish by creating spatial outputs in a GIS. Knebl *et al.* (2005) applied the Map-to-map tool, using NEXRAD rainfall imagery with HEC-HMS and HEC-RAS, to monitor hydrological model performance at a regional level in the San Antonia river basin, Texas. To date, no research has been conducted into using the HEC-HMS model with UK-based rainfall radar imagery. Developing a workflow that would exploit this could be extremely beneficial to hydrologists in the UK, as both the radar images and models are freely available to download from the internet (subject to licence agreements). Ongoing collaboration with ECS will continue to develop these applied workflow systems using hydrometeorology as the pioneering application.

9.3.4 Alternative catchments

One final suggestion for further research would be to apply methods used in this research within the Severn Uplands to other catchment locations. Of particular interest would be to use the radar rainfall data in an upland area where the rain gauge network is sparse but there are adequate flow records to assess hydrological model accuracy. Future predictions would be modelled using the UKCP09 scenarios.

9.4 SUMMARY

To summarise, research conducted has provided a comprehensive analysis of changes in extremes and climate variability for the Severn Uplands over the last 30 years and an insight into future extremes for winter events has been analysed using a hydrological model and UK climate change scenarios. This chapter has attempted to provide a

qualitative analysis of the error and uncertainty associated with the procedures undertaken. Quantitative analysis of future hydrological extremes for a winter event was provided in Chapter 8. Limitations have been discussed and improvements suggested along with ideas for furthering research in hydrological extremes of the Severn Uplands and in similar upland catchments.

Generally, the GIS community has shown little regard for issues of uncertainty and spatio-temporal variability apart from geometric precision. This is not because of computational problems, but because market forces have determined that many GIS applications need not address these issues (Burrough, 2001). The spatial distribution and characteristics of hydrological extremes are becoming increasingly important in terms of flood inundation and flood risk mapping. Consequently, to accurately address the spatiality of climate change impacts on hydrological extremes it is essential to quantify associated uncertainty surrounding predictions. If research is to be made more accessible to a variety of users through the construction of simple workflow systems, then uncertainty will need to be incorporated into these models.

CHAPTER 10

Conclusions

The overall aim of this research was to determine how hydrological extremes within a climate sensitive catchment have changed over recent years and how they are likely to be affected under future conditions given current climate change predictions. The Severn Uplands was selected as a relatively rural site where hydro-climate interactions are particularly responsive, especially in the mountainous upper reaches of the catchment. Time-series analysis of precipitation and flow across the catchment revealed some trends in hydrological extremes over the last 30 years. Significant trends in the precipitation record indicated increases in winter and autumn precipitation and decreases in summer precipitation. Trends show spring precipitation has increased in the Vyrnwy catchment but decreased in the main Severn basin. No obvious patterns were concluded from monthly precipitation analysis. Flow time-series exhibited increasing trends in winter and decreasing trends in spring. Additionally, the monthly analysis revealed a general catchment increase in July flows. Time-series analysis of climate variability in the Severn Uplands indicated some correlation of increasing air temperature, SST and a reduction in snow cover with precipitation and flow extremes. Extremes were found to be linked to certain weather types and largely influenced by the NAO. Changes may be attributable to a recent shift in climate variability of the Severn Uplands, particularly given the changes in extremes relative to snow cover and temperature change. This is likely to be explained by underlying global temperature increases. Other influential factors which are likely to have affected flow regimes are physical catchment changes, in particular soil desiccation and evapotranspiration, which are linked to temperature changes and minor alterations in land use.

To investigate possible future changes in hydrological extremes for the Severn Uplands the HEC-HMS hydrological model was parameterised to simulate conditions within the catchment. An extreme event was modelled and the effects of using different precipitation inputs were quantified. No increase in flow prediction accuracy was apparent when using gauge-corrected radar data compared to the precipitation gauge catchment network, despite an increase in prediction accuracy when correcting raw radar imagery locally using the mean field bias from an interpolated gauge precipitation surface. Despite this, both data inputs were altered under future climates to investigate the uncertainty propagation of using different data inputs.

UK climate scenario projections of temperature and precipitation were used to force the hydrological model to predict future changes in flow extremes. This was achieved at event-level, where an extreme hydrological event was used as the baseline and predictions were made for changes in wintertime flows. The model predicted an increase in extreme flows (peak flow and outflow volume) over the course of the 21st century. These flow increases were as much as 8% by the 2020s, 18% by the 2050s and 30% by the 2080s. Discrepancies were recorded between outputs relative to the precipitation inputs used to drive the hydrological model. This highlighted the importance of ensemble simulations to reduce uncertainty and the inability to conclude too much from the findings at a detailed applications scale.

This research has provided an insight into hydrological extremes and climate variability within the Severn Uplands. The development of methods and research ideas is plentiful, with further research to strengthen findings envisaged. As with the majority of UK upland river basins, the Severn Uplands was found to be a complex system with intricate interactions between climate and hydrology. The major drawback of predicting future environments is that the climate is a chaotic phenomenon and feedback is infinite and largely unpredictable. Much speculation can be inferred, but essentially the future remains unknown. By investigating past trends, processes and interactions can be understood more accurately, and the past provides a good starting point for predicting the future; trends in the Severn Uplands hydrological extremes and climate shifts may be set to continue. One such future environment was described by the Severn catchment flood management plan (Environment Agency, 2008) indicating a possible shift towards a Mediterranean climate within the Severn catchment. French wine companies have already bought land within the catchment in anticipation of climatic problems in Eastern France. A shift in climate would

provide the possibility of increased planting of Mediterranean trees and if climate aridity should drastically reduce then commercial olive production may be a viable option. This is where science meets adaptation. Developing knowledge of hydroclimate systems through scientific processes aids the ability to make informed decisions about how the environment will respond under envisaged future climate systems. Successful management of predicted changes comes with successful mitigation and the ability to adapt to a changing world.

References

Abdul, O.I., Burn, D.H., 2006. Trends and variability in the hydrological regime of the Mackenzie River Basin. *Journal of Hydrology* **319** 282-294

Abramson, D., Kommineni, J., McGregor, J.L., Katzfey, J., 2005. An atmospheric sciences workflow and its implementation with web services. *Future Generation Computer Systems* **21** 69-78

Adamowski, K., Bougadis, J., 2003. Detection of trends in annual extreme rainfall. *Hydrological Processes* **17** 3547-3560

Agnew, M.D., Palutikof, J.P., 2000. GIS-based construction of baseline climatologies for the Mediterranean using terrain variables. *Climate Research* **14** 115-127

Ahrens, S.R., Maidment, D.R., 1999. Flood forecasting for the Buffalo Bayou using CRWR-PrePro and HEC-HMS. Center for research in water resources, Austin, Texas. CRWR online report 99-6 available at http://www.crwr.utexas.edu/online.html (accessed November 2006)

Alexander, L.V., Jones, P.D., 2001. Updated precipitation series for the UK and discussion of recent extremes. *Atmospheric Science Letters* **1** 142-150

Amengual, A., Romero, R., Gómez, M., Martin, A., Alonso, S., 2007. A hydrometeorological modelling study of a flash-flood event over Catalonia, Spain. *Journal of Hydrometeorology* **8** 282-303

Anagnoustou, E.N., Krejewski, W.F., 1999. Uncertainty quantification of mean-areal radar-rainfall estimates. *Journal of Atmospheric and Oceanic Technology* **16** 206-215

Anderson, M.L., Chen, Z.-Q., Kavvas, M.L., Feldman, A., 2002. Couple HEC-HMS with atmospheric models for prediction of watershed runoff. *Journal of Hydrologic Engineering*, doi: 10.1061/(ASCE)1084-0699(2002)7:4 312-318

Andrieu, H., Creutin, J.D., Delrieu, G., Faure, D., 1997. Use of a weather radar for the hydrology of a mountainous area. Part I: radar measurement interpretation. *Journal of Hydrology* **193** 1-25

Apaydin, H., Sonmez, F.K., Yildirim, Y.E., 2004. Spatial interpolation techniques for climate data in the GAP region in Turkey. *Climate Research* **28** 31-40

Arnell, N.W., 1999. The effect of climate change on hydrological regimes in Europe: a continental perspective. *Global Environmental Change* **9** 5-23

Arnell, N.W., 2003a. Relative effects of multi-decadal climatic variability and changes in the mean and variability of climate due to global warming: future streamflows in Britain. *Journal of Hydrology* **270** 195-213

Arnell, N.W., 2003b. Effects of IPCC SRES emissions scenarios on river runoff: a global perspective. *Hydrology and Earth System Sciences* **7** (5) 619-641

Arnell, N.W., 2004. Climate change and global water resources: SRES emissions and socioeconomic scenarios. *Global Environmental Change* **14** 31-52

Arnell, N.W., Jones, R.G., 2003. Climate change scenarios from a regional climate model: Estimating change in runoff in southern Africa. *Journal of Geophysical* Research **108** (16) 4519

Arnell, N.W., Osborn, T., 2006. *Interfacing climate and impacts models in integrated assessment modelling.* Technical Report 52, Tyndall Centre for Climate Change Research, 63pp

Arnell, N.W., Reynard, N.S., 1996. The effects of climate change due to global warming on river flows in Great Britain. *Journal of Hydrology* **183** 397-424

ASCE, 1996. *Hydrology Handbook*. 2nd Edition, American Society of Civil Engineers, New York

Atkinson, P.M., Lloyd, C.D., 1998. Mapping precipitation in Switzerland with ordinary and indicator kriging. *Journal of Geographic Information and Decision Analysis* **2** (2) 65-76

Aziz, O.I.A., Burn, D., 2006. Trends and variability in the hydrological regime of the Mackenzie River Basin. *Journal of Hydrology* **319** 282-294

Bacchi, B., Kottegoda, D.P., 1995. Identification and calibration of spatial correlation patterns of rainfall. *Journal of Hydrology* **165** 311-348

Bailey, R.A., 1981. Forecasting for floods in the river Severn catchment. *Journal of the Institution of Water Engineers and Scientists* **35** 168-178

Ball, J.E., Luk, K.C., 1998. Modelling spatial variability of rainfall over a catchment. *Journal of Hydrologic Engineering* **3** (2) 122-130

Bell, V.A., Kay, A.L., Jones, R.G., Moore, R.J., 2007. Development of a high resolution grid-based river flow model for use with regional climate model output. *Hydrological Earth System Sciences* **11** (1) 532-549

Bell, V.A., Moore, R.J., 1998. A grid-based distributed flood forecasting model with weather radar data: Part 1 Formulation. *Hydrology and Earth Systems Sciences* **2** 265-281

Bell, V.A., Moore, R.J., 1998. A grid-based distributed flood forecasting model with weather radar data: Part 2 Case studies. *Hydrology and Earth Systems Sciences* **2** 283-298

Benner, T.C., 1999. Central England temperatures: long-term variability and teleconnections. *International Journal of Climatology* **19** 391-403

Beven, K.J., 1989. Changing ideas in hydrology – the case of physically-based models. *Journal of Hydrology* **105** 157-172

Beven, K.J., 1993. Prophecy, reality and uncertainty in distributed hydrological modelling. *Advances in Water Resources Research* **16** 41-51

Beven, K.J., 2001. *Rainfall-Runoff Modelling: The Primer.* John Wiley & Sons LTD, England, 360pp

Beven, K.J., 2003. Riverine flooding in a warmer Britain. *The Geographical Journal* **159** (2) 157-161

Beven, K.J., Binley, A.M., 1992. The future of distributed models: model calibration and uncertainty prediction. *Hydrological Processes* **6** 279-298

Blazkova, S., Beven, K.J., 2004,.Flood frequency estimation by continuous simulation of subcatchment rainfalls and discharges with the aim of improving dam safety assessment in a large basin in the Czech Republic. *Journal of Hydrology* **292** 153-172

Bonaccorso, B., Cancelliere, A., Rossi, G., 2005. Detecting trends of extreme rainfall series in Sicily. *Advances in Geosciences* **2** 7-11

Borga, M., 2002. Accuracy of radar rainfall estimated for streamflow simulation. *Journal of Hydrology* **267** 26-39

Borga, M., Anagnostou, E.N., Frank, E., 2000. On the use of real-time radar rainfall estimates for flood prediction in mountainous basins. *Journal of Geophysical Research* **105** 2269-2280

Bower, D., Hannah, D.M., McGregor, G.R., 2004. Techniques for assessing the climate sensitivity of river flow regimes. *Hydrological Processes* **18** 2515-2543

Bradley, A.A., Kruger, A., 1998. Recalibration of hydrologic models for use with WSR-88D precipitation estimates. Preprints, Special Symposium on Hydrology, 78th Annual AMS Conference, American Meteorology Society, Boston. Online at http://citeseerx.ist.psu.edu/viewdoc/summary?doi=10.1.1.40.4340 (accessed June 2006)

Bradley, A.A., Peters-Lidard, C., Nelson, B.R., Smith, J.A., Young, C.B., 2002. Raingage network design using NEXRAD precipitation estimates. *Journal of American Water Resources Association* **38** (5) 1-15

Brandt, C., Robinson, M., Finch, J.W., 2004. Anatomy of a catchment: the relation of physical attributes of the Plynlimon catchments to variations in hydrology and water status. *Hydrology and Earth Systems Sciences* **8** (3) 345-354

Brohan, P., Kennedy, J.J., Harris, I., Tett, S.F.B., Jones, P.D., 2006. Uncertainty estimates in regional and global observed temperature changes: a new dataset from 1850. *Journal of Geophysical Research* **111**: D12106, doi:10.1029/2005JD006548

Brown, J.D. and Damery, S.D., 2002. Managing flood risk in the UK: towards an integration of social and technical perspectives. *Trans Inst Br Geogr* **27** 412-426

Brunetti, M., Buffoni, L., Maugeri, M., Nanni, T., 2000. Precipitation intensity trends in northern Italy. *International Journal of Climatology* **20** 1027-1031

Buffoni, L., Maugeri, M., Nanni, T., 1999. Precipitation in Italy from 1833 to 1996. *Theoretical Applied Climatology* **63** 33-40

Bürger, C.M., Kolditz, O., Fowler, H.J., Blenkinsop, S., 2007. Future climate scenarios and rainfall-runoff modelling in the Upper Gallego catchment (Spain). *Environmental Pollution* **148** 842-854

Burn, D.H., Climatic influences on streamflow timing in the headwaters of the Mackenzie River Basin. *Journal of Hydrology* **352** 225-238

Burn, D.H., Hag Elnur, M.A., 2002. Detection of hydrologic trend and variability. *Journal of Hydrology* 255 **107**-122

Burrough, P.A., 2001. GIS and geostatistics: essential partners for spatial analysis. *Environmental and Ecological Statistics* **8** 361-377

Butts, M.B., Payne, J.T., Kristensen, M., Madsen, H., 2004. An evaluation of the impact of model structure on hydrological modelling uncertainty for streamflow simulation. *Journal of Hydrology* **298** 242-266

Cameron, D., 2007. Flow, frequency, and uncertainty estimation for an extreme historical flood event in the Highlands of Scotland. *Hydrological Processes* **21** 1460-1470

Cameron, D., Beven, K, Naden, P., 2000, Flood frequency estimation by continuous simulation under climate change (with uncertainty). *Hydrology and Earth Systems Sciences* **4** (3) 393-405

CEH Wallingford, 2005. 54014 – Severn at Abermule: Elevation. Spatial catchment information, online at http://www.nwl.ac.uk/ih/nrfa/spatialinfo/Elevation/elevation054014.html (accessed November 2007)

Charley, W.J., 1988. *The estimation of rainfall for flood forecasting using radar and rain gage data*. Technical Paper. US Army Corps of Engineers, Davis, CA. 12pp

Christensen, J.H., B. Hewitson, A. Busuioc, A. Chen, X. Gao, I. Held, R. Jones, R.K. Kolli, W.-T. Kwon, R. Laprise, V. Magaña Rueda, L. Mearns, C.G. Menéndez, J. Räisänen, A. Rinke, A. Sarr and P. Whetton, 2007: Regional Climate Projections. In: *Climate Change 2007: The Physical Science Basis. Contribution of Working Group I to the Fourth Assessment Report of the Intergovernmental Panel on Climate Change* [Solomon, S., D. Qin, M. Manning, Z. Chen, M. Marquis, K.B. Averyt, M. Tignor and H.L. Miller (eds.)]. Cambridge University Press, Cambridge, United Kingdom and New York, NY, USA.

Clark, C.O., 1945. Storage and the unit hydrograph. *Trans. Am. Soc. Civil Engrs* **110** 1419-1488

Cole, S.J., Moore, R.J., 2008. Hydrological modelling using rain gauge- and radar-based estimators of areal rainfall. *Journal of Hydrology* **358** 159-181

Collier, C.G., Fox, N.I., 2003. Assessing the flooding susceptibility of river catchments to extreme rainfall in the United Kingdom. *Intl. J. River Basin Management* **1** (3) 1-11

Collier, C.G., Fox, N.I., Hand, W.H., 2002. *Extreme rainfall and flood event recognition*. R&D Technical Report FD2201, DEFRA 61pp

Cowan, W. L., 1956. Estimating hydraulic roughness coefficients. *Agricultural Engineering* **37** 473-475

Cranston M.D., Black A.R., 2006. Flood warning and the use of weather radar in Scotland: a study of flood events in the Ruchill Water catchment. *Meteorological Applications* **13** 43–52.

Creutin, J.D., Andrieu, H., Faure, D., 1997. Use of a weather radar for the hydrology of a mountainous area. Part II: radar measurement validation. *Journal of Hydrology* **193** 26-44

Creutin, J.D., Obled, C., 1982. Objective analysis and mapping techniques for rainfall fields: an objective comparison. *Water Resources Research* **18** (2) 413-431

Crowley, T.J., 2000. Causes of climate change of the last 1000 years. *Science* **289** (5477) 270-277

Culshaw, M.G., Nathanail, C.P., Leeks, G.J.L., Alker, S., Bridge, D., Duffy, T., Fowler, D., Packman, J.C., Sewtnam, R., Wadsworth, R., and Wyatt, B., 2006. The role of web-based environmental information in urban planning – the environmental information systems for planners. *Science of the Total Environment* **360** 233-345

Cunderlik, J.M., Simonovic, S.P., 2004. *Calibration, verification and sensitivity analysis of the HEC-HMS hydrologic model.* CFCAS project: assessment of water resources risk and vulnerability to changing climate conditions. Project report IV. 113pp

Cunderlik, J.M., Simonovic, S.P., 2005. Hydrological extremes in a south-western Ontario river basin under future climate conditions. *Hydrological Sciences* **50** (4) 361-654

Cunderlik, J.M., Simonovic, S.P., 2007. Inverse flood risk modelling under changing climatic conditions. *Hydrological Processes* **21** 563-577.

Curtis, D.C., Clyde, B.S., 1999. Comparing spatial distributions of rainfall derived from rain gages and radar. NEXRAIN Corporation. Online at http://www.onerain.com/includes/pdf/whitepaper/Spatial_Dist_of_Rainfall.pdf (accessed December 2007)

Dahmen, E.R., Hall, M.J., 1990. *Screening of hydrological data: tests for stationarity and relative consistency.* Publication 49, International Institute for Land Reclamation and Improvement, The Netherlands, 58pp

Dale, M., 2005. Impact of climate change on UK flooding and future predictions. *Proceedings of the Institute of Civil Engineers, Water Management* **158** 135-140

De Bruijn, E.I.F., Brandsma, T., 2000. Rainfall prediction for a flooding event in Ireland caused by the remnants of Hurricane Charley. *Journal of Hydrology* **239** 148-161

DEFRA, 2001a. *National Appraisal of Assets at Risk from Flooding and Coastal Erosion, including the potential impact of climate change: Final Report*. Halcrow, Swindon, 61pp.

DEFRA, 2001b. *To what degree can the October/November 2000 flood events be attributed to climate change?* FD2304 Technical Report, CEH Wallingford and the Met Office, 116pp

DEFRA, 2004. *Review of UK climate change indicators*. Contract EPG /1/1/158, Centre for Ecology and Hydrology, Penicuik 74pp

Dessai, S., Hulme, M., 2001. Climatic implications of revised IPCC emission scenarios, the Kyoto Protocol and quantification of uncertainties. *Integrated Assessment* **21** 158-170

Dinku, T., Anagnostou, E.N., 2002. Improving radar-based estimation of rainfall over complex terrain. *Journal of Applied Meteorology* **41** 1163-1178

Diskin, M.H., Simon, F., 1977. A procedure for the selection of objective functions fro hydrologic simulation models. *Journal of Hydrology* **34** 129-149

Doerr, S.H., Shakesby, R.A., Walsh, R.P.D., 2000. Soil water repellency: its causes, characteristics and hydrogeomorphological significance. *Earth Sciences Review* **51** 33–65

Donigian, A.S. , 2002. Watershed Model Calibration and Validation: The HSPF Experience. WEF-National TMDL Science and Policy 2002, November 13-16, 2002. Phoenix AZ, WEF-2002 Specialty Conference Proceedings

Douville, H., F., Chauvin, F., Planton, S., Royer, J-F., Salas-Melia, D., Tyteca, S., 2002. Sensitivity of the hydrological cycle to increasing amounts of greenhouse gases and aerosols. *Climate Dynamics* **20** 45-68

Earls, J., Dixon, B., 2007. Spatial interpolation of rainfall data using ArgGIS: A comparative study. ESRI professional papers. Online at http://gis.esri.co,/library/userconf/proc07/papers/abstracts/a1451.html (accessed November 2008)

Ekström, M., Fowler, H.J., Kilsby, C.G., Jones, P.D., 2005. New estimates of future changes in extreme rainfall across the UK using regional climate model integrations: 2. Future estimates and use in impact studies. *Journal of Hydrology* **300** 234-251

Engen-Skaugen, T., Roald, L. A., Beldring, S., Førland, E. J., Tveito, O. E., Engeland, K., Benestad, R., 2005. *Climate change impacts on water balance in Norway Climate*. Report 1/2005, Norwegian Meteorological Institute, Oslo

Environment Agency, 2000. *Local Environment Agency Plan: Severn Uplands Environmental Overview*. 88pp

Environment Agency, 2001. *Lesson learned: Autumn 2000 floods.* Environment Agency, Bristol. 58pp

Environment Agency, 2001b. Flooding in Wales – October/November 2000. Environment Agency Wales, online at http://www.environment-agency.gov.uk/research/library/publications/33885.aspx (accessed March 2009)

Environment Agency, 2002a. *River Severn Regulation – fact sheet 2: Llyn Clywedog and Lake Vyrnwy* 2pp

Environment Agency, 2002b. *River Severn strategy: a flood management strategy for the Severn Corridor.* Scoping Report, Project Ref. No. 5009. Solihull, West Midlands. 41pp

Environment Agency, 2003. *Impact of climate change on flood flows in river catchments – interim report.* R&D Technical Report W5-032/TR, Bristol, 49pp

Environment Agency, 2005. *River Severn catchment flood management plan (CFMP)*. Final Report 510, Solihull. 156pp + 270pp appendices

Environment Agency, 2006. *Fluvial Severn flood risk management strategy.* Final Report 5009, Solihull. 400pp + 446pp appendices

Environment Agency, 2008. *Severn catchment flood management plan – draft report.* Online at http://www.environment-agency.gov.uk/regions/midlands/1192964/2048445/?version=1&lang=_e (accessed September 2008)

Environment Agency, 2009a. *Flood in England: a national assessment of flood risk*. Environment Agency, Bristol, UK, 33pp

Environment Agency, 2009b. *Investing for the future. Flood and coastal risk management in England; a long-term investment strategy*. Environment Agency, Bristol, UK, 23pp

Evans, E., Ashley, R., Hall, J., Penning-Roswell, E., Saul, A., Sayers, P., Thorne, C., Watkinson, A., 2004. *Foresight. Future Flooding. Scientific Summary: Volume I – Future risks and their drivers.* Office of Science and Technology, London. 366pp

Feldman, A.D. 2000. *Hydrologic Modelling System HEC-HMS Technical Reference Manual.* US Army Corps of Engineers. Davis, California, USA.

Fleming, M., Neary, V., 2004. Continuous hydrologic modelling study with the Hydrologic Modelling System. *J. Hydrological Engineering* **9** (3) 175-183

Fohrer, N., Eckhardt, K., Frede, H.G., 2001. Hydrologic response to land use changes on the catchment scale. *Physical Chemical Earth* **26** (7-8) 577-582

Foody, G.M., Cgoneim, E.M., Arnell, N.W., 2004. Predicting locations sensitive to flash flooding in an arid environment. *Journal of Hydrology* **292** 48-58

Ford, D.T., Hamilton, D., 1996. *Computer models for water excess management*. Larry W. Mays ed., Water resources handbook. Mc-Graw Hill, New York, 1568pp

Fowler, H.J., Ekstrom, M., Kilsby, C.G., Jones, P.D., 2005. New estimates of future changes in extreme rainfall across the UK using regional climate model integrations: 1. Assessment of control climate. *Journal of Hydrology* **300** 212-233

Fowler, H.J., Hennessy, K.J., 1995. Potential impacts of global warming on the frequency and magnitude of heavy precipitation. *Natural Hazards* **11** (3) 283-303

Fowler, H.J., Kilsby, C.G., 2002. Precipitation and the North Atlantic Oscillation: a study of climatic variability in northern England. *International Journal of Climatology* **22** 843-866

Fowler, H.J., Kilsby, C.G., 2003. A regional frequency analysis of United Kingdom extreme rainfall from 1964 to 2000. *International Journal of Climatology* **23** (11) 1313-1334

Fowler, H.J., Kilsby, C.G., 2007. Using regional climate model data to simulated historical and future river flows in northwest England. *Climatic Change* **80** (3-4) 337-367

Fowler, H.J., Kilsby, C.G., Stunell, J., 2006. Modelling the impacts of projected future climate change on water resources in northwest England. *Hydrological Earth Systems Science* **11** 1115-1126

Fraedrich, K.,1994. An ENSO impact on Europe? *Tellus A* **46** 541-552

Fraedrich, K., Müller, K., 1992. Climate anomalies in Europe associated with ENSO extremes. International *Journal of Climatology* **12** 25-31

Frei, C., Schär, C., 2001. Detection probability of trends in rare event: theory and application to heavy precipitation in the Alpine region. *Journal of Climate* **14** 1568-1584

Frei, C., Davies, H.C., Gurtz, J., Schär, C., 2000. Climate dynamics and extreme precipitation and flood events in Central Europe. *Integrated Assessment* **1** 281-299

Gan, T.Y., Dlamini, E.M., Biftu, G.F., 1997. Effects of model complexity and structure, data quality, and objective functions on hydrologic modelling. *Journal of Hydrology* **192** 81-103

Garcia, A., Sainz, A., Revilla, J.A., Alvarez, C., Juanes, J.A., Puente, A., 2008. Surface water resources assessment in scarcely gauged basins in the north of Spain. *Journal of Hydrology* **356** 312-326

Garcia, B.I.L., Sentelhas, P.C., Tapia, L., Sparovek, G., 2006. Filling in missing rainfall data in the Andes region of Venezuela, based on a cluster analysis approach. *Rev. Bra. Agrometerologica* **14** (2) 225-233

Giannoni, F., Smith, J.A., Zhang, Y., Roth, G., 2003. Hydrologic modelling of extreme floods using radar rainfall estimates. *Advances in Water Resources* **26** 195-203

Gil, Y., Deelman, E., Blythe, J., Kesselman, C., Tangmunarunkit, H., 2004. Artificial intelligence and Grids: workflow planning and beyond. *IEEE Intelligent Systems* 26-33 Online at www.computer.org/intelligent (accessed December 2007)

Gillett, N.P., Graf, H.F., Osborn, T.J., 2003. Cimate change and the North Atlanitc Oscilliation In *The North Atlantic Oscillation: climatic significance and environmental impact*. Hurrell, J.W., Kushnir, Y., Ottersen, G., Visheck, M. (Eds.) Geophysical Monograph Series 134

Gilman, K., 2002. *Modelling the effect of land use change in the upper Severn catchment on flood levels downstream.* English Nature Research Reports, No. 471, Peterborough, 104pp

Giorgi, F., Whetton, P., Jones, R., Christensen, J., Mearns, L., Hewitson, L., Von Storch, H., Francisco, R., Jack, C, 2001. Emerging patterns of simulated regional climatic changes for the 21st century due to anthropogenic forcing. *Geophysical Research Letters* **28** 3317-3320

Gjertsen, U., Salek, M., Michelson, D.B., 2004. Gauge adjustment of radar-based precipitation estimated in Europe. Proceedings of ERAD 2002, *ERAD Publication Series*, 7-11

Gleick, P.H., 1989. Climate change, hydrology and water resources. *Reviews of Geophysics* **27** 329-344

Golding, B.W., 1998. Nimrod: A system for generating automated very short range forecasts. *Meteorological Applications* ***5*** 1-16

Golding, B.W., 2000. Quantitative precipitation forecasting in the UK. *Journal of Hydrology* **239** 286-305

Goodall, J., Maidment., D.R., 2002. *The Geostatistical Analyst Exercise*. GIS Course Material. The University of Texas, Austin, USA

Goovaerts, P., 1997. *Geostatistics for natural resources evaluation*. Oxford University Press, New York, 483pp

Goovaerts, P., 2000. Geostatistical approaches for incorporating elevation into the spatial interpolation of rainfall. *Journal of Hydrology* **228** 113-129

Gordon, C., Cooper, C., Senior, C.A., Banks, H., Gregory, J.A., Johns, T.C., Mitchell, J.F.B., Wood, R.A., 2000. The simulation of SST, sea ice extents and ocean heat transports in a version of the Hadley Centre coupled model without flux adjustments. *Climate Dynamics* **16** 147-168

Gregory, K.J., 1997. *Fluvial Geomorphology of Great Britain*. Geological Conservation Review Series (13) 348pp

Groisman, P.Y., Knight, R.W., Easterling, D.R., Karl, T.R., Hegerl, G.C., Razuvaev, V.N., 2005. Trends in intense precipitation in the climate record. *Journal of Climate* **18** 1326-1350

Guan, H., Wilson, J.L., 2005. Geostatistical mapping of mountainous precipitation incorporating autosearched effects of terrain and climate characteristics. *Journal of Hydrometeorology* **6** 1018-1031

Gumbel, E.J., 1941. The return period of flood flows. *The Annals of Mathematical Statistics* **12** (2) 163-190

Gutowski, W.J., Decker, S.G., Donovan, R.A, Pan, Z., Arritt, R.W., Tackle, E.S., 2003. Temporal-spatial scales of observed precipitation in central US climate. *Journal of Climate* **16** 3841-3847

Haberlandt, U., 2007. Geostatistical interpolation of houly precipitation from rain gauges and radar for a large-scale extreme rainfall event. *Journal of Hydrology* **332** 144-157

Hall, G., Cratchley, R., 2006. Coupling of MODFLOW with the MM5 mesoscale meteorological model for real-time input of high resolution rainfall patterns in a mountainous area. Conference paper from MODFLOW and more 2006: Managing ground water systems. 5pp

Hamed, K.H., 2008. Trend detection in hydrologic data: the Mann-Kendall trend test under the scaling hypothesis. *Journal of Hydrology* **349** 350-363

Hamed, K.H., 2008. Discussion of "To prewhiten or not to prewhiten in trend analysis?". *Hydrological Sciences Journal* **53** (3) 667-668

Hamed, K.H., Rao, A.R., 1998. A modified Mann-Kendall trend test for autocorrelated data. *Journal of Hydrology* **204** 182-196

Hand, W.H., Fox, N.I., Collier, C.G., 2004. A study of twentieth century extreme rainfall events in the United Kingdom with implications for forecasting. *Meteorological Applications* **11** 15-31

Hanna, E., Mayes, J., Beswick, M., Prior, J., Wood, L., 2008. An analysis of the extreme rainfall in Yorkshire, June 2007, and its rarity. *Weather* **63** (9) 253-260

Hannaford, J., Marsh, T.J., 2007. High-flow and flood trends in a network of undisturbed catchments in the UK. *International Journal of Climatology* **10** 1325-1338

Hardman-Mountford, N.J., Leaper, N., 2003. Marine indicators of climate change. In *Review of UK climate change indicators*. Eds Wilkins, D. and Wright, K. Contract EPG 1/1/158 DEFRA. Online at http://www.ecn.ac.uk/iccuk/reportjune2003/Jan2004.htm (accessed November 2007)

Haria, A.H., Shand, P., 2004. Evidence for deep sub-surface flow routing in forested upland Wales: implications for containment transport and stream flow generation. *Hydrology and Earth Systems Sciences* **8** (3) 334-344

Harrison, D.L., Driscoll, S.J., Kitchen, M., 2000. Improving precipitation estimated from weather radar using quality control and correction techniques. *Meteorological Applications* **6** 135-144

Harrison, G. 1997. *Manual Severn Basin Version 3 (Autumn 2005)*. Regional monitoring and forecasting duty officers, Environment Agency Region

Harrison, J., Winterbottom, S., Johnson, R., 2001. *Climate change and changing patterns of snowfall in Scotland.* The Scottish Executive Central Research, Edinburgh, 48pp

Hay, L.E., Clark, M.P., Wilby, R.L., Gutowski Jr.., W.J., Leavesley, G.H., Pan, Z., Arritt, R.W., Takle, E.S., 2002. Use of regional climate model output for hydrologic simulations. *Journal of Hydrometeorology* **3** 571–590.

Haylock, M.,R., Goodess, C.M., 2004. Interannual variability of European extreme winter rainfall and links with mean large-scale circulation. *International Journal of Climatology* **24** 759-776

Haylock, M.R., Nichols, N., 2000. Trends in extreme rainfall indices for an updated high quality dataset for Australia, 1910-1998. *International Journal of Climatology* **20** (13) 1533-1541

Haylock, M.R., Peterson, T.C., Alves, L.M., Ambrizzi, T., Anunciação, Baez, J., Barros, V.R., Berlato, M.A., Bidegain, M., Coronel, G., Corradi, V., Garcia, V.J., Grimm, A.M., Karoly, D., J.A., Marengo, Marino, M.B., Moncunill, D.F., Nechet, D., Quintana, J., Rebello, E., Rusticucci, M., Santos, J.L., Trebejo, I., Vincent, L.A., 2006. Trends in total and extreme South American rainfall in 1960-2000 and links with sea surface temperatures. *Journal of Climate* **19** 1490-1512

Hegerl, G.C., F. W. Zwiers, P. Braconnot, N.P. Gillett, Y. Luo, J.A. Marengo Orsini, N. Nicholls, J.E. Penner and P.A. Stott, 2007: Understanding and Attributing Climate Change. In: *Climate Change 2007: The Physical Science Basis. Contribution of Working Group I to the Fourth Assessment Report of the Intergovernmental Panel on Climate Change* [Solomon, S., D. Qin, M. Manning, Z. Chen, M. Marquis, K.B. Averyt, M. Tignor and H.L. Miller (eds.)]. Cambridge University Press, Cambridge, United Kingdom and New York, NY, USA.

Hennessy, K.J., Gregory, J.M., Mitchell, J.F.B., 1997. Changes in daily precipitation under enhanced greenhouse conditions. *Climate Dynamics* **13** 667-680

Higgs, G. 1987 Environmental change and hydrological response: flooding in the upper Severn catchment. In Gregory, K.J., Lewin, J. and Thornes, J. B.,eds. *Palaeohydrology in practice*. Wiley, Chichester, UK

Hoblit, B.C., Curtis, D.C, 2001. Integrating radar rainfall estimates with digital elevation models and land use data to create an accurate hydrologic model. Conference paper, Floodplain Management Association Spring 2001 Conference, San Diego, California, 13-16 March, 9pp

Hossain, F., Anagnostou, E.N., Dinku, T., Borga, M., 2004. Hydrological model sensitivity to parameter and radar rainfall estimation uncertainty. *Hydrological Processes* **18** 3277-3291

Hough, M.N., Jones, R.J.A., 1997. The United Kingdom Meteorological Office rainfall and evaporation calculation system: MORECS version 2.0 – an overview. *Hydrology and Earth Systems Sciences* **1** (2) 227-239

Howe, G.M., Slaymaker, H.O., Harding, D.M., 1967. Some aspects of the flood hydrology of the upper catchments of the Severn and Wye. *Transactions Institute of British Geographers* **41** 33-58

Howe, J., White, I., 2002. The Geography of the Autumn 2000 Floods in England and Wales. *Geography* **87** (2) 116-124

HR Wallingford, 2005. *Guidance on National Flood Risk Assessments*. Department for International Development, Wallingford, 18pp.

Hudson, J.A., Gilman, K., 1993. Long-term variability in the water balances of the Plynlimon catchments. *Journal of Hydrology* **143** 355–380.

Hulme, M., Jenkins, G.J., 1998. *Climate change scenarios for the UK. Scientific Report, UKCIP Technical Report No. 1*. Climatic Research Unit, Norwich, p80

Hulme, M., Jenkins, G.L, Lu, X., Turnpenny, J.R., Mitchell, T.D., Jones, R.G., Lowe, J., Murphy, J.M., Hasell, D., Boorma, P., McDonald, R., Hill, S., 2002. *Climate change scenarios for the United Kingdom: The UKCIP02 scientific report.* Tyndall Centre for Climate Change Research, School of Environmental Sciences, University of East Anglia, Norwich, UK. 120pp

Hundecha, Y., Bárdossy, A., 2005. Trends in daily precipitation and temperature extremes across western Germany in the second half of the 20th century. *International Journal of Climatology* **25** 1189-1202

Huntingford, C., Jones, R.G., Prudhomme, C., Lamb, R., Gash, J.H.C., Jones, D.A., 2003. Regional climate model predictions of extreme rainfall for a changing climate. *Quarterly Journal of the Royal Meteorological* Society **129** 1607-1621

IPCC, 2001. *Climate Change 2001: Impacts, Adaptations and Vulnerability*. (McCarthy *et al*. Eds). Cambridge University Press, Cambridge. 1032pp

Jackson, B.M., Wheater, H.S., McIntyre, N.R., Chell, J., Francis, O.J., Frogbrook, Z., Marshall, M., Reynolds, B., Solloway, I., 2008. The impact of upland management on flooding: insights from a multiscale experimental and modelling programme. *Journal of Flood Risk Management* **1** 71-80

Jakeman, A.J., Hornberger, G.M., 1993. How much complexity is warranted in a rainfall-runoff model? *Water Resources Research* **29** (8) 2637-2649

Jenkins, G.J., Murphy, J.M., Sexton, D.M.H., Lowe, J.A., Jones, P., Kilsby, C.G., 2009. *UK climate projections briefing report.* Met Office, Hadley Centre, Exeter, UK.

Jenkinson, A.F., Collison, F.P., 1977. *An initial climatology of gales over the North Sea.* Meteorological Office Branch Memorandum No.62, 18pp

Jiang, T., Su, B., Hartmann, H., 2007. Temporal and spatial trends of precipitation and river flow in the Yangtze River Basin, 1961-2000. *Geomorphology* **85** 143-154

Jones, P., 2006. CRU Information Sheet No. 1: Global Temperature Record. Climatic Research Unit, Online at http://www.cru.uea.ac.uk/cru/info/warming/ (Accessed February 2007)

Jones, P.D., Conway, D., Briffa, K.R., 1997. Precipitation variability and drought. In *Climates of the British Isles: present, past and future* (M Hulme and E Barrow, Eds), Routledge, London, 197-219

Jones, P.D., Hulme, M., 1997. The changing temperature of 'Central England'. In *Climates of the British Isles: present, past and future* (M Hulme and E Barrow, Eds), Routledge, London, 173-196

Jones, P.D., Reid, P.A., 2001. Assessing future changes in extreme precipitation over Britain using Regional Climate Model integrations. *International Journal of Climatology* **21** 1337-1356

Jones, R.G., Murphy, J.M., Noguer, M., 1995. Simulation of climate change over Europe using a nested regional climate model I: assessment of control climate, including sensitivity to location of lateral boundaries. *Journal of the Royal Meteorological Society* **121** 1413-1449

Jones, R.N., 2000. Managing uncertainty in climate change projections – issues for impact assessment. *Climatic Change* **45** 403-419

Karl, T.R., Knight, R.W., 1998. Secular trends of precipitation amount, frequency and intensity in the United States. *Bulletin of the American Meteorological Society* **76** (2) 231-241

Karl, T.R., Knight, R.W., Plummer, N., 1995. Trends in high-frequency climate variability in the twentieth century. *Nature* **377** 217-220

Katz, R.W., 2002. Techniques for estimating uncertainty in climate change scenarios and impact studies. *Climate Research* **20** 167-185

Kay, A.L., Davies, H.N., 2008. Calculating potential evaporation from climate model data: a source of uncertainty for hydrological climate change impacts. *Journal of Hydrology* **358** 221-239

Kay, A.L., Reynard, N.S., Jones, R.G., 2006. RCM rainfall for UK flood frequency estimation. I. Method and validation. *Journal of Hydrology* **318** 151-162

Kay, A.L., Jones, R.G., Reynard, N.S., 2006. RCM rainfall for UK flood frequency estimation. II. Climate change results. *Journal of Hydrology* **318** 163-172

Kelly, R.E.J., Atkinson, P.M., 1999. Modelling and efficient mapping of snow cover in the UK for remote sensing validation. In *Advances in remote sensing and GIS analysis*. Eds. Atkinson, P.M. and Tate, N.J. John Wiley & Sons Ltd pp75-94

Kendall, M.G., 1975. *Rank Correlation Methods*. Griffin, London, England.

Kent, K.M., 1973. *A method for estimating volume and rate or runoff in small watersheds.* SCS-TP 149, USDA-SCS, Washington DC, USA

Khatibi, R., 2005. Treating uncertainty in flood forecasting – development, uptake and barriers, Proceedings of the 2nd ACTIF Workshop in Delft. Online at http://www.actif-ec.net/Workshop2/papers/ACTIF_S1_05.pdf (accessed May 2009)

Kilsby, C.G., Jones, P.D., Burton, A., Ford, A.C., Fowler, H.J., Harpham, C., James, P., Smith, A., Wilby, R.L., 2007. A daily weather generator for use in climate change studies. *Environmental Modelling and Software* **22** 1705-1719

Kirby, C., Newson, M.D., Gilman, K., 1991. *Plynlimon research: the first two decades.* Report 109, Institute of Hydrology, Wallingford, UK

Kitchen, M., and Blackall, R.M., 1992. Representativeness errors in comparisons between radar and gauge measurements of rainfall. *Journal of Hydrology* **134** 13-33

Kitchen, M., Brown, R., and Davies, A. G., 1994. Real-time correction of weather radar data for the effects of bright band, range and orographic growth in widespread precipitation. *Quarterly Journal of the Royal Meteorological Society* **120** 1231-1254.

Knapp, B., 1986. *Systematic Geography*. London, 540pp

Knebl, M.R., Yang, Z.L., Hutchinson, K., Maidment, D.R., 2005. Regional scale flood modelling using NEXRAD rainfall, GIS and HEC-HMS/RAS: a case study for the San Antonio River Basin Summer 2002 storm event. *Journal of Environmental Management* **75** 325-336

Kothyari, U.C., Singh, V.P., 1996. Rainfall and temperature trends in India. *Hydrological Processes* **10** 357-372

Koutsoyiannis, D., Baloutsos, G., 2000. Analysis of a long record of annual maximum rainfall in Athens, Greece, and design rainfall influences. *Natural Hazards* **22** (1) 29-48

Krajewski W.F., 1987. Cokriging radar-rainfall and rain gauge data. *Journal of Geophysical Research* **92** 9571–9580

Krajewski, W.F., Smith, J.A., 2002. Radar hydrology: rainfall estimation. *Advances in Water Resources* **25** 1387-1394

Kundzewicz, Z.W., Graczyk, D., Maurer, T., Pinskwar, I., Radziejewski, M., Svensson, C., Szwed, M., 2005. Trend detection in river flow series: 1. Annual maximum flow. *Hydrological Sciences Journal* **50** 797-810

Kyriakidis, P.C., Kim, J., Miller, N.L., 2001. Geostatistical mapping of precipitation from rain gauge data using atmospheric and terrain characteristics. *Journal of Applied Meteorology* **40** 1855-1877

Lamb, H.H., 1950. Types and spells of weather around the year in the British Isles: annual trends, seasonal structure of the year, singularities. *The Quarterly Journal of the Royal Meteorological Society* **76** (330) 393-429

Lamb, H.H., 1972. *British Isles weather types and a register of daily sequence of circulation patterns, 1861-1971.* Geophysical Memorandum No. 110, Meteorological Office, London, UK.

Lamb, R., 2001. *To what extent can the October/November 2000 floods be attributed to climate change?* DEFRA FD2304 Final Report, 40pp

Lane, S.N., 2008. Climate change and the summer 2007 floods in the UK. *Geography* **93** 91-97

Lane, S.N., Tayefi, V., Reid, S.C., Hardy, R.J., 2007. Interactions between sediment delivery, channel change, climate change and flood risk in a temperate upland environment. *Earth Surface Processes and Landforms* **32** 429-446

Lang, H., Grebner, D., 1998. On large-scale topographic control of the spatial distribution of extreme precipitation and floods in high mountain regions. In *Hydrology, Water Resources and Ecology in Headwaters, Proceedings of the HeadWater'98 Conference*, Merano, Italy, IASH Publication **248** 47-50

Lawrimore, J.H., Halpert, M.S., Bell, G.D., Menne, M.J., Lyon, B., Schnell, R.C., Gleason, K.L., Easterling, D.R., Thiaw, W., Wright, W.J., Heim, R.R., Robinson, D.A., Alexander, L., 2001. Climate Assessment for 2000. *Bulletin of the American Meteorological Society* **82** (6) S1-S55pp

Lázaro, R., Rodrigo, F.S, Gutiérrez, L., Domingo, F., Puigdefábregas, J., 2001. Analysis of a 30-year rainfall record (1967-1997) in semi-arid SE Spain for implications on vegetation. *Journal of Arid Environments* **48** 376-395

Leander, R., Buishand, T.A., 2007. Resampling of regional climate model output for the simulation of extreme river flows. *Journal of Hydrology* **332** 487-496

Legates, D.R., McCabe, G.J., 1999. Evaluating the use of Goodness of Fit measures in hydrologic and hydroclimatic model validation. *Water Resources Research* **35** 233–241

Lewis, H.W., Harrison, D.L., 2007. Assessment of radar data quality in upland catchments. *Meteorological Applications* **14** 441-445

Lloyd, C.D., 2005. Assessing the effect of integrating elevation data into the estimation of monthly precipitation in Great Britain. *Journal of Hydrology* **308** 128-150

Longley, P.A., Goodchild, M.F., Maguire, D.J., Rhind, D.W., 2005. *Geographic Information Systems and Science (2nd Edition)*. John Wiley and Sons, Chichester, UK. 517pp

Madsen, H., Butts, M.B., Khu, S.T., Liong, S.Y., 2000. Data assimilation in rainfall-runoff forecasting. Conference paper, Hydroinformatics 2000: 4th International Conference on Hydroinformatics, Iowa, 23-27 July, 8pp

Maidment, 1993. *Handbook of Hydrology*. McGraw-Hill, USA, 1424pp

Mandapaka, P.V., Krajewski, W.F., Ciach, G.J., Villarini, G., Smith, J.A., 2008. Estimation of radar-rainfall error spatial correlation. *Advance in Water Resources* doi: 10.1016/j.advwatres.2008.08.014

Mann, H.B., 1945. Non-parametric tests against trend. *Econometrica* **13** 245-259

Marc, V., Robinson, M., 2007. The long-term water balance (1972-2004) of upland forestry and grassland at Plynlimon, mid-Wales. *Hydrology Earth Systems Sciences* **11** (1) 44-60

Marsh, T.J., 1999a. River flows in northwest and southeast Britain. In *Indicators of climate change in the UK*. Editors Cannell, M.G.R, Palutikof, J.P., Sparks, T.H. Departments for the Environment, Transport and the Regions, pp 16-17

Marsh, T.J., 1999b. Frequency of low and high river flows in northwest and southeast Britain. In *Indicators of climate change in the UK*. Editors Cannell, M.G.R, Palutikof, J.P., Sparks, T.H. Departments for the Environment, Transport and the Regions, pp 18-19

Marsh, T.J., 2002. Capitalising on river flow data to meet changing national needs – a UK perspective. *Flow Measurement and Instrumentation* **13** 291-298

Marsh, T.J., Dale, M., 2002. The UK floods of 2000-2001: a hydrometeorlogical appraisal. *CIWEM* **16** 180-188

Marsh, T.J., Hannaford, J., 2007. *The summer 2007 floods in England and Wales – a hydrological appraisal.* Centre for Ecology & Hydrology, 32pp

Marshall. M.R., Francis, O.J., Frogbrook, Z.L., Jackson, B.M., McIntyre, N., Reynolds, B., Solloway, I., Wheater, H.S., Chell, J., 2009. The impact of upland land management on flooding: results from an improved pasture hillslope. *Hydrological Processes* **23** 464-475

Marshall, M.R., Frogbrook, Z.L., Francis, O.J., Reynolds, B., McIntyre, N., Wheater, H.S., 2006. The impact of upland land management on flooding: preliminary results from a multi-scale experimental programme. BHS 9th National Hydrology Symposium, Durham.

Matalas, N.C., Langbei, W.B., 1962. Information content of the mean. *Journal of Geophysical Research* **67** (9) 3441-3448

McColl, C., Aggett, G., 2007. Land-use forecasting and hydrologic model integration for improved land-use decision support. *Journal of Environmental Management* **84** 494-512

McCuen, R.H., 1973. The role of sensitivity analysis in hydrologic modeling. *Journal of Hydrology* **18** 37-53

McCuen, R.H., Knightm Z., Cutter, G., 2006. Evaluation of the Nash-Sutcliffe Efficiency Index. *Journal of Hydrologic Engineering* 597-602

McElwain, L., Sweeney, J., 2003. Climate change in Ireland – recent trends in temperature and precipitation. *Irish Geography* **36** (2) 97-111

McEwen, L.J., 1989 Extreme rainfall and its implications for flood frequency: a case study of the Middle River tweed Basin, Scotland. *Transactions of the Institute of British Geographers* **14** (3) 287-298

McGuffie, K., Henderson-Sellers, A., Holbrook, N., Kothavala, Z., Balachova, O., Hoekstra, J., 1999. Assessing simulations of daily temperature and precipitation variability with global climate models for present and enhanced greenhouse climates. *International Journal of Climatology* **19** 1-26

McSweeney, 2007. Daily Rainfall Variability at Point and Areal Scales: Evaluating Simulations of Present and Future Climate. PhD thesis. Online at http://www.cru.uea.ac.uk/cru/pubs/thesis/2007-mcsweeney/ (accessed August 2008)

MCRM , 2005. Midlands catchment runoff model parameter values. Sourced directly from Environment Agency, Shrewsbury, UK

Mearns, L.O., Giorgi, F., Whetton, D., Pabon, M., Hulme, M., 2003. Guidelines for use of climate scenarios developed from regional climate model experiments. 38pp Online at http://ipcc-data.org/guidelines/dgm_no1_v1_10-2003.pdf (accessed May 2009)

Meehl, G.A., Karl, T., Easterling, D.R., Changnon, S., Pielke, R., Changnon, D., Evans, J., Groisman, P.Y., Knutson, T.R., Kunkel, K.E., Mearns, L.O., Parmesan, C., Pulwarty, R., Root, T., Syleves, R.T., Whetton, P., Zwiers, F., 2000. An introduction to trends in extreme weather and climate events: observations, socioeconomic impacts, terrestrial ecological impacts and model projections. *Bulletin of the American Meteorological Society* **81** (3) 431-416

Melching, C.S., 1995. Reliability estimation. In Singh, V.P. (ed.) *Computer Models of Watershed Hydrology.* Water Resources Publications, Highlands Ranch, Colorado, USA 1144pp

Met Office, 2007. Online at http://www.metoffice.gov.uk/climate/uk/averages/19712000/areal/england_nw_&_wales_n.html (accessed January 2008)

Michaelides, D., 2008. School of Electronics and Computer Science, University of Southampton, Southampton, UK

Miller, W.A., Cunge, J.A., 1975. Simplified equations of unsteady flow, in Mahmood K., Yevjevich V., eds., *Unsteady flow in open channels: Volume 1.* Water Resources Publications, Colorado State University, Fort Collins, Colorado 183-249

Militino, A.F., Palacios, M.B., Ugate, M.D., 2001. Robust predictions of rainfall in Navarre, Spain. In *Eds*. Monestiez, P., Allard, D., Froideveaux, R., (2001) *GeoENV III: Geostatistics for environmental applications.* Proceedings of the 3rd European conference on geostatistics for environmental applications. Avignon, France, 540pp

Miller, N.L., 2003. *California climate change, hydrologic responses and flood forecasting*. International expert meeting on urban flood management, World Trade Centre, Rotterdam, The Netherlands, 11pp

Modarres, R., Silva, V.P.R., 2007. Rainfall trends in arid and semi-arid regions of Iran. *Journal of Arid Environments* **70** 344-355

Molnár, P., Ramírez, J.A., 2001. Recent trends in precipitation and streamflow in the Rio Puerco Basin. *Journal of Climate* **14** (10) 2317-2328

Montero-Martinez, G., Kostinski, A.B., Shaw, R.A., Garcia-Garcia, F., 2009. Do all raindrops fall at terminal speed? *Geophysical Research Letters* **36** L11818 doi:10.1029/2008GL037111

Moore, R.J., 2002. Aspects of uncertainty, reliability and risk in flood forecasting systems incorporating weather radar. In Bogardi, J.J. and Kundzewicz, Z.W. (eds.) *Risk, reliability, uncertainty and robustness of water resources systems.* Cambridge University Press, pp30-40

Moore, R.J. and Bell, V.A. 2000. *Comparison of rainfall-runoff models for flood forecasting. Part 1: Literature review of models.* Report prepared by the Institute of Hydrology, Environment Agency R&D Technical Report W241, 94pp

Moore, R.J., Bell, V.A., Jones, D.A. 2005. Forecasting for flood warning. *C. R. Geoscience* **337** 203-217

Moore, R.J., Jones, A.E., Jones, D.A., Black, K.B., Bell, V.A., 2004. Weather radar for flood forecasting: some UK experiences. Sixth international symposium on hydrological applications of weather radar, Melbourne, Australia

Muleta, M.K., Nicklow, J.W., 2005. Sensitivity and uncertainty analysis couple with automatic calibration fro a distributed watershed model. *Journal of Hydrology* **306** 127-145

Murphy, C., Charlton, R., 2006. Climate change impact on catchment hydrology and water resources for selected catchments in Ireland. National hydrology seminar paper 2006, online at http://www.ria.ie/committees/pdfs/hydrology/Murphy.pdf (accessed January 2008)

Nadarajah, S., Shiau, J.T., 2005. Analysis of extreme flood events for the Pachang River, Taiwan. *Water Resources Management **19*** (4) 363-374

Nakicenovic, N., Alcamo, J., Davis, G., Vries, B., Fenhann, J., Gaffin, S., Gregory, K., Grübler, A., Jung, T.Y., Kram, T., Rovere, E.L., Michaelis, L., Mori, S., Morita, T., Pepper, W., Pitcher, H., Price, L., Riahi, K., Roehrl, A., Rogner, H-H., Sankovski, A., Schlesinger, M., Shukla, P., Smith, S., Swart, R., Rooijen, A., Victor, N., Dadi, Z., 2000. *Special Report on Emissions Scenarios: A Special Report of Working Group III of the Intergovernmental Panel on Climate Change*. Cambridge University Press, Cambridge, U.K., 599pp. Online at http://www.grida.no/climate/ipcc/emission/index.htm (accessed January 2008)

Nash, J.E., Sutcliffe, J.V., 1970. River flow forecasting through conceptual models. Part 1: A discussion of principles. *Journal of Hydrology* **10** (3) 282-290

Neary, V.S., Habib, E., Felming, M., 2004. Hydrologic modelling with NEXRAD precipitation in Middle Tennessee. *Journal of Hydrologic Engineering*, Sept/Oct 2004 339-349

Ness, L., Neal, C., Davies, T.D., Reynolds, B., 2004. Impacts of the North Atlantic Oscillation on stream water chemistry in mid-Wales. *Hydrology and Earth Systems Sciences* **8** (3) 409-421

Newson, M., 1997. *Land, Water and Development: Sustainable Management of River Basin Systems.* 2nd Edition. Routledge, London, New York.

NOAA, 2007. ISAT software. Online at http://www.csc.noaa.gov/crs/cwq/isat.html (accessed June 2007).

O'Connell, E., Ewen, J., O'Donnell, G., Quinn, P., 2007. Is there a link between agricultural land-use management and flooding? *Hydrological Earth Systems Science* **11** 69-107

Önöz, B. and Bayazit, M., 2003. The power of statistical tests for trend detection. *Turkish Journal of Engineering and Environmental Sciences*, **27** 247-251

Osborn, T.J., 2000. *Climatic Research Unit: Information Sheet No. 11: North Atlantic Oscillation.* Climatic Research Unit, online at http://www.cru.uea.ac.uk/cru/info/nao/ (accessed February 2007)

Osborn, T.J., Hulme, M., 2002. Evidence for trends in heavy rainfall events over the UK. *Philosophical Transactions of the Royal Society Land A* **360** 1313-1325

Osborn, T.J., Hulme, M., Jones, P.S., Basnett, T.A., 2000. Observed trends in the daily intensity of United Kingdom precipitation. *International Journal of Climatology* **20** 347-364

Pal, I., Al-Tabbaa, A., 2009. Trends in seasonal precipitation extremes – an indicator of climate change' in Kerala, India. *Journal of Hydrology* **367** 62-69

Parker, D.E., Legg, T.P., Folland C.K., 1992. A new daily Central England Temperature Series, 1772-1991. *International Journal of Climatology* **12** 317-342

Paz, A., R., Collischonn, W., Risso, A., Mendes, C.A.B., 2008. Errors in river lengths derived from raster digital elevation models. *Computers and Geosciences* **34** 1584-1596

Pelling, M., 2004. Visions of Risk: A Review of International Indicators of Disaster Risk and its Management. A report for the ISDR Inter-Agency Task force on Disaster Reduction – Working Group 3: Risk, Vulnerability and Disaster Impact Assessment. United Nations development programme. Online at http://www.preventionweb.net/files/2549_visionsofrisk.pdf (accessed June 2009)

Perrin, C., Michel, C., Andreassian, V., 2001. Does the large number of parameters enhance model performance? Comparative assessment of common catchment model structures on 429 catchments. *Journal of Hydrology* **242** 275-301

Perry, M., 2006. *A spatial analysis of trends in the UK climate since 1914 using grid datasets.* Climate Memorandum No 21, National Climate Information Centre, Met Office, Exeter. 29pp

Perry, M., Hollis, D., 2005. The generation of monthly gridded datasets for a range of climatic variables over the United Kingdom. *International Journal of Climatology* **25** 1041-1054

Peters, J.C., Easton, D.J., 1996. Runoff simulation using radar rainfall data. Technical paper No. 155, Hydrologic Engineering Center, Davis, California, 13pp

Pilling, C.G., Jones, J.A.A., 1999. High resolution climate change scenarios: implications for British runoff. *Hydrological Processes* **13** 2877-2895

Pilling, C.G., Jones, J.A.A., 2002. The impact of future climate change on seasonal discharge, hydrological processes and extreme flows in the Upper Wye experimental catchment, mid-Wales. *Hydrological Processes* **16** 1201-1213

Pilon, P.J., Yue, S., 2002. Detecting climate-related trends in streamflow data. *Water Science and Technology* **45** (8) 89-104

Pitt, M., 2008. *The Pitt Review: Learning lessons from the 2007 floods*. 505pp Online at http://www.cabinetoffice.gov.uk/thepittreview/final_report.aspx (accessed Sept 2008)

Post, P., Truilja, V., Tuulik, J., 2002. Clirculation weather types and their influence on temperature and precipitation in Estonia. *Boreal Environment Research* **7** 281-289

Prudhomme, C., Jakob, D., Svensson, C., 2003. Uncertainty and climate change impact on the flood regime of small catchments. *Journal of Hydrology* **277** 1-23

Prudhomme, C., Reed, D.W., 1999. Mapping extreme rainfall in a mountainous region using geostatistical techniques: a case study in Scotland. International *Journal of Climatology* **19** 1337-1356

Prudhomme, C., Reynard, N., Crooks, S., 2002. Downscaling of global climate models for flood frequency analysis: where are we now? *Hydrological Processes* **16** 1137-1150

Qian, W., Lin, X., 2005. Regional trends in recent precipitation indices in China. *Meteorological Atmospheric Physics* **90** 196-207

Randall, D.A., R.A. Wood, S. Bony, R. Colman, T. Fichefet, J. Fyfe, V. Kattsov, A. Pitman, J. Shukla, J. Srinivasan, R.J. Stouffer, A. Sumi and K.E. Taylor, 2007: Cilmate Models and Their Evaluation. In: Climate Change 2007: The Physical Science Basis. Contribution of Working Group I to the Fourth Assessment Report of the Intergovernmental Panel on Climate Change [Solomon, S., D. Qin, M. Manning, Z. Chen, M. Marquis, K.B. Averyt, M.Tignor and H.L. Miller (eds.)]. Cambridge University Press, Cambridge, United Kingdom and New York, NY, USA.

Rao, P.G., 1993. Climatic changes and trends over a major river basin in India. *Climatic Research* **2** 215-223

Rayner, N.A., Parker, D.E., Horton, E.B., Folland, C.K., Alexander, L.V., Rowell, D.P., Kent, E.C., Kaplan, A., 2003. Global analyses of sea surface temperature, sea ice, and night marine air temperature since the late nineteenth century. *Journal of Geophysical Research* **108** doi:10.1029/2002JD002670

Reed, D.W., Robson, A.J., 1999. *Flood Estimation Handbook Volume 3: Statistical procedures for flood frequency estimation.* Institute of hydrology, Wallingford, UK. 338pp

Reynard, N., Prudhomme, C., Crooks, S., 1999. *Climate change impacts for fluvial flood defence*. Institute of Hydrology report to MAFF.

Reynard, N.S., Prudhomme, C., Crooks, S.M., 2001. The flood characteristics of large UK rivers: potential effects of changing climate and land use. *Climatic Change* **28** 343-359

RHS, 2008. River habitat survey online database at http://www8.geodata.soton.ac.uk/ (accessed September 2008)

Robayo, O., Whiteaker, T., Maidment, D., 2004. Converting a NEXRAD map to a floodplain map. Proceedings of the 2004 AWRA spring conference: GIS and water resources III, American Water Resources Association

Robson, A.J., 2002, Evidence for trends in UK flooding. *Philosophical Transactions of the Royal Society Land A* **360** 1327-1343

Robson, A.J., Jones, T.K., Reed, D.W., Bayliss, A.C., 1998. A study of national trend and variation in UK floods. *International Journal of Climatology* **18** 165-182

Robson, A.J., Reed, D.W., 1996. *Non-stationarity in UK flood series*. Flood Estimation Handbook Note 25, Report to MAFF, Project FD0409. 37pp

Rodionov, S.N., 2006. Use of prewhitening in climate regime shift detection. *Geophysical Research Letters* **33** L12707, doi:10.1029/2006GL025904

Rodrigo, F.S., Esteban-Parra, M.J., Pozo-Vázquez, D., Castro-Díez, Y., 1999. A 500-year precipitation record in Southern Spain. *International Journal of Climatology* **149** 1233-1253

Romanowicz R.J., K. J. Beven, 1998. Dynamic real time predictions of flood inundation probabilities. *IAHS Hydrological Sciences Journal* **43** 181-196.

Romanowicz, R., Beven, K.J., Young, P.C., 2004. Assessing the risk of flooding in real time. Proceedings of ACTIF Conference on Quantification, reduction and dissemination of uncertainty in flood forecasting, Delft, Netherlands, Online at http://www.actif-ec.net/Workshop2/papers/ACTIF _S1_06.pdf (accessed June 2008)

Salinger, M.J., Griffiths, G.M., 2001. Trends in New Zealand daily temperatures and extreme rainfall. *International Journal of Climatology* **21** (12) 1437-1452

Samuels, P., 2004. *Some research needs for river flood forecasting in FP6*. ACTIF report EVK1-CT-2002-80014 5pp

Savin, N.E., White, K.J., 1977. The Durbin-Watson test for serial correlation with extreme sample sizes of many regressors. *Econometrica* **45** (8) 1989-1996

Sayers, P.B., Hall, J.W., Meadowcroft, I.C., 2002. Towards risk-based flood hazard management in the UK. Proceedings of the ICE, *Civil Engineering* **150** 36-42

Schaefer, J.T., 1990. The critical success index as an indicator of warming skill. *Weather and Forecasting* **5** 570-575

Scharffenberg, W.A., Fleming, M.J., 2006. *HEC-HMS User's Manual Version 3.1*. US Army Corps of Engineers, Hydrological Engineering Centre, Davis, California, USA.

Semenov, M.A., 2007. Development of high-resolution UKCIP02-based climate change scenarios in the UK. *Agricultural and Forest Meteorology* **144** 127-138

Semonov, M.A., 2008. Simulation of extreme weather events by a stochastic weather generator. *Climate Research* **35** 203-212

Semenov, M.A., Barrow, E.M., 1997. Use of a stochastic weather generator in the development of climate change scearios. *Climatic Change* **35** 397-414

Semenov, M.A., Brooks, R.J., 1999. Spatial interpolation of the LARS-WG stochastic weather generator in Great Britain. *Climate Research* **11** 137-148

Seo, D.-J., 1998. Real-time estimation of rainfall fields using radar rainfall and rain gauge data. *Journal of Hydrology* **208** 37-52

Seo, D.J., Krajewski, W.F., Bowles, D.S., 1990a. Stochastic interpolation of rainfall data from rain gauges and radar using cokriging 1. Design of experiments. *Water Resources Research* **26** (3) 469-477

Seo, D.J., Krajewski, W.F., Azimi-Zonooz, A., Bowles, D.S., 1990b. Stochastic interpolation of rainfall data from rain gauges and radar using cokriging 2. Results. *Water Resources Research* **26** (5) 915-924

Seo, D.J., Breidenbach, J.P., Johnson, E.R., 1999. Real-time estimation of mean field bias in radar rainfall data. *Journal of Hydrology* **223** 131-147

Sefton, C.E.M., Boorman, D.B., 1997. A regional investigation of climate change impacts on UK streamflows. *Journal of Hydrology* **195** 26-44

Sharma, D., Das, Gupta, A., Babel, M.S., 2007. Spatial disaggregation of bias-corrected GCM precipitation fro improved hydrologic simulation: Ping River Basin, Thailand. *Hydrology and Earth System Sciences Discussions* **4** 35-74

Shorthouse, C., Arnell, N., 1999. The effects of climate variability on spatial characteristics of European river flows. *Physics and Chemistry of the Earth, Part B: Hydrology, Oceans and Atmosphere* **24** (1-2) 7-13

Sibley, A., 2005. Analysis of the heavy orographic rainfall over North Wales, 3 and 4 February 2004. *Weather* **60** (2) 31-36

Sinclair, S., Pegram, G., 2005. Combining radar and rain gauge rainfall estimates using conditional merging. *Atmospheric Science Letters* **6** 19-22

Smith, P.J., Kojiri, T., 2003. Probabilistic short-term distributed flood forecasting. *Annuals of Disaster Prevention Research Institute*, Kyoto University **46**

Sneyers, R., 1990. *On the statistical analysis of series of observations*. WMO technical note 143, Geneva. 143pp

Sneyers, R., 1992. On the use of statistical analysis for objective determination of climate change. *Meteorologische Zeitschrift* **1** 247-256

Starkel, L., 1991. Long-distance correlation of fluvial events in the temperate zone. In Starkel, L., Gregory, K.J. and Thornes, J.B., eds, *Temperate palaeohydrology: fluvial procevves in the temperate zone during the last 15,000 years*. John Wiley, Chichester, UK 473-95.

Steele-Dunne, S., Lynch, P., McGrath, R., Semmler, T., Wang, S., Hanafin, J., Noland, P., 2008. The impacts of climate change on hydrology in Ireland. *Journal of Hydrology* **356** 28-45

Stein, A., Corsten, L.C.A., 1991. Universal kriging and cokriging as a regression procedure. *Biometrics* **47** (2) 575-587

Stein, A., Staritsky, I.G., Bouma, J., Van Eunsbergen, A.C., Bregt, A.K., 1991. Simulation of moisture deficits and areal interpolation by universal cokriging. *Water Resources Research* **8** 1963-1973

Stellman, K.M., Fuelberg, H.F., Garza, R., Mullusky, M., 2001. An examination of radar and rain gauge-derived mean areal precipitation over Georgia watersheds. *American Meteorological Society*. **Feb 2001** 133-144

Sumner, G., 1996. Daily precipitation patterns over Wales: towards a detailed precipitation climatology. *Transactions of the Institute of British Geographers*, New Series **21** (1) 157-176

Sun, X., Mein, R.G., Keenan, T.D., Elliot, J.F., 2000. Flood estimation using radar and rain gauge data. *Journal of Hydrology* **239** 4-18

Suppiah R., Hennessy K.J., 1998. Trends in total rainfall, heavy rain events and number of dry days in Australia, 1910-1990. *International Journal of Climatology* **18** 1141-1164.

Svensson, C., Hannaford, J., Kundzewicz, Z.W., Marsh, T., 2006. Trends in river floods: why is there no clear signal in observations? In Tchigurinskaia, I., Thein, K.N.N., Hubert (Eds.), *Frontiers in Flood Research*, IAHS Publ. 305 pp1-18

Svensson, C., Jakob, D., Reed, D.W., 2002. Diurnal characteristics of heavy precipitation according to weather type at an upland site in Scotland. *International Journal of Climatology* **22** 569-585

Teschl, R., Randeu, W.L., Teschl, F., 2006. Weather radar estimated of rainfall adjusted to rain gauge measurements using neural networks. 2006 International Joint Conference on Neural Networks, Vancouver, Canada 5126-5131

Thom, H.C.S., 1966. *Some methods of climatological analysis*. Technical report No. 81, World Meteorological Organisation, Geneva. 53pp

Tilford, K.A., Sene, K., Chatterton, J.B., and Whitlow, C., 2003. *Flood Forecasting – Real Time Modelling.* Defra/Environment Agency R&D Technical Report W5C-013/5/TR

Timbe, L. and P Willems. 2004. "Uncertainties in Hydrodynamic Flood Simulation." ACTIF workshop on Quantification, Reduction and Dissemination of Uncertainty. November 22-23 2004. Delft, Netherlands, p.1-15.

Trapero, L., Rigo, T., Bech, J., Pineuda, N., Forcadell, D., Franco, M., Sánchez-Diezma, R., 2006. Assessing the uncertainty of quantitative precipitation estimated of the Meteorlogical Sevive of Catalonia weather radar network. Proceedings of ERAD 2006, *ERAD Publication Series*, 217-220

Trenberth, K.E., 1999. Conceptual framework for changes of extremes of the hydrological cycle with climate change. *Climatic Change* **42** 327-339

Trenberth, K.E., P.D. Jones, P. Ambenje, R. Bojariu, D. Easterling, A. Klein Tank, D. Parker, F. Rahimzadeh, J.A. Renwick, M. Rusticucci, B. Soden and P. Zhai, 2007: Observations: Surface and Atmospheric Climate Change. In: *Climate Change 2007: The Physical Science Basis*. Contribution of Working Group I to the Fourth Assessment Report of the Intergovernmental Panel on Climate Change [Solomon, S., D. Qin, M. Manning, Z. Chen, M. Marquis, K.B. Averyt, M. Tignor and H.L. Miller (eds.)]. Cambridge University Press, Cambridge, United Kingdom and New York, NY, USA.

Trigo, R.M., DaCamara, C.C., 2000. Circulation weather types and their influence on the precipitation regime in Portugal. *International Journal of Climatology* **20** 1559-1581

Upton, G.J.G., Rahimi, A.R., 2003. Online detection of errors in tipping-bucked rain gauges. *Journal of Hydrology* **278** 197-212

USACE, 1996. Hydrologic aspects of flood warning preparedness programs. US Army Corps of Engineers, Engineering Technical Letter, ETL 1110-2-540.

USACE, 2000. *HEC-HMS technical reference manual*. Online at http://www.hec.usace.army.mil/software/hec-hms/documentation/CPD-74B_2000Mar.pdf (accessed November 2005)

USACE 2003. *HEC-GeoHMS Version 1.1.* US Army Corps of Engineers, Hydrological Engineering Centre, Davis, California, USA.

USACE 2005. *HEC-DSSVue Version 1.2*. US Army Corps of Engineers, Hydrological Engineering Centre, Davis, California, USA.

USACE 2006. *HEC-HMS Version 3.1*. US Army Corps of Engineers, Hydrological Engineering Centre, Davis, California, USA.

USGS 2002. *Shuttle Radar Topography Mission (SRTM) Elevation Data Set.* Online at http://seamless.usgs.gov (accessed November 2005)

Vehvilainen, B., Cauwenberghs, M.K., Cheze, J-L., Jurczyk, A., Moore, R.J., Olsson, J., Salek, M., Szturc, J., 2004. Evaluation of operational flow forecasting systems that use weather radar. COST717, Working group 1, task 6, available online at http://www.smhi.se/cost717/doc/WDD_01_200408_1.pdf (accessed November 2008)

Vincente-Serrano, S.M., Saz-Sánchez, M.A., Curadrat, J.M., 2003. Comparative analysis of interpolation methods in the middle Ebro Valley (Spain): application to annual precipitation and temperature. *Climate Research* **24** 161-180

Vieux, B.E., 2004. Distributed hydrologic modelling for flood forecasting. GIS and Remote Sensing. In *Hydrology, Water Resources and Environment*. IAHS 289 pp.1-10

Walsh C.L., Kilsby C.G., 2007. Implications of climate change on flow regime affecting Atlantic salmon. *Hydrological Earth Systems Science* **11** 1127-1143

catchment, Cumbria, UK. Hydrol. Earth. Syst. Sci. Wang, S., McGrath, R., Semmler, T., Sweeney, C., Nolan, P., 2006. The impact of climate change on discharge of Suir River catchment (Ireland) under different climate scenarios. *Natural Hazards Earth Systems Science* **6** 387-395

Wang, X.L., Swail, V.R., 2001. Changes of extreme heights in northern hemisphere oceans and related atmospheric circulation regimes. *Journal of Climate* **14** 2204-2221

Weatherhead, E.K., Knox, J.W., de Vries, T.T., Ramsden, S., Gobbons, J., Arnell, N.W., Odoni, N., Hiscock, K., Sandhu, C., Saich, A., Conway, D., Warwick, C., Bharwani, S., Hossell, J., Clemence, B., 2005. *Sustainable water resources: a framework for assessing adaptation options in the rural sector*. Technical Report 44, Tyndall Centre for Climate Change Research, 72pp

Wetherald, R.T., Manabe, S. 2002. Simulation of hydrologic changes associated with global warming. *Journal of Geophysical Research* **107** doi:10.1029/2001JD001195 4379

Wheater, H.S., 2002. Progress in and prospects for fluvial flood modelling. *Phil. Trans.: Mathematical, Phys. and Eng.* Sciences **360** 1409-1431

Wheater, H.S., 2006. Flood hazard and management: a UK perspective. *Phil. Trans. R. Soc. A* **364** 2135-2145

White, W.R., 2001. Water in rivers: flooding. *Proceedings of the Institute of Civil Engineers. Water and Maritime Engineering* **148** (2) 107-118

White, I., Howe, J., 2002. Flooding and role of planning in England and Wales: a critical review. *Journal of Environmental Planning and Management* **45** (5) 735-745

Whiteaker, T., Robayo, O., Maidment, D.R., Obenour, D., 2006. From a NEXRAD rainfall map to a flood inundation map. *Journal of Hydrologic Engineering* **11** (1) 37-45

Wilby, R., 1993. Evidence of ENSO in the synoptic climate of the British Isles since 1880. *Weather* **48** 234-239

Wilby, R.L., 2005. Uncertainty in water resource model parameters used for climate change impact assessment. *Hydrological Process* **19** 3201-3219

Wilby, R.L., Hay, L.E., Gutowski, W.J., Arritt, R.W., Takle, E.S., Pan, Z., Leavesley, G.H., Clark, M.P., 2000. Hydrological responses to dynamically and statistically downscaled climate model output. *Geophysical Research Letter* **27** (8) 1199-1202

Wilby, R.L., Wigley, T.M.L., 1997. Downscaling general circulation model output: a review of methods and limitations. *Progress in Physical Geography* **21** 530-548

Williams, J., 2007. Personal communication. E. Biggs, Southampton.

Wilson, J.W., Brandes, E.A., Radar measurement of rainfall – a summary. *Bulletin on the American Meteorological Society* **60** (9) 1048-1058

Wood, T.R., 1987. The present-day hydrology of the River Severn. In Gregory, K.J., Lavin, J., Thomas, J.B., (Eds.) *Palaeoecology in Practice: A River Basin Analysis*. John Wiley & Sons Ltd, pp79-163

Wood, A.W., Leung, L.R., Sridhar, V., Lettenmaier, D.P., 2004. Hydrologic implications of dynamical and statistical approaches to downscaling climate model outputs. *Climatic Change* **62** 189-216

Xu, C-Y., 1999. From GCMs to river flow: a review of downscaling methods and hydrological modelling approaches. *Progress in Physical Geography* **23** 229-249

Yapo, P.O., Gupta, H.V., Sorooshian, S., 1996. Automatic calibration of conceptual rainfall-runoff models: sensitivity to calibration data. *Journal of Hydrology* **181** 23-48

Yener, M.K., Sorman, A.U., Sorman, A.A., Sensoy, A., Gexgin, T., 2007. Modelling studies with HEC-HMS and runoff scenarios in Yuvacik basin, Turkiye. *River Basin Management*. International Congress on River Basin Management. 621-634

Young, E.F., Holt, J.T., 2007. Prediction and analysis of long-term variability of temperature and salinity in the Irish Sea. *Journal of Geophysical Research* **112** 1-18

Yue, S., Hasino, M., 2003. Long term trends of annual and monthly precipitation in Japan. *Journal of the American Water Resources Association*. **39** (3) 587-596

Yue, S., Pilon, P., Cavadias, G., 2002. Power of Mann-Kendall and Spearman's rho tests for detecting monotonic trends in hydrological time-series. *Journal of Hydrology* **259** 254-271

Yue, S., Pilon, P., Phinney, B., Cavadias, G., 2002. The influence of autocorrelation on the ability to detect trend in hydrological series. *Hydrological Processes* **16** 1807-1829

Yue, S., Wang, C.Y., 2002a. Applicability of prewhitening to eliminate the influence of serial correlation on the Mann-Kendall test. *Water Resources Research* **38** (6) 1-7

Yue, S., Wang, C.Y., 2002b. Regional streamflow trend detection with consideration of both temporal and spatial correlation. *International Journal of Climatology* **22** 933-946

Yue, S., Wang, C.Y., 2004. The Mann-Kendall test modified by effective sample size to detect trend in serially correlation hydrological series. *Water Resources Management* **18** 201-218

Zapert, R., Gaertner, P.S., Filar, J.A., 1998. Uncertainty propagation within an integrated model of climate change. *Energy Economics* **20** 571-598.

Zhang, X., Vincent, L.A., Hogg, W.D., Niitsoo, A., 2000. Temperature and precipitation trends in Canada during the 20th Century. *Atmosphere-Ocean* **38** (3) 395-429

Appendices

APPENDIX 1: DURBIN-WATSON TEST SCORES

Test results for serial correlation using the Durbin-Watson test statistics. Table A1 refers to section 5.2.

Table A1 Durbin-Watson test statistic scores for annual and monthly flow time-series. Bold indicates the presence of serial correlation and italics are inconclusive results, for a sample size of 30 with critical bounds $d_L = 1.35$ and $d_U = 1.49$ for 1 regressor at $\alpha < 0.05$.

	Abermule	Llanyblodwel	Llanymynech	Montford	Rhos-y-Pentref
Annual	2.04	2.41	**1.29**	2.07	1.66
Autumn	1.87	1.7	1.91	2.14	1.98
Winter	1.66	2.47	1.65	1.55	1.94
Spring	1.88	1.9	1.52	*1.34*	*1.44*
Summer	1.77	2.25	1.82	2.15	2.07
Oct	2	1.82	1.66	2.04	2.25
Nov	2.61	2.44	2.49	2.31	2.66
Dec	1.61	*1.38*	**1.29**	1.57	2.02
Jan	2.12	2.23	2.04	2.05	2.41
Feb	2	2.1	1.95	1.97	2.16
Mar	1.6	1.95	1.63	*1.36*	1.59
Apr	2.25	2.35	2.09	2.27	2.29
May	1.68	2.27	2.19	1.98	1.88
Jun	2.03	1.97	1.97	1.87	2.25
Jul	2.55	2.62	1.95	2.11	1.95
Aug	1.71	1.59	1.9	*1.72*	1.92
Sep	1.66	1.54	1.55	*1.45*	*1.44*

APPENDIX 2: CLIMATE VARIABLES CORRELATION MATRICES

The correlation matrices indicate correlation coefficient values between climate variables and hydrological extremes (flow and precipitation) at gauge locations. Table A2 refers to sections 5.4.2, 5.4.3 and 5.4.4.

Table A2 Coefficients of correlation between flow and precipitation extremes and climate variables. *p* value is indicated below the coefficient value. Correlations significant at $\alpha < 0.05$ are indicated in bold. Key to table abbreviations as follows:

Temp	Air temperature
SST	Sea surface temperature
Snow cover	Days of snow cover at more than 50 % of cell
Snow level	Snow depth for Snowdonia
NAO	North Atlantic oscillation
SON	Autumn
DJF	Winter
MAM	Spring
JJA	Summer
Ann	Annual maxima
Ann3	Annual 3-day maximum
Ann7	Annual 7-day maximum
Ann10	Annual 10-day maximum
Ann30	Annual 30-day maximum
Ann90	Annual 90th percentile
Ann95	Annual 95th percentile
Ann97	Annual 97th percentile

Key is the same for *seasonal* frequency, intensity and persistence.

ANNUAL	Intensity	Persistence				Frequency		
	ann	ann3	ann7	ann10	ann30	ann90	ann95	ann97
Temp	0.047	0.403	0.265	0.205	0.223	0.378	0.426	0.249
	0.826	0.051	0.211	0.337	0.295	0.069	0.038	0.24
SST	-0.117	0.31	0.271	0.223	0.237	0.185	0.259	0.066
	0.579	0.131	0.19	0.284	0.255	0.377	0.212	0.753
Snow cover	-0.256	**-0.561**	**-0.439**	-0.361	-0.327	**-0.657**	**-0.655**	**-0.484**
	0.227	**0.004**	**0.032**	0.083	0.119	**0**	**0.001**	**0.017**
Snow level	0.073	**-0.407**	-0.279	-0.197	-0.201	-0.372	**-0.411**	-0.26
	0.73	**0.043**	0.177	0.345	0.336	0.067	**0.041**	0.21
NAO	0.286	0.272	0.124	0.121	0.124	0.26	0.153	0.292
	0.166	0.188	0.556	0.565	0.556	0.21	0.465	0.157

Precipitation gauge:
Cefn Coch

SEASONAL	Frequency											
	aut90	aut95	aut97	win90	win95	win97	spr90	spr95	spr97	sum90	sum95	sum97
SON Temp	-0.171	-0.098	0.066	0.324	0.229	0.165	0.228	0.097	0.095	**-0.408**	-0.296	-0.116
	0.425	0.65	0.758	0.142	0.305	0.464	0.295	0.659	0.665	**0.048**	0.16	0.59
DJF Temp	0.255	0.253	0.248	0.198	-0.05	0.028	0.036	0.009	0.244	0.035	0.015	-0.12
	0.228	0.233	0.243	0.378	0.824	0.903	0.871	0.968	0.262	0.873	0.944	0.577
MAM Temp	0.384	0.335	0.287	-0.211	-0.177	-0.006	0.137	0.072	0.277	0.214	0.042	0.003
	0.064	0.11	0.174	0.345	0.43	0.98	0.534	0.745	0.202	0.315	0.847	0.991
JJA Temp	-0.093	-0.014	0.153	0.298	0.199	0.168	0.015	-0.191	-0.076	-0.394	-0.233	-0.047
	0.666	0.948	0.476	0.178	0.373	0.454	0.946	0.383	0.731	0.057	0.273	0.827
DJF SST	-0.093	-0.073	-0.062	0.142	0.105	0.139	0.016	-0.064	0.254	-0.268	-0.273	-0.258
	0.657	0.729	0.768	0.518	0.633	0.527	0.942	0.765	0.231	0.195	0.186	0.213
MAM SST	0.193	0.179	0.195	0	-0.075	-0.003	0.179	0.019	0.25	0.095	-0.1	-0.035
	0.355	0.393	0.349	0.999	0.733	0.988	0.403	0.931	0.238	0.653	0.634	0.867
JJA SST	0.119	0.097	0.2	-0.04	-0.156	-0.053	0.126	-0.075	0.143	-0.173	-0.03	0.057
	0.57	0.645	0.337	0.856	0.476	0.811	0.558	0.727	0.504	0.407	0.887	0.786
SON SST	0.108	0.147	0.27	-0.084	-0.122	-0.034	0.106	-0.137	-0.056	-0.15	-0.085	0.106
	0.608	0.484	0.193	0.703	0.578	0.878	0.621	0.524	0.794	0.475	0.687	0.613
MAM Snow	0.044	-0.11	-0.017	0	-0.116	-0.038	-0.14	0	0	0.176	0.369	**0.412**
	0.837	0.608	0.937	0.999	0.607	0.865	0.525	0.999	0.999	0.411	0.076	**0.046**
DJF NAO	0.061	0.026	0.112	**0.49**	0.196	0.141	-0.095	-0.129	0.025	0.15	-0.067	-0.1
	0.772	0.903	0.593	**0.018**	0.369	0.52	0.659	0.549	0.906	0.473	0.749	0.635

SEASONAL	Intensity				Persistence															
	aut	win	spr	sum	3aut	3win	3spr	3sum	7aut	7win	7spr	7sum	10aut	10win	10spr	10sum	30aut	30win	30spr	30sum
SON Temp	0.033	0.078	-0.064	-0.182	-0.045	-0.007	0.175	-0.357	-0.083	0.014	0.266	-0.343	-0.048	0.062	0.179	**-0.425**	-0.095	0.184	0.106	-0.397
	0.883	0.731	0.772	0.396	0.839	0.975	0.424	0.087	0.707	0.949	0.22	0.101	0.828	0.783	0.415	**0.039**	0.666	0.411	0.632	0.055
DJF Temp	0.39	0.073	-0.088	-0.231	0.367	0.04	0.284	-0.162	0.182	0.14	0.293	-0.109	0.169	0.128	0.304	-0.126	0.195	0.218	0.239	-0.05
	0.066	0.748	0.691	0.277	0.085	0.859	0.189	0.45	0.406	0.536	0.176	0.613	0.441	0.571	0.159	0.557	0.372	0.331	0.272	0.817
MAM Temp	0.114	0.127	0.06	-0.238	0.102	0.189	**0.416**	0.006	0.044	0.218	0.384	-0.083	0.026	0.222	0.352	-0.051	0.057	0.159	0.297	0.151
	0.606	0.573	0.787	0.263	0.644	0.399	**0.048**	0.979	0.842	0.33	0.07	0.701	0.905	0.32	0.1	0.812	0.797	0.479	0.169	0.482
JJA Temp	0.039	0.086	-0.238	-0.132	-0.26	0.056	0.01	-0.238	-0.374	-0.032	-0.034	-0.213	-0.337	-0.065	-0.042	-0.388	-0.352	-0.025	0.098	**-0.446**
	0.858	0.704	0.274	0.54	0.231	0.804	0.964	0.262	0.079	0.888	0.877	0.318	0.116	0.775	0.85	0.061	0.1	0.914	0.657	**0.029**
DJF SST	0.007	0.053	-0.062	-0.13	0.107	0.07	0.162	-0.189	0.063	0.125	0.036	-0.203	0.052	0.059	-0.025	-0.157	0.099	-0.007	-0.043	-0.315
	0.973	0.81	0.775	0.535	0.62	0.752	0.449	0.366	0.769	0.57	0.867	0.329	0.808	0.788	0.909	0.454	0.644	0.974	0.841	0.126
MAM SST	0.19	0.029	0.06	-0.37	0.169	0.121	0.304	-0.157	0.081	0.218	0.293	-0.219	0.072	0.214	0.293	-0.188	0.103	0.193	0.138	-0.078
	0.373	0.895	0.78	0.069	0.429	0.581	0.148	0.453	0.705	0.318	0.164	0.292	0.738	0.328	0.164	0.367	0.633	0.376	0.521	0.712
JJA SST	-0.005	-0.096	-0.087	-0.202	-0.099	0.044	0.236	-0.108	-0.243	0.043	0.172	-0.101	-0.217	-0.019	0.22	-0.177	-0.212	0.011	0.207	-0.275
	0.983	0.663	0.687	0.333	0.644	0.842	0.267	0.608	0.252	0.845	0.423	0.632	0.308	0.932	0.302	0.397	0.32	0.961	0.332	0.183
SON SST	-0.189	-0.181	-0.198	-0.099	-0.126	-0.097	0.158	-0.148	-0.261	-0.112	0.21	-0.103	-0.3	-0.084	0.186	-0.129	-0.344	0.057	0.181	-0.245
	0.378	0.408	0.353	0.636	0.559	0.661	0.462	0.481	0.219	0.61	0.326	0.624	0.154	0.705	0.384	0.539	0.1	0.797	0.397	0.238
MAM Snow	-0.01	0.006	0.213	0.374	-0.024	-0.005	-0.034	0.204	0.089	0.026	-0.149	0.234	0.109	0.008	-0.103	0.21	0.035	0.021	-0.335	0.01
	0.966	0.98	0.328	0.071	0.913	0.982	0.876	0.338	0.687	0.909	0.497	0.271	0.62	0.972	0.639	0.324	0.872	0.928	0.119	0.961
DJF NAO	**0.437**	0.278	0.076	-0.182	0.236	0.194	0.055	-0.131	0.005	0.248	0.061	-0.183	0.09	0.252	0.105	-0.252	0.125	**0.42**	0.299	-0.076
	0.033	0.2	0.723	0.385	0.267	0.374	0.8	0.534	0.983	0.253	0.778	0.38	0.675	0.247	0.626	0.225	0.56	**0.046**	0.155	0.719

ANNUAL	Intensity	Persistence				Frequency		
	ann	ann3	ann7	ann10	ann30	ann90	ann95	ann97
Temp	0.331	0.381	0.298	0.214	0.355	0.323	0.234	0.192
	0.098	0.055	0.14	0.294	0.075	0.107	0.251	0.347
SST	0.189	0.231	0.21	0.089	0.189	0.125	0.061	0.011
	0.345	0.247	0.293	0.658	0.345	0.534	0.762	0.957
Snow cover	-0.173	-0.243	-0.29	-0.287	-0.374	**-0.496**	-0.288	-0.248
	0.398	0.231	0.151	0.155	0.06	**0.01**	0.153	0.221
Snow level	0.043	0.015	-0.06	-0.024	-0.214	-0.25	-0.027	-0.079
	0.83	0.94	0.765	0.904	0.283	0.209	0.894	0.697
NAO	0.214	0.216	0.038	0.073	0.303	0.343	0.221	0.162
	0.283	0.278	0.85	0.718	0.125	0.08	0.268	0.419

Precipitation gauge:
Dolydd

SEASONAL	Frequency											
	aut90	aut95	aut97	win90	win95	win97	spr90	spr95	spr97	sum90	sum95	sum97
SON Temp	-0.018	0.226	0.25	-0.296	-0.027	0.156	-0.055	-0.013	0.128	-0.332	-0.146	-0.188
	0.929	0.267	0.218	0.141	0.894	0.448	0.788	0.95	0.532	0.098	0.478	0.359
DJF Temp	-0.072	-0.066	-0.031	-0.329	-0.21	-0.093	-0.057	-0.098	-0.027	-0.081	-0.157	-0.139
	0.728	0.75	0.881	0.1	0.302	0.653	0.781	0.634	0.895	0.693	0.443	0.497
MAM Temp	0.112	0.074	0.24	0.03	-0.026	-0.035	0.219	0.207	0.288	0.158	0.085	-0.023
	0.586	0.721	0.239	0.886	0.899	0.866	0.282	0.311	0.153	0.442	0.68	0.91
JJA Temp	0.079	0.212	0.13	-0.067	0.039	0.245	-0.214	-0.239	-0.085	**-0.48**	-0.25	-0.283
	0.703	0.298	0.526	0.743	0.85	0.229	0.293	0.24	0.678	**0.013**	0.219	0.161
DJF SST	-0.322	-0.189	-0.186	-0.029	-0.135	-0.036	-0.149	-0.236	-0.156	-0.099	-0.182	-0.089
	0.102	0.344	0.353	0.884	0.502	0.86	0.458	0.237	0.438	0.624	0.364	0.659
MAM SST	0.05	0.062	0.168	-0.136	-0.201	-0.091	-0.034	-0.088	0.137	0.129	0.097	0.05
	0.804	0.758	0.402	0.5	0.315	0.653	0.865	0.662	0.496	0.52	0.629	0.804
JJA SST	0.059	0.078	0.105	-0.028	-0.075	0.138	-0.045	-0.109	0.051	-0.229	-0.136	-0.155
	0.77	0.698	0.602	0.888	0.709	0.493	0.823	0.59	0.8	0.25	0.497	0.44
SON SST	0	0.122	0.049	-0.103	-0.239	-0.071	-0.147	-0.216	-0.02	-0.353	-0.216	-0.262
	0.999	0.543	0.808	0.609	0.231	0.726	0.466	0.28	0.92	0.071	0.278	0.186
MAM Snow	0.134	0.037	-0.12	-0.308	-0.241	-0.089	-0.24	-0.16	-0.209	0.158	0.218	0.28
	0.514	0.859	0.558	0.126	0.236	0.665	0.238	0.436	0.305	0.441	0.285	0.165
DJF NAO	0.007	0.062	0.145	-0.171	0.188	0.316	-0.081	0.028	0.067	-0.077	-0.09	-0.076
	0.971	0.76	0.47	0.394	0.349	0.109	0.69	0.89	0.74	0.703	0.656	0.707

SEASONAL	Intensity				Persistence															
	aut	win	spr	sum	3aut	3win	3spr	3sum	7aut	7win	7spr	7sum	10aut	10win	10spr	10sum	30aut	30win	30spr	30sum
SON Temp	0.098	0.255	-0.102	-0.235	-0.122	0.291	0.025	0.016	-0.066	0.249	0.005	-0.266	0.007	0.254	0	-0.272	-0.052	0.366	0.023	**-0.483**
	0.632	0.209	0.621	0.248	0.552	0.15	0.902	0.938	0.748	0.221	0.982	0.189	0.974	0.21	1	0.179	0.8	0.066	0.912	**0.012**
DJF Temp	0.225	0.101	0.04	-0.281	0.299	0.349	0.171	-0.122	0.166	0.4	0.118	-0.101	0.072	0.38	0.124	-0.107	0.166	**0.46**	0.126	-0.2
	0.27	0.623	0.846	0.164	0.137	0.081	0.403	0.552	0.418	0.043	0.565	0.624	0.725	0.056	0.545	0.604	0.417	**0.018**	0.539	0.327
MAM Temp	-0.174	0.115	0.33	-0.175	0.008	0.226	**0.454**	-0.032	-0.089	0.19	0.371	-0.061	-0.196	0.166	0.368	-0.063	-0.024	0.286	**0.395**	0.031
	0.394	0.576	0.1	0.394	0.97	0.266	**0.02**	0.879	0.667	0.352	0.062	0.766	0.338	0.417	0.065	0.758	0.906	0.156	**0.046**	0.88
JJA Temp	-0.069	0.133	-0.198	-0.235	-0.176	**0.395**	-0.21	-0.224	-0.308	0.216	-0.242	-0.152	-0.256	0.198	-0.249	-0.253	-0.249	0.286	-0.174	**-0.395**
	0.737	0.517	0.333	0.247	0.39	**0.046**	0.302	0.271	0.125	0.289	0.233	0.457	0.208	0.332	0.219	0.212	0.22	0.156	0.397	**0.046**
DJF SST	0.111	0.034	-0.081	-0.266	0.156	0.107	0.013	-0.141	0.161	0.056	0.014	-0.085	0.098	-0.007	0.012	-0.028	0.14	-0.007	-0.155	-0.139
	0.582	0.866	0.689	0.179	0.437	0.595	0.949	0.484	0.422	0.782	0.945	0.674	0.627	0.972	0.954	0.889	0.485	0.973	0.441	0.489
MAM SST	0.032	0.064	0.199	-0.181	0.182	0.129	0.302	0.034	0.116	0.132	0.281	-0.011	-0.024	0.1	0.264	-0.033	0.082	0.249	0.177	-0.083
	0.875	0.75	0.32	0.367	0.364	0.523	0.126	0.865	0.565	0.512	0.156	0.958	0.905	0.62	0.183	0.872	0.684	0.21	0.378	0.681
JJA SST	-0.09	0.077	0.056	-0.303	-0.113	0.307	0.085	-0.116	-0.239	0.158	0.044	-0.18	-0.259	0.106	0.047	-0.217	-0.16	0.202	0.051	-0.318
	0.654	0.704	0.78	0.124	0.573	0.119	0.674	0.566	0.23	0.433	0.827	0.37	0.192	0.598	0.815	0.278	0.424	0.311	0.8	0.106
SON SST	-0.17	0.187	-0.17	**-0.407**	-0.281	0.193	0.062	-0.067	-0.326	0.032	0.03	-0.331	-0.36	0.025	0.009	**-0.39**	-0.312	0.146	0.001	-0.481
	0.395	0.351	0.397	**0.035**	0.156	0.334	0.76	0.74	0.097	0.873	0.881	0.092	0.065	0.903	0.963	**0.044**	0.113	0.468	0.997	0.011
MAM Snow	0.12	0.196	-0.112	0.176	0.105	0.22	-0.16	0.317	0.173	0.208	-0.179	0.097	0.177	0.178	-0.219	0.207	0.052	0.026	-0.32	-0.059
	0.558	0.338	0.586	0.391	0.609	0.279	0.435	0.114	0.397	0.309	0.382	0.637	0.387	0.383	0.283	0.311	0.8	0.899	0.111	0.776
DJF NAO	0.232	0.243	0.117	0.06	0.322	**0.455**	0.074	-0.097	0.116	0.376	0.018	0.067	0.095	0.34	0.002	-0.054	0.099	**0.48**	0.167	-0.241
	0.245	0.221	0.56	0.767	0.101	**0.017**	0.715	0.629	0.564	0.053	0.927	0.738	0.636	0.083	0.994	0.79	0.624	**0.011**	0.404	0.225

ANNUAL	Intensity	Persistence				Frequency		
	ann	ann3	ann7	ann10	ann30	ann90	ann95	ann97
Temp	-0.135	0.009	0.138	0.268	0.271	0.108	0.226	0.216
	0.52	0.965	0.52	0.206	0.2	0.608	0.277	0.301
SST	-0.128	0.016	0.197	0.284	0.142	0.01	0.124	0.136
	0.532	0.94	0.346	0.169	0.497	0.963	0.547	0.507
Snow cover	0.14	-0.111	-0.252	-0.372	-0.344	-0.15	-0.119	-0.159
	0.504	0.607	0.234	0.073	0.1	0.474	0.57	0.447
Snow level	**0.463**	0.152	-0.075	-0.218	-0.07	-0.04	-0.034	-0.025
	0.017	0.469	0.722	0.295	0.74	0.846	0.868	0.904
NAO	-0.103	0.036	-0.085	0.033	0.122	-0.178	-0.118	0.072
	0.617	0.864	0.685	0.874	0.561	0.385	0.566	0.727

Precipitation gauge:
Llanfyllin

SEASONAL	Frequency											
	aut90	aut95	aut97	win90	win95	win97	spr90	spr95	spr97	sum90	sum95	sum97
SON Temp	0.069	0.168	0.172	**0.463**	**0.515**	0.38	0.121	-0.006	0.179	-0.136	-0.04	-0.05
	0.737	0.413	0.401	**0.02**	**0.008**	0.061	0.574	0.978	0.402	0.525	0.852	0.818
DJF Temp	-0.007	0.106	0.023	0.352	0.207	0.179	-0.209	-0.243	-0.043	-0.216	-0.279	-0.097
	0.973	0.605	0.91	0.084	0.321	0.392	0.327	0.253	0.841	0.311	0.187	0.654
MAM Temp	0.123	0.276	0.189	0.051	-0.03	-0.162	-0.052	-0.207	-0.218	0.264	0.206	0.182
	0.55	0.172	0.355	0.807	0.887	0.44	0.811	0.331	0.307	0.213	0.334	0.396
JJA Temp	0.1	0.071	0.044	0.293	**0.542**	0.469	0.106	0.204	0.303	-0.119	0.073	0.195
	0.628	0.732	0.832	0.155	**0.005**	0.018	0.621	0.339	0.151	0.581	0.736	0.361
DJF SST	-0.333	-0.122	-0.112	0.142	0.094	0.114	-0.08	0.028	0.159	-0.326	-0.284	-0.18
	0.089	0.544	0.578	0.488	0.648	0.58	0.705	0.893	0.447	0.112	0.169	0.388
MAM SST	-0.054	0.212	0.166	0.195	0.069	0.013	0.032	-0.154	-0.079	0.146	0.092	-0.012
	0.789	0.288	0.407	0.34	0.738	0.951	0.878	0.462	0.707	0.487	0.662	0.954
JJA SST	0.148	0.216	0.11	0.14	0.189	0.073	0.047	0.021	0.161	0.004	0.161	0.294
	0.462	0.278	0.587	0.495	0.355	0.723	0.824	0.919	0.443	0.987	0.441	0.153
SON SST	0.09	0.262	0.146	0.133	0.152	0.086	0.176	0.097	0.248	-0.227	-0.029	0.039
	0.654	0.187	0.466	0.519	0.459	0.678	0.4	0.645	0.233	0.276	0.89	0.853
MAM Snow	0.147	0	0.01	0.121	0.023	0.073	-0.283	-0.116	-0.079	-0.138	0.149	0.204
	0.474	0.999	0.96	0.564	0.913	0.728	0.18	0.588	0.715	0.52	0.488	0.34
DJF NAO	-0.073	-0.02	-0.077	0.306	0.303	**0.402**	-0.222	-0.297	-0.089	-0.127	-0.288	-0.016
	0.718	0.922	0.703	0.129	0.132	**0.042**	0.286	0.149	0.674	0.546	0.162	0.938

SEASONAL	Intensity				Persistence															
	aut	win	spr	sum	3aut	3win	3spr	3sum	7aut	7win	7spr	7sum	10aut	10win	10spr	10sum	30aut	30win	30spr	30sum
SON Temp	0.189	0.337	0.104	0.07	0.109	0.365	0.147	-0.075	0.071	0.318	-0.258	-0.059	0.067	0.342	-0.239	-0.054	-0.009	**0.397**	-0.026	-0.183
	0.378	0.1	0.63	0.744	0.614	0.073	0.493	0.727	0.743	0.121	0.224	0.784	0.757	0.094	0.261	0.801	0.968	**0.05**	0.905	0.391
DJF Temp	0.056	0.168	0.044	-0.197	0.212	0.377	0.085	-0.238	0.096	**0.421**	0.015	-0.276	0.063	**0.461**	-0.018	-0.192	0.039	0.436	-0.043	**-0.43**
	0.795	0.423	0.839	0.357	0.32	0.063	0.693	0.262	0.654	**0.036**	0.946	0.191	0.768	**0.02**	0.934	0.368	0.858	0.029	0.841	**0.036**
MAM Temp	0.137	-0.03	-0.216	-0.399	0.255	0.172	0.033	-0.292	0.156	0.217	0.15	-0.07	0.124	0.271	0.157	0.004	0.035	0.106	-0.03	-0.043
	0.523	0.887	0.31	0.053	0.228	0.412	0.879	0.166	0.468	0.297	0.484	0.743	0.563	0.19	0.465	0.987	0.869	0.615	0.889	0.843
JJA Temp	0.011	0.371	0	0.167	-0.121	0.333	-0.007	-0.047	-0.336	0.223	-0.145	0.024	-0.312	0.234	-0.206	0.084	-0.31	0.285	0.252	-0.206
	0.958	0.068	1	0.434	0.573	0.104	0.975	0.827	0.108	0.284	0.498	0.911	0.138	0.261	0.334	0.696	0.14	0.168	0.236	0.333
DJF SST	-0.116	0.17	0.094	-0.092	0.045	0.186	0.261	-0.179	0.011	0.241	0.024	-0.122	-0.034	0.189	0.014	-0.026	0.042	0.066	-0.093	-0.379
	0.581	0.407	0.655	0.661	0.832	0.363	0.208	0.393	0.957	0.236	0.911	0.563	0.873	0.354	0.949	0.903	0.842	0.748	0.658	0.062
MAM SST	0.255	0.129	-0.005	**-0.468**	0.338	0.212	0.145	-0.371	0.206	0.309	0.135	-0.189	0.166	0.353	0.09	-0.115	0.053	0.177	-0.11	-0.257
	0.219	0.53	0.982	**0.018**	0.098	0.297	0.49	0.068	0.322	0.125	0.519	0.366	0.428	0.077	0.67	0.583	0.801	0.388	0.6	0.215
JJA SST	-0.005	0.096	0.006	-0.08	0.051	0.22	0.027	-0.206	-0.157	0.185	0.044	-0.036	-0.134	0.205	0.018	0.084	-0.188	0.188	0.174	-0.187
	0.981	0.642	0.978	0.703	0.807	0.28	0.896	0.323	0.455	0.365	0.834	0.866	0.522	0.315	0.93	0.69	0.368	0.359	0.407	0.371
SON SST	0.018	0.122	0.087	-0.102	0.148	0.111	0.12	-0.217	-0.046	0.063	-0.098	-0.154	-0.087	0.119	-0.146	-0.086	-0.231	0.195	-0.03	-0.277
	0.932	0.553	0.681	0.627	0.48	0.591	0.569	0.297	0.828	0.76	0.64	0.462	0.68	0.563	0.485	0.683	0.267	0.339	0.887	0.181
MAM Snow	0.032	-0.08	0.384	0.293	-0.121	0.026	-0.051	0.236	0.015	0.041	-0.219	-0.023	0.009	-0.031	-0.068	-0.062	-0.082	0.05	-0.174	-0.1
	0.882	0.702	0.064	0.165	0.572	0.904	0.814	0.268	0.945	0.847	0.303	0.916	0.967	0.883	0.753	0.775	0.703	0.812	0.417	0.643
DJF NAO	0.138	0.15	0.092	0.009	0.246	0.282	0.036	-0.047	0.005	0.182	0.081	-0.123	0.036	0.239	0.041	-0.103	0.076	0.38	0.301	-0.28
	0.51	0.463	0.663	0.967	0.237	0.162	0.865	0.823	0.98	0.374	0.702	0.559	0.863	0.239	0.844	0.623	0.718	0.055	0.143	0.175

ANNUAL	Intensity	Persistence				Frequency		
	ann	ann3	ann7	ann10	ann30	ann90	ann95	ann97
Temp	-0.221	0.2	0.134	0.089	0.068	0.078	0.015	0.207
	0.299	0.348	0.531	0.678	0.752	0.716	0.945	0.332
SST	-0.271	0.167	0.195	0.164	-0.022	0.004	-0.125	0.027
	0.19	0.424	0.351	0.434	0.915	0.984	0.55	0.898
Snow cover	0.047	**-0.422**	-0.227	-0.224	-0.188	-0.281	-0.192	-0.373
	0.828	**0.04**	0.287	0.293	0.378	0.184	0.368	0.073
Snow level	0.329	-0.197	-0.147	-0.178	-0.018	-0.122	0.062	-0.133
	0.108	0.346	0.484	0.394	0.932	0.56	0.77	0.526
NAO	-0.127	0.006	-0.062	-0.066	0.185	0.363	**0.457**	0.278
	0.544	0.976	0.769	0.754	0.377	0.075	**0.022**	0.179

Precipitation gauge:
Llangynog

SEASONAL	Frequency											
	aut90	aut95	aut97	win90	win95	win97	spr90	spr95	spr97	sum90	sum95	sum97
SON Temp	-0.081	0.201	0.151	0.207	0.149	0.256	0.1	0.154	-0.123	-0.381	-0.349	-0.347
	0.708	0.345	0.481	0.333	0.486	0.239	0.649	0.482	0.575	0.073	0.102	0.104
DJF Temp	0.005	0.001	0.259	0.256	0.254	0.211	0.025	0.087	0.032	-0.232	-0.203	-0.305
	0.983	0.998	0.221	0.228	0.23	0.333	0.91	0.692	0.885	0.287	0.352	0.157
MAM Temp	0.173	0.048	0.268	0.047	-0.028	0.201	0.167	0.058	0.187	0.099	0.07	-0.095
	0.418	0.825	0.206	0.827	0.896	0.357	0.446	0.792	0.394	0.653	0.751	0.665
JJA Temp	-0.026	0.061	0.101	0.179	0.334	0.354	0.157	0.358	0.079	-0.288	-0.267	-0.286
	0.904	0.776	0.638	0.402	0.111	0.097	0.474	0.093	0.719	0.183	0.218	0.185
DJF SST	-0.327	-0.2	0.015	0.016	0.106	0.204	0.033	0.199	-0.088	-0.264	-0.187	-0.296
	0.111	0.338	0.943	0.938	0.613	0.339	0.877	0.351	0.681	0.212	0.381	0.16
MAM SST	0.077	0.017	0.232	0.059	0.019	0.153	0.172	0.156	0.162	0.029	0.001	-0.174
	0.714	0.936	0.265	0.78	0.929	0.475	0.422	0.467	0.45	0.892	0.995	0.416
JJA SST	0.17	0.141	0.308	-0.057	0	0.097	0.369	**0.421**	0.219	-0.199	-0.179	-0.258
	0.416	0.501	0.134	0.787	1	0.652	0.076	**0.04**	0.305	0.351	0.402	0.223
SON SST	0.093	0.201	0.323	-0.054	0.017	0.175	0.413	0.338	0.03	**-0.517**	-0.446	**-0.5**
	0.66	0.334	0.115	0.799	0.934	0.412	0.045	0.106	0.89	**0.01**	0.029	**0.013**
MAM Snow	0.224	0.375	0.126	0.015	-0.035	-0.254	-0.047	0.11	-0.113	-0.073	0.028	0.156
	0.293	0.071	0.556	0.946	0.871	0.242	0.83	0.617	0.607	0.739	0.897	0.478
DJF NAO	-0.074	-0.081	0.076	**0.409**	**0.533**	0.369	0.002	-0.023	0.05	-0.02	0.023	-0.036
	0.725	0.7	0.717	**0.042**	**0.006**	0.076	0.994	0.916	0.816	0.926	0.915	0.867

SEASONAL	Intensity				Persistence															
	aut	win	spr	sum	3aut	3win	3spr	3sum	7aut	7win	7spr	7sum	10aut	10win	10spr	10sum	30aut	30win	30spr	30sum
SON Temp	0.126	0.053	-0.116	-0.075	0.014	0.067	-0.037	-0.16	-0.109	0.216	-0.244	-0.29	-0.016	0.201	-0.245	-0.286	-0.035	0.212	0.028	**-0.48**
	0.566	0.805	0.597	0.735	0.949	0.757	0.866	0.466	0.622	0.311	0.263	0.18	0.941	0.347	0.261	0.186	0.872	0.32	0.897	**0.02**
DJF Temp	0.16	0.077	-0.184	-0.127	0.295	0.219	0.034	-0.322	0.108	**0.433**	-0.16	-0.412	0.078	0.379	-0.217	-0.344	0.039	0.362	-0.148	**-0.432**
	0.465	0.721	0.401	0.564	0.171	0.303	0.877	0.134	0.624	**0.035**	0.466	0.051	0.724	0.068	0.32	0.108	0.859	0.083	0.5	**0.04**
MAM Temp	-0.047	0.161	-0.025	-0.239	0.184	0.238	0.162	-0.233	-0.015	0.399	0.009	-0.157	-0.025	**0.442**	0.056	-0.007	-0.08	0.2	0.122	-0.138
	0.83	0.452	0.909	0.271	0.401	0.263	0.459	0.285	0.948	0.054	0.968	0.475	0.909	**0.031**	0.801	0.975	0.717	0.349	0.579	0.53
JJA Temp	-0.227	0.052	-0.059	0.015	-0.281	0.102	-0.083	-0.259	**-0.451**	0.122	-0.279	-0.268	-0.399	0.06	-0.242	-0.241	-0.363	0.078	0.085	**-0.556**
	0.298	0.81	0.79	0.947	0.194	0.635	0.708	0.233	**0.031**	0.57	0.197	0.216	0.059	0.782	0.266	0.268	0.089	0.718	0.701	**0.006**
DJF SST	-0.012	-0.121	-0.398	-0.069	0.157	-0.082	-0.083	-0.13	0.004	0.13	-0.224	-0.103	0.004	0.041	-0.289	-0.072	0.003	-0.073	-0.349	-0.285
	0.955	0.564	0.054	0.749	0.464	0.696	0.701	0.545	0.985	0.536	0.292	0.633	0.986	0.846	0.171	0.737	0.989	0.728	0.095	0.177
MAM SST	0.081	-0.024	-0.126	-0.321	0.279	0.047	0.092	-0.305	0.088	0.288	-0.007	-0.212	0.084	0.322	-0.053	-0.076	0.02	0.176	-0.006	-0.287
	0.708	0.911	0.558	0.126	0.186	0.822	0.668	0.147	0.683	0.163	0.975	0.319	0.695	0.116	0.806	0.724	0.927	0.401	0.978	0.174
JJA SST	-0.17	-0.127	0.009	-0.165	-0.052	-0.056	0.212	-0.289	-0.281	0.102	0.034	-0.256	-0.24	0.092	0.027	-0.191	-0.245	0.056	0.176	**-0.599**
	0.428	0.547	0.966	0.44	0.809	0.789	0.321	0.171	0.184	0.628	0.874	0.227	0.26	0.663	0.901	0.372	0.248	0.791	0.41	**0.002**
SON SST	-0.148	-0.05	-0.119	-0.203	-0.086	-0.107	0.184	-0.24	-0.269	0.025	-0.059	-0.275	-0.277	0.067	-0.102	-0.242	-0.298	0.075	0.096	**-0.636**
	0.491	0.813	0.579	0.341	0.69	0.612	0.39	0.259	0.204	0.906	0.786	0.193	0.191	0.749	0.637	0.254	0.157	0.722	0.656	**0.001**
MAM Snow	0.26	-0.31	0.375	0.279	0.02	-0.169	0.203	0.214	0.2	-0.17	0.129	-0.017	0.166	-0.19	-0.009	-0.121	0.083	0.017	-0.233	-0.127
	0.232	0.141	0.077	0.197	0.928	0.43	0.353	0.327	0.36	0.428	0.557	0.937	0.449	0.375	0.967	0.582	0.707	0.938	0.284	0.563
DJF NAO	0.178	0.287	0.019	-0.015	0.171	0.31	-0.095	-0.27	0.031	0.311	-0.137	-0.27	0.035	0.279	-0.201	-0.218	0.016	**0.428**	0.074	-0.224
	0.404	0.164	0.928	0.943	0.424	0.131	0.658	0.201	0.887	0.131	0.523	0.202	0.87	0.177	0.345	0.306	0.942	**0.033**	0.731	0.292

ANNUAL	Intensity	Persistence				Frequency		
	ann	ann3	ann7	ann10	ann30	ann90	ann95	ann97
Temp	0.241	**0.427**	**0.408**	0.368	**0.413**	0.365	**0.452**	**0.439**
	0.257	**0.037**	**0.048**	0.077	**0.045**	0.079	**0.026**	**0.032**
SST	0.119	0.307	0.395	0.379	0.384	0.27	0.39	0.354
	0.57	0.136	0.051	0.062	0.058	0.191	0.054	0.083
Snow cover	-0.127	-0.392	**-0.405**	-0.395	-0.402	**-0.404**	-0.371	-0.289
	0.555	0.058	**0.05**	0.056	0.051	**0.05**	0.074	0.17
Snow level	-0.017	-0.219	-0.308	-0.354	-0.374	-0.301	-0.228	-0.125
	0.935	0.293	0.134	0.082	0.065	0.144	0.273	0.552
NAO	-0.004	0.053	-0.098	-0.157	-0.046	0.03	0.018	-0.004
	0.985	0.8	0.641	0.454	0.828	0.886	0.932	0.984

Precipitation gauge:
Pen-y-Coed

SEASONAL	Frequency											
	aut90	aut95	aut97	win90	win95	win97	spr90	spr95	spr97	sum90	sum95	sum97
SON Temp	0.147	0.392	0.381	**0.467**	**0.468**	**0.412**	0.036	0.186	0.211	-0.214	-0.301	-0.231
	0.492	0.058	0.066	**0.021**	**0.021**	**0.045**	0.869	0.395	0.333	0.327	0.163	0.289
DJF Temp	0.019	0.038	0.091	0.397	0.334	0.125	-0.118	-0.036	0.033	-0.202	-0.106	-0.059
	0.932	0.86	0.673	0.055	0.11	0.562	0.59	0.87	0.88	0.356	0.629	0.788
MAM Temp	0.216	0.191	0.08	0.25	0.225	0.039	0.183	0.296	**0.43**	0.044	0.165	0.049
	0.31	0.372	0.712	0.239	0.289	0.856	0.404	0.17	**0.04**	0.84	0.45	0.823
JJA Temp	0.186	0.296	0.286	0.315	0.314	**0.47**	-0.109	-0.175	0.018	-0.406	**-0.52**	-0.32
	0.385	0.161	0.176	0.133	0.135	**0.02**	0.621	0.423	0.936	0.055	**0.011**	0.137
DJF SST	-0.188	-0.04	-0.053	0.224	0.128	-0.079	-0.153	-0.119	0.036	-0.185	-0.201	-0.24
	0.369	0.849	0.8	0.282	0.542	0.709	0.475	0.579	0.866	0.388	0.346	0.259
MAM SST	0.15	0.24	0.131	0.326	0.204	-0.035	-0.039	0.102	0.355	0.104	0.195	0.036
	0.475	0.249	0.532	0.112	0.329	0.868	0.857	0.636	0.089	0.63	0.36	0.867
JJA SST	0.273	0.315	0.189	0.255	0.243	0.167	0.134	0.085	0.257	-0.286	-0.312	-0.123
	0.187	0.125	0.365	0.219	0.243	0.425	0.532	0.694	0.226	0.176	0.138	0.567
SON SST	0.212	0.372	0.299	0.284	0.19	0.18	0.348	0.205	0.163	-0.485	-0.381	-0.259
	0.31	0.067	0.146	0.169	0.362	0.39	0.095	0.336	0.446	0.016	0.066	0.222
MAM Snow	-0.156	-0.018	0.012	0.08	-0.005	-0.062	0.016	-0.176	-0.251	0.103	0.161	0.345
	0.466	0.932	0.957	0.71	0.983	0.774	0.942	0.421	0.248	0.639	0.464	0.106
DJF NAO	-0.107	-0.03	0.134	0.316	0.296	0.266	**-0.439**	-0.137	0.037	-0.019	-0.043	0.004
	0.609	0.885	0.522	0.124	0.151	0.198	**0.032**	0.523	0.865	0.931	0.843	0.985

SEASONAL	Intensity				Persistence															
	aut	win	spr	sum	3aut	3win	3spr	3sum	7aut	7win	7spr	7sum	10aut	10win	10spr	10sum	30aut	30win	30spr	30sum
SON Temp	0.084	0.302	0.253	0.08	0.059	0.361	0.282	-0.106	0.005	0.36	0.237	-0.225	0.056	0.34	0.202	-0.261	0.006	0.398	0.174	**-0.488**
	0.705	0.152	0.243	0.717	0.785	0.084	0.192	0.629	0.983	0.084	0.277	0.302	0.796	0.104	0.356	0.229	0.977	0.054	0.429	**0.018**
DJF Temp	0.141	0.197	0.117	-0.084	0.384	0.292	0.249	-0.077	0.285	0.383	0.166	-0.281	0.255	0.33	0.179	-0.203	0.354	**0.412**	0.156	-0.253
	0.522	0.357	0.594	0.703	0.064	0.166	0.251	0.728	0.178	0.065	0.448	0.194	0.23	0.115	0.415	0.352	0.098	**0.045**	0.479	0.245
MAM Temp	0.033	0.144	0.269	-0.124	0.378	0.194	**0.432**	0.022	0.273	0.258	**0.418**	-0.074	0.239	0.247	0.372	0.05	0.231	0.244	0.39	0.079
	0.881	0.501	0.215	0.573	0.068	0.363	**0.04**	0.922	0.196	0.223	**0.047**	0.736	0.261	0.245	0.08	0.82	0.288	0.25	0.066	0.722
JJA Temp	-0.088	0.296	-0.09	-0.064	-0.016	**0.406**	-0.203	-0.23	-0.157	0.34	-0.156	-0.33	-0.112	0.28	-0.113	-0.375	-0.053	0.307	0.078	**-0.522**
	0.689	0.161	0.683	0.772	0.942	**0.049**	0.353	0.29	0.464	0.104	0.477	0.124	0.601	0.185	0.609	0.078	0.81	0.144	0.723	**0.011**
DJF SST	0.096	0.16	0.05	-0.09	0.248	0.165	0.1	-0.088	0.209	0.114	0.066	-0.095	0.193	0.063	0.053	-0.015	0.195	0.037	-0.018	-0.178
	0.656	0.445	0.815	0.675	0.233	0.43	0.642	0.682	0.317	0.587	0.759	0.658	0.356	0.765	0.804	0.943	0.36	0.86	0.933	0.407
MAM SST	0.086	0.101	0.324	-0.021	**0.473**	0.133	0.338	0.042	0.356	0.211	0.317	-0.077	0.332	0.173	0.305	-0.01	0.349	0.207	0.199	-0.069
	0.689	0.632	0.122	0.923	**0.017**	0.527	0.106	0.844	0.08	0.312	0.131	0.722	0.105	0.408	0.147	0.963	0.094	0.321	0.35	0.75
JJA SST	-0.114	0.155	0.261	-0.141	0.197	0.3	0.209	-0.042	0.039	0.387	0.262	-0.183	0.048	0.324	0.255	-0.129	0.06	0.315	0.319	**-0.368**
	0.596	0.46	0.218	0.512	0.344	0.145	0.328	0.845	0.854	0.056	0.217	0.393	0.821	0.115	0.229	0.548	0.782	0.125	0.129	**0.077**
SON SST	-0.051	0.201	0.207	-0.262	0.135	0.198	0.372	-0.174	-0.027	0.248	0.367	-0.189	-0.043	0.267	0.298	-0.207	-0.147	0.307	0.282	**-0.451**
	0.813	0.336	0.332	0.216	0.521	0.344	0.074	0.416	0.899	0.232	0.077	0.376	0.838	0.196	0.157	0.331	0.494	0.135	0.181	**0.027**
MAM Snow	0.114	-0.025	-0.009	0.38	-0.06	0.057	-0.093	0.189	0.032	0.097	-0.147	0.088	0.02	-0.012	-0.142	0.033	-0.175	-0.093	-0.252	-0.171
	0.605	0.907	0.969	0.073	0.78	0.79	0.673	0.389	0.881	0.651	0.504	0.689	0.927	0.955	0.517	0.881	0.425	0.667	0.246	0.435
DJF NAO	-0.034	0.252	0.029	0.197	0.111	0.337	-0.052	0.007	-0.036	0.309	-0.13	-0.202	0.04	0.226	-0.109	-0.238	0.217	**0.399**	0.049	-0.233
	0.875	0.225	0.893	0.355	0.599	0.1	0.808	0.973	0.864	0.132	0.545	0.343	0.848	0.277	0.612	0.263	0.308	**0.048**	0.822	0.273

ANNUAL	Intensity	Persistence				Frequency		
	ann	ann3	ann7	ann10	ann30	ann90	ann95	ann97
Temp	-0.107	-0.093	0.123	0.165	0.142	0.066	0.072	-0.098
	0.603	0.652	0.55	0.42	0.489	0.748	0.725	0.634
SST	-0.09	-0.062	0.152	0.163	0.057	-0.022	0.047	-0.088
	0.654	0.757	0.448	0.416	0.778	0.911	0.816	0.661
Snow cover	-0.016	-0.058	-0.172	-0.211	-0.337	-0.262	-0.22	-0.017
	0.936	0.779	0.4	0.302	0.092	0.197	0.281	0.933
Snow level	0.035	-0.068	-0.244	-0.224	-0.265	-0.058	-0.129	0.011
	0.864	0.737	0.219	0.26	0.181	0.773	0.521	0.957
NAO	0.393	0.253	0.258	0.339	0.311	0.059	0.267	0.21
	0.042	0.203	0.193	0.083	0.115	0.769	0.179	0.294

Precipitation gauge:
Welshpool

SEASONAL	Frequency											
	aut90	aut95	aut97	win90	win95	win97	spr90	spr95	spr97	sum90	sum95	sum97
SON Temp	-0.024	0.083	0.084	0.137	0.053	0.11	0.056	0.147	-0.087	-0.166	0.001	-0.204
	0.912	0.699	0.696	0.513	0.801	0.6	0.785	0.472	0.673	0.429	0.997	0.328
DJF Temp	0.168	0.002	-0.05	0.03	0.073	0.083	-0.156	-0.14	-0.228	-0.092	-0.213	-0.349
	0.431	0.993	0.815	0.886	0.729	0.692	0.448	0.497	0.263	0.66	0.306	0.087
MAM Temp	0.142	0.34	0.317	-0.355	-0.128	-0.06	-0.278	-0.285	-0.299	0.09	-0.027	-0.087
	0.507	0.104	0.131	0.082	0.541	0.777	0.168	0.159	0.137	0.67	0.897	0.681
JJA Temp	-0.28	-0.191	-0.121	0.183	-0.147	-0.013	0.246	0.247	0.168	-0.343	-0.133	-0.142
	0.185	0.371	0.574	0.38	0.484	0.952	0.225	0.223	0.412	0.094	0.525	0.499
DJF SST	-0.193	-0.297	-0.211	0.155	0.254	0.289	-0.124	-0.077	-0.117	-0.209	-0.373	-0.36
	0.356	0.15	0.31	0.45	0.211	0.153	0.538	0.703	0.562	0.306	0.061	0.071
MAM SST	0.079	0.141	0.117	-0.091	0.08	0.066	-0.189	-0.199	-0.233	0.146	0.009	-0.208
	0.709	0.501	0.577	0.658	0.698	0.748	0.345	0.32	0.241	0.477	0.964	0.307
JJA SST	-0.022	0.032	-0.022	-0.188	-0.291	-0.142	-0.033	-0.063	-0.079	-0.175	0.009	-0.07
	0.916	0.878	0.916	0.359	0.149	0.488	0.871	0.756	0.695	0.392	0.965	0.735
SON SST	0.004	0.15	0.127	-0.146	-0.198	-0.17	0.015	-0.083	-0.178	-0.162	-0.081	-0.332
	0.985	0.475	0.546	0.477	0.332	0.406	0.942	0.682	0.374	0.43	0.693	0.097
MAM Snow	0.163	-0.193	-0.156	0.181	0.009	0.084	0.004	-0.041	-0.057	0.007	0.216	0.091
	0.448	0.366	0.468	0.387	0.967	0.691	0.984	0.841	0.782	0.972	0.299	0.667
DJF NAO	0.062	-0.049	-0.039	0.226	0.128	0.113	-0.138	-0.04	0.025	-0.128	-0.173	-0.242
	0.769	0.816	0.851	0.268	0.532	0.583	0.491	0.842	0.902	0.534	0.397	0.233

SEASONAL	Intensity				Persistence														
	aut	win	spr	sum	3aut	3win	3spr	3sum	7aut	7win	7spr	7sum	10aut	10win	10spr	10sum	30aut	30win	30spr	30sum
SON Temp	0.295	-0.053	-0.141	-0.167	0.13	-0.027	-0.157	-0.317	0.249	-0.026	-0.176	-0.244	0.236	0.054	-0.252	-0.126	0.102	0.128	-0.303	-0.244
	0.152	0.801	0.492	0.424	0.535	0.898	0.444	0.123	0.23	0.901	0.39	0.241	0.256	0.798	0.215	0.549	0.626	0.54	0.132	0.239
DJF Temp	-0.013	0.077	-0.218	-0.218	0.097	0.053	-0.121	-0.289	0.106	0.197	-0.191	-0.169	0.08	0.19	-0.171	-0.042	0.155	0.206	-0.264	-0.181
	0.951	0.714	0.284	0.295	0.644	0.803	0.557	0.16	0.615	0.346	0.35	0.419	0.702	0.364	0.403	0.842	0.46	0.323	0.193	0.386
MAM Temp	0.112	0.03	-0.316	-0.24	0.16	-0.153	-0.204	-0.173	0.13	0.025	-0.163	0.045	0.108	0.102	-0.17	0.205	0.046	0.006	-0.259	0.197
	0.595	0.888	0.115	0.247	0.445	0.465	0.316	0.407	0.535	0.907	0.426	0.829	0.608	0.627	0.407	0.326	0.826	0.977	0.201	0.344
JJA Temp	-0.111	-0.061	-0.185	-0.232	-0.157	-0.088	-0.112	-0.377	-0.207	-0.119	-0.088	-0.234	-0.179	-0.027	-0.167	-0.106	-0.254	-0.075	0.009	-0.357
	0.599	0.773	0.367	0.265	0.454	0.675	0.586	0.063	0.321	0.572	0.671	0.259	0.391	0.896	0.416	0.613	0.221	0.721	0.965	0.08
DJF SST	-0.234	0.213	-0.172	-0.285	-0.316	0.148	-0.062	-0.442	-0.214	0.281	-0.194	-0.333	-0.241	0.239	-0.269	-0.193	-0.022	-0.011	-0.393	**-0.404**
	0.25	0.297	0.391	0.158	0.116	0.47	0.76	0.024	0.294	0.164	0.333	0.096	0.236	0.239	0.174	0.346	0.913	0.959	0.043	**0.041**
MAM SST	0.137	0.113	-0.116	-0.329	0.096	0.047	-0.069	-0.282	0.107	0.238	-0.101	-0.033	0.095	0.275	-0.164	0.17	0.033	0.057	-0.259	0.029
	0.506	0.583	0.565	0.101	0.639	0.821	0.733	0.163	0.603	0.242	0.614	0.874	0.645	0.175	0.413	0.406	0.871	0.782	0.192	0.887
JJA SST	-0.139	-0.12	-0.253	-0.161	-0.095	-0.246	-0.171	-0.179	-0.128	-0.176	-0.115	-0.063	-0.098	-0.104	-0.127	0.101	-0.106	-0.205	-0.151	-0.218
	0.499	0.561	0.203	0.432	0.643	0.225	0.395	0.382	0.534	0.391	0.567	0.76	0.633	0.612	0.529	0.624	0.605	0.316	0.451	0.286
SON SST	0.015	-0.229	-0.231	-0.32	-0.059	-0.253	-0.247	-0.255	-0.075	-0.181	-0.255	-0.174	-0.114	-0.092	-0.347	-0.051	-0.144	-0.132	-0.269	-0.316
	0.941	0.26	0.247	0.111	0.774	0.213	0.213	0.209	0.716	0.375	0.199	0.397	0.578	0.656	0.076	0.803	0.483	0.522	0.175	0.115
MAM Snow	-0.076	-0.059	0.361	0.098	-0.038	0.124	0.177	0.046	0.043	0.107	0.128	-0.138	0.068	0.003	0.178	-0.206	0.034	0.138	0.038	-0.312
	0.72	0.778	0.07	0.642	0.857	0.554	0.387	0.826	0.837	0.612	0.533	0.509	0.748	0.988	0.384	0.324	0.873	0.511	0.854	0.129
DJF NAO	0.146	0.182	-0.037	0.021	0.295	0.144	0.074	-0.086	0.126	0.136	-0.006	-0.015	0.172	0.209	0.008	0.015	0.142	0.371	0.143	-0.075
	0.477	0.374	0.853	0.92	0.143	0.481	0.713	0.675	0.539	0.506	0.978	0.94	0.4	0.306	0.969	0.944	0.489	0.062	0.476	0.716

Flow gauge:
Abermule

ANNUAL	Intensity	Frequency		
	ann	ann90	ann95	ann97
Temp	0.285	0.1	0.191	0.252
	0.134	0.607	0.322	0.188
SST	0.118	-0.138	-0.048	0.003
	0.534	0.469	0.8	0.986
Snow cover	-0.23	-0.222	-0.192	-0.206
	0.23	0.247	0.317	0.284
Snow level	-0.092	0.019	0.012	0.086
	0.649	0.924	0.953	0.669
NAO	0.207	0.212	0.32	0.196
	0.272	0.262	0.084	0.243

SEASONAL	Intensity				Frequency											
	aut	win	spr	sum	aut90	aut95	aut97	win90	win95	win97	spr90	spr95	spr97	sum90	sum95	sum97
SON Temp	-0.094	0.017	**-0.434**	0.18	0.087	0.208	0.172	0.08	0.058	0.02	**-0.468**	-0.331	-0.339	0.262	0.262	0.253
	0.628	0.929	**0.019**	0.349	0.655	0.279	0.371	0.679	0.764	0.918	**0.01**	0.08	0.072	0.169	0.169	0.186
DJF Temp	0.098	0.11	-0.111	**0.401**	0.076	0.086	0.109	-0.247	-0.259	-0.287	-0.082	-0.119	-0.104	0.356	0.315	0.316
	0.612	0.569	0.565	**0.031**	0.696	0.658	0.573	0.197	0.176	0.131	0.674	0.539	0.59	0.058	0.096	0.095
MAM Temp	-0.035	0.185	0.031	0.174	0.279	0.236	0.326	-0.22	-0.198	-0.245	0.051	0.033	0.083	0.093	0.13	0.087
	0.856	0.337	0.872	0.367	0.143	0.219	0.084	0.251	0.304	0.2	0.792	0.866	0.668	0.633	0.503	0.654
JJA Temp	-0.359	-0.166	-0.073	0.334	-0.038	-0.108	-0.011	-0.274	-0.247	-0.276	**-0.417**	-0.361	-0.28	0.287	0.27	0.288
	0.056	0.39	0.706	0.077	0.845	0.576	0.955	0.151	0.196	0.148	**0.024**	0.055	0.141	0.131	0.156	0.13
DJF SST	0.048	-0.054	-0.285	0.234	-0.203	-0.172	-0.224	-0.202	-0.224	-0.249	-0.136	-0.104	-0.148	0.083	0.115	0.12
	0.805	0.777	0.128	0.213	0.281	0.364	0.234	0.284	0.234	0.185	0.475	0.585	0.435	0.663	0.546	0.528
MAM SST	0.023	0.123	-0.143	0.1	0.144	0.133	0.091	-0.284	-0.296	-0.332	0.099	0.09	0.091	0.09	0.096	0.04
	0.905	0.517	0.451	0.599	0.447	0.483	0.631	0.129	0.113	0.073	0.603	0.635	0.633	0.636	0.615	0.835
JJA SST	-0.117	0.052	-0.132	0.113	0.078	0.017	0.102	-0.18	-0.236	-0.332	-0.278	-0.255	-0.181	0.051	0.066	0.086
	0.546	0.786	0.487	0.552	0.682	0.93	0.591	0.342	0.209	0.073	0.137	0.173	0.339	0.787	0.729	0.651
SON SST	-0.206	-0.05	**-0.468**	-0.043	0.115	0.119	0.089	-0.034	-0.16	-0.282	-0.339	-0.292	-0.286	0.053	0.065	0.033
	0.283	0.795	**0.009**	0.821	0.544	0.533	0.641	0.859	0.399	0.132	0.067	0.118	0.126	0.78	0.735	0.864
MAM Snow	0.135	0.248	-0.06	0.006	-0.044	0.061	-0.062	0.256	0.244	0.328	0.074	0.091	0.049	0.094	0.049	0.01
	0.484	0.194	0.758	0.974	0.822	0.753	0.749	0.18	0.202	0.082	0.704	0.638	0.799	0.629	0.802	0.96
DJF NAO	-0.081	0.105	0.113	**0.467**	0.036	-0.008	0.018	-0.11	-0.087	-0.142	-0.064	-0.069	-0.038	**0.48**	**0.411**	**0.437**
	0.675	0.581	0.553	**0.009**	0.851	0.966	0.927	0.563	0.649	0.456	0.736	0.718	0.842	**0.007**	**0.024**	**0.016**

Flow gauge:
Llanyblodwel

ANNUAL	Intensity	Frequency		
	ann	ann90	ann95	ann97
Temp	0.074	0.08	0.212	0.262
	0.702	0.679	0.27	0.17
SST	0.062	-0.042	0.123	0.176
	0.746	0.824	0.516	0.352
Snow cover	-0.141	-0.076	-0.15	-0.127
	0.466	0.695	0.437	0.513
Snow level	0.14	0.059	0.015	0.019
	0.485	0.768	0.942	0.926
NAO	-0.169	0.009	0.039	0.065
	0.373	0.961	0.837	0.734

SEASONAL	Intensity				Frequency											
	aut	win	spr	sum	aut90	aut95	aut97	win90	win95	win97	spr90	spr95	spr97	sum90	sum95	sum97
SON Temp	0.155	0.056	-0.045	-0.238	0.104	0.241	**0.435**	-0.041	-0.022	0.007	**-0.465**	**-0.431**	**-0.434**	0.196	0.23	0.117
	0.422	0.775	0.817	0.213	0.59	0.207	**0.018**	0.837	0.91	0.971	**0.011**	**0.02**	**0.019**	0.318	0.238	0.553
DJF Temp	0.148	0.1	-0.012	-0.111	-0.019	0.011	0.112	-0.183	-0.195	-0.047	-0.073	-0.147	-0.163	**0.405**	0.27	0.066
	0.445	0.611	0.952	0.566	0.922	0.954	0.563	0.352	0.32	0.811	0.707	0.447	0.399	**0.032**	0.164	0.738
MAM Temp	0.065	0.165	0.118	-0.166	0.177	0.146	0.181	-0.095	-0.01	0.171	0.13	0.074	0.068	0.155	0.091	0.04
	0.739	0.402	0.542	0.39	0.359	0.448	0.347	0.629	0.959	0.385	0.5	0.705	0.726	0.432	0.644	0.839
JJA Temp	-0.163	0.076	-0.072	0.09	-0.055	0.095	0.26	-0.044	-0.018	0.083	**-0.425**	-0.318	-0.267	0.202	0.239	0.128
	0.399	0.7	0.71	0.643	0.776	0.624	0.174	0.822	0.928	0.675	**0.022**	0.092	0.162	0.302	0.221	0.515
DJF SST	0.036	0.02	-0.186	-0.213	-0.29	-0.127	-0.021	-0.122	-0.097	-0.104	-0.133	-0.24	-0.356	0.132	0.137	0.027
	0.852	0.919	0.326	0.259	0.121	0.503	0.912	0.529	0.616	0.592	0.483	0.202	0.054	0.495	0.478	0.889
MAM SST	0.135	0.052	0.014	-0.268	0.098	0.099	0.161	-0.186	-0.105	0.068	0.115	0	-0.035	0.172	0.051	-0.005
	0.485	0.788	0.942	0.152	0.606	0.602	0.397	0.333	0.587	0.725	0.545	1	0.853	0.371	0.791	0.981
JJA SST	0.012	-0.037	0.109	-0.134	0.113	0.232	0.347	0.056	0.141	0.248	-0.332	-0.267	-0.215	0.097	0.082	-0.017
	0.95	0.847	0.565	0.481	0.554	0.217	0.06	0.773	0.467	0.195	0.073	0.154	0.254	0.615	0.673	0.93
SON SST	-0.018	-0.209	-0.029	-0.277	0.249	**0.397**	**0.522**	0.05	0.135	0.127	-0.407	-0.381	-0.311	-0.017	-0.012	-0.107
	0.925	0.278	0.879	0.138	0.185	**0.03**	**0.003**	0.795	0.486	0.513	0.026	0.038	0.095	0.932	0.952	0.581
MAM Snow	-0.002	-0.101	0.173	-0.048	0.074	0.157	0.091	0.377	0.36	0.21	-0.125	-0.119	-0.105	0.012	-0.026	-0.08
	0.991	0.609	0.368	0.805	0.704	0.416	0.638	0.048	0.06	0.283	0.517	0.539	0.588	0.953	0.897	0.684
DJF NAO	0.01	0.216	0.071	0.131	-0.113	-0.096	-0.021	-0.087	-0.113	-0.016	-0.032	-0.053	-0.054	**0.498**	**0.384**	0.296
	0.958	0.259	0.71	0.489	0.551	0.615	0.91	0.655	0.56	0.934	0.866	0.78	0.779	**0.006**	**0.04**	0.119

Flow gauge:
Llanymynech

ANNUAL	Intensity	Frequency		
	ann	ann90	ann95	ann97
Temp	0.281	0.048	0.096	0.202
	0.14	0.804	0.622	0.293
SST	0.125	-0.195	-0.163	0.029
	0.511	0.302	0.388	0.881
Snow cover	**-0.367**	-0.148	-0.116	-0.139
	0.05	0.443	0.55	0.471
Snow level	-0.059	0.078	0.221	0.155
	0.77	0.699	0.269	0.439
NAO	0.225	0.294	0.258	0.208
	0.231	0.115	0.168	0.27

SEASONAL	Intensity				Frequency											
	aut	win	spr	sum	aut90	aut95	aut97	win90	win95	win97	spr90	spr95	spr97	sum90	sum95	sum97
SON Temp	0.051	0.084	0.138	**-0.469**	-0.029	0.178	0.27	0.001	0.035	-0.029	**-0.519**	**-0.482**	**-0.508**	0.145	0.344	0.335
	0.793	0.666	0.475	**0.01**	0.881	0.356	0.156	0.994	0.858	0.883	**0.004**	**0.008**	**0.005**	0.452	0.068	0.075
DJF Temp	0.071	0.333	0.137	-0.268	-0.002	0.009	0.052	-0.235	-0.185	-0.089	-0.07	-0.092	-0.082	0.255	0.349	0.331
	0.715	0.077	0.479	0.159	0.991	0.964	0.79	0.219	0.336	0.646	0.718	0.635	0.671	0.182	0.064	0.08
MAM Temp	0.044	0.241	0.255	-0.182	0.198	0.124	0.085	-0.155	-0.112	-0.01	0.164	0.089	0.137	-0.033	0.099	0.191
	0.821	0.207	0.183	0.345	0.304	0.521	0.661	0.423	0.565	0.959	0.396	0.644	0.479	0.865	0.611	0.322
JJA Temp	-0.317	0.231	0.004	-0.233	-0.035	0.005	-0.026	-0.145	-0.175	-0.169	**-0.497**	**-0.424**	-0.34	0.227	0.371	0.32
	0.093	0.228	0.984	0.224	0.858	0.98	0.893	0.451	0.364	0.381	**0.006**	**0.022**	0.071	0.237	0.047	0.09
DJF SST	0.015	0.081	-0.073	**-0.368**	-0.301	-0.192	-0.111	-0.226	-0.123	-0.185	-0.154	-0.109	-0.134	0.076	0.205	0.215
	0.937	0.669	0.7	**0.045**	0.106	0.309	0.558	0.23	0.517	0.329	0.416	0.566	0.481	0.688	0.276	0.253
MAM SST	0.098	0.096	0.219	**-0.361**	0.031	0.033	0.068	-0.297	-0.226	-0.136	0.118	0.098	0.096	-0.031	0.155	0.188
	0.612	0.614	0.246	**0.05**	0.869	0.863	0.72	0.112	0.23	0.473	0.533	0.605	0.613	0.871	0.412	0.32
JJA SST	-0.148	0.059	0.221	**-0.385**	0.093	0.113	0.091	-0.074	-0.045	-0.045	-0.325	-0.288	-0.224	-0.053	0.149	0.194
	0.444	0.755	0.241	**0.036**	0.623	0.551	0.633	0.696	0.812	0.814	0.079	0.123	0.233	0.782	0.432	0.304
SON SST	-0.193	-0.168	0.138	**-0.577**	0.06	0.183	0.27	-0.04	-0.01	-0.123	**-0.463**	**-0.455**	**-0.446**	-0.132	0.087	0.125
	0.317	0.376	0.466	**0.001**	0.753	0.334	0.149	0.834	0.958	0.518	**0.01**	**0.011**	**0.014**	0.486	0.649	0.511
MAM Snow	-0.012	-0.213	0.158	-0.011	0.056	0.178	0.247	0.197	0.253	0.226	-0.075	0.016	-0.116	0.047	0.071	-0.048
	0.952	0.267	0.414	0.954	0.771	0.357	0.197	0.305	0.186	0.238	0.698	0.935	0.548	0.81	0.713	0.805
DJF NAO	-0.008	**0.436**	0.172	-0.016	0.01	-0.017	-0.047	-0.051	-0.072	0.027	-0.031	-0.035	0.006	**0.387**	**0.464**	**0.396**
	0.966	**0.016**	0.364	0.934	0.96	0.93	0.805	0.79	0.704	0.889	0.87	0.853	0.973	**0.034**	**0.01**	**0.03**

Flow gauge:
Montford

ANNUAL	Intensity	Frequency		
	ann	ann90	ann95	ann97
Temp	0.303	0.215	0.238	0.26
	0.11	0.263	0.213	0.173
SST	0.237	0.01	0.098	0.144
	0.206	0.959	0.606	0.447
Snow cover	-0.258	-0.194	-0.131	-0.145
	0.176	0.314	0.499	0.454
Snow level	-0.145	0.012	0.01	0.033
	0.469	0.953	0.96	0.87
NAO	0.135	0.254	0.26	0.259
	0.478	0.176	0.165	0.167

SEASONAL	Intensity				Frequency											
	aut	win	spr	sum	aut90	aut95	aut97	win90	win95	win97	spr90	spr95	spr97	sum90	sum95	sum97
SON Temp	0.004	0.105	0.066	-0.246	0.009	0.155	0.123	0.116	0.04	0.029	**-0.539**	**-0.41**	**-0.425**	0.176	0.197	0.143
	0.985	0.587	0.737	0.206	0.963	0.422	0.525	0.548	0.835	0.881	**0.003**	**0.027**	**0.022**	0.362	0.305	0.459
DJF Temp	0.136	0.327	0.08	-0.289	0.068	0.045	-0.035	-0.047	-0.119	-0.128	-0.086	-0.12	-0.197	0.302	**0.367**	0.318
	0.491	0.083	0.685	0.136	0.726	0.815	0.857	0.808	0.539	0.508	0.656	0.535	0.305	0.111	**0.05**	0.093
MAM Temp	0.054	0.217	0.232	0.092	0.234	0.062	-0.024	-0.035	-0.056	-0.067	0.13	0.12	0.087	0.074	0.163	0.2
	0.786	0.258	0.235	0.64	0.223	0.751	0.9	0.858	0.774	0.731	0.503	0.537	0.654	0.704	0.398	0.299
JJA Temp	-0.227	0.205	-0.166	0.008	0.135	0.104	-0.001	-0.071	-0.143	-0.179	**-0.424**	-0.297	-0.261	0.277	0.292	0.305
	0.245	0.285	0.398	0.969	0.484	0.59	0.996	0.714	0.458	0.354	**0.022**	0.118	0.171	0.146	0.124	0.108
DJF SST	0.003	0.181	-0.008	-0.196	-0.206	-0.15	-0.203	-0.077	-0.164	-0.149	-0.124	-0.158	-0.285	0.239	0.268	0.234
	0.987	0.338	0.969	0.308	0.275	0.428	0.282	0.687	0.388	0.431	0.514	0.404	0.127	0.203	0.152	0.213
MAM SST	0.118	0.16	0.227	0.058	0.124	0.034	-0.068	-0.119	-0.14	-0.091	0.075	0.076	-0.025	0.149	0.188	0.145
	0.543	0.397	0.237	0.765	0.515	0.859	0.722	0.531	0.46	0.632	0.695	0.689	0.896	0.433	0.32	0.446
JJA SST	-0.144	0.115	0.05	0.072	0.205	0.191	0.091	0.084	-0.048	-0.09	-0.301	-0.201	-0.218	0.066	0.16	0.166
	0.457	0.545	0.797	0.709	0.276	0.311	0.631	0.66	0.8	0.638	0.107	0.287	0.246	0.728	0.398	0.38
SON SST	-0.283	-0.133	0.017	0.136	0.183	0.271	0.175	0.09	-0.084	-0.13	**-0.449**	**-0.388**	**-0.416**	0.028	0.036	0.027
	0.136	0.484	0.931	0.483	0.333	0.147	0.355	0.637	0.659	0.495	**0.013**	**0.034**	**0.022**	0.883	0.848	0.888
MAM Snow	-0.012	0.116	0.194	-0.06	0.032	0.265	0.346	0.274	0.31	**0.424**	-0.03	-0.065	-0.128	0.079	0.007	0.001
	0.953	0.55	0.323	0.76	0.867	0.164	0.066	0.15	0.101	**0.022**	0.876	0.738	0.51	0.682	0.971	0.998
DJF NAO	0.1	0.306	0.097	-0.187	0.044	-0.036	-0.108	0.044	0.001	0.029	-0.018	-0.004	-0.023	**0.408**	**0.422**	**0.4**
	0.606	0.1	0.617	0.332	0.817	0.85	0.569	0.818	0.994	0.88	0.926	0.981	0.906	**0.025**	**0.02**	**0.028**

Flow gauge:
Rhos-y-Pentref

ANNUAL	Intensity	Frequency		
	ann	ann90	ann95	ann97
Temp	0.371	0.101	0.312	0.322
	0.047	0.603	0.099	0.088
SST	0.228	-0.104	0.135	0.204
	0.225	0.583	0.478	0.28
Snow cover	-0.271	-0.253	-0.353	-0.25
	0.156	0.185	0.06	0.19
Snow level	-0.207	-0.005	-0.051	-0.059
	0.3	0.982	0.799	0.769
NAO	0.094	0.266	0.187	0.186
	0.622	0.155	0.323	0.326

SEASONAL	Intensity				Frequency											
	aut	win	spr	sum	aut90	aut95	aut97	win90	win95	win97	spr90	spr95	spr97	sum90	sum95	sum97
SON Temp	0.019	0.364	-0.008	-0.434	0.03	0.172	0.256	-0.095	0.029	0.073	**-0.493**	**-0.472**	**-0.394**	0.28	0.344	0.252
	0.92	0.052	0.968	0.019	0.877	0.372	0.18	0.625	0.881	0.707	**0.007**	**0.01**	**0.034**	0.141	0.068	0.187
DJF Temp	0.111	0.421	0.152	-0.154	0.189	0.129	0.1	-0.196	-0.288	-0.099	-0.069	-0.091	-0.094	**0.463**	**0.388**	0.273
	0.567	0.023	0.431	0.426	0.327	0.504	0.606	0.308	0.13	0.61	0.724	0.639	0.627	**0.012**	**0.037**	0.152
MAM Temp	-0.071	**0.367**	0.211	-0.059	0.322	0.258	0.234	-0.27	-0.229	-0.034	0.086	0.096	0.018	0.178	0.133	0.072
	0.714	**0.05**	0.272	0.761	0.088	0.176	0.223	0.157	0.232	0.861	0.655	0.622	0.928	0.357	0.491	0.709
JJA Temp	-0.222	0.297	-0.114	-0.1	-0.023	-0.023	-0.079	**-0.417**	-0.326	-0.273	**-0.369**	-0.361	-0.357	**0.378**	0.333	0.165
	0.247	0.117	0.557	0.604	0.905	0.907	0.682	**0.025**	0.084	0.152	**0.049**	0.054	0.058	**0.043**	0.078	0.393
DJF SST	0.086	0.298	-0.001	-0.29	-0.072	-0.088	-0.078	-0.199	-0.289	-0.08	-0.206	-0.173	-0.158	0.195	0.265	0.233
	0.657	0.109	0.994	0.12	0.704	0.643	0.683	0.292	0.122	0.675	0.275	0.361	0.403	0.301	0.156	0.216
MAM SST	0.012	0.357	0.212	-0.236	0.226	0.211	0.181	-0.318	-0.283	-0.012	0.091	0.11	0.042	0.264	0.241	0.201
	0.95	0.053	0.261	0.209	0.23	0.264	0.338	0.087	0.13	0.951	0.631	0.564	0.827	0.158	0.2	0.288
JJA SST	-0.061	0.247	0.128	-0.19	0.088	0.141	0.057	-0.312	-0.26	-0.039	-0.236	-0.233	-0.265	0.207	0.19	0.082
	0.754	0.189	0.501	0.315	0.642	0.457	0.765	0.093	0.165	0.839	0.209	0.215	0.157	0.273	0.315	0.667
SON SST	-0.132	0.172	-0.009	**-0.52**	0.117	0.237	0.201	-0.158	-0.15	0.051	-0.36	**-0.365**	**-0.368**	0.153	0.137	0.039
	0.493	0.363	0.964	**0.003**	0.54	0.207	0.287	0.404	0.43	0.788	0.051	**0.047**	**0.045**	0.419	0.469	0.837
MAM Snow	0.298	-0.008	0.15	-0.028	-0.17	0.066	0.026	0.293	0.323	0.34	0.014	-0.028	0.038	0.075	0.185	0.22
	0.116	0.968	0.439	0.885	0.378	0.732	0.893	0.123	0.088	0.071	0.941	0.884	0.845	0.698	0.338	0.251
DJF NAO	-0.025	0.277	0.178	0.079	0.139	0.013	-0.052	-0.088	-0.09	-0.089	-0.03	-0.031	-0.046	**0.436**	0.355	0.226
	0.897	0.139	0.347	0.68	0.464	0.946	0.784	0.643	0.636	0.642	0.875	0.869	0.809	**0.016**	0.054	0.229

APPENDIX 3: CROSS SECTIONS

Cross-sections for the HEC-HMS Muskingum-Cunge routing model. Table A3 refers to Section 6.3 and links to the reaches listed in Table 6.1.

Table A3 Cross-sections for each reach of the HEC-HMS model

Reach: R11910	
Station	Elevation
0	310
136	300
204	300
206	299
212	298.5
214	300
279	300
502	310

Reach: R11950	
Station	Elevation
0	70
185	70
700	65
705	61
722	60
727	65
844	70
854	75

Reach: R7870	
Station	Elevation
0	270
32	260
69	260
69.1	234.4
668.9	234.4
669	260
682	260
694	270

Reach: R7910	
Station	Elevation
0	65
752	60
823	55
825.5	51
875.5	51
878	55
1287	60
1472	65

Reach: R7950	
Station	Elevation
0	90
115	80
567	75
569.25	73.4
594.25	72.5
596.5	75
621.5	80
833.5	85

Reach: R11920	
Station	Elevation
0	290
66	280
117	280
118	278
138	278
139	280
214	280
264	290

Reach: R7830	
Station	Elevation
0	80
206	70
300	60
322.5	58.4
327.25	57.5
329.5	60
488.5	70
799.5	75

Reach: R7890	
Station	Elevation
0	60
501	60
537	60
542	56
559	55
564	60
661	60
1586	60

Reach: R7920	
Station	Elevation
0	60
168	60
1017	60
1017.1	56
1019.4	58
1019.5	60
1861.5	65
1898.5	70

Reach: R8010	
Station	Elevation
0	130
33	120
114	110
118	106
131.5	108
135.5	110
200.5	120
238.5	130

Reach: R11940	
Station	Elevation
0	230
57	220
63	220
66	218.5
82	218
85	220
133	220
169	230

Reach: R7840	
Station	Elevation
0	65
317	65
833	65
838	61

855	55
860	60
2254	60
2487	60

Reach: R7900	
Station	Elevation
0	60
39	60
983	60
994.5	57
1019.5	57.8
1031	60
1852	60
2632	60

Reach: R7940	
Station	Elevation
0	140
18	130
58	120
59.75	115
82.25	113
94	120
110	130
130	140

Reach: R8040	
Station	Elevation
0	75
30	70
541	65
546	62
566	62
571	65
1530	70
1621	75

Reach: R8060	
Station	Elevation
0	80
654	75
683	75
688	73
722	72.5
727	75
937	75
977	75

Reach: R8100	
Station	Elevation
0	110
162	100
284	90
288.5	87.5
327.5	88.2
332	90
820	100
858	110

Reach: R8160	
Station	Elevation
0	180
21	170
95	170
98.75	168
116.25	169.5
120	170
275	170
588	180

Reach: R8180	
Station	Elevation
0	200
54	190
70	190
72	188
90	188
92	190
131	190
203	200

Reach: R8230	
Station	Elevation
0	220
68	210
101	210
102	208
110	208
111	210
129	210
196	220

Reach: R8080	
Station	Elevation
0	85
267	80
772	80
776.5	77.5
815.5	78.2
820	80
1059	80
1310	80

Reach: R8150	
Station	Elevation
0	170
106	160
424	160
438	160
458	158.7
472	160
616	160
647	170

Reach: R8170	
Station	Elevation
0	150
153	140
216	140
226	136
248	130
258	140
455	140
491	150

Reach: R8190	
Station	Elevation
0	170
111	160
184	150
198	150
218	148.7
232	150
477	160
527	170

Reach: R8250	
Station	Elevation
0	200
68	190
200	180
202	178
220	179.5
222	180
363	190
538	200

APPENDIX 4: TEMPERATURE CHANGE PREDICTIONS

Predicted changes in temperature for November and December in the Severn Uplands subbasins under future UKCIP02 emission scenarios. Table A4 refers to Section 8.3.

Table A4 Percentage change in temperature for (a) predicted, (b) low uncertainty margin, and (c) high uncertainty margin

(a) predicted

November		Low			Medium-Low			Medium-High			High		
Subbasin	**Present**	**2020**	**2050**	**2080**	**2020**	**2050**	**2080**	**2020**	**2050**	**2080**	**2020**	**2050**	**2080**
Banwy	5.48	6.23	6.83	7.4	6.32	7.08	7.72	6.32	7.27	8.64	6.38	7.63	9.21
Camlad	6.06	6.83	7.43	8.01	6.92	7.68	8.34	6.92	7.88	9.26	6.97	8.24	9.83
Clywedog	5.03	5.79	6.38	6.95	5.88	6.63	7.28	5.88	6.83	8.19	5.93	7.18	8.76
Dulas	5.16	5.92	6.52	7.09	6.01	6.77	7.41	6.01	6.96	8.33	6.07	7.32	8.9
Hafren	4.27	5.03	5.62	6.19	5.12	5.87	6.52	5.12	6.07	7.43	5.17	6.42	8
Lake Vyrnwy	5.42	6.18	6.77	7.34	6.27	7.02	7.67	6.27	7.22	8.58	6.32	7.57	9.15
Lower Vyrnwy Lat	6.18	6.94	7.54	8.11	7.03	7.79	8.44	7.03	7.99	9.36	7.09	8.35	9.93
Mid Vyrnwy Lat	6.02	6.78	7.38	7.95	6.87	7.63	8.27	6.87	7.82	9.19	6.93	8.18	9.76
Mule Lat	6.42	7.18	7.78	8.35	7.27	8.03	8.68	7.27	8.23	9.6	7.33	8.59	10.17
Rhiw	5.94	6.7	7.3	7.87	6.79	7.55	8.2	6.79	7.75	9.12	6.85	8.11	9.69
Tanat	5.4	6.16	6.75	7.32	6.25	7	7.65	6.25	7.2	8.56	6.3	7.55	9.13
Trannon	5.52	6.28	6.88	7.45	6.37	7.13	7.77	6.37	7.32	8.69	6.43	7.68	9.26
Vyrnwy Conf Lat	6.67	7.44	8.05	8.62	7.53	8.3	8.95	7.53	8.49	9.88	7.59	8.86	10.46
Welshpool Lat	6.51	7.28	7.88	8.45	7.36	8.13	8.78	7.36	8.32	9.7	7.42	8.68	10.27

December		Low			Medium-Low			Medium-High			High		
Subbasin	**Present**	**2020**	**2050**	**2080**	**2020**	**2050**	**2080**	**2020**	**2050**	**2080**	**2020**	**2050**	**2080**
Banwy	3.85	4.5	5.01	5.5	4.57	5.23	5.78	4.57	5.39	6.56	4.62	5.7	7.05
Camlad	4.22	4.88	5.39	5.89	4.95	5.61	6.17	4.95	5.78	6.96	5	6.09	7.45
Clywedog	3.35	4	4.51	5	4.07	4.73	5.28	4.07	4.89	6.06	4.12	5.2	6.55
Dulas	3.52	4.17	4.69	5.17	4.25	4.9	5.45	4.25	5.07	6.24	4.3	5.37	6.73
Hafren	2.66	3.31	3.82	4.31	3.38	4.04	4.59	3.38	4.2	5.37	3.43	4.51	5.86
Lake Vyrnwy	3.85	4.5	5.01	5.5	4.57	5.23	5.78	4.57	5.39	6.56	4.62	5.7	7.05
Lower Vyrnwy Lat	4.39	5.05	5.56	6.05	5.12	5.78	6.33	5.12	5.94	7.12	5.17	6.25	7.61
Mid Vyrnwy Lat	4.27	4.92	5.44	5.92	5	5.65	6.2	5	5.82	6.99	5.05	6.12	7.48
Mule Lat	4.56	5.21	5.73	6.21	5.29	5.94	6.49	5.29	6.11	7.28	5.34	6.41	7.77
Rhiw	4.22	4.87	5.39	5.87	4.95	5.6	6.15	4.95	5.77	6.94	5	6.07	7.43
Tanat	3.74	4.39	4.9	5.39	4.46	5.12	5.67	4.46	5.28	6.45	4.51	5.59	6.94
Trannon	3.79	4.44	4.96	5.44	4.52	5.17	5.72	4.52	5.34	6.51	4.57	5.64	7
Vyrnwy Conf Lat	4.72	5.38	5.9	6.4	5.46	6.12	6.68	5.46	6.29	7.48	5.51	6.6	7.97
Welshpool Lat	4.67	5.33	5.84	6.34	5.4	6.06	6.62	5.4	6.23	7.41	5.45	6.54	7.9

(b) Low uncertainty margin

November		Low			Medium-Low			Medium-High			High		
Subbasin	**Present**	**2020**	**2050**	**2080**	**2020**	**2050**	**2080**	**2020**	**2050**	**2080**	**2020**	**2050**	**2080**
Banwy	5.48	5.73	6.33	6.9	5.32	6.08	6.72	4.82	5.77	7.14	4.38	5.63	7.21
Camlad	6.06	6.33	6.93	7.51	5.92	6.68	7.34	5.42	6.38	7.76	4.97	6.24	7.83
Clywedog	5.03	5.29	5.88	6.45	4.88	5.63	6.28	4.38	5.33	6.69	3.93	5.18	6.76
Dulas	5.16	5.42	6.02	6.59	5.01	5.77	6.41	4.51	5.46	6.83	4.07	5.32	6.9
Hafren	4.27	4.53	5.12	5.69	4.12	4.87	5.52	3.62	4.57	5.93	3.17	4.42	6
Lake Vyrnwy	5.42	5.68	6.27	6.84	5.27	6.02	6.67	4.77	5.72	7.08	4.32	5.57	7.15
Lower Vyrnwy Lat	6.18	6.44	7.04	7.61	6.03	6.79	7.44	5.53	6.49	7.86	5.09	6.35	7.93
Mid Vyrnwy Lat	6.02	6.28	6.88	7.45	5.87	6.63	7.27	5.37	6.32	7.69	4.93	6.18	7.76
Mule Lat	6.42	6.68	7.28	7.85	6.27	7.03	7.68	5.77	6.73	8.1	5.33	6.59	8.17
Rhiw	5.94	6.2	6.8	7.37	5.79	6.55	7.2	5.29	6.25	7.62	4.85	6.11	7.69
Tanat	5.4	5.66	6.25	6.82	5.25	6	6.65	4.75	5.7	7.06	4.3	5.55	7.13
Trannon	5.52	5.78	6.38	6.95	5.37	6.13	6.77	4.87	5.82	7.19	4.43	5.68	7.26
Vyrnwy Conf Lat	6.67	6.94	7.55	8.12	6.53	7.3	7.95	6.03	6.99	8.38	5.59	6.86	8.46
Welshpool Lat	6.51	6.78	7.38	7.95	6.36	7.13	7.78	5.86	6.82	8.2	5.42	6.68	8.27

December		Low			Medium-Low			Medium-High			High		
Subbasin	**Present**	**2020**	**2050**	**2080**	**2020**	**2050**	**2080**	**2020**	**2050**	**2080**	**2020**	**2050**	**2080**
Banwy	3.85	4	4.51	5	3.57	4.23	4.78	3.07	3.89	5.06	2.62	3.7	5.05
Camlad	4.22	4.38	4.89	5.39	3.95	4.61	5.17	3.45	4.28	5.46	3	4.09	5.45
Clywedog	3.35	3.5	4.01	4.5	3.07	3.73	4.28	2.57	3.39	4.56	2.12	3.2	4.55
Dulas	3.52	3.67	4.19	4.67	3.25	3.9	4.45	2.75	3.57	4.74	2.3	3.37	4.73
Hafren	2.66	2.81	3.32	3.81	2.38	3.04	3.59	1.88	2.7	3.87	1.43	2.51	3.86
Lake Vyrnwy	3.85	4	4.51	5	3.57	4.23	4.78	3.07	3.89	5.06	2.62	3.7	5.05
Lower Vyrnwy Lat	4.39	4.55	5.06	5.55	4.12	4.78	5.33	3.62	4.44	5.62	3.17	4.25	5.61
Mid Vyrnwy Lat	4.27	4.42	4.94	5.42	4	4.65	5.2	3.5	4.32	5.49	3.05	4.12	5.48
Mule Lat	4.56	4.71	5.23	5.71	4.29	4.94	5.49	3.79	4.61	5.78	3.34	4.41	5.77
Rhiw	4.22	4.37	4.89	5.37	3.95	4.6	5.15	3.45	4.27	5.44	3	4.07	5.43
Tanat	3.74	3.89	4.4	4.89	3.46	4.12	4.67	2.96	3.78	4.95	2.51	3.59	4.94
Trannon	3.79	3.94	4.46	4.94	3.52	4.17	4.72	3.02	3.84	5.01	2.57	3.64	5
Vyrnwy Conf Lat	4.72	4.88	5.4	5.9	4.46	5.12	5.68	3.96	4.79	5.98	3.51	4.6	5.97
Welshpool Lat	4.67	4.83	5.34	5.84	4.4	5.06	5.62	3.9	4.73	5.91	3.45	4.54	5.9

(c) High uncertainty margin

November		Low			Medium-Low			Medium-High			High		
Subbasin	**Present**	**2020**	**2050**	**2080**	**2020**	**2050**	**2080**	**2020**	**2050**	**2080**	**2020**	**2050**	**2080**
Banwy	5.48	6.73	7.33	7.9	7.32	8.08	8.72	7.82	8.77	10.14	8.38	9.63	11.21
Camlad	6.06	7.33	7.93	8.51	7.92	8.68	9.34	8.42	9.38	10.76	8.97	10.24	11.83
Clywedog	5.03	6.29	6.88	7.45	6.88	7.63	8.28	7.38	8.33	9.69	7.93	9.18	10.76
Dulas	5.16	6.42	7.02	7.59	7.01	7.77	8.41	7.51	8.46	9.83	8.07	9.32	10.9
Hafren	4.27	5.53	6.12	6.69	6.12	6.87	7.52	6.62	7.57	8.93	7.17	8.42	10
Lake Vyrnwy	5.42	6.68	7.27	7.84	7.27	8.02	8.67	7.77	8.72	10.08	8.32	9.57	11.15
Lower Vyrnwy Lat	6.18	7.44	8.04	8.61	8.03	8.79	9.44	8.53	9.49	10.86	9.09	10.35	11.93
Mid Vyrnwy Lat	6.02	7.28	7.88	8.45	7.87	8.63	9.27	8.37	9.32	10.69	8.93	10.18	11.76
Mule Lat	6.42	7.68	8.28	8.85	8.27	9.03	9.68	8.77	9.73	11.1	9.33	10.59	12.17
Rhiw	5.94	7.2	7.8	8.37	7.79	8.55	9.2	8.29	9.25	10.62	8.85	10.11	11.69
Tanat	5.4	6.66	7.25	7.82	7.25	8	8.65	7.75	8.7	10.06	8.3	9.55	11.13
Trannon	5.52	6.78	7.38	7.95	7.37	8.13	8.77	7.87	8.82	10.19	8.43	9.68	11.26
Vyrnwy Conf Lat	6.67	7.94	8.55	9.12	8.53	9.3	9.95	9.03	9.99	11.38	9.59	10.86	12.46
Welshpool Lat	6.51	7.78	8.38	8.95	8.36	9.13	9.78	8.86	9.82	11.2	9.42	10.68	12.27

December		Low			Medium-Low			Medium-High			High		
Subbasin	**Present**	**2020**	**2050**	**2080**	**2020**	**2050**	**2080**	**2020**	**2050**	**2080**	**2020**	**2050**	**2080**
Banwy	3.85	5	5.51	6	5.57	6.23	6.78	6.07	6.89	8.06	6.62	7.7	9.05
Camlad	4.22	5.38	5.89	6.39	5.95	6.61	7.17	6.45	7.28	8.46	7	8.09	9.45
Clywedog	3.35	4.5	5.01	5.5	5.07	5.73	6.28	5.57	6.39	7.56	6.12	7.2	8.55
Dulas	3.52	4.67	5.19	5.67	5.25	5.9	6.45	5.75	6.57	7.74	6.3	7.37	8.73
Hafren	2.66	3.81	4.32	4.81	4.38	5.04	5.59	4.88	5.7	6.87	5.43	6.51	7.86
Lake Vyrnwy	3.85	5	5.51	6	5.57	6.23	6.78	6.07	6.89	8.06	6.62	7.7	9.05
Lower Vyrnwy Lat	4.39	5.55	6.06	6.55	6.12	6.78	7.33	6.62	7.44	8.62	7.17	8.25	9.61
Mid Vyrnwy Lat	4.27	5.42	5.94	6.42	6	6.65	7.2	6.5	7.32	8.49	7.05	8.12	9.48
Mule Lat	4.56	5.71	6.23	6.71	6.29	6.94	7.49	6.79	7.61	8.78	7.34	8.41	9.77
Rhiw	4.22	5.37	5.89	6.37	5.95	6.6	7.15	6.45	7.27	8.44	7	8.07	9.43
Tanat	3.74	4.89	5.4	5.89	5.46	6.12	6.67	5.96	6.78	7.95	6.51	7.59	8.94
Trannon	3.79	4.94	5.46	5.94	5.52	6.17	6.72	6.02	6.84	8.01	6.57	7.64	9
Vyrnwy Conf Lat	4.72	5.88	6.4	6.9	6.46	7.12	7.68	6.96	7.79	8.98	7.51	8.6	9.97
Welshpool Lat	4.67	5.83	6.34	6.84	6.4	7.06	7.62	6.9	7.73	8.91	7.45	8.54	9.9

APPENDIX 5: UNCERTAINTY MARGIN PREDICTIONS

Predicted flow changes under the low and high uncertainty margins for precipitation and temperature. Table A5 refers to Section 8.6.

Table A5 Percentage change in peak flow and output volume predictions under changing precipitation and temperature uncertainty margins for (a) gauge- and (b) radar- driven hydrological modelling

(a) gauge

Decrease in precipitation – decrease in temperature

	Low			Medium-Low			Medium-High			High		
	2020	2050	2080	2020	2050	2080	2020	2050	2080	2020	2050	2080
Peak Flow												
Rhos-y-Pentref	-2.09	2.09	5.76	-8.38	-3.14	1.05	-14.14	-8.38	-0.52	-19.90	-13.61	-4.71
Abermule	-2.26	1.59	5.09	-9.51	-4.42	-0.62	-15.38	-10.04	-3.41	-22.30	-15.76	-8.60
Llanymynech	-1.87	1.75	5.53	-10.76	-4.35	-0.38	-16.36	-10.76	-2.97	-23.30	-16.63	-8.05
Montford	-2.25	1.72	5.60	-5.74	-4.69	-0.56	-11.96	-6.01	-3.46	-18.10	-12.34	-8.82
Volume												
Rhos-y-Pentref	-3.08	0.47	3.71	-10.68	-5.68	0.46	-17.29	-12.26	-5.26	-24.36	-18.29	-10.49
Abermule	-3.56	-0.60	2.11	-11.28	-7.04	-1.59	-17.75	-13.66	-8.03	-24.79	-19.78	-13.81
Llanymynech	-3.09	-0.54	2.12	-11.24	-6.69	-1.66	-17.07	-13.04	-7.55	-23.96	-19.09	-12.96
Montford	-3.35	-0.74	1.84	-11.30	-7.08	-1.80	-17.36	-13.42	-8.10	-24.42	-19.57	-13.62

Decrease in precipitation – increase in temperature

	Low			Medium-Low			Medium-High			High		
	2020	2050	2080	2020	2050	2080	2020	2050	2080	2020	2050	2080
Peak Flow												
Rhos-y-Pentref	-2.09	2.09	5.76	-8.90	-3.14	1.05	-14.14	-8.90	-1.05	-20.42	-13.61	-5.24
Abermule	-2.26	1.59	5.09	-9.51	-4.47	-0.62	-15.38	-10.04	-3.41	-22.35	-15.81	-8.60
Llanymynech	-1.87	1.75	5.53	-10.76	-4.35	-0.38	-16.40	-10.79	-2.97	-23.34	-16.67	-8.09
Montford	-2.28	1.69	5.58	-5.79	-4.72	-0.59	-12.01	-6.06	-3.51	-18.18	-12.39	-8.90
Volume												
Rhos-y-Pentref	-3.41	0.19	3.44	-11.12	-6.17	-0.08	-17.92	-12.90	-5.87	-25.09	-19.20	-11.46
Abermule	-3.85	-0.94	1.78	-11.85	-7.64	-2.21	-18.54	-14.50	-8.82	-25.78	-20.80	-14.82
Llanymynech	-3.44	-0.86	1.77	-11.83	-7.31	-2.31	-18.06	-13.94	-8.46	-25.02	-20.16	-13.90
Montford	-3.80	-1.18	1.40	-12.08	-7.96	-2.67	-18.62	-14.64	-9.28	-25.95	-21.11	-15.18

Increase in precipitation – increase in temperature

	Low			Medium-Low			Medium-High			High		
	2020	2050	2080	2020	2050	2080	2020	2050	2080	2020	2050	2080
Peak Flow												
Rhos-y-Pentref	11.52	15.18	15.18	18.85	24.61	28.80	25.13	31.94	42.93	31.94	41.88	54.45
Abermule	12.54	16.72	18.89	20.62	26.38	31.28	28.35	36.09	47.38	36.67	47.33	60.69
Llanymynech	12.47	16.86	20.86	20.71	26.58	27.65	28.99	35.96	47.25	36.50	47.03	60.34
Montford	13.73	18.42	21.86	22.55	28.88	34.27	31.19	39.39	51.92	39.98	51.62	65.97
Volume												
Rhos-y-Pentref	12.08	15.68	16.31	19.82	24.78	29.04	27.20	33.85	43.30	35.16	43.97	55.76
Abermule	11.63	14.86	16.71	19.88	24.46	28.38	27.94	33.99	42.53	36.35	44.41	54.26
Llanymynech	10.88	14.03	16.89	18.61	22.84	26.40	25.93	31.53	39.80	33.72	41.55	51.70
Montford	11.12	14.26	16.74	19.04	23.34	27.00	26.65	32.36	40.64	34.71	42.60	52.59

Increase in precipitation – decrease in temperature

	Low			Medium-Low			Medium-High			High		
	2020	**2050**	**2080**	**2020**	**2050**	**2080**	**2020**	**2050**	**2080**	**2020**	**2050**	**2080**
Peak Flow												
Rhos-y-Pentref	11.52	15.71	15.71	18.85	24.61	29.32	25.13	32.46	42.93	32.46	42.41	54.97
Abermule	12.54	16.72	18.93	20.62	26.38	31.28	28.35	36.09	47.43	36.71	47.38	60.69
Llanymynech	12.47	16.86	20.86	20.71	26.62	31.46	28.99	36.00	47.29	36.54	47.06	60.37
Montford	13.78	18.42	21.88	22.61	28.94	34.33	31.27	39.45	51.97	40.09	51.70	66.08
Volume												
Rhos-y-Pentref	12.48	15.99	16.63	20.67	25.70	29.86	28.54	35.19	44.54	36.94	45.84	57.56
Abermule	11.91	15.19	17.12	20.49	25.12	29.04	28.88	34.98	43.57	37.63	45.79	55.74
Llanymynech	11.23	14.37	17.24	19.19	23.50	27.09	26.79	32.41	40.85	34.82	42.72	53.12
Montford	11.56	14.70	17.21	19.85	24.22	27.88	27.91	33.65	42.00	36.39	44.38	54.61

(b) radar

Decrease in precipitation – decrease in temperature

	Low			Medium-Low			Medium-High			High		
	2020	**2050**	**2080**	**2020**	**2050**	**2080**	**2020**	**2050**	**2080**	**2020**	**2050**	**2080**
Peak Flow												
Rhos-y-Pentref	6.48	8.10	9.72	-0.41	1.62	9.72	-7.29	-4.86	-1.22	-14.17	-11.34	-7.29
Abermule	2.91	7.85	12.43	-5.38	0.88	6.17	-15.61	-7.05	3.44	-18.34	-15.61	-2.47
Llanymynech	-4.56	-0.75	2.90	-11.15	-6.66	-2.71	-18.15	-9.45	-5.27	-24.77	-18.34	-10.13
Montford	0.84	4.06	7.21	-4.81	-0.92	2.48	-10.96	-6.31	0.33	-16.97	-11.10	-3.87
Volume												
Rhos-y-Pentref	7.85	10.56	13.25	0.22	3.46	19.93	-7.74	-3.85	1.61	-15.35	-10.68	-4.87
Abermule	1.91	5.52	8.22	-5.56	-1.75	4.97	-13.31	-8.87	-2.40	-20.78	-15.32	-8.40
Llanymynech	-3.05	-0.32	1.94	-9.83	-6.60	-1.10	-16.87	-13.10	-7.65	-23.63	-19.02	-13.17
Montford	4.45	7.46	10.08	-3.01	0.55	6.84	-10.81	-6.66	-0.65	-18.25	-13.18	-6.74

Decrease in precipitation – increase in temperature

	Low			Medium-Low			Medium-High			High		
	2020	2050	2080	2020	2050	2080	2020	2050	2080	2020	2050	2080
Peak Flow												
Rhos-y-Pentref	6.48	8.10	9.72	-0.41	1.62	9.72	-7.29	-4.86	-1.22	-14.17	-11.34	-7.29
Abermule	2.91	7.85	12.43	-5.38	0.88	6.17	-15.70	-7.14	3.35	-18.43	-15.61	-2.47
Llanymynech	-4.56	-0.75	2.90	-11.15	-6.66	-2.71	-18.15	-9.86	-8.58	-24.77	-18.37	-10.17
Montford	0.86	4.06	7.21	-4.84	-0.95	2.45	-10.99	-6.32	-1.86	-17.00	-11.13	-3.90
Volume												
Rhos-y-Pentref	7.61	10.39	13.05	-0.09	3.08	11.07	-8.30	-4.45	1.03	-15.92	-11.29	-5.48
Abermule	1.64	4.82	7.90	-6.12	-2.32	4.36	-14.13	-9.67	-3.24	-21.71	-16.34	-9.49
Llanymynech	-3.35	-0.62	1.94	-10.35	-7.15	-1.69	-17.71	-13.93	-8.58	-24.71	-20.17	-14.47
Montford	4.07	7.06	9.89	-3.77	-0.25	6.07	-11.89	-7.77	-1.86	-19.64	-14.65	-8.39

Increase in precipitation – increase in temperature

	Low			Medium-Low			Medium-High			High		
	2020	2050	2080	2020	2050	2080	2020	2050	2080	2020	2050	2080
Peak Flow												
Rhos-y-Pentref	20.65	22.27	24.29	27.94	31.98	44.13	34.82	38.46	43.32	42.15	46.96	52.63
Abermule	20.02	25.31	30.42	29.28	36.60	42.95	37.92	47.35	61.29	47.18	60.41	75.84
Llanymynech	13.91	18.39	22.68	22.33	28.37	33.59	30.13	38.08	49.57	38.47	49.45	63.17
Montford	14.58	19.17	23.57	23.04	29.35	34.84	31.02	39.29	51.59	39.57	51.31	62.74
Volume												
Rhos-y-Pentref	24.41	27.55	35.44	33.39	39.09	51.31	42.01	47.77	55.47	51.26	58.79	68.10
Abermule	18.06	21.72	30.47	26.91	32.96	42.66	35.41	42.06	51.69	44.38	53.63	64.81
Llanymynech	13.01	14.49	24.27	19.26	24.31	31.77	26.66	32.12	39.90	34.56	42.04	51.48
Montford	20.37	23.76	35.25	29.09	34.70	43.54	31.02	43.32	52.05	46.05	54.41	64.82

Increase in precipitation – decrease in temperature

	Low			Medium-Low			Medium-High			High		
	2020	**2050**	**2080**	**2020**	**2050**	**2080**	**2020**	**2050**	**2080**	**2020**	**2050**	**2080**
Peak Flow												
Rhos-y-Pentref	20.65	22.27	22.27	27.94	32.39	44.13	35.22	38.46	43.32	42.32	46.96	52.63
Abermule	20.02	25.31	30.34	29.28	36.60	42.95	38.01	47.44	61.29	47.18	60.49	75.93
Llanymynech	10.43	14.38	18.49	18.07	24.02	28.99	25.72	38.04	44.50	33.77	44.39	57.64
Montford	14.61	19.23	23.48	23.07	29.38	34.86	31.05	39.34	51.64	39.62	51.39	62.80
Volume												
Rhos-y-Pentref	24.70	27.83	30.75	34.21	39.91	52.19	43.36	49.16	56.80	53.05	60.68	70.07
Abermule	18.35	22.07	25.57	27.60	33.66	43.39	36.51	43.16	52.81	45.75	55.16	66.43
Llanymynech	11.76	14.82	17.35	19.96	25.39	32.51	27.81	33.18	41.07	36.08	43.60	53.17
Montford	20.80	24.19	27.18	29.94	35.59	44.43	38.68	44.76	53.51	47.78	56.26	59.58

APPENDIX 6: PEER-REVIEWED PUBLICATIONS FROM THESIS RESEARCH

Biggs, E.M., Atkinson, P.M., De Roure, D.C., 2009. Modelling the hydrological extreme event of summer 2007 in the Severn Uplands from gauge and radar rainfall sources. Proceedings of the 12th Biennial International Conference of the Euromediterranean Network of Experimental and Representative Basins (ERB) Kraków, Poland, 18–20 September 2008. *IHP-VII Technical Documents in Hydrology* **84** UNESCO Working Series SC-2009/WS/11, UNESCO, Paris

This publication used data analysis which was not included within the thesis itself, but the research contributed to the selection of methods and analysis subsequently performed.

MODELLING THE HYDROLOGICAL EXTREME EVENT OF SUMMER 2007 IN THE SEVERN UPLANDS FROM GAUGE AND RADAR RAINFALL SOURCES

E.M. Biggs [1], P.M. Atkinson[1] and D.C. De Roure[2]

[1] *School of Geography, University of Southampton, Southampton, SO17 1BJ, UK*

[2] *School of Electronics and Computer Science, University of Southampton, Southampton, SO17 1BJ, UK*

Corresponding author: Eloise Biggs, e-mail: Eloise.Biggs@soton.ac.uk

ABSTRACT

This paper provides a comparison of gauge interpolated and radar derived precipitation data sources for an upland catchment in the UK for a time period when extreme hydrological conditions were prevalent. Subsequently, a performance measure was used to evaluate the accuracy of hydrological simulation of extreme conditions using the two independent precipitation data sources within a HEC-HMS modelling framework. Discrepancies between gauge and radar time-series precipitation records were found to coincide with elevation, spatial distribution of precipitation and distance from the radar source. The Nash-Sutcliffe performance measure indicated that despite the higher temporal and spatial resolution of the radar data, interpolated gauging station records produced comparative accuracy when replicating the extreme hydrological event of Summer 2007.

Key words: extremes, radar rainfall, HEC-HMS, rainfall-runoff modelling

INTRODUCTION

Global changes in climate are likely to induce an increase in the frequency and magnitude of hydrological extremes (Cunderlik and Simonovic, 2005). There is evidence to suggest that both precipitation and flow extremes have increased in the UK over the last 30–40 years (DEFRA, 2001; Osborn *et al*., 2000; Fowler and Kilsby, 2003). Flooding is the most damaging and costly natural hazard in the UK, costing the nation billions of pounds every year (Brown and Damery, 2002) and extreme floods such as those experienced in 1998, 2000 and 2007 are likely to occur more frequently due to changes in precipitation. Accurate monitoring and modelling of these extreme events is essential if future extremes under a changing climate are to be characterised accurately. The quality of hydrological forecasts will, in general, depend on the quality of the simulation model, the accuracy of the precipitation and boundary forecasts, and the efficiency of the data assimilation procedure. Recent efforts in fluvial forecasting have focused on quantifying rainfall amounts from radar images. As the spatial and temporal resolution of distributed gridded data has increased it has become more desirable to incorporate gauge-corrected radar imagery into hydrological modelling to increase accuracy. This paper investigates the effectiveness of tipping-bucket rain gauges and Nimrod radar rainfall imagery to simulate a recent extreme flood event in the UK and to determine where the differences in accuracy lie given the different data resources used for model simulation.

STUDY SITE AND DATA

The Severn Uplands

The Severn Uplands is located at the headwaters of the River Severn, UK, and encompasses a drainage area of approximately 2000 km² (Fig. 1). The strong maritime influence in the Severn Uplands leads to high rainfall quantities and frequencies. To the west, the catchment is bordered by the Cambrian Mountains and prevailing

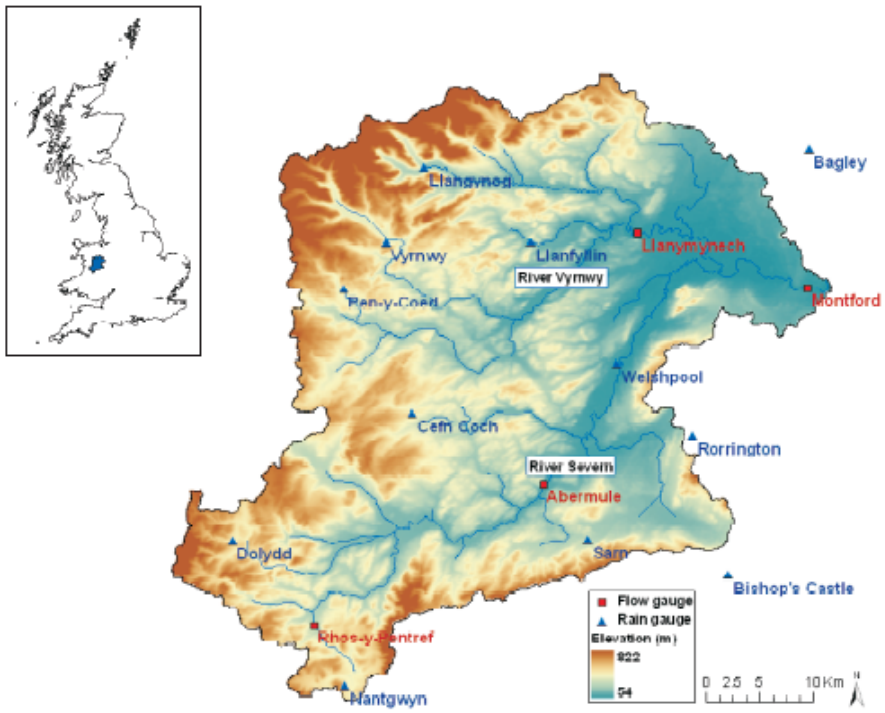

Fig. 1: The Severn Uplands catchment.

weather systems from the south-west bring precipitation as air streams are forced to uplift by the mountains. Rainfall is high in the west, totalling more than 2500 mm·annum^{-1}, and runoff regimes are flashy. Towards the east of the basin rainfall reduces to around 660 mm·annum^{-1} and drastic reductions in elevation give way to a wider fluvial system which meanders through low-lying floodplains. Elevation ranges from heights of approximately 820 m AOD in the west to lows of 50 m AOD in the east. The Vyrnwy, a major tributary, adjoins the River Severn just upstream of the catchment outlet at the Severn-Vyrnwy confluence zone where flood inundation occurs frequently. The Severn Uplands is a predominantly rural catchment with widespread grassland constituting approximately two-thirds of the land cover and woodland comprising the majority of the remaining third. The catchment largely constitutes impermeable geology, which leads to the generation of rapid runoff processes, particularly in the upper reaches where slopes are steep.

Summer 2007

During the summer of 2007 many parts of the UK were inundated following a series of unseasonably low depression systems throughout June and July. The heavy rainfall was the result of a series of statistically unusual weather patterns that have been attributed to two major causes; the position of the Polar Front Jet Stream and high North Atlantic sea surface temperatures (Marsh and Hannaford, 2007). In June, heavy thunderstorms led to wide extents of ground saturation, then in July slow moving depressions resulted in the largest flood inundation peaks. Rainfall intensity was high and June was one of the wettest months on record in the UK.

Two main sources of precipitation data are available in the UK; (i) gauged data recorded by the Environment Agency and (ii) Nimrod radar imagery sourced from the Met Office and supplied through the British Atmospheric Data Centre (BADC). Gauge records were obtained at 15-minute intervals for 12 gauges across the catchment (Figure 1) and radar images were acquired at 5-minute temporal resolution with 1 km^2 spatial resolution. Flow gauge data (Environment Agency) for model calibration were retrieved at 15-minute intervals for four locations (Figure 1). Radar data were aggregated to 15-minute intervals to temporally coincide with

the gauge time-series. All precipitation and flow records were retrieved for the time period 1st June to 31st July 2007, which is referred to in this paper as 'Summer 2007'.

METHODS

HEC-HMS, a one-dimensional rainfall-runoff model, was used to replicate hydrological processes in the Severn Uplands. Rainfall inputs were used to drive the hydrological model where subbasin (Clark unit hydrograph (gauge) and ModClark (radar) transform; recession baseflow; initial and constant loss) and river routing (Muskingum-Cunge) parameters acted to translate rainfall into runoff. Model calibration was undertaken using the HEC-HMS optimisation procedure with a combination of two objective functions and two minimising algorithms to determine optimal accuracy. The models (gauge- and radar-driven) were calibrated independently and optimum parameter sets were derived which generated the most accurate hydrograph simulations. Gauge rainfall was modelled within HEC-HMS using time and depth weights. Rainfall inputs were compared using error and correlation calculations and model outputs were assessed using a performance measure as described below.

Rainfall comparison

Root-mean square error (RMSE) was used as a measure of the quantitative agreement between the gauge and radar time-series. Lewis and Harrison (2007) state that RMSE is highly correlated with the magnitude of land surface rain-rate such that poorly performing radars in light rain could appear more accurate in predicting reference data than relatively accurately performing radar in heavy rainfall. Therefore, in addition to RMSE, the root-mean square factor (RMSF) was used as it overcomes this problem. RMSF is interpreted as giving scale to the multiplicative error (Golding, 1998) and is calculated as

$$RMSF = \exp\left\{\frac{1}{n}\sum_{i=1}^{n}\left[\mathrm{h}\left(\frac{R_i}{G_i}\right)\right]^2\right\}^{½} \qquad \text{Eq.1}$$

where R_i is radar precipitation and G_i is rain gauge precipitation at observation i and n is number of observations. Radar time-series were calculated by extracting cell values located at each of the gauging station locations and amalgamated to coincide with the temporal resolution of the gauge time-series. To avoid division by zero, only values ≥ 0.05 mm (a quarter of the standard 0.2 mm threshold for hourly readings) present in both 15-minute time-series were analysed. In addition to RMSE and RMSF, the Pearson product-moment correlation coefficient r was used to determine correlation and systematic bias was estimated as the difference between time-series totals.

Performance measure

The Nash-Sutcliffe efficiency index E_f (Nash and Sutcliffe, 1971) is a performance measure which compares optimal model simulations, rendered from strategic sampling of the parameter space, to that of the observational data, as follows

$$E_f = 1 - \frac{\sum_{i=1}^{n}(\hat{Y}_i - Y_i)^2}{\sum_{i=1}^{n}(Y_i - \overline{Y})^2} \qquad \text{Eq. 2}$$

where: $\hat{Y}_i$ is the predicted value and Y_i is the measured value of the dependent variable Y for observation i, $\overline{Y}$ is the mean of the measured values and n is the sample size. E_f will return a value of 1 for a perfect fit.

A value close to 0 is equivalent to saying that the hydrological model is equal to a one-parameter "no-knowledge" model. Negative values indicate that the model is performing below that of a "no-knowledge" model (Beven, 2001).

RESULTS

Time-series precipitation residuals at 15-minute intervals for Summer 2007 indicate an average RMSE of 0.18 mm across the Severn Uplands catchment (Table 1). No obvious spatial pattern in RMSE is apparent. However, RMSF values are generally smaller towards the east of the catchment and larger in the west (Table 1). Harrison *et al.* (2000) found that sampling difference alone can account for a RMSF difference of between 1.26 and 2.51 for hourly radar data at a 5 km² spatial resolution. Quality controlled and corrected Nimrod radar data have a typical RMSF value of around 2 when compared to surface gauges (Harrison *et al.*, 2000). With respect to these findings, RMSF values for the Severn Uplands indicate less error between precipitation residuals at analysed sites than expected, with a maximum observed RMSF value of 1.29. Correlations between the two time-series are large, particularly at sites in the south-east of the catchment where large positive correlations indicate a near-perfect fit (Table 1). Bias between Summer 2007 precipitation totals (radar minus gauge) indicates systematic errors of approximately ± 50 mm (Table 1). Radar time-series data over-predict ground observations at half of the gauging station locations. In terms of absolute error the most accurate radar predictions (in relation to reference data for the Summer 2007 hydrological event) are situated in the north-west of the catchment.

Table 1: Comparison of gauge and radar time-series at gauge station locations.

Station	RMSE [mm]	RMSF	r	Bias [mm]
Bagley	0.15	1.22	0.85	15.22
Bishop's Castle	0.13	1.22	0.85	30.71
Cefn Coch	0.20	1.26	0.63	41.97
Dolydd	0.18	1.29	0.81	-40.76
Llanfyllin	0.19	1.22	0.74	-56.37
Llangynog	0.18	1.25	0.79	4.22
Nantgwyn	0.19	1.26	0.75	17.46
Pen-y-Coed	0.21	1.29	0.71	0.77
Rorrington	0.17	1.19	0.90	-53.87
Sarn	0.16	1.21	0.86	-51.10
Vyrnwy	0.15	1.26	0.80	-1.29
Welshpool	0.22	1.23	0.80	-59.86

Table 2: Nash-Sutcliffe performance measure E_f for calibrated gauge- and radar-driven model simulations in comparison to observed flows.

	July		Summer 2007	
	Radar	Gauge	Radar	Gauge
Rhos-y-rentref	0.813	0.835	0.522	0.653
Abermule	0.672	0.597	0.315	0.540
Llanymynech	0.607	0.448	0.405	0.802
Montford	0.406	0.397	0.197	0.578

Model simulations were run initially to test the July 2007 predictions only. E_f indices of these preliminary results indicate little difference between simulated and observed flows derived from gauge and radar data inputs (Table 2). E_f values signify greater prediction accuracy in the upper reaches of the catchment, with accuracy decreasing with distance downstream. The gauge network generates a larger E_f value at Rhos-y-Pentref than that produced from the radar, but all three other sites are predicted more accurately using radar data. In contrast, when the entire Summer 2007 period is modelled the gauging network predicts more accurately in all cases (Table 2). The differences between July and Summer 2007 predictions are visualised in Figure 2 for Rhos-y-Pentref where the latter part of the gauge and radar time-series clearly fit the observed data more accurately.

INTERPRETATION AND DISCUSSION

Differences between the precipitation time-series are likely to have arisen from the ability of the radar to represent rainfall accurately. Several sources of uncertainty are present when processing radar data and two main factors seem to influence accuracy in the Severn Uplands. Firstly, the occultation and echoes of the radar

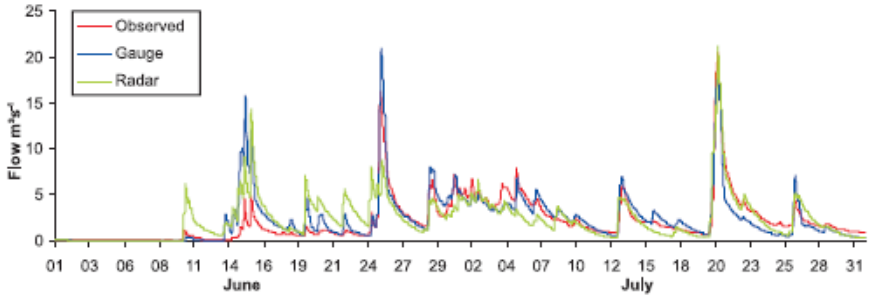

Fig. 2: Calibrated gauge- and radar-driven model simulations and observational data at Rhos-y-Pentref.

beam due to topographic changes and issues arising from orographic enhancement may have resulted in larger inaccuracies in the higher elevations to the north and west of the Severn Uplands. Secondly, the greater the distance from the radar source the greater the error, which could be due to the overshooting of precipitation by the radar beam at long ranges (Tilford *et al.*, 2003). In addition to these radar-sourced inaccuracies, the actual total amount of precipitation may have an effect on gauge-radar residuals.

These three factors are illustrated in Figure 3 where RMSF has been plotted against Summer 2007 rainfall totals, the distance of the site from the radar source and the elevation of the site. Significant positive correlations ($p < 0.05$) are identified between RMSF and all variables with values of 0.64 (radar), 0.91 (gauge), 0.73 (distance) and 0.68 (elevation). Larger error values at sites in the west of the Severn Uplands are likely to have

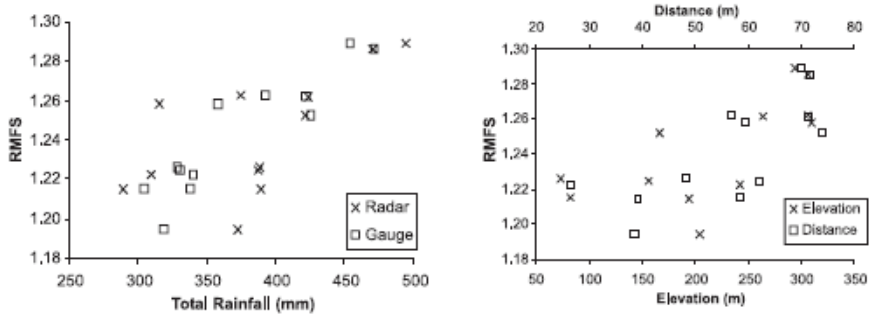

Fig. 3: Variations in RMSF in accordance with changes in total Summer 2007 rainfall (left) and elevation and distance from nearest radar source for time-series recorded locations (right).

resulted from higher rainfall due to orographic enhancement (elevation) which in turn results in increased radar distortion. These locations also happen to be furthest away from the nearest radar source which is situated to the south-east of the catchment. By multiplying the radar variables together, then scaling the values from 0 to 1, the spatial distribution of error likelihood was defined (Fig. 4). The scaled values show a significant positive correlation with RMSF at a value of 0.92 ($p < 0.001$).

The increased predictive power at upstream locations is likely to have occurred due to more clearly defined rainfall-runoff processes, as the steep topography and impermeable geology aid rapid transition of rainfall into runoff which directly inputs into river channels. Contrastingly, further downstream clear-cut rainfall-runoff processes diminish as the topography flattens out and basin properties such as floodplain storage and groundwater aquifers become increasingly influential. In terms of model output differences arising from precipitation data inputs, the E_f values suggest that HEC-HMS is capable of using both gauge and radar sources

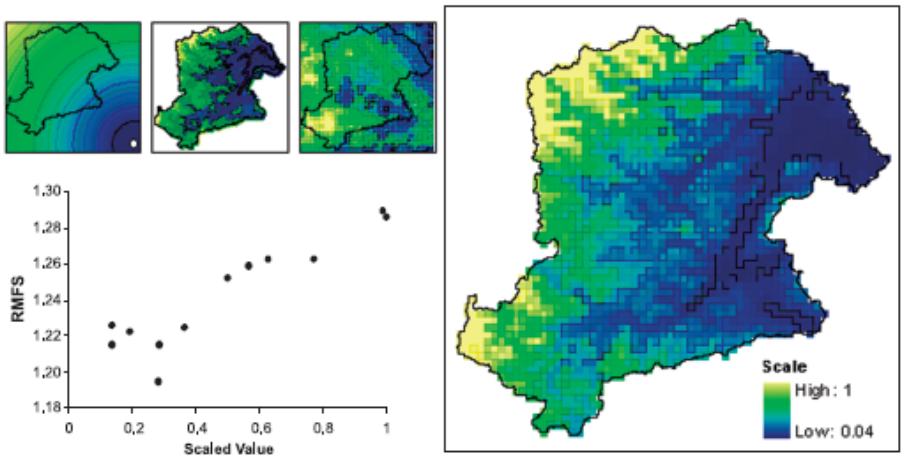

Fig. 4: Distance from radar source (top left), elevation (top middle) and rainfall total (top right) were multiplied and scaled then mapped (right) and plotted against RMSF.

to replicate Summer 2007 extreme flows with suitable accuracy, particularly at the more upstream locations. The lack of difference between the time-series E_f values may be due to the effectiveness of the modelling and calibration procedures within HEC-HMS. It may be beneficial in future research to correct the bias within the radar data by using the variables discussed above.

CONCLUSIONS

It has to be reiterated that neither rain gauge nor weather radar data can be taken as 'truth' (Tilford *et al.*, 2003). Despite differences in the gauge and radar time-series records, both point-interpolated and grid-distributed precipitation produced comparable results when using HEC-HMS to model the extreme hydrological event of Summer 2007 in the Severn Uplands. Greater accuracy was achieved in the upper reaches of the catchment and simulation accuracy increased in the latter part of the time period simulated. Overall, although some error remains, the Summer 2007 extreme hydrological event, one of the wettest events on record in the UK, was modelled adequately using both gauge and radar precipitation inputs. This provides encouragement for using the HEC-HMS software to model other extreme events which have occurred in the Severn Uplands; firstly, to validate the parameter sets for alternative extreme hydrological conditions, and secondly, to further research on how future precipitation extremes will influence fluvial extremes given current climate change predictions.

Acknowledgements: This research was jointly funded by the School of Geography and School of Electronics and Computer Science (ECS) at the University of Southampton. The authors wish to thank Danius Michaelides (ECS) and Thomas Eva0 (US Army Corps) for their assistance in data processing.

REFERENCES

Brown J.D. and Damery S.D. (2002). Managing flood risk in the UK: towards an integration of social and technical perspectives. *Transactions of the Inst. of Br. Geogr.*, **27**: 412–426.

Cunderlik J.M. and Simonovic S.P. (2005). Hydrological extremes in a south-western Ontario river basin under future climate conditions. *Hydrol. Sci. J.*, **50**(4): 361–654.

DEFRA (2001). *National Appraisal of Assets at Risk from Flooding and Coastal Erosion, including the potential impact of climate change: Final Report*. Halcrow, Swindon: 61pp.

Fowler H.J. and Kilsby C.G. (2003). A regional frequency analysis of United Kingdom extreme rainfall from 1964 to 2000. *Int. J. Climatol.*, **23**(11): 1313–1334.

Golding B.W. (1998). Nimrod: system for generating automated very short forecasts. *Meteorol. Appl.*, **5**: 1–16.

Harrison D.L., Driscoll S.J. and Kitchen M. (2000). Improving precipitation estimated from weather radar using quality control and correction techniques. *Meteorol. Appl.*, **6**: 135–144.

Lewis H.W. and Harrison D.L. (2007). Assessment of radar data quality in upland catchments. *Meteorol. Appl.*, **14**: 441–454.

Marsh T.J. and Hannaford J. (2007). *The summer 2007 floods in England and Wales – a hydrological appraisal*. Centre for Ecology and Hydrology, Wallingford, UK: 32pp.

Nash J.E. and Sutcliffe J.V. (1971). River flow forecasting through conceptual models. Part 1: A discussion of principles. *J. Hydrol.*, **10**(3): 282–290.

Osborn T.J., Hulme M., Jones P.S. and Basnett T.A. (2000). Observed trends in the daily intensity of United Kingdom precipitation. *Int. J. Climatol.*, **20**: 347–364.

Tilford K.A., Sene K., Chatterton J.B., and Whitlow C. (2003). *Flood Forecasting – Real Time Modelling*. Defra/Environment Agency R&D Technical Report W5C-013/5/TR.